

Pretreatment options for micropollutant abatement
before aquifer recharge in drinking water production:
Assessment of UV/H₂O₂ and dense membranes

Présentée le 22 avril 2022

Faculté de l'environnement naturel, architectural et construit
Laboratoire pour le traitement et la qualité de l'eau
Programme doctoral en génie civil et environnement

pour l'obtention du grade de Docteur ès Sciences

par

Robin WÜNSCH

Acceptée sur proposition du jury

Prof. K. Schirmer, présidente du jury
Prof. U. von Gunten, Prof. T. Wintgens, directeurs de thèse
Prof. H. Lutze, rapporteur
Prof. K. G. Linden, rapporteur
Dr C. McArdell, rapporteuse

Acknowledgements

Without the valuable support of many people, I would not have been able to complete this thesis. My cordial thanks to all of them.

I sincerely thank Urs von Gunten for his great support, many valuable discussions, careful revisions and comments on various manuscripts, and the many hours he invested in me and my studies. I felt that your supervision was a privilege.

I deeply thank Thomas Wintgens for his invested time, valuable inputs and great support. Thank you for being an architect of the projects and for making my time at the School of Life Sciences FHNW possible.

Many thanks to Kristin Schirmer, who presided the committee of my oral examination. I also thank the members of the examination committee: Christa McArdell, Holger Lutze, and Karl G. Linden.

I thank Michael Thomann for his great support of my studies as well as the manifold, valuable inputs and discussions. Thank you to the members of the UWT group. You made my time at FHNW what it was: a time rich in good memories and valuable experiences. I would like to thank the following people by name: Jan Svojitka, Patrik Eckert, David Cayon Diaz, Mario Strässle, Rita Hochstrat, Nadja Rastetter, Kirsten Remmen, Thérèse Krahnstöver, Sebastian Hedwig, Meret Amrein, Luca Loreggian. I also thank all other current and former members of the UWT group. Thank you, Felix Schmidt, for your manifold diligent support. Also, I thank Timm Hettich for fruitful collaborations. I thank Fredy Dinkel for his support in many projects. Erik Ammann is thanked for his hands-on support.

I thank Industrielle Werke Basel (IWB) for many good collaborations and discussions. Especially, I thank Richard Wülser, Julia Plattner, Fabienne Eugster and Pascal Temmler for the great projects, as well as trusting and respectful cooperation.

I thank the members of Urs von Gunten's group at Eawag for supporting me whenever needed.

Acknowledgements

A special thanks goes to Silvio Canonica, Elisabeth Muck and Joanna Houska.

Thank you, Uwe Hübner, for many fruitful discussions and good collaborations.

I thank all project partners for good cooperation and manifold support. The following persons deserve a special thank: Axel Jakob, Sven Bressmer, Jens Gebhardt, Steffen Rüting, Stephan Neumayer, Andree Blesgen, and Jozef Kochan.

I thank all the master's thesis writers for their excellent work: Michael Jau, Carina Mayer, Marlies Prahtel, Milena Sbarai Feuerhammel Silva, Christine Roth.

In addition, I thank the funding agencies and sponsors of my research. AquaNES was funded by the European Union's Horizon 2020 research and innovation program [grant agreement number 689450] and by the State Secretary for Education, Research and Innovation (SERI) of Switzerland [contract number: 16.0053-1]. INSPIREWATER was funded by the European Union's Horizon 2020 research and innovation program [grant agreement number 723702]. The School of Life Sciences FHNW funded the HLS research project ANNETTe: Artificial Neural Networks for Efficient Tailoring of Nanofiltration Membranes in Advanced Drinking Water Treatment. The Swiss Water Works Association (SVGW) co-funded the project OXIBIEAU.

I thank my family and friends for the unconditional support and for the good time that we shared. Linda, I am sure I could not have done all this without you. Your huge support was an essential pillar for me. Thank you.

Dübendorf, December 17, 2021

R. W.

Zusammenfassung

Mikroverunreinigungen (MV) wie Rückstände von Arzneimitteln, Industriechemikalien oder Pestiziden können in nahezu allen Wasserressourcen nachgewiesen werden. Um sie in der Trinkwasseraufbereitung zu entfernen, werden verschiedene Verfahren eingesetzt, z.B. Ozonung, weitergehende Oxidationsverfahren (Advanced Oxidation Processes, AOP), Adsorption an Aktivkohle oder Membranfiltration. Die Auswahl eines geeigneten Verfahrens stellt Wasserversorger vor eine komplexe Aufgabe.

Die vorliegende Arbeit vergleicht zwei Verfahrensketten im Kontext eines Multi-Barriere-Systems, das eine künstliche Grundwasseranreicherung (GWA) anwendet. Um künftig Böden und Aquifere vor MV zu schützen, wird eine zusätzliche Barriere gegen MV vor der GWA untersucht: (1) Eine Vollstrombehandlung mit dem AOP UV/H₂O₂, (2) eine Teilstrombehandlung mittels Niederdruckumkehrosmose (low-pressure reverse osmosis, LPRO) oder Nanofiltration (NF) mit einer Ozonung des Retentats zur Behandlung der aufkonzentrierten MV.

In Pilotversuchen wurden die relativen Abnahmen der MV durch UV/H₂O₂-Behandlung sowie durch eine nachgeschaltete Bodensäule ermittelt. Im Vergleich zu einer weiteren Bodensäule, die ohne vorgeschaltete UV/H₂O₂-Vorbehandlung betrieben wurde, nahmen die relativen Konzentrationen aller MV durch das kombinierte Verfahren (UV/H₂O₂ + Bodensäule) stärker ab. Dies konnte durch einen additiven Effekt der beiden Einzelprozesse erklärt werden.

Relative Konzentrationsabnahmen basieren im UV/H₂O₂-Verfahren im Wesentlichen auf der eingebrachten UV-Fluenz und der •OH-Exposition. Diese Parameter konnten auf Basis gemessener Konzentrationsabnahmen zweier im Wasser vorhandener MV und ihrer kinetischen Daten (Geschwindigkeitskonstante 2. Ordnung für die Reaktion mit •OH, Absorption, Quantenausbeute) mit einem Modell berechnet werden. Kombiniert mit weiteren kinetischen Daten war die Vorhersage relativer Konzentrationsabnahmen anderer MV mit einer Genauigkeit von ±20 % möglich. Für genaue Ergebnisse sollten die gemessenen relativen Konzentrationsabnahmen der Probesubstanzen > 50 % sein. In diesem Fall hängt die Genauigkeit der berechneten Parameter vor allem von der Präzision der kinetischen Daten ab.

Zusammenfassung

Wenn MV-Konzentrationen in Konzentraten membranbasierter Verfahren durch Ozonung vermindert werden sollen, kann aus vorliegendem Bromid das potenziell karzinogene Bromat entstehen. Um möglichst hohe MV-Konzentrationsabnahmen bei gleichzeitig geringer Bromatbildung zu erreichen, wurde das Zusammenspiel zwischen Membranauswahl und Konzentrat-Ozonung untersucht. In Laborversuchen mit standardisierten Konzentraten wurde festgestellt, dass weder die Herkunft des Wassers noch der Membrantyp eine Veränderung der Bromatausbeute bei gleicher relativer MV-Konzentrationsabnahme bewirkt. NF-Membranen weisen jedoch einen geringeren relativen Rückhalt von Bromid und MV auf als LPRO-Membranen, weshalb NF-Konzentrate besser für eine Ozonung geeignet sind.

Eine Multi-Kriterien-Analyse der betrachteten Verfahren zeigte, dass die Vollstrombehandlung mit UV/H₂O₂ ca. vierfach geringere Kosten verursacht, rund fünfmal geringere Umweltauswirkungen hat und zusätzlich eine signifikant höhere mikrobielle Inaktivierung erreicht. Hingegen ist die Teilstrombehandlung mit LPRO bis zu zweimal günstiger für die Umwelt, wenn Strom aus Wind- oder Wasserkraft bezogen wird. Diese Studie trägt somit zu einer ganzheitlichen Bewertung der Verfahren hinsichtlich technischer, ökonomischer und ökologischer Aspekte bei.

Stichwörter: UV/H₂O₂, Umkehrosmose, Nanofiltration, Ozonung, Mikroverunreinigungen, Multi-Barrieren System, Multi-Kriterien Analyse

Abstract

Micropollutants (MP) such as residues of pharmaceuticals, industrial chemicals or pesticides can be detected in almost all water resources. Various processes can be used to abate them in drinking water treatment, e.g., ozonation, advanced oxidation processes (AOP), adsorption on activated carbon or membrane filtration. The selection of a suitable process combination is a complex task for water suppliers.

This thesis compares two process chains in the context of a multi-barrier system including managed aquifer recharge (MAR). To protect soils and aquifers from MP in the future, an additional barrier against MP upstream of the MAR was investigated: (1) a full-stream treatment using the AOP UV/H₂O₂, and (2) a side-stream treatment with low-pressure reverse osmosis (LPRO) or nanofiltration (NF) and ozonation of the retentate to treat the concentrated MPs.

Pilot-scale experiments were conducted to determine the relative abatements of MP by UV/H₂O₂ treatment and by a subsequent soil column treatment. Compared to a soil column fed with water without UV/H₂O₂ pretreatment, the performance of the combined process (UV/H₂O₂ + soil column) was more efficient. However, this could be explained by an additive effect of the individual processes.

Relative abatements in the UV/H₂O₂ process are mainly based on the introduced UV fluence and hydroxyl radical exposure. These parameters could be calculated with a model based on the measured relative abatements of two MPs (probe compounds) and their kinetic data (second-order rate constants for the reactions with hydroxyl radical, absorbance and quantum yield). With this information, the relative abatements of other MPs could be predicted with an accuracy of $\pm 20\%$. A sensitivity analysis of the model showed that the relative abatements of the selected probe compounds should be $> 50\%$. In this case, the accuracy of the calculated parameters depends mainly on the precision of the kinetic data.

In the case of membrane-based treatment of water by LPRO or NF, a concentrate is produced. Ozonation to treat MP in the concentrate is accompanied by a formation of the possibly carcinogenic bromate by oxidation of bromide. To achieve the highest possible MP abate-

Abstract

ment with simultaneously low bromate formation, both membrane selection and subsequent concentrate ozonation were investigated. In laboratory tests with standardized concentrates, neither the water source nor the membrane type caused a change in bromate yield for similar relative MP abatements. However, NF membranes have lower relative retentions of bromide and MP than LPRO membranes, making NF concentrates more suitable for ozonation with limited bromate formation.

A comparison of UV/H₂O₂ with membrane treatment showed that full-stream treatment with UV/H₂O₂ has about four times lower costs and an about five times lower environmental impact. In addition it achieves significantly better disinfection. In contrast, side-stream treatment with LPRO results in up to two times lower impacts for the environment when the electrical energy source is wind or hydropower. This study thus contributes technical, economic, and environmental aspects to a holistic evaluation of the two process options.

Keywords: UV/H₂O₂, reverse osmosis, nanofiltration, ozonation, micropollutants, multi-barrier system, multi-criteria assessment

Contents

Acknowledgements	i
Abstracts (Deutsch/English)	iii
List of Figures	ix
List of Tables	xi
I Multi-Barrier Systems for the Abatement of Micropollutants in Drinking Water Production	1
1 Introduction	3
2 Materials and Methods	9
II UV/H₂O₂ before Soil Infiltration	17
3 Impact on Micropollutants, Dissolved Organic Matter and Biological Activity	19
4 Micropollutants as Internal Probe Compounds to Assess UV/H ₂ O ₂ Treatment	31
III Dense Membrane Filtration before Soil Infiltration	53
5 Ozone Treatment of Concentrates	55
IV Which Way to Go?	75
6 Multi-Criteria Assessment of the Investigated Treatment Options	77
7 Summary and Outlook	95
Appendix A: Supporting Information for Chapter 3	101
Appendix B: Supporting Information for Chapter 4	111

Contents

Appendix C: Supporting Information for Chapter 5	121
Appendix D: Supporting Information for Chapter 6	139
Bibliography	159
Curriculum Vitae	189

List of Figures

1.1	Schemes of assessed process trains	5
2.1	Drinking water production at IWB	10
2.2	Map of IWB's Lange Erlen Infiltration Site	11
2.3	Schemes of the pilot plant	13
3.1	Abatement of micropollutants by UV/H ₂ O ₂ treatment	23
3.2	Abatement of micropollutants by soil column treatment	24
3.3	LC-OCD chromatograms of different treatment steps	27
3.4	Intact cell counts and bacterial ATP along soil columns	28
4.1	Predicted abatement of selected micropollutants by in laboratory experiments with river Rhine sand filtrate.	40
4.2	Predicted abatement of selected micropollutants by in laboratory experiments with river Rhine sand filtrate.	42
4.3	Overview on possible combinations of probe compounds in river Rhine filtrate	43
4.4	Predicted abatement of selected micropollutants by in laboratory experiments with river Rhine sand filtrate.	46
4.5	Sensitivity analysis of the model.	49
5.1	Comparison of carbamazepine abatement in different water sources	64
5.2	Negative natural logarithm of the relative concentrations of benzotriazole and bezafibrate as functions of the negative natural logarithm of the relative concen- trations of ibuprofen	66
5.3	Molar bromate yields as functions of the specific ozone dose for various mem- brane in of River Wiese, River Rhine and Lake Biel water standardized concen- trates	67
5.4	Bromate yields as functions of the abatement of selected micropollutants. . . .	68
5.5	Different types of micropollutants in the process chain of membrane filtration and subsequent abatement in concentrate ozonation.	69
6.1	ILCD Single Scores of Treatment Alternatives	87
A1	Concentrations of micropollutants along the treatment chains	104

List of Figures

A2	Concentrations of EDTA in the raw Rhine river water	105
A3	Dissolved organic carbon concentrations along the soil columns	106
A4	Bacterial ATP per intact cell in the water phase along the soil columns	109
B1	Schematic drawing of a collimated beam device	112
B2	"Dark experiment" with river Rhine and river Wiese sand filtrates	115
B3	CBD laboratory experiments with river Wiese sand filtrate	116
B4	Pilot-scale experiments with river Rhine sand filtrate	119
B5	Pilot-scale experiments with river Wiese sand filtrate	120
C1	Membrane bench-scale test unit	123
C2	Membrane pilot-scale test unit	123
C3	Relative abatement of micropollutants as functions of the specific O ₃ dose in standardized concentrates	133
C4	Relative diclofenac abatement as a function of the specific ozone dose in stan- dardized concentrates	134
C5	Relative residual concentration of ibuprofen as a function of the relative residual concentration of atrazine	134
C6	Relative abatements of micropollutants as functions of the specific ozone dose in standardized and non-standardized River Wiese water concentrates.	136
C7	Molar bromate yields as a function of the specific ozone dose for RW standard- ized LPRO concentrate and non-standardized LPRO concentrate.	137
C8	Molar bromate yields as a function of the specific ozone dose for RW standard- ized LPRO concentrate and non-standardized LPRO concentrate.	137
D1	Possible Designs of a UV/H ₂ O ₂ Process	142
D2	Assessment of UV/H ₂ O ₂ Design	144
D3	Bromide in River Rhine and Bromate Yield	147
D4	Membrane Unit Capital Cost	151
D5	Ozone Unit Capital Cost	153
D6	UV/H ₂ O ₂ Climate Impact per Total Unit Cost	155
D7	UV/H ₂ O ₂ Single Score per Total Unit Cost	156

List of Tables

1.1	Overview on advanced water treatment processes	6
4.1	Water Quality Parameters of Rivers Rhine and Wiese Rapid Sand Filtrates	36
4.2	Fitted Rate Constants of Selected Micropollutants	48
5.1	Specified Membrane Characteristics	59
5.2	Kinetic data of selected micropollutants	60
5.3	Relative Retentions by Membranes	62
5.4	Electron Donating Capacities of Concentrates	63
5.5	Retentions in dense membranes, observed second-order rate constants for ozone and hydroxyl radical, experimental or predicted relative abatements of se- lected micropollutants during ozonation, hydroxyl radical exposure and bromate yield in the non-standardized LPRO concentrate.	71
6.1	Criteria in published multi-criteria assessments	79
6.2	Capital expenditures of the UV/H ₂ O ₂ treatment	81
6.3	Operating expenditures of the UV/H ₂ O ₂ treatment system	82
6.4	Capital expenditures of the low-pressure reverse osmosis membrane treatment with ozone treatment of the concentrate	83
6.5	Operating expenditures of the low-pressure reverse osmosis membrane treat- ment with ozone treatment of the concentrate	84
6.6	Process Inputs	85
6.7	Environmental Impact Points	86
6.8	Non-Target Screening Results	90
6.9	Summary of the Multi-Criteria Assessment	93
A1	Device list of sensors and probes	102
A2	Operational parameters of the UV/H ₂ O ₂ process	102
A3	Operational parameters of the soil columns	102
A4	Selected properties of investigated micropollutants	103
A5	Performance parameters of the analytical methods	104
A6	Evaluation by categories of the dissolved organic matter	107
A7	Performance parameters of the analytical methods	108

List of Tables

B1	Calculation scheme for CBD irradiation times	113
B2	List of suppliers and purity of utilized chemicals	114
B3	Overview of analytical parameters for micropollutant analyses	115
B4	Uncertainties and types of distribution considered in the model	116
B5	Differences between calculated and set UV fluences	117
B6	Statistical evaluation of single probe compounds in bench-scale experiments .	118
B7	Statistical evaluation of single probe compounds in pilot-scale experiments . .	118
C1	Studies reporting on bromate formation upon ozonation of reverse osmosis concentrates	122
C2	Review of pK_a , $k_{O_3,MP}$ and $k_{OH,MP}$ for selected micropollutants	124
C3	Purities and suppliers of chemicals	127
C4	Water quality parameters of the water samples before ozonation	128
C5	Limits of detection and maximum standard measurement errors of the micropollutants	131
C6	Slopes, their standard error and R^2 of EDC measurements	132
D1	Concentrations of Selected Micropollutants in river Rhine rapid sand filtrate water	140
D2	Abatement of Selected Micropollutants in Soil Aquifer Treatment Columns . . .	140
D3	Required abatement of a UV/H ₂ O ₂ or a membrane system	141
D4	Comparison of Metformin Abatements	143
D5	Membrane Screening in Bench-Scale Tests	145

Multi-Barrier Systems for the Abatement of Micropollutants in Drinking Water Production

Part I

1 Introduction

Organic compounds of anthropogenic origin with potential adverse effects on human health or the aquatic ecosystem at concentrations in the ng L^{-1} to $\mu\text{g L}^{-1}$ range are often termed "micropollutants" (MP). Typical MPs can be, e.g., industrial chemicals, pharmaceuticals, X-ray contrast media, food additives, personal care products, pesticides, hormones, and their respective metabolites [1]. They can have undesired effects on water organisms, such as the sexual disruption of wild fish in rivers upon exposure to endocrine-disrupting compounds from wastewater effluents [2]. Adverse effects of MPs in complex mixtures such as wastewaters can be significantly higher than effects determined in single compounds assays [3]. Specifically, MPs that are persistent in the environment, accumulate in organisms and have toxic or other adverse effects are of major concern [4].

MPs are a global issue due to their ubiquitous presence in surface waters and groundwaters [1], [5]–[12]. At the same time, drinking water is mostly produced from these sources [13], [14]. Simple water treatment processes, e.g., coagulation, flocculation, sedimentation, or sand filtration, are not designed to abate MPs and do not abate many MPs sufficiently [15]–[19]. Consequently, to maintain safe drinking water of high quality at low costs, strategies for resource protection are necessary [20], [21]. In addition to the protection of water resources, water treatment processes are required in drinking water production as effective barriers against MPs. For compound which are non-toxic to humans, this might be regarded pre-emptive and a consumer's confidence-building measure, because MPs can indicate that the source water is impaired, e.g., with wastewater [22], [23]. Nevertheless, from a precautionary point of view, MPs should be abated during drinking water production to avoid (yet unknown) adverse effects upon consumption of potable water. This is underpinned by the fact that analytical

limitations exist for, e.g., very polar compounds [24] and therefore a "complete picture" of the risks associated with a particular potable water is unlikely to ever be obtained [25].

Globally, the aquifers are over-exploited due to an increasing water demand. Managed aquifer recharge (MAR) is a umbrella-term for the intended artificial augmentation of an aquifer's water level to enable a sustainable abstraction of drinking water [26], [27]. Some forms of MAR have been applied since more than a century in Europe, such as river bank filtration or infiltration basins [27]. Today, a web-based global inventory lists about 1'200 sites where different types of MAR are applied [28]. Though local differences exist for the purpose of the water treated by MAR, it is predominantly for domestic uses in Europe, North America and Africa [28]. MAR is applied in Europe and North America with different treatment targets [29]. In certain European countries, MAR is used to produce high quality water suitable for drinking with hardly any additional treatment and no chlorine disinfection. Therefore, the treatment aims at biodegradable dissolved organic carbon (BDOC) and pathogen removal, as well as MP abatement [29]. In North America, the primary intention is to remove pathogens from surface waters, especially *cysts* and *oocysts*, and to reduce costs for conventional drinking water treatment [29]. Here, the removal of turbidity and dissolved organic carbon (DOC) is a secondary treatment goal [29].

Contaminant removal during MAR is based on a complex combination and interaction of effects such as physicochemical filtration of suspended particulate matter, solute precipitation, sorption and biodegradation [30]. These processes are affected by various site-specific parameters, such as soil characteristics, infiltration rate, water source and quality, climate, as well as pollutant characteristics [30]. The capability of MAR systems to abate MPs has been widely studied and results have been critically reviewed [17], [31]. Some MPs are well removed in MAR systems (e.g., atenolol, naproxen, trimethoprim), whereas other MPs are persistent upon this treatment (e.g., atrazine, carbamazepine, primidone, sucralose, tramadol) [31]. Typically, parameters considered to affect the removal of MPs are the concentration and type of BDOC in the feed water, redox conditions during the MAR treatment, mineral composition of the subsurface material and the hydraulic residence time or traveling distance [17], [31]. Hence, if the water source is contaminated with, e.g., MPs that are hardly removed during MAR, it might be necessary to pretreat the raw water before MAR treatment to protect soil, aquifers and groundwater [30] as groundwater pollution through contaminated infiltrated water could potentially be a legal issue [32].

In addition, drinking water producers utilizing MAR systems experienced that contaminations of the past are now being released. The Dutch drinking water company Oasen can serve as an illustrative example. Oasen produces drinking water from river bank filtration water (rivers Nieuwe Maas and Lek) near Rotterdam in the western Netherlands [33]. Historically, the rivers were impacted by discharged perfluorooctanoic acid (PFOA) from a chemical production plant upstream of the bank filtrate extraction wells. Pollution of the river waters with PFOA was back-calculated to have taken place during a period from around 1970 until around 2000. PFOA is very persistent in the environment, mobile and has adverse effects on human health

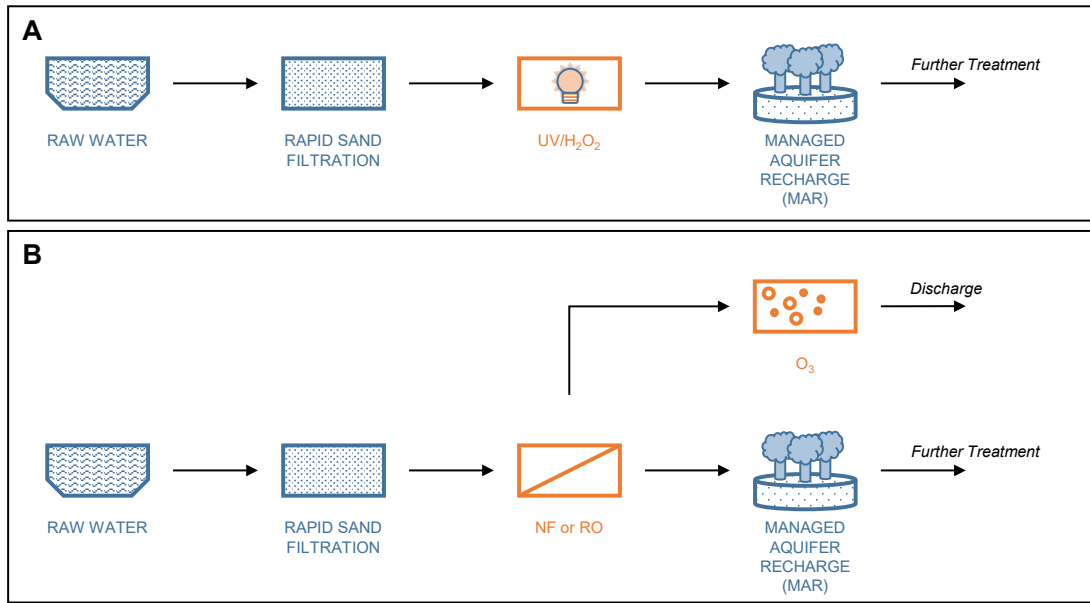


Figure 1.1: Schemes of the assessed process trains. After raw water extraction and rapid sand filtration, either (A) a UV/H₂O₂ or (B) a dense membrane filtration with concentrate ozonation is used as a pretreatment before managed aquifer recharge (MAR). Further treatment after MAR can be, e.g., a disinfection. This thesis focuses on the assessment of the processes highlighted in orange. UV: Ultraviolet. NF: Nanofiltration. RO: Reverse osmosis.

[34]. Based on the measured concentrations in their pumping wells and hydrodynamic models, Oasis expects that the pollution of their raw water (mixed groundwaters) peaked around 2010 with concentrations partially above 200 ng L⁻¹ and will continue to affect their raw water (concentrations > 10 ng L⁻¹) until at least 2050 [33]. This showcases that the pollution of soils and aquifers with persistent chemicals can have a long-term impact on the drinking water resources. Therefore, it seems reasonable to investigate pretreatment options to protect MAR sites from pollution with MPs.

Clearly, there is no universal solution to target all MPs with one process at reasonable costs and environmental impacts, as physico-chemical properties of MPs largely vary. Instead, the combination of different treatment processes in a multi-barrier approach is currently regarded the most feasible option for the abatement of a wide spectrum of MPs [25], [35]–[38]. Table 1.1 lists some technologies that proved effective for MP abatement and that are currently deployed in full-scale. Typically, currently deployed processes are based on activated carbon, dense membranes or partial oxidation processes. Among the partial oxidation processes are the so-called advanced oxidation processes (AOP). AOPs aim at the *in situ* generation of hydroxyl radicals ([•]OH). [•]OH react relatively unspecifically and typically with second-order rate constants near the diffusion limit, i.e., in the range of 10⁹ to 10¹⁰ M⁻¹ s⁻¹.

This thesis focuses on the assessment of two pretreatment options before MAR (Figure 1.1).

Chapter 1. Introduction

Table 1.1: Overview on water treatment processes for the abatement of micropollutants utilized in full-scale drinking water treatment.

Technology	Working principle	Target compounds	Short description
Powdered Activated Carbon (PAC)	Adsorption	Non-polar to moderately polar compounds	Activated carbon is dosed in powdered form. Loaded PAC must be removed, e.g., by coagulation-flocculation and sedimentation or ultrafiltration.
Granular Activated Carbon (GAC)	Adsorption	Non-polar to moderately polar compounds	Filtration over GAC bed.
Biological Activated Carbon (BAC)	Biological degradation	Biologically degradable compounds	(Slow) Filtration over (exhausted) granular activated carbon bed.
Ozonation (O_3)	(Partial) Chemical oxidation	Compounds with electron-rich sites	O_3 generated on-site is transferred to the water. Contact chamber and off-gas treatment required.
O_3/H_2O_2	(Partial) Chemical oxidation	Compounds with sites for OH addition or H-abstraction	O_3 generated on-site is transferred to the water. H_2O_2 quickly decomposes O_3 to hydroxyl radicals.
Ultraviolet (UV)/ H_2O_2	(Partial) Chemical oxidation	UV-susceptible compounds, or with sites for OH addition or H-abstraction	Direct photolysis of compounds and generation of hydroxyl radicals from H_2O_2 photolysis.
Nanofiltration (NF)	Size-exclusion, electro-static repulsion and diffusion through a semi-permeable membrane	Compounds with a molecular weight (MW) above the MW cut-off and (divalent) ionic compounds of similar charge as the membrane surface.	Water is forced through a membrane by mechanical force. Concentrate management required.
Reverse Osmosis (RO)	Size-exclusion and diffusion through a semi-permeable membrane	Compounds with a molecular weight (MW) above the MW cut-off.	Water is forced through a membrane by mechanical force. Concentrate management required.

One pretreatment option is an AOP consisting of a hydrogen peroxide (H_2O_2) dosage and subsequent irradiation with monochromatic ultraviolet (UV) light at a wavelength of 254 nm (UV/ H_2O_2 , Figure 1.1A). Hypothetically, this option in combination with MAR might lead to synergistic effects [39] if the products of the partial oxidation process are more biodegradable than their parent compounds [40]. The other investigated pretreatment is the treatment of a part of the volume flow by nanofiltration (NF) or reverse osmosis (RO) (Figure 1.1B). The NF or RO permeate is mixed with rapid sand filtrate before MAR and the respective concentrate is treated with ozone (O_3) before discharge to a river.

If a pretreatment prior to MAR is deemed necessary, which of the selected options would be the better choice? The present study intends to contribute to answering this overarching question in the context of a multi-criteria assessment (MCA). The information required for this assessment was collected in laboratory and pilot-scale experiments. Chapter 2 describes the most relevant analytical methods and experimental setups. In addition, the drinking water production site of Industrielle Werke Basel in Basel, Switzerland, is introduced, because large parts of this study are based on experiments with water from this site.

Chapter 3 investigates UV/H₂O₂ pretreatment before MAR simulated by a soil aquifer treatment (SAT) column. How strongly are MPs abated and can synergistic effects of the two treatments be observed? What is the impact on the dissolved organic matter (DOM)? How is the microbiology impacted by the treatments? These questions are investigated with data from a pilot-scale experiment, including two SAT-columns operated in parallel. One column was fed with rapid sand filtrate after UV/H₂O₂ treatment. The other was fed with the rapid sand filtrate without further pretreatment and served as a reference column. The presented results, obtained in the Horizon2020 project AquaNES, were published previously [38].

Chapter 4 presents a model that facilitates an assessment of fundamental performance parameters of the UV/H₂O₂ treatment, i.e., the UV fluence (H_{calc}) and •OH exposure ($CT_{\text{OH,calc}}$). Can H_{calc} and $CT_{\text{OH,calc}}$ be calculated from the abatement of two MPs serving as internal probe compounds? How accurately can the abatement of other MPs be predicted based on the calculated values of H_{calc} and $CT_{\text{OH,calc}}$? Which parameters are most critical to obtain reliable results from the model? This chapter was published previously [41].

With respect to the side-stream membrane treatment, Chapter 5 highlights the interaction of membrane choice and subsequent concentrate treatment by ozonation. It is known that the membrane selection impacts the ion composition and pH of the concentrate. However, the membrane hypothetically has an effect on the DOM as well, because some DOM fractions might be able to permeate through "looser" NF membranes, but are retained by RO. How do the hypothetically differing DOM compositions impact the abatement of MPs and formation of bromate upon ozone treatment? Do the water source and the membrane type impact the tradeoff between MP abatement and bromate formation? To answer these research questions, two river water rapid sand filtrates and one lake water were treated with up to three membranes, i.e., two NF membranes and one low-pressure RO (LPRO) membrane. Concentrates were standardized to the same pH and concentrations of DOC, total inorganic carbon and Br⁻ to rule out the impact of these parameters on the bromate formation upon ozone treatment. In addition the concentrates were spiked with well-known MPs to investigate the potential impact of the membrane on the trade-off between MP abatement and bromate formation. The results are prepared for a submission to a scientific journal for publication [42].

Finally, the two pretreatment options are compared in a MCA. Chapter 6 first gives a short overview on existing MCAs in the field of water treatment with a focus on MP abatement. Subsequently, the pretreatment designs are derived for a specific treatment goal, using the

Chapter 1. Introduction

river Rhine rapid sand filtrate as an example raw water. The MCA considers technical aspects, as well as cost, environmental and other aspects, such as disinfection. For the cost assessment, equations were derived based on a publication by Plumlee *et al.* (2014) [43] to facilitate high transferability. Environmental aspects were investigated by means of a life cycle assessment (LCA). A similar LCA was conducted in the OXIBIEAU project, which was published before [44]. Here, in comparison to the submitted manuscript, some modifications of the LCA were done with respect to the assessed process chains and input data. In addition to costs and environmental impacts, advantages of the respective treatment approaches are briefly discussed, such as the formation and fate of oxidation products during the UV/H₂O₂ treatment. Chapter 7 summarizes the main findings of this thesis and provides an outlook for further research.

2 Materials and Methods

This chapter introduces the drinking water production of Industrielle Werke Basel (IWB) and a pilot plant for the investigations of UV/H₂O₂ treatment and soil aquifer treatment (SAT) columns. Furthermore, the most important analytical methods for this thesis are described. In parts, the descriptions are copied from previously published articles from this thesis [38], [41], [42]. Additional methods relevant for individual chapters are described in the respective section.

IWB's Drinking Water Production Process

The city of Basel, Switzerland, and surrounding areas receive about 50 % of their drinking water from IWB. The production of drinking water by IWB is shown in Figure 2.1 and is based on the managed recharge of the aquifers with water from the river Rhine. The water is abstracted from the river Rhine after traveling almost 170 km from Lake Constance (Figure 2.2). The abstracted water is filtered by rapid sand filters for particle removal (20 filters with 50 m² surface area each, varying volume flow around 700 – 900 L s⁻¹, 0.8 m sand bed height). Filtration is stopped when the filtrate turbidity is ≥ 4.0 FNU to protect the infiltration sites from clogging. The sand filtrate is infiltrated into the aquifer in the Lange Erlen forest at an infiltration rate of 1 to 2 m d⁻¹ in an intermittent mode of operation (10 days infiltration, then a 20 days drying and aeration phase of the soil). The artificial groundwater augmentation in Lange Erlen has been in operation since 1911 without a loss of performance. Initially, the water resource was unfiltered water from the river Wiese (Figure 2.2) and this was changed to river Rhine rapid sand filtrate water in 1964 [45]. The infiltrate mixes with natural groundwater after passing a

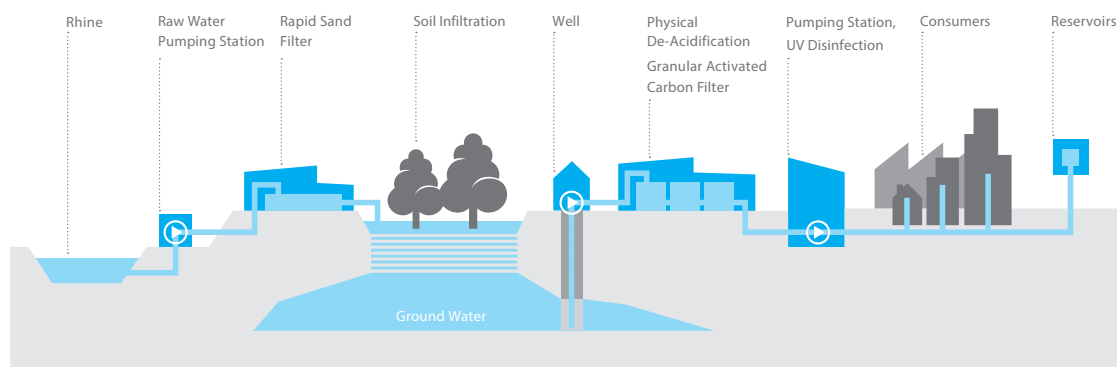


Figure 2.1: Scheme of IWB's drinking water production process chain. Figure provided by IWB [47] and modified by the author.

humus layer of about 0.2 to 0.3 m thickness and a subsequent gravel and sand layer of about 2.5 m thickness [45]. The water is collected and abstracted by several wells in the catchment area after traveling 10 to 30 days underground [46]. Abstracted groundwater is further treated by partial physical de-acidification by aeration, activated carbon filtration, pH adjustment to 7.7 by NaOH addition and medium-pressure UV disinfection before the water is distributed to the consumers. [41]

The Lange Erlen site was subject of previous PhD theses [45], [46], [48] and research other than presented here [49]. In his PhD thesis, D. Rüetschi (2004) [45] investigated the fundamental working principles of the Lange Erlen infiltration site. It was not well understood why the system could be operated with a sustainable performance without the need to mechanically clean the topsoil layer, as known from slow sand filters. The research identified the infiltration-drying-cycle as an important feature for the sustainability of the site's performance. Additionally, the structure of the topsoil layer with macro-pore diameters in the range of 0.1 to 5.0 cm (from earthworm and mouse tunnels) contributes significantly to the practically maintenance-free operation of the site. Investigations of the microbial activity along the infiltration path showed that the DOC removal hardly took place within the first few cm of the (biologically highly active) humus layer. Instead, the DOC was removed across the whole infiltration path, i.e., 2/3 in the gravel and sand layer and 1/3 in the aquifer. Rüetschi concluded that in the unsaturated zones, water purification is mainly based on microbial degradation of the DOC, which partly takes place during the infiltration cycle, partly during the drying and aeration cycle from DOC-deposits adsorbed, e.g., on iron oxide. In the saturated zone, i.e., the aquifer, the DOC removal could not be explained entirely, but likely bases on dilution with natural groundwater and adsorption. Longer phases of operational interruption are therefore likely responsible to maintain the permeability of the aquifer, which is then regenerated by microbial degradation of the adsorbed organic matter [45].

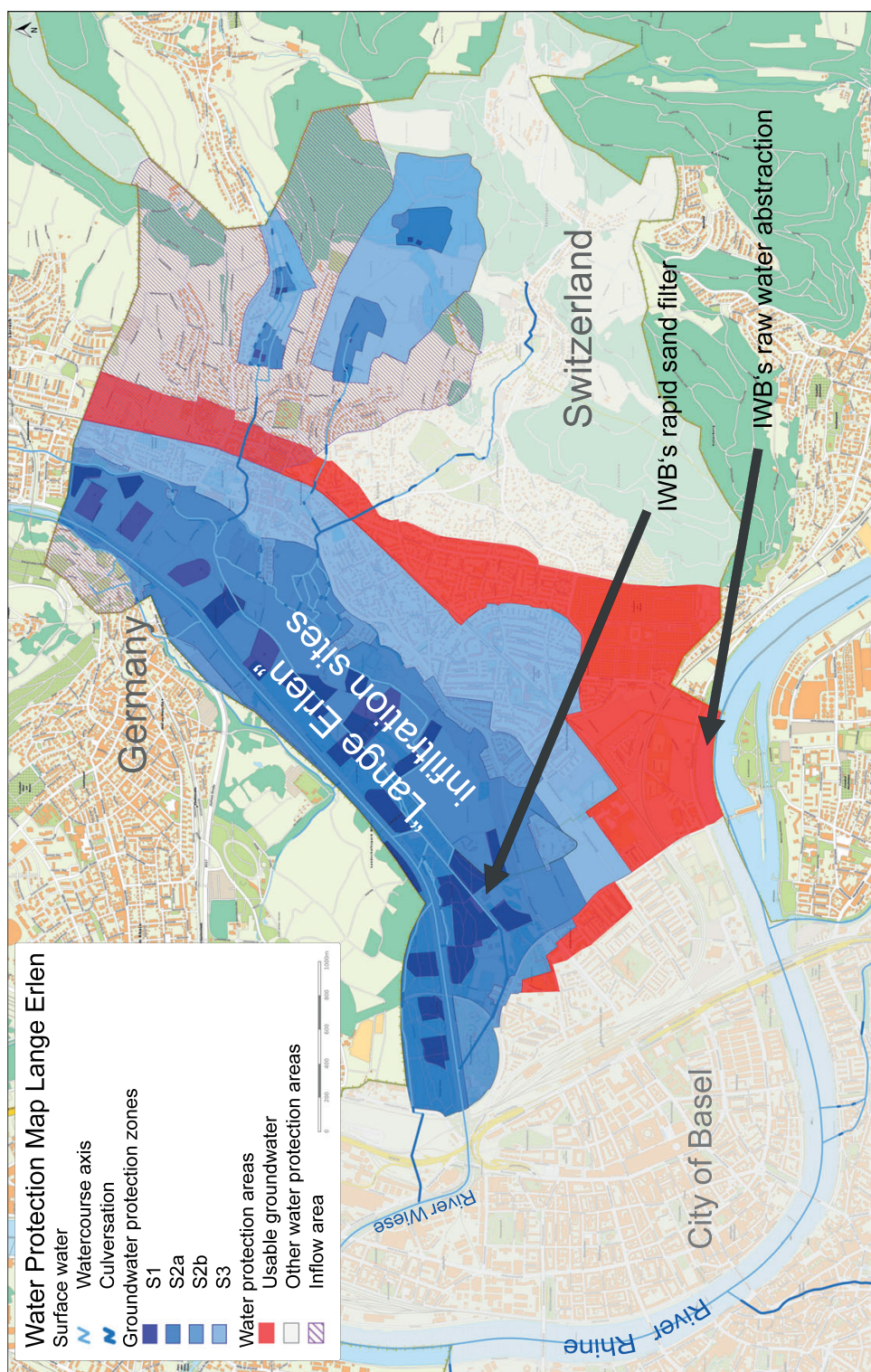


Figure 2.2: Map of the Lange Erlen infiltration site. Water and groundwater protection zones are also shown, as well as locations of IWB's river Rhine raw water extraction and rapid sand filter building. Map obtained from <https://map.geo.bs.ch> and modified by the author.

A subsequent PhD thesis by K. Schütz (2008) [46] detailed the roles of soil fauna and microbiology. In a preliminary study, she found that infiltration fields periodically in use for groundwater augmentation ('active fields') provided better habitats for earthworms than an infiltration field that was not in use for groundwater augmentation since a longer period ('inactive field'). In contrast, the active fields were less optimal for mites (Acari) and springtails (Collembola) than the inactive field. Detailed investigations of the earthworm populations in the Lange Erlen underpinned that the interrupted mode of infiltration favored the growth of earthworms and they likely contribute to the long-term sustainability of the soil infiltration site. Furthermore, Schütz found significant differences in microbial communities between active and inactive fields in vertical soil profiles to ≈ 4 m, assessed by phospholipid fatty acids. Differences were mostly observed in the vadose zone and were attributed to the flooding of the active fields. It remained unclear whether these differences occurred from physical transport of microorganisms of the river water or from nutrients and dissolved substances transported by the infiltrate leading to distinct growth of populations. Schütz further confirmed that considerable fractions of the soil's biomass were located in 0.4 to 3.2 m depth and thus significantly contribute to the DOC removal. Finally, she studied the enzyme activity in two active fields and an inactive field as a control. While the microbial activity measured by CO_2 and specific respiration was higher at the active fields, no difference to inactive field was detected for the biomass, absolute and specific enzyme activities. Site-specific differences in the relative enzyme activity pattern were explained by different soil characteristics. Schütz concluded that the DOC introduced to the infiltration fields by the infiltration of river water leads to an increased microbial activity, but not to growth of microbial biomass.

Finally, the PhD thesis of F. R. Storck (2014) [48] further investigated the roles of adsorption, microbiological degradation and dilution with natural groundwater for the removal of DOC and selected MPs. In field experiments, Storck determined a DOC abatement of 47% across an infiltration site, which was explained by 35% adsorption and biological degradation and 12% dilution with natural groundwater. In a depth of 1.3 to 2.6 m, a biologically highly active zone was detected. At some locations, the formation of NO_2 and CH_4 indicated temporary N-limited conditions in the fully oxic water. Storck confirmed the hypothesized oxidative biological degradation of DOM by mass balances and isotopic signatures. In pilot-scale column experiments, Storck investigated the abatement of ten MPs, i.e., iohexol, iomeprol, iopromid, ioxitalamic acid, caffeine and galaxolide (all removed by >30% to >73%), as well as atrazine, tris-(2-chloroethyl)phosphat (TCEP), iopamidol and diatrizoic acid (all recalcitrant). He found that a short-term moderate pollution of the feed water (river Rhine rapid sand filtrate) with quickly biodegradable substances simulated by sucrose addition should not negatively impact the drinking water production, but could even increase the removal of some MPs. In contrast, strong contamination with bio-available substrates result in a change of the redox conditions (oxic to anoxic) and inhibit abatement of some MPs, e.g., iomeprol, ioxitalamic acid and iopromide. The same columns as used by Storck were re-used for the research conducted in this thesis with a different soil material, as described below.

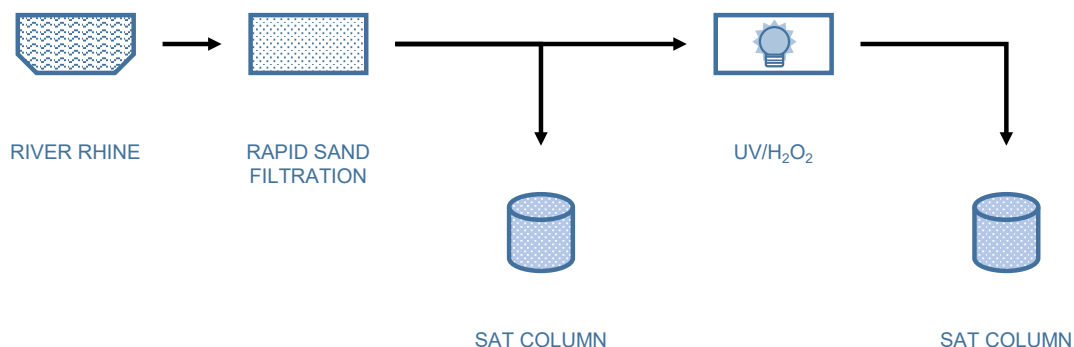


Figure 2.3: Scheme of the pilot plant used for the treatment of river Rhine rapid sand filtrate water. Further details can be found elsewhere [38], [41].

Recently, Zawadzka *et al.* (2019) [49] investigated ecosystem services provided by the Lange Erlen site and two other combined natural and engineered water treatment sites in the context of the AquaNES project. The authors reported that the Lange Erlen site plays an important role for carbon storage, pollination, water retention, sediment retention, nutrient retention and habitat connectivity for biodiversity [49]. Also, the research highlighted the higher aesthetic visual value of the natural treatment processes in comparison to engineered processes.

Pilot Plant

It is known that the river Rhine is polluted with various MPs such as chelating agents, iodinated X-ray contrast media, artificial sweeteners, pharmaceutical active compounds and industrial chemicals [41], [44], [50]. In the current drinking water production of IWB, not all of these compounds are fully abated during MAR, but some MPs are still present after soil infiltration of the rapid sand filtrate water and abstraction of the groundwater. These include, e.g., ethylenediaminetetraacetic acid (EDTA), acesulfame, and iopamidol [48]. Most of these compounds are well abated by UV-based AOPs [38], [41]. For this reason, and to exclude the formation of bromate from bromide in ozone-based treatments [51], a UV/H₂O₂ treatment was selected as one pretreatment option before MAR.

A pilot plant was used to investigate the UV/H₂O₂ process alone (Chapters 3 and 4) or in combination with a soil aquifer treatment (SAT) (Chapter 3). It was installed in the rapid sand filter of IWB's full-scale drinking water treatment plant and is schematically shown in Figure 2.3. SAT is a sub-group of MAR and describes the (intermittent) infiltration of water to an unconfined aquifer [52].

The UV/H₂O₂ process was continuously operated at different set points in a fully automated mode from March 2017 until February 2021. Mostly, a treatment with 4 mg H₂O₂ L⁻¹ and 6'000 J m⁻² was selected based on results of bench-scale batch experiments [41], [53] and a

treatment goal of $\geq 80\%$ abatement of the iodinated X-ray contrast media.

The UV fluence was adjusted by controlling the flow through the respective UV reactor by a controllable valve upstream of the UV reactor. The target flow was determined from a correlation with the UV transmissivity of the respective influent, measured *online* by photometers (ColorPlus, Sigrist-Photometer, Switzerland). H_2O_2 was dosed by dosing pumps (gamma/X, ProMinent, Germany) before the UV reactors (Spektron 6, Xylem Services, Germany) from a 2 % (w/w) stock solution, prepared by dilution with ultrapure water from a 35 % (w/w) solution. After the dosing point for H_2O_2 , a static mixer ensured complete mixing before entering the UV reactor. The flow through the reactor was measured after the UV reactors by online flow meters (3021, GEMÜ, Germany). Grab samples were collected from sampling ports upstream of the H_2O_2 dosing point and after the UV reactor [41]. Table A1 (Appendix A) gives an overview on the devices and probes utilized at the pilot plant. For the treatment with $4 \text{ mg } \text{H}_2\text{O}_2 \text{ L}^{-1}$ and $6'000 \text{ J m}^{-2}$, Table A2 summarizes the operational parameters of the UV/ H_2O_2 treatment, such as the average volume flow through the UV reactor ($566 \pm 51 \text{ L h}^{-1}$).

In addition to UV/ H_2O_2 treatment of the river Rhine rapid sand filtrate water, an identical second UV/ H_2O_2 line was operated in parallel with rapid sand filtrate water from the river Wiese, as described elsewhere [41].

The SAT columns were made of stainless steel and were of the dimensions $1.0 \text{ m} \times 0.5 \text{ m}$ (filling height \times inner diameter, respectively). They were filled with a disturbed soil sample from the Lange Erlen (Basel, Switzerland) infiltration site of IWB (first meter, sieved fraction $< 2 \text{ cm}$). The soil sample was mixed with sand from the full-scale rapid sand filters in a 1:1 volumetric ratio to ensure sufficient permeability during the piloting phase. The SAT columns were operated in continuous overflow and were manually adjusted to a target flow of 6 L h^{-1} (EBCT = 24 h, i.e., infiltration velocity = 1 m d^{-1}) by a needle valve at the respective column outlet. Grab samples were collected from sampling ports along the columns, located at the column walls after a soil passage of 0.05 m, 0.1 m, 0.5 m and 1.0 m, respectively. The continuous SAT operation was divided in a startup phase (March 2017 to October 2017) and a test phase (November 2017 to August 2018) for the data presented in Chapter 3 [38]. A summary of the treatment conditions in the columns is provided in Table A3 (Appendix A).

Analytical Methods

Dissolved organic carbon (DOC) was measured by size exclusion chromatography (SEC) coupled with an organic carbon detector (OCD), a UV absorption detector at 254 nm (UVD) and an organic nitrogen detector (OND) (model 8, DOC-Labor Dr. Huber, Germany) [54]. A 26.8 mM phosphate buffer at pH 6.58 was used as eluent, prepared by dissolving 12.5 g KH_2PO_4 and 7.5 g $\text{Na}_2\text{HPO}_4 \times 2 \cdot \text{H}_2\text{O}$ in 5 L pure water ($\geq 18.2 \text{ M}\Omega$). The chromatograms were evaluated using the manufacturer's software (ChromCALC, DOC-Labor Dr. Huber, Germany). The standard error of the DOC was estimated to be 7% from replicate measurements of the same sample. [42]

Bromide and bromate were analyzed by ion chromatography (IC) coupled with an inductively coupled plasma (ICP), using a mass spectrometer (MS) as detector. No sample preparation was necessary. Samples were injected (100 μL) to the IC (ICS-2100, Thermo Fisher Analytics, USA) equipped with a guard column (Dionex IonPac AG-18, 2x50 mm, Thermo Fisher Analytics, USA) and a separation column (Dionex IonPac AS-18, 2x250 mm, Thermo Fisher Analytics, USA). KOH was applied as eluent with a gradient method. Bromide and bromate were detected as bromine at the ICP-MS (8800 QqQ, Agilent Technologies, USA) in no-gas mode at mass 81, as this showed the highest sensitivity. The limit of detection (LoD) and limit of quantification (LoQ) were derived at 0.7 and 2 $\mu\text{g L}^{-1}$, respectively, from blank injection measurements. The calibrated range was 2 to 20 $\mu\text{g L}^{-1}$ for bromate and 100 to 600 $\mu\text{g L}^{-1}$ for bromide, respectively, and showed a high linearity ($R^2 > 0.99$, five-point calibrations, respectively). Standard measurement errors were determined to be 8% for both species from replicate standard injections. [42]

MPs were measured by different methods. Data presented in Chapters 3 and 4 were measured by IWB as described in the following. Concentrations of 5-methyl-1H-benzotriazole (5BTZ), 1H-benzotriazole (BTZ), carbamazepine (CBZ), metformin (MET), metoprolol (MPL), sotalol (STL) and sulfamethoxazole (SMX) were measured by HPLC-MS/MS (Qtrap 5500, AB Sciex) with electron spray ionization in positive and negative mode based on a modified standard method (DIN 38407-47). A separation column (Aquity UPLC HSS T3, 3.0 mm \times 150 mm, particle size 1.8 μm , Waters, MA, USA) was used for separation on a high performance liquid chromatography (HPLC, UltiMate 3000, Thermo Scientific, MA, USA) after direct injection (250 μL). Deuterated internal standards were BTZ-d4 for BTZ and 5BTZ, CBZ-d10 for CBZ, SMX-d4 for MPL and SMX, MET-d6 for MET and STL-d4 for STL. Purities of the chemicals are provided in Table B2 (Appendix B).

Acesulfame (ACE), diatrizoic acid (DTA), iohexol (IHx), iopamidol (IPA) and iopromide (IPR) were measured after 10-fold pre-concentration, which was achieved by evaporation to dryness under vacuum at 54 $^{\circ}\text{C}$, subsequent elution with eluent (ultrapure water with 5 mM ammonium formate and 0.1% formic acid) and sterile filtration (0.2 μm). The same HPLC-MS/MS system was used as above, but a different set of columns was applied (pre-column: Eclipse XBD-C18, 12.5 mm \times 4.6 mm, particle size: 5 μm ; separation column: Eclipse XBD-C18, 50 mm \times 4.6 mm, particle size: 1.8 μm , both Agilent Technologies, CA, USA). Deuterated internal standards were IPA-d8 for IPA, IME, IPR and IHx, DTA-d6 for DTA and ACE-d4 for ACE. [38] Details on chemical purities and suppliers of the standards are provided in Table B2 (Appendix B). Measurement uncertainties are described in Table B3 (Appendix B).

EDTA was analyzed according to a modified method from Geschke and Zehring [55] as Fe(III)-EDTA after solid phase extraction using a Bakerbond SPE Quaternary Amine (N+) column (Avantor, PA, USA). Samples were biologically stabilized by the addition of 7 mL formaldehyde (37%) to 500 mL of sample, as EDTA samples were prepared and usually measured about two weeks after sampling. The compounds were eluted with formic acid, achieving a concentration factor of 800. Separation was achieved by an UltiMate 3000 HPLC (Thermo

Chapter 2. Materials and Methods

Scientific, MA, USA), equipped with a Superspher 60 RP-select B (Merck, Germany) column. Signals were detected by a Dionex DAD-3000RS (Thermo Scientific, MA, USA) diode array detector at 258 nm. [38]

MPs reported in Chapter 5 were measured by FHNW School of Life Sciences, Institute for Chemistry and Bioanalytics, via by ultra-high performance liquid chromatography (UHPLC) coupled with an MS/MS detector. No sample preparation was necessary. Samples were directly injected (1 μ L) to the UHPLC system (1260 Infinity II Prime, Agilent Technologies, USA). Separation was achieved using a C18 column (Halo AQ-C18, 2.1 \times 50 mm, 2.7 μ m particle size, Advanced Materials Technology, USA) and a gradient method with eluent A (ultrapure water with 2 mM ammonium fluoride) and eluent B (methanol with 2 mM ammonium fluoride). The MPs were detected with a MS/MS system (6465B Ultivo, Agilent Technologies, USA) after electrospray ionization in positive and/or negative mode. [42] Further details are described in Chapter 5.

UV/H₂O₂ before Soil Infiltration Part II

3 Impact on Micropollutants, Dissolved Organic Matter and Biological Activity

This chapter is a copy of the post-print version of the publication [38]:

Wünsch, R., Plattner, J., Cayon, D., Eugster, F., Gebhardt, J., Wülser, R., von Gunten, U., and Wintgens, T.: Surface water treatment by UV/H₂O₂ with subsequent soil aquifer treatment: impact on micropollutants, dissolved organic matter and biological activity. *Environ. Sci.: Wat. Res. & Technol.*, **5** (2019), 10, 1709-1722. DOI: 10.1039/c9ew00547a.

Reproduced from [38] with permission from the Royal Society of Chemistry.

R.W.'s contributions: Design, preparation and execution of experiments; measurement of bulk water quality parameters and size exclusion chromatography of the dissolved organic matter; data analysis and interpretation; writing and critically reviewing the draft manuscript.

Abstract

The impact of an UV/H₂O₂ AOP before soil aquifer treatment (SAT) on the abatement of selected MPs (EDTA, acesulfame, iopamidol, iomeprol, metformin, 1H-benzotriazole, iopromide), dissolved organic matter (DOM) (apparent molecular size distribution, specific UV absorbance at 254 nm – SUVA) and microbial parameters (intact cell count, cell-bound ATP) was investigated. The pilot plant study revealed a shift towards longer retention times of the humic substances peak in LC analysis of DOM, lower SUVA and higher biodegradability of DOM after UV/H₂O₂ treatment. In addition, an overall higher abatement of all investigated MPs by the combined treatment was observed (AOP with subsequent SAT) compared to either process alone. This observation could be explained by an addition of the single treatment effects. The strong primary disinfection effect of the AOP was detectable along the first meter of infiltration, but did not lead to a change in the column performance with respect to DOM abatement. In contrast, the abatement of some MPs was slightly lower in the column receiving the UV/H₂O₂ effluent, especially the Xray contrast media iomeprol and iopromide.

Introduction

UV/H₂O₂ oxidation processes usually do not lead to a full mineralization of MPs. Instead, potentially toxic transformation products can be formed [40]. In addition, the dissolved organic matter (DOM) is transformed to products, which are partially bio-available [56]–[59] and an increased formation potential for disinfection by-products upon post-chlorination was observed [56], [59]. Therefore, AOP treated water should be biologically treated before its distribution [40], [60].

Soil aquifer treatment (SAT) systems are applied in integrated water management systems for the removal of dissolved organic carbon (DOC) and pathogens [29], [61], but MPs have also been demonstrated to be partially degraded during SAT [17], [29], [62]–[64]. Yet during SAT, full mineralization of MPs is often not accomplished and (partly stable) metabolites are formed.

Approaches to combine technical and natural treatment systems are considered highly useful, e.g., by the UNESCO to ensure good water quality and robust treatment systems at reasonable costs [65]. Ozonation and AOPs before natural and/or technical biological treatment systems have been considered in many previous studies [35], [36], [39], [40], [57], [59], [62], [66]–[78], however, currently predominantly in the fields of enhanced wastewater treatment [68], [69], [71], [78] or indirect potable reuse schemes [71], [75], [79]. Nevertheless, implementations of treatment schemes combining technical and natural treatment systems in full-scale are still scarce, especially for drinking water production from conventional water sources, i.e., surface water or groundwater.

In a previous study the combination of H₂O₂, O₃ and UV was investigated to treat river water after coagulation, flocculation, sedimentation, micro-sieving and dual media filtration before dune infiltration for an improved abatement of MPs [39], [57], [80]–[82]. In comparative pilot tests with different treatment combinations (O₃, UV/H₂O₂, UV/O₃ and O₃/H₂O₂), all investigated MPs except methyl tert-butyl ether (MTBE) were abated by >90 % with UV/H₂O₂. However, the O₃/H₂O₂ process showed similar or better efficiency, apart from the X-ray contrast media amidotrizoic acid, and that limited bromate formation was found [39]. Different AOP combinations (O₃/H₂O₂/LP-UV) were compared with respect to MP removal efficiency, investment and operational costs. For the specific treatment case, a combination of 2 mg O₃ L⁻¹, 6 mg H₂O₂ L⁻¹ and a LP-UV fluence of 6500 J m⁻² yielded the best abatement per treatment costs [81]. This is probably due to the “bleaching effect” by O₃/H₂O₂ (decrease in UV absorption at 254 nm), which makes subsequent UV/H₂O₂ treatment more efficient. In laboratory experiments, spiked MPs showed a similar biodegradation in an ozonated water matrix as in a non-oxidized matrix, except for naproxen, ibuprofen and gemfibrozil, which had a lower extent of abatement in the oxidized matrix [57].

In another study, urban surface water was treated either with ozonation before SAT column treatment, or bank filtration and aeration before SAT column treatment [59]. The authors concluded that O₃ - SAT is a feasible option for water treatment due to the overall higher

abatement of MPs and removal of precursors for disinfection by-products, but did not investigate bromate formation [59]. Similar results were also obtained with municipal wastewater effluents [69], [71].

Despite these previous studies, no long-term data are currently available for a UV/H₂O₂ treatment of surface water with subsequent SAT. The aim of this study was to evaluate the performance of a UV/H₂O₂ – SAT column treatment system in comparison to SAT column treatment only. Selected MPs were analyzed to investigate their abatement by the different treatment steps. Measurements by liquid chromatography coupled with an organic carbon detector (LC-OCD) were conducted to study the impact of distinct treatment steps on the molecular size distribution of the dissolved organic matter (DOM). Microbiological parameters, such as intact cell counts and cell-bound ATP, were analyzed to investigate their evolution along the treatment train. With this approach, this study provides an assessment of the performance and impacts of UV/H₂O₂ treatment with subsequent SAT for drinking water production.

Materials and Methods

The pilot plant, the feed water (Rhine river rapid sand filtrate) and the analytical methods for the quantification of MPs and DOC were described in detail before (Chapter 2).

Biodegradable dissolved organic carbon (BDOC) was determined according to the French norm AFNOR XP T90-319 in duplicate batches as the difference in DOC before and after a seven-day incubation at 25 °C using a washed sand inoculum. Before setting up the BDOC batches, all samples were treated with catalase immobilized on a resin (sepabeads EC-EP, particle size: 200 to 500 µm) for quenching residual peroxide [83]. 1 to 2 g catalase resin L⁻¹ were added to the samples, placed on a shaker for 1 h at 100 rpm and separated by sedimentation. Quenching success was confirmed by H₂O₂ quantification.

H₂O₂ was quantified photometrically by titanium oxalate [84], [85]. In brief, 0.5 mL of a titanium(IV) oxysulphate solution in concentrated sulphuric acid (≈1.3 % Ti) was added to 10 mL of a sample. After about five minutes of reaction, the absorbance at 420 nm was measured (see Table A5, Appendix A for details).

Soil respiration was measured in triplicates along the reference method Agroscope B-BA-IS [86], [87]. In brief, produced CO₂ is trapped in 25 mM NaOH within 72 h incubation at 25 °C. Then, CO₃²⁻ is precipitated with 0.5 M BaCl₂ and residual NaOH determined by titration with 25 mM HCl, using a phenolphthalein indicator. Produced CO₂ is calculated from the used volume of HCl. Details on the performance of all applied analytical methods other than for MPs are provided in Table A5 (Appendix A).

Intact cell counts (ICC) were measured along an adopted method from Prest et al. [88]. In brief, 10 µL of a SYBR Green I (SG) stain stock solution and 20 µL of 30 mM propidium iodide in dimethyl sulfoxide (DMSO, ≥ 99.9 %) were mixed, then filled up to 1 mL with DMSO (ICC

stain working solution). Samples were prepared by 1:10 dilution in 0.22 µm-filtered bottled water before staining and then heated to 37 °C for 3 minutes. Subsequently, 10 µL of the ICC stain working solution was added to 990 µL of the sample. Samples were incubated in the dark (37 °C, 10 minutes) before the measurement with an Accuri C6 (BD Biosciences, NJ, USA) flow cytometer.

Total adenosine tri-phosphate (ATP) of the samples was measured in duplicates according to a protocol adopted from Hammes et al. [89]. In brief, 1.6 mL sample was incubated (38 °C, 5 to 10 minutes) in parallel to 50 µL aliquots of prepared ATP reagent (10 mL ATP reagent with 1.6 mL of 1M MgCl₂). Then, 500 µL of the heated sample was transferred to the ATP reagent and incubated for exactly 20 seconds before measuring the luminescence at 490 to 575 nm on a GloMax 20/20 (Promega, WI, USA) luminometer. Quantification was done by a calibration with pure ATP standards. Free ATP was measured by the same method after filtration of the samples with 0.22 µL syringe filters. Bacterial, i.e., cell-bound ATP was calculated by subtracting free ATP from total ATP.

Results and Discussion

Abatement of Selected Target Micropollutants

Micropollutant Abatement by UV/H₂O₂ Treatment. By the treatment with UV/H₂O₂, all MP abatements were found to be statistically significant in paired two-sided t-tests, except for MET (Figure 3.1). According to the method described in Chapter 4, the average UV fluence was about 5'100 J m⁻² and the average ·OH exposure was 1.2×10^{-10} M s, when 1H-benzotriazole (BTZ) and iopamidol (IPA) were used as internal probe compounds with kinetic data presented in Chapter 5. The results agree well with published data on the MPs, e.g. acesulfame (ACE), iomeprol (IME), IPA and iopromide (IPR) are known to be well abated by direct photolysis [90]–[92].

Ethylenediaminetetraacetic acid (EDTA) and metformin (MET) are relatively recalcitrant substances even in reactions with ·OH [92], [93]. However, depending on the complexed metal ion, direct photolysis of EDTA complexes can proceed quickly, e.g., with Fe(III) [94]. Calculations with the average molar concentrations of the sand filtrate's cations in the ChemEQL chemical speciation software [95] confirmed that EDTA should be prevalent as [Fe(III)OH(EDTA)]²⁻ (57 mol-%), [Fe(III)(EDTA)]⁻ (39 mol-%) and [Ca(EDTA)]²⁻ (3 mol-%). Therefore, the relatively strong abatement is attributed to direct photolysis of the predominant Fe(III)EDTA complexes [94].

For MET, with the average process conditions stated above, $k_{\text{OH},\text{MET}} = (0.7 \pm 1.0) \times 10^9 \text{ M}^{-1} \text{ s}^{-1}$ (average value of [96], [97]), $\epsilon_{254,\text{MET}} = 940 \text{ M}^{-1} \text{ cm}^{-1}$ [92], and $\Phi_{254,\text{MET}} = 0.014 \text{ mol einstein}^{-1}$ [92], an abatement of 11 % was expected, which is inside the measured range of 0 to 20 %.

The water temperature of river sand filtrate ranged from 3.2 to 27.0 °C during the experiments. It is known that both ·OH reactions [98]–[100] and photo-physical properties [100], [101] can

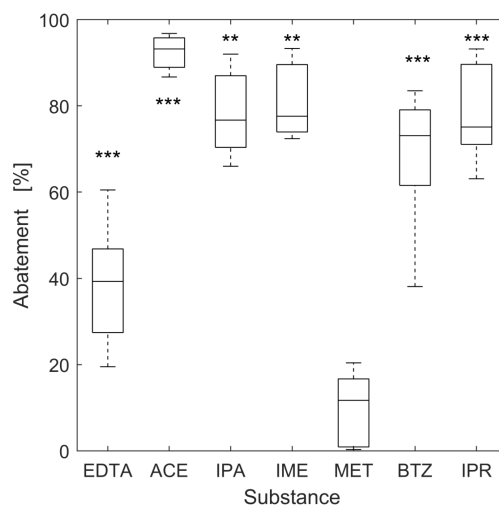


Figure 3.1: Abatement of selected micropollutants by UV/H₂O₂ treatment with 4 mg H₂O₂ L⁻¹ and 6'000 J m⁻². Abatement calculated relative to the LOQ, if effluent concentration was below. $n = 7$ for all MPs. Significance of abatement in paired two-sided t-tests (sand filtrate and after UV/H₂O₂ treatment) marked with “**” and “***” for $p < 0.01$ and < 0.001 , respectively.

be temperature dependent, while the influence of the latter is expected to be minimal [98]. In addition, the efficiency of the UV lamps also changes with temperature [102]. This might translate into a lower applied UV dose in low water temperatures than at elevated temperatures, consequently in lower direct photolysis of target MPs and generation of $\cdot\text{OH}$, and finally in lower observed reaction rates. However, this study was not designed to systematically investigate the temperature effects; hence, the impact of the water temperature on the observed reaction rates are not evaluated.

Abatement by Soil Column Treatment. After the soil column treatment of river sand filtrate, five substances were prevalent in median concentrations above $0.1 \mu\text{g L}^{-1}$. These were EDTA (Swiss drinking water threshold $200 \mu\text{g L}^{-1}$ [103]), ACE, IPA, IME, and BTZ (Figure A1, Appendix A). Abatement during soil treatment alone was statistically significant for ACE, IME, MET and IPR (Figure 3.2). In contrast, the abatements of IPA and BTZ were negligible by the column receiving river sand filtrate. IPA and BTZ are known to be recalcitrant in biological wastewater treatment [104]–[106]. Overall, the soil treatment alone does not appear to be very effective for the removal of the investigated MPs, except for MET.

After pre-treatment with UV/H₂O₂, only MET and IPR abatements were found to be statistically significant in the column fed with the AOP effluent (Figure A1, Appendix A). In contrast to the column receiving river sand filtrate, the abatements of ACE and IME were probably not significant in the column receiving the AOP effluent because of the often very low influent concentrations. Statistically significant differences between the performances of the soil columns were only found for EDTA and MET.

EDTA concentrations in the raw water were often higher in the past years than during the

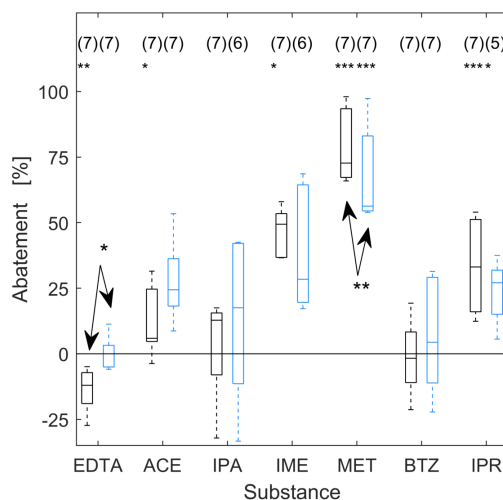


Figure 3.2: Abatement of micropollutants along the soil columns, relative to the influent concentration of the respective column receiving river sand filtrate (black) or UV/H₂O₂ treated river sand filtrate (blue, 4 mg H₂O₂ L⁻¹ and 6'000 J m⁻²). Abatement calculated to the LOQ, if effluent concentration was below. *n* indicated by numbers in brackets. Significance of abatement along columns and significance of difference between groups in paired two-sided *t*-tests marked with “*”, “**” and “***” for *p* < 0.05, < 0.01 and < 0.001, respectively.

test phase and tended to decrease throughout the last years (Figure A2, Appendix A). We hypothesize that the soil material is likely saturated with EDTA, leading to a leaching due to competitive adsorption of DOM. As further discussed below, the organic matter in the AOP effluent tends to be more hydrophilic. Hence, its lower adsorption on the soil column might provide an explanation for the lower leaching of EDTA after the AOP.

MET is known to be well biodegradable [106]–[112]. Differences between the soil column performances for MET are explained by a lower biological activity in the water phase receiving UV/H₂O₂ effluent. The strong primary disinfection effect in combination with the residual H₂O₂ may hamper the biological regrowth in the water phase along the top few centimetres, as further discussed below. However, the lower removal of MET in the soil column after UV/H₂O₂ due to less co-metabolism or less enzymatic diversity as a consequence of increased concentrations of biodegradable DOM cannot be ruled out completely (see below) [113].

Temperatures were controlled neither in the column influents, nor along the columns. The effluent temperatures, measured in grab samples, were 1.0 to 1.5 °C above the sand filtrate's temperature due to temperature equilibration with the environment. They ranged between 7.9 to 27.3 °C and 8.0 to 27.6 °C for the column receiving river sand filtrate and AOP effluent, respectively (*n* = 14 for both). The varying temperature is expected to impact the performance of the soil columns as well, in terms of removal of both bulk organic matter and MPs [63]. However, for the soil columns as well, the study was not designed to assess the impact of temperature on the removal efficiency; hence, it is not further evaluated.

Abatement of the Combined UV/H₂O₂ - Soil Column Treatment. The combined treatment (AOP with subsequent SAT) led to higher abatements for the majority of the investigated substances compared to soil or UV/H₂O₂ treatment alone. By the use of the selected UV/H₂O₂ process, it was possible to abate all investigated MPs to below 0.1 µg/L after subsequent soil treatment, except for EDTA. Such an extent of abatement could not be accomplished by soil treatment alone (Figure A1, Appendix A). It is hence concluded that the combined treatment can be a useful approach to reach a certain treatment goal. Furthermore, the AOP can act as an additional barrier to avoid target MPs to accumulate in the soil. The overall abatement can be explained by the sum of the effects of UV/H₂O₂ and soil treatment and the soil column performance did not significantly change due to AOP pre-treatment (Figure 3.2). Therefore, no enhanced or synergistic abatement of target substances in the soil column was observed after the AOP for the investigated compounds. This confirms previous results for a surface water matrix, which was treated with a specific ozone dose of 1 mg O₃ per mg DOC before a biodegradation batch test with an adapted sand inoculum to remove various spiked MPs [57]. Transformation products (TP) of the MPs are formed upon the UV/H₂O₂ treatment and they are typically more polar than their parent compounds. Hence, they less efficiently adsorb on the soil material. In addition, the biological stability of TPs is mostly unknown and not explored in this study. A theoretical assessment of TPs from ozonation indicated that some TPs might be better removed in subsequent biological treatment steps, whereas others would be recalcitrant, depending on the type of ozonated parent compound [114]. Only very limited information from pilot or full-scale applications is available on this topic. Results from wastewater ozonation indicate that some TPs are relatively stable in subsequent biological treatments [78], [115]. Therefore, it is uncertain whether a higher degree of MPs' mineralization can be expected from a combined AOP - SAT treatment.

Nevertheless, AOP treated water should be biologically re-stabilized before its distribution to remove biologically available organic matter formed during the AOP [116]. Therefore, the proposed configuration appears particularly interesting for surface waters with low background [•]OH scavenging rates, *k*_{OH,S} [35]. In addition, previous studies demonstrated an increase of the disinfection by-product formation potential upon chlorination in AOP treated water, which was lowered again by a biological post-treatment [56], [117], [118], e.g., a SAT.

A previous study was able to link lower concentrations of primary substrate and a higher share of its refractory substances with a higher biological abatement of MPs in laboratory-scale column tests [113]. As during the AOP treatment parts of the DOM became more biodegradable, i.e., less refractory [56]–[59], this might imply a worse performance of the combined treatment (AOP + soil column) than the sum of the single treatment steps in certain waters. However, the small differences of the soil column performances with or without AOP pre-treatment in our study does not confirm these previous observations (Figure 3.2).

Impact on Bulk Organic Parameters

In natural waters, DOM is prevalent at concentrations several orders of magnitude higher than MPs. As the generated $\cdot\text{OH}$ react relatively unselectively, DOM is one of their major sinks: based on the estimated $k_{\text{OH},\text{S}} = 5.3 \times 10^4 \text{ s}^{-1}$ [38], the fraction of $\cdot\text{OH}$ reacting with DOM is about 60 % and with bicarbonate about 40 %. As expected, [56], [58], [119], the applied UV/H₂O₂ process did not lead to mineralization of the DOM (Figure A3, Appendix A), but DOM becomes more biodegradable by the application of an AOP [56]–[59]. Laboratory measurements of the BDOC ($n = 3$, March 2018 – June 2018) confirmed an increase of the biodegradable fraction by the AOP treatment from an average of 0.1 mg/L (sand filtrate) to 0.5 mg/L BDOC (UV/H₂O₂ effluent, $p < 0.05$). However, this did not lead to an increased abatement of the DOC by the soil column treatment after AOP and the difference between the performances of the tested columns was statistically not significant (Figure A3, Appendix A). In fact, both soil columns (with and without UV/H₂O₂ pre-treatment) did not contribute much to the DOC removal (median removal of 0.2 mg L⁻¹ (18 %) and 0.3 mg L⁻¹ (23 %) without and with UV/H₂O₂ pre-treatment, respectively). This is in contrast to full-scale SAT applications, where DOC removals between 33 to 88 % were reported [17]. However, here, the utilized columns had a much lower residence time (24 h) and shorter travelling distance (1 m) compared to the reviewed full-scale applications (residence times: 3 days to 96 months, travelling distance: 6 to 2700 m [17]). In addition, the sand filtrated feed water was biologically already very stable in terms of low BDOC values (see above), which might explain the overall low DOC removal.

Figure 3.3 shows LC-OCD chromatograms of the different treatment steps. The peak around 44 minutes (associated with humic substances, HS [54]) was abated, while a peak at around 48 minutes (associated with building blocks, [54]) was built up. On average, the HS peak maximum was slightly shifted ($p < 0.01$) from $43.9 \pm 0.5 \text{ min}$ (river sand filtrate) to $44.5 \pm 0.5 \text{ min}$ (after UV/H₂O₂ treatment). Our measurements cannot exclude that this results from a matrix effect of the changed background matrix after the AOP. However, along with the slight increase of the peak around 48 minutes, this indicates a slight shift towards smaller molecules, which is in line with the widely assumed de-polymerization mechanism of DOM upon UV/H₂O₂ treatment [120]. Subsequent soil column treatment led to a decrease of all peaks, indicating that all fractions were removed by the SAT treatment, regardless of the UV/H₂O₂ pre-treatment. In fact, the slightly shifted HS peak was the only parameter in LC-OCD measurements that differed between the two soil column influents and effluents (Tables A6 and A7, Appendix A). The UV/H₂O₂ treatment also decreased the specific UV absorbance at 254 nm ($\text{SUVA} = \text{UVA} / \text{DOC}$), an indicator for aromaticity of the DOM and, by that, for hydrophobicity. Median SUVA values significantly ($p < 0.01$, $n = 3$) decreased from $2.0 \text{ L mg}^{-1} \text{ m}^{-1}$ after sand filtration to $1.7 \text{ L mg}^{-1} \text{ m}^{-1}$ after UV/H₂O₂ treatment. This indicates that UV/H₂O₂ reaction products tended to be less aromatic. It is known that $\cdot\text{OH}$ react readily with DOM by $\cdot\text{OH}$ addition to C-C double bonds and aromatic rings, H-abstraction and to a minimal extent by electron transfer [121]. Further, it is known that UV/H₂O₂ treatment can lead to ring opening reactions,

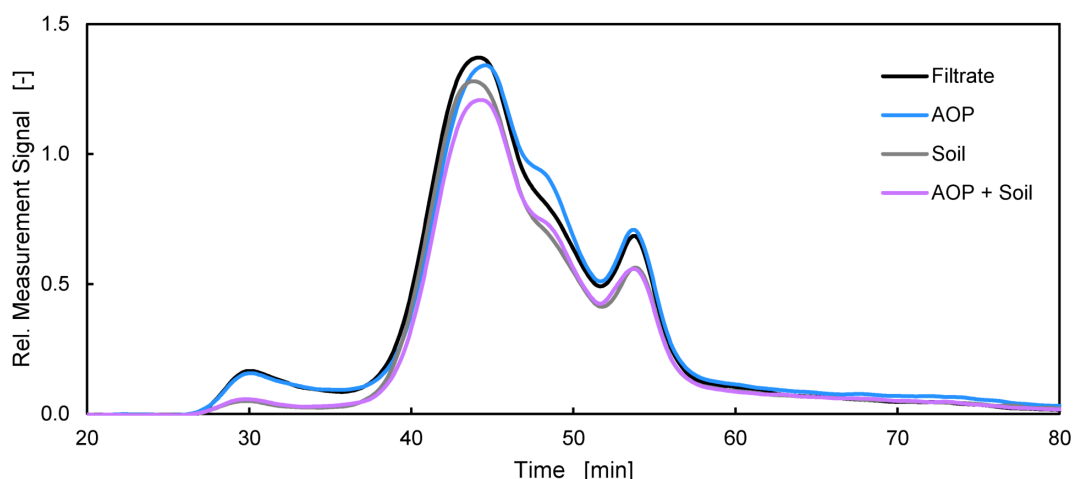


Figure 3.3: LC-OCD chromatograms of the dissolved organic matter after the indicated treatments, averages from $n = 7$ measurement campaigns (November 2017 to August 2018, one measurement after a rain-event excluded). Black: river sand filtrate. Blue: after UV/H₂O₂ with 4 mg H₂O₂ L⁻¹ and 6'000 J m⁻² (AOP). Grey: after soil column. Lavender: after AOP and soil column.

e.g., of phenols [122]. In addition, studies on direct photolysis of natural DOM confirmed that irradiation at 254 nm is able to reduce the SUVA values even at doses comparable to those applied in this study (6'000 J m⁻²) [123], [124]. Therefore, the decrease in SUVA by the AOP treatment is attributed to both direct photolysis of DOM and its reactions with $\cdot\text{OH}$. Soil column treatment resulted in an increase of the SUVA value in both treatment lines (2.4 L mg⁻¹ m⁻¹ and 1.9 L mg⁻¹ m⁻¹ for the columns receiving river sand filtrate without and with UV/H₂O₂ treatment, respectively). It was shown before that an increase of SUVA during soil passage is due to an accumulation of slowly- and non-biodegradable DOM in the water phase, as this fraction of DOM is typically associated with a higher molecular weight and SUVA [59], [125].

Impact on Microbial Activity. UV irradiation during water treatment is known to effectively inactivate microorganisms [126]. The applied AOP utilizes UV doses that are about 15 to 20 times higher than those commonly used for drinking water disinfection [127]. This leads to a strong primary disinfection effect of the water during AOP treatment, which is reflected by the ICC measurements in the water phase at the column influent (Figure 3.4 A). The corresponding measurements of bacterial, i.e., cell-bound ATP in the water phase support this observation (Figure 3.4 B).

ICC measurements along the columns showed that the disinfection effect of the AOP was still detectable throughout the subsequent column receiving the AOP effluent. Of note, ICC measurements are not a proper method to distinguish between living and dead cells after UV/H₂O₂ treatment. As UV irradiation primarily targets the DNA of cells, the cell membrane

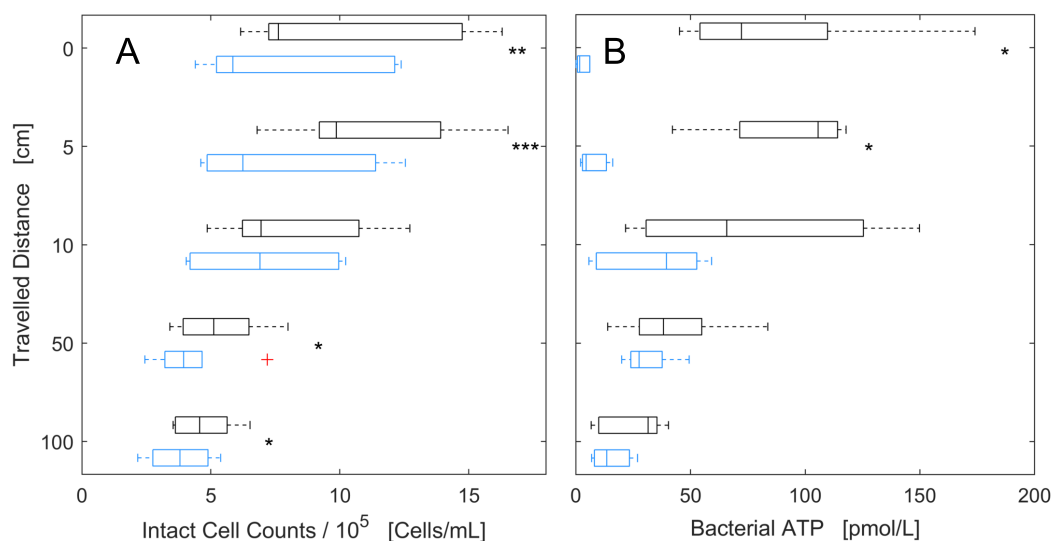


Figure 3.4: A: Intact cell counts in the water phase along the columns receiving river sand filtrate (black) and UV/H₂O₂ effluent (blue). $n = 6$ for all. Outliers marked as a red cross. B: Bacterial ATP in the water phase along the columns receiving river sand filtrate (black) and UV/H₂O₂ effluent (blue). $n = 5$ for all, except $n = 4$ for river sand filtrate after 5 cm travel distance. For A and B, significant differences between groups in paired two-sided t-tests marked with “*”, “**” and “***” for $p < 0.05$, < 0.01 and < 0.001 , respectively.

might still be intact after treatment. Hence, the reduction of ICC by UV/H₂O₂ is not discussed (travel distance = 0 cm). However, lower ICC values in the water phase along the column after the UV/H₂O₂ treatment remained visible and probably contributed to the lower values of bacterial ATP, as discussed below. Overall, the filter effect of the soil columns for the removal of intact cells was relatively low ($0.3 \pm 0.1 \log_{10}$ -steps for both columns). A median reduction of $1.5 \pm 0.6 \log_{10}$ -steps in bacterial ATP was observed by the UV/H₂O₂ treatment (Figure 6). Residual ATP in inactivated (but still intact) cells might explain the low reduction values of bacterial ATP. However, heterotrophic plate counts (HPC) before and after the UV/H₂O₂ treatment during the start-up phase showed a relatively low reduction of only $1.3 \pm 0.4 \log_{10}$ -steps ($n=5$, March 2017 – July 2017). This is less than expected, as the UV dose ($6'000 \text{ J m}^{-2}$) should be sufficient for an inactivation of more than 4 \log_{10} -steps for bacteria, viruses and protozoa [126], [128]. Probably, the relatively low reduction values of the HPCs are explained by non-sanitized equipment. The similar \log_{10} reduction values of bacterial ATP and HPC is probably fortuitous because there is no general correlation between cell-bound ATP and HPC [89]. The soil column receiving river sand filtrate was able to reduce the bacterial ATP concentrations by $0.6 \pm 0.4 \log_{10}$ -steps, which falls in a similar range as the removal of ATP of slow sand filters in previous studies (about $0.2 \log_{10}$ -steps, [129]).

The bacterial activity in the water phase was consistently higher along the column receiving river sand filtrate compared to the column receiving the UV/H₂O₂ effluent (Figure 3.4 B).

In the river sand filtrate column, the bacterial ATP peaked after 5 cm (110 pM). After that, the concentration of the bacterial ATP constantly decreased towards the column effluent. In the column after UV/H₂O₂ treatment, the bacterial ATP increased from around 0 pM at the column influent to a maximum of about 40 pM after a filtration distance of 10 cm. At the same time, the median residual H₂O₂ concentration in the UV/H₂O₂ effluent was 3.6 ± 0.7 mg H₂O₂ L⁻¹ (Table A2, Appendix A). Along the subsequent column receiving the AOP effluent, H₂O₂ was still present in low concentrations after 5 cm (0.2 ± 0.1 mg H₂O₂ L⁻¹, i.e. partially < LOQ, $n = 3$) and was depleted (< LOD) after 10 cm (i.e., contact time around 2 hours), which is in good agreement with published results from laboratory batch tests [130]. The increase in bacterial ATP is explained by detachment of soil bacteria. However, as H₂O₂ inhibits microbial activity even at 1 mg H₂O₂ L⁻¹, [130], H₂O₂ can serve as an explanation for the slow recovery of bacterial ATP along the first centimeters in the column after the AOP treatment.

Respiratory measurements of soil samples from the columns' tops confirmed that both column materials were biologically active, i.e., the residual H₂O₂ did not inhibit biological activity at the influent zone of the column. The soil respiration of the column material receiving AOP pre-treated water was much higher ($30 \mu\text{g CO}_2 (\text{g}_{\text{dry mass soil}})^{-1} (24 \text{ h})^{-1}$) than the material in the column receiving river sand filtrate ($17 \mu\text{g CO}_2 (\text{g}_{\text{dry mass soil}})^{-1} (24 \text{ h})^{-1}$). This finding is not necessarily in contradiction to the ATP data, as the ATP values were measured for the water phase only. The observation might be related to the higher availability of BDOC after the AOP treatment. In addition, the decay of H₂O₂ gives rise to additional O₂, stimulating additional bacterial activity. However, as the water along both SAT columns was fully oxidic at all times and almost oxygen saturated in the sand filtrate, the latter hypothesis is considered more relevant for full-scale applications with different redox conditions along the infiltration path.

The specific cell activity (i.e., bacterial ATP / ICC) in the water phase along the column receiving the UV/H₂O₂ effluent never exceeded the activity of the river sand filtrate column at the sampling points in a statistically significant way (Figure A4, Appendix A). As more BDOC was produced by the UV/H₂O₂ treatment, it was expected that the specific cell activity might be higher due to the additional substrate available. However, this could not be demonstrated in this study. It is known that the microbial density is orders of magnitudes higher on the soil compared to the water phase. For the soil, a higher activity could be demonstrated in the top layer after the AOP treatment (see above).

Conclusions

- A combination of UV/H₂O₂ with a subsequent soil aquifer treatment (SAT) is a feasible process combination for micropollutant abatement in drinking water production. Residual hydrogen peroxide hampers microbial regrowth in the water phase unless it is depleted to below $0.3 \text{ mg H}_2\text{O}_2 \text{ L}^{-1}$ (5 – 10 cm infiltration depth in this study). Despite this, the soil was still biologically active.

- Micropollutant abatement by the UV/H₂O₂ process with subsequent SAT is generally higher than by UV/H₂O₂ or SAT only. However, the abatement could be well explained by an additive effect of the unit processes. The investigated substances (EDTA, acesulfame, iopamidol, iomeprol, metformin, 1H-benzotriazole, iopromide) were primarily abated by the UV/H₂O₂ process and metformin mainly during SAT.
- A slight shift of the humic substances peak maximum towards longer retention times, along with a small build-up of the building blocks fraction, indicates a shift towards smaller substances as a consequence of UV/H₂O₂ treatment. This is accompanied with an increase of the biodegradable fraction of the dissolved organic matter (DOM). In addition, a loss in specific UV absorbance of the DOM (SUVA) by the oxidation process was observed. However, the investigated soil columns did not contribute much to the removal of DOC, probably due to the relatively short residence time compared to full-scale SAT systems.
- The UV/H₂O₂ process had a strong primary disinfection effect on the suspended microorganisms, mainly due to the high UV doses applied. This effect was conserved in the water phase, likely due to the inhibitory effect of the residual H₂O₂ within the first 10 cm. Along the full length of the investigated columns (1 m), both intact cell counts and cell-bound ATP measurements were lower in the column with compared to without UV/H₂O₂ treatment.

4 Micropollutants as Internal Probe Compounds to Assess UV/H₂O₂ Treatment

This chapter is a copy of the post-print version of the publication [41]:

Wünsch, R., Mayer, C., Plattner, J., Eugster, F., Wülser, R., Gebhardt, J., Hübner, U., Canonica, S., Wintgens, T., and von Gunten, U.: Micropollutants as internal probe compounds to assess UV fluence and hydroxyl radical exposure in UV/H₂O₂ treatment. *Wat. Res.* (2021), 116940. DOI: 10.1016/j.watres.2021.116940. [41]

The article was published by Elsevier under a creative commons license (CC BY 4.0).

R.W.'s contributions: Design of the model; data sourcing and analysis; interpretation and discussion of the results; writing and critically reviewing the draft manuscript.

Abstract

A model is presented that calculates the applied UV fluence (H_{calc}) and the $\bullet\text{OH}$ exposure ($CT_{\bullet\text{OH,calc}}$) from the abatement of two selected MPs, which act as internal probe compounds. Quantification of the H_{calc} and $CT_{\bullet\text{OH,calc}}$ was generally accurate when a UV susceptible and a UV resistant probe compound were selected, and both were abated at least by 50 %. Based on these key parameters a model was developed to predict the abatement of other MPs. The prediction of abatement was verified in various waters (sand filtrates of rivers Rhine and Wiese, and a tertiary wastewater effluent) and at different scales (laboratory experiments, pilot plant). The accuracy to predict the abatement of other MPs was typically within ± 20 % of the respective measured abatement. The model was further assessed for its ability to estimate unknown rate constants for direct photolysis ($k_{\text{UV,MP}}$) and reactions with $\bullet\text{OH}$ ($k_{\bullet\text{OH,MP}}$). In most cases, the estimated rate constants agreed well with published values, considering the uncertainty of kinetic data determined in laboratory experiments. A sensitivity analysis revealed that in typical water treatment applications, the precision of kinetic parameters ($k_{\text{UV,MP}}$ for UV susceptible and $k_{\bullet\text{OH,MP}}$ for UV resistant probe compound) have the strongest impact on the model's accuracy.

Introduction

To mitigate the impact of organic micropollutants (MPs), advanced oxidation processes (AOPs) are a treatment option in utilities for drinking water production ([40], [81], [100], [131]) or (in)direct potable water reuse ([100], [132], [133]). AOPs are based on in situ generation of highly reactive radicals (e.g., $\bullet\text{OH}$, $\text{SO}_4\bullet^-$), that react almost diffusion-controlled with many constituents in water ([40], [134]). Despite the many options for radical generation, AOPs deployed in full-scale drinking water treatment are currently either ozone-based (O_3 , $\text{O}_3/\text{H}_2\text{O}_2$) or ultraviolet (UV) radiation based ($\text{UV}/\text{H}_2\text{O}_2$, UV/Cl_2), [135]. Ozone-based processes can form the possibly carcinogenic bromate (BrO_3^-), if bromide (Br^-) is present in the raw water, [51]. Strategies exist for the mitigation of bromate formation. However, for waters containing high concentrations of bromide ($> 100 \mu\text{g L}^{-1}$, [51]), the $\text{UV}/\text{H}_2\text{O}_2$ process is often preferred because there is no bromate formation, [136]. In addition, other considerations can lead to the selection of a UV-based AOP, if e.g., the targeted MPs are more efficiently abated by direct photolysis, as in the case of N-nitrosodimethylamine (NDMA) or most X-ray contrast media, [81].

The UV/H₂O₂ process. The abatement of MPs in the $\text{UV}/\text{H}_2\text{O}_2$ process is based on a combination of the direct photolysis of the MP and reactions with $\bullet\text{OH}$, that are formed upon photolysis of H_2O_2 , [100], [137]. The abatement can be described as follows:

$$\ln\left(\frac{c_{0,\text{MP}}}{c_{\text{MP}}}\right) = H \times k_{\text{UV,MP}} + CT_{\bullet\text{OH}} \times k_{\bullet\text{OH,MP}} \quad (4.1)$$

$c_{0,\text{MP}}$ and c_{MP} ($\text{mol L}^{-1} = \text{M}$) describe the concentrations of a MP before and after the $\text{UV}/\text{H}_2\text{O}_2$ treatment, respectively. H is the UV fluence (J m^{-2}), $CT_{\bullet\text{OH}}$ is the $\bullet\text{OH}$ exposure (M s). $k_{\bullet\text{OH,MP}}$ ($\text{M}^{-1} \text{s}^{-1}$) is the second-order rate constant for the reaction of a MP with $\bullet\text{OH}$. $k_{\text{UV,MP}}$ is the fluence-based rate constant for direct photolysis of the MP ($\text{m}^2 \text{J}^{-1}$), which can be calculated from Eq. 4.2, [138]:

$$k_{\text{UV}} = \frac{\ln(10)}{10} \times \frac{\lambda}{h c N_A} \times \varepsilon \times \Phi \quad (4.2)$$

λ denotes the wavelength, i.e., 254 nm; h : Planck's constant ($6.62 \times 10^{-34} \text{ J s}$), c : speed of light ($3.0 \times 10^8 \text{ m s}^{-1}$), N_A : Avogadro's number ($6.02 \times 10^{23} \text{ einstein}^{-1}$). ε and Φ are the decadic molar absorption coefficient ($\text{M}^{-1} \text{cm}^{-1}$) and quantum yield at 254 nm (mol einstein^{-1}), respectively. For some selected MPs, $k_{\bullet\text{OH,MP}}$, ε and Φ are summarized in Table 4.1. For reported pH-dependent values for ε , the values at the actual pH can be calculated by Eq. 4.3, [90]:

$$\varepsilon = \varepsilon_1 + (\varepsilon_2 - \varepsilon_1) \times \alpha_2 \quad (4.3)$$

ε_1 and ε_2 are the decadic molar absorption coefficients of the protonated and deprotonated form of a MP, respectively. The fraction of the deprotonated form of the MP at a given pH, α_2 , is calculated by Eq. 4.4 and employing the pK_a of the MP's protonated form.

$$\alpha_2 = \frac{1}{1 + 10^{pK_a - pH}} \quad (4.4)$$

The pH-dependent quantum yield is calculated analogously, [90].

Second-order rate constants for the reactions of a large number of MPs with $\bullet OH$ are compiled in a database, [139], or can be deduced theoretically, [140]. Possible temperature effects on the rate constants are discussed below (Eq. 4.12). Molar absorption coefficients and photolysis quantum yields are also reported in literature, [90], [96], [141], [142], however, for these parameters no simple estimations are possible.

Approaches to assess UV fluence and $\bullet OH$ exposure. Commonly, a UV fluence rate E ($W m^{-2}$) is measured either by chemical actinometry, e.g., potassium iodide-iodate, [138], [143], or by previously calibrated radiometers. Chemical actinometers are based on a known photochemical reaction with a known quantum yield.

The hydroxyl radical exposure (CT_{OH} , M s) is commonly determined indirectly by measurement of the abatement of an $\bullet OH$ probe compound such as para-chlorobenzoic acid (*p*CBA), [137], [144], [145], or a dye such as methylene blue, [146]–[148], rhodamine B, [149], or fluorescein, [146]. Alternatively, it can be estimated as $CT_{OH} = c_{OH,SS} \times t$, where t (s) is the reaction time and $c_{OH,SS}$ (M) is the pseudo steady-state concentration of $\bullet OH$ obtained from given initial water quality parameters, the average H_2O_2 concentration ($\overline{c_{H_2O_2}}$, M) and the UV fluence rate, [138], [142], [150]:

$$c_{OH,SS} = E \times \frac{\ln(10)}{10} \times \frac{\lambda}{h c N_A} \times \frac{\varepsilon_{H_2O_2} \times \Phi_{H_2O_2} \times \overline{c_{H_2O_2}}}{S + k_{OH,H_2O_2} \times \overline{c_{H_2O_2}}} \quad (4.5)$$

$\varepsilon_{H_2O_2} \approx 18.6$ to $19.2 M^{-1} cm^{-1}$ at 254 nm, [100], [135], $\Phi_{H_2O_2} = 1.0$, [100], and $k_{OH,H_2O_2} = 2.7 \times 10^7 M^{-1} s^{-1}$, [151]. The *pseudo*-first-order $\bullet OH$ scavenging rate constant of the background water matrix, S (s^{-1}), can be measured directly, [148], or calculated from the individual contributions of the main $\bullet OH$ scavengers, i , which are essentially dissolved organic carbon, carbonate and bicarbonate for surface waters:

$$S = \sum_i c_i \times k_{OH,i} \quad (4.6)$$

Approaches to predict micropollutant abatement. Current *a priori* approaches to predict the abatement of MPs in UV/ H_2O_2 systems are often based on the above described theories,

which may be coupled, for sophisticated assessments, with computational fluid dynamics methods, [92], [98], [152]–[154]. Alternatively, empirical correlations with online measurements of optical water matrix parameters, such as UV absorbance or fluorescence, were suggested for indirect monitoring of the MP abatement by the UV/H₂O₂ process, [155], [156]. For ozonation and ozone-based AOPs, an a posteriori approach was suggested, in which the measured abatement of MPs with known second-order reaction rate constants for the reactions with O₃ and •OH was used to predict the abatement of other MPs, [157]–[161]. The abatement of MPs by ozonation and O₃/H₂O₂ treatment in ultrapure and drinking water was successfully modelled using the aforementioned approach, and oxidant exposures were determined from the abatement of an ozone-resistant and an ozone-reactive compound, [157], [158]. Also for wastewater ozonation, the •OH exposure could be well determined by back-calculation from ozone-resistant compounds, such as iopromide, clofibric acid, ibuprofen, ketoprofen or primidone, [159]–[161]. In contrast, the use of prevalent MPs as internal probe compounds to determine the ozone exposure in wastewater and subsequently model the abatement of other MPs was not successful, [159], [161], [162]. A mass transfer limitation related to sample mixing at low ozone dosages is assumed, which was probably the cause for similar removal of MPs despite several orders of magnitude difference in some second-order rate constants, [159].

Lester *et al.* proposed sucralose as an internal probe compound to monitor full-scale UV-AOP treatments, [163]. They suggested to predict the abatement of other MPs based on empirical, water-specific correlations factors. Here, a model is presented that can be applied without prior water-specific calibration, as it is based on widely accepted, fundamental (photo)chemical reaction theories. While this approach does not provide a real-time control option, it is useful, (i), to predict the abatement of MPs with known second-order rate constants for their reactions with •OH ($k_{\text{OH,MP}}$), molar absorption coefficients at 254 nm (ϵ) and quantum yields at 254 nm (Φ) that were not monitored. By this, (ii), the model allows to extrapolate from indicator compounds during performance validation tests to any other compound that might appear in the source water. Further, (iii), the model allows to check the plausibility of experimental results (data consistency).

In this chapter, a model based on the measured abatement of two MPs is developed for low pressure UV/H₂O₂ processes. Two main potential applications of the model are presented, (i), the assessment of UV fluence and •OH exposure and, (ii), the prediction of abatement of MPs with known (photo)chemical reactivity. The applications are verified with data from own experiments and literature representing different treatment systems (laboratory and pilot-scale) and water matrices (surface waters and a wastewater effluent). Finally, the sensitivity of the model is assessed to elucidate the most relevant experimental parameters for accurate predictions.

Materials and Methods

Water samples. Water samples were taken from two river water rapid sand filtrates, i.e., Rhine and Wiese in northwestern Switzerland. The production of the river Rhine rapid sand filtrates is described in Chapter 2. The river Wiese rapid sand filtrate production is described elsewhere, [41]. Sand filtrate water grab samples of the rivers Rhine and Wiese were collected for laboratory experiments in annealed glassware at different time points (May 2016 – January 2019). Samples were stored at 4 °C until use and the UV/H₂O₂ experiments were conducted within seven days after sampling. A summary of characteristic water quality parameters and MP concentrations of the sand filtrates of rivers Rhine and Wiese is provided in Table 4.1. The MPs were selected because of their presence in the raw waters and relevance for drinking water treatment, as well as reported specific (photo)chemical and physical data, i.e., $k_{\text{OH},\text{MP}}$, ε and Φ (Table 4.1).

Experimental setup.

Laboratory Experiments. Laboratory experiments were conducted on a collimated beam device (CBD), [138], at room temperature to verify the model under well-defined conditions. Experiments were conducted with varying H₂O₂ concentrations (0 to 8 mg L⁻¹) and UV fluences (1'900 to 8'000 J m⁻², low pressure mercury UV lamps irradiating almost monochromatically at 254 nm, supplied by Xylem Services) to assess the model under process conditions relevant for realistic water treatment applications. A description of the CBD experimental procedure is provided in Appendix B, lists with details on the experimental set points in the laboratory experiments are described elsewhere [41]. In some laboratory experiments with river Rhine sand filtrate, selected MPs were spiked for a better quantification of the abatement at elevated H₂O₂ concentrations and UV fluences. Therefore, a mix stock solution was prepared in ultrapure water with concentrations of 1 mg L⁻¹ acesulfame (ACE), diatrizoic acid (DTA), iohexol (IHX), iopamidol (IPA), iopromide (IPR) and metformin (MET), and 0.5 mg L⁻¹ 5-methyl-1H-benzotriazole (5BTZ) as described in Appendix B. Prior to the experiment, 25 µL of this stock solution were spiked into a 250 mL water sample, thus supplementing the final concentration by 100 ng L⁻¹ for these MPs (exception: 50 ng L⁻¹ for 5BTZ). All chemicals were of the highest available quality and used without further purification.

Pilot Plant Experiments. Pilot plant experiments were conducted to validate the model under operational conditions and at different times throughout the year. A description of the pilot plant is provided in Chapter 2. Lists with details on the respective operational set points are described elsewhere [41]. The pilot plant was mostly operated at 4 mg H₂O₂ L⁻¹ and a UV fluence of 6'000 J m⁻² (600 mJ cm⁻²) (low pressure mercury UV lamp irradiating almost monochromatically at 254 nm, supplied by Xylem Services). This set point was selected because the results of CBD experiments indicated that, under these conditions, X-ray contrast

Table 4.1: Water quality parameters of rapid sand filtrates of rivers Rhine and Wiese. Data base: 14 (Rhine sand filtrate) and 13 (Wiese sand filtrate) grab samples, June 2017 to April 2019, unless stated otherwise. All values are presented as average \pm standard deviation.

Parameter	Unit	Rhine	Wiese	Mol. weight (g mol ⁻¹)	pK _a	k _{OH,MP} /10 ⁹ M ⁻¹ s ⁻¹	ϵ or ϵ_1 M ⁻¹ cm ⁻¹	Φ or Φ_1 mol Einst. ⁻¹	ϵ_2 M ⁻¹ cm ⁻¹	Φ_2 mol Einst. ⁻¹
DOC	mg L ⁻¹	1.4 \pm 0.3, ^a	1.3 \pm 0.3, ^b	12		2.3 \times 10 ⁴ , ^c				
TIC	mg L ⁻¹	28.5 \pm 5.1	12.9 \pm 4.1	12	6.35	0.0085, ^d				
					10.33	0.39, ^d				
pH	-	8.1 \pm 0.1	7.8 \pm 0.2							
UVA ₂₅₄	m ⁻¹	3.5 \pm 0.8	4.4 \pm 1.1							
Temp.	°C	14.9 \pm 7.2	14.1 \pm 7.2							
Nitrate	mg L ⁻¹	5.5 \pm 1.5, ^e	4.7 \pm 0.8, ^f							
5BTZ	ng L ⁻¹	26 \pm 9	22 \pm 20	133.2	8.5 \pm 0.3, ^g	8.71 \pm 0.06, ^g	5230 \pm 77, ^g	0.016 \pm 0.001, ^g	3440 \pm 153, ^g	0.0049 \pm 0.0008, ^g
ACE	ng L ⁻¹	244 \pm 87	79 \pm 30	163.2	\approx 2, ^h	3.8 \pm 0.3, ⁱ	3600, ^j	0.187, ^j		
BTZ	ng L ⁻¹	176 \pm 41	230 \pm 142	119.1	8.3 \pm 0.2, ^g	8.3 \pm 0.2, ^g	6140 \pm 97, ^g	0.016 \pm 0.001, ^g	4500 \pm 301, ^g	0.0026 \pm 0.0003, ^g
CBZ	ng L ⁻¹	4 \pm 10	17 \pm 17	236.3	16.0, ^k	8.0 \pm 1.9, ^l	6070, ^m	0.00060 \pm 0.00009, ^m		
DTA	ng L ⁻¹	26 \pm 7	37 \pm 26	613.9	2.2, ^k	0.59 \pm 0.06, ⁿ	19000 \pm 818, ^o	0.039 \pm 0.002, ^o		
IHX	ng L ⁻¹	31 \pm 21	n.d., ^p	821.1	11.7, ^k	3.5 \pm 0.4, ^q	27620, ^m	0.04030 \pm 0.00009, ^m		
IPA	ng L ⁻¹	193 \pm 129	n.d., ^p	777.1	10.7, ^r	3.4 \pm 0.3, ^s	22700, ^t	0.03318, ^t		
IPR	ng L ⁻¹	112 \pm 50	n.d., ^p	797.1	11.1, ^k	3.32 \pm 0.03, ^u	21470 \pm 608, ^v	0.034 \pm 0.008, ^v		
MET	ng L ⁻¹	204 \pm 68	98 \pm 66	129.2	12.3, ^k	1.4 \pm 0.1, ^o	940 \pm 5, ^o	0.014 \pm 0.003, ^o		
MPL	ng L ⁻¹	5 \pm 3	19 \pm 10	267.4	9.7, ^k	7.6 \pm 0.7, ^o	519 \pm 318, ^w	0.045 \pm 0.034, ^o		
SMX	ng L ⁻¹	17 \pm 5	13 \pm 8	253.3	5.7, ^x	5.9 \pm 1.6, ^w	11890 \pm 117, ^y	0.212 \pm 0.009, ^y	16760 \pm 194, ^y	0.046 \pm 0.011, ^y
STL	ng L ⁻¹	3 \pm 6	11 \pm 7	272.4	8.2, 9.8, ^r	7.9 \pm 1.6, ^z	370 \pm 20, ^A	0.39 \pm 0.02, ^A		

^a $n = 24$ (February 2017 – April 2019). ^b $n = 18$ (February 2017 – April 2019). ^c Average of five surface water sources, [164], unit: L mgC⁻¹ s⁻¹.
^d [151]. ^e Data from periodic river Rhine raw water monitoring; $n = 28$ (March 2017 – April 2019). ^f Data from an upstream river monitoring station, $n = 28$ (March 2017 – April 2019), (Landesanstalt für Umwelt Baden-Württemberg, 2021) [165]. ^g [141]. ^h [166]. ⁱ [167].
^j [168]. ^k Predicted by MarvinSketch (V.19.18), ChemAxon. ^l [142]. ^m [169]. ⁿ Average of [96], [170]. ^o Average of [92], [142]. ^p Not detected.
^q Average of [169], [171]. ^r The Merck Index Online, accessed: February 2020. ^s [171]. ^t [91]. ^u Average of [158], [171]. ^v Average of [90], [168].
^w Average of [96], [142]. ^x [158]. ^y [90]. ^z [96]. ^A [92].

media occurring in the river Rhine sand filtrate were abated by $\geq 80\%$, [53]. Furthermore, such a treatment constitutes some additional “broad band barrier” for MPs due to the $\bullet\text{OH}$ generation, [53]. In an additional set of experiments, the operational set points were varied (0 to $10'000\text{ J m}^{-2}$, 0 to $10\text{ mg H}_2\text{O}_2\text{ L}^{-1}$) to verify the model at other set points relevant for water treatment. Water temperatures during the pilot trials varied in the range of 5.0 to 24.5 °C.

Analytical Methods. Residual H_2O_2 in all samples was quenched by addition of 2 mol sodium thiosulfate (from a stock solution) per mol H_2O_2 . The sodium thiosulfate stock solution was prepared by dissolving 1.7 g $\text{Na}_2\text{S}_2\text{O}_3$ in 50 mL ultrapure water. Even though H_2O_2 quenching was not complete under these conditions, [38], possible Fenton-like reactions of residual H_2O_2 with Fe(III) and Cu(II) present in the surface water filtrates were shown to be irrelevant in a “dark experiment” (no UV fluence) with $4\text{ mg H}_2\text{O}_2\text{ L}^{-1}$ at pilot scale with river Rhine and Wiese sand filtrates (Figure B2, Appendix B).

Analytical methods for the measurements of the MPs are described in Chapter 2. In brief, 5-methyl-1H-benzotriazole (5BTZ), 1H-benzotriazole (BTZ), carbamazepine (CBZ), metformin (MET), metoprolol (MPL), sulfamethoxazole (SMX) and sotalol (STL) were measured on an HPLC-MS/MS system after direct injection. Acesulfame (ACE), diatrizoic acid (DTA), iohexol (IHX), iopamidol (IPA) and iopromide (IPR) were measured on the same system after 10-fold pre-concentration but employing a different set of separation columns.

Model for Prediction of Micropollutant Abatement. This paragraph describes the proposed model. The underlying assumptions are:

- The abatement of MPs during the UV/ H_2O_2 process can be described by direct photolysis at 254 nm and reactions with $\bullet\text{OH}$. Reactions with other reactive species, e.g., carbonate radicals ($\text{CO}_3^{\bullet-}$), are neglected. Note that these reactions can become more important than reactions with $\bullet\text{OH}$, e.g., if the ratio of the steady-state concentrations of $\text{CO}_3^{\bullet-}$ to $\bullet\text{OH}$ exceeds two to three orders of magnitude, and second-order rate constants for reactions of MPs with carbonate radicals are $> 1.0 \times 10^7\text{ M}^{-1}\text{ s}^{-1}$, [92], [172].
- All MPs face the same reaction conditions (e.g., no competition for $\bullet\text{OH}$ or UV photons between the MPs). This is justified by the high pseudo-first-order $\bullet\text{OH}$ scavenging rate constant for the water matrix ($5.7 \times 10^4\text{ s}^{-1}$ and $4.0 \times 10^4\text{ s}^{-1}$ for average sand filtrates of river Rhine and river Wiese, respectively) as compared to the MPs (25 s^{-1} and 23 s^{-1} based on average measured concentrations of all MPs in sand filtrates of river Rhine and river Wiese, respectively), calculated with Eq. 4.6, respectively.
- MPs are assumed not to be re-formed during or after the UV/ H_2O_2 treatment in the water matrix.
- The analyzed probe compounds represent average concentrations of the whole UV/ H_2O_2 feed and effluent.

Chapter 4. Micropollutants as Internal Probe Compounds to Assess UV/H₂O₂ Treatment

- Fundamentally, it is assumed that rate constants reported from experiments elsewhere are transferable to real water systems, i.e., no water matrix interactions alter the observed rate constants.
- The UV fluence is assumed to have a narrow distribution, i.e., H in Eqs. 4.1 and 4.7 is assumed to be relatively constant throughout the entire flow traveling across the UV reactor, which should be valid for laboratory experiments conducted on collimated beam devices and for typical water treatment systems with well-designed UV reactors, i.e., close to an ideal continuously stirred tank reactor or ideal plug flow reactor.

Under these conditions, the abatement of MPs can be described by Eq. 4.1. To predict the abatement of MPs in one experimental data set, two MPs (denoted by the subscripts '1' and '2' in the following equations) are selected as internal probe compounds. Their abatements are inserted into Eq. 4.1 to obtain the calculated UV fluence, H_{calc} , and the calculated $\bullet\text{OH}$ exposure, $CT_{\bullet\text{OH,calc}}$. Solving the corresponding system of two linear equations for H_{calc} and $CT_{\bullet\text{OH,calc}}$, yields:

$$H_{\text{calc}} = \frac{\ln\left(\frac{c_{0,1}}{c_1}\right) - \ln\left(\frac{c_{0,2}}{c_2}\right) \frac{k_{\bullet\text{OH},1}}{k_{\bullet\text{OH},2}}}{k_{\text{UV},1} - k_{\text{UV},2} \frac{k_{\bullet\text{OH},1}}{k_{\bullet\text{OH},2}}} \quad (4.7)$$

$$CT_{\bullet\text{OH,calc}} = \frac{\ln\left(\frac{c_{0,2}}{c_2}\right) - \ln\left(\frac{c_{0,1}}{c_1}\right) \frac{k_{\text{UV},2}}{k_{\text{UV},1}}}{k_{\bullet\text{OH},2} - k_{\bullet\text{OH},1} \frac{k_{\text{UV},2}}{k_{\text{UV},1}}} \quad (4.8)$$

where $c_{0,1}$ and $c_{0,2}$ are the initial and c_1 and c_2 the transient concentrations of MP1 and MP2, respectively, $k_{\bullet\text{OH},1}$ and $k_{\bullet\text{OH},2}$ the respective second-order rate constants for the reactions of the MPs with $\bullet\text{OH}$; and $k_{\text{UV},1}$ and $k_{\text{UV},2}$ the respective rate constants for direct photolysis of the MPs. The internal probe compounds should be selected based on different predominant abatement mechanisms. Mathematically, this corresponds to the condition that $k_{\bullet\text{OH},1}/k_{\text{UV},1}$ has to be clearly different from $k_{\bullet\text{OH},2}/k_{\text{UV},2}$, which prevents the denominators of Eqs. 4.7 and 4.8 to be close to zero. This increases the robustness of the method against analytical uncertainty. Ideally, MP '1' – the UV susceptible probe compound – is abated predominantly by UV irradiation, whereas MP '2' – the UV resistant $CT_{\bullet\text{OH}}$ probe compound – predominantly by reactions with $\bullet\text{OH}$. Knowing H_{calc} and $CT_{\bullet\text{OH,calc}}$, the expected abatement of all other MPs with known $k_{\bullet\text{OH,MP}}$, ϵ_{MP} and Φ_{MP} can be calculated by Eq. 4.1.

To estimate the confidence intervals of H_{calc} , $CT_{\bullet\text{OH,calc}}$ and the predicted abatements, the uncertainties of all relevant influencing factors (i.e., pH, photochemical parameters, second-order rate constants for reactions with $\bullet\text{OH}$, analytical measurement uncertainties) are accounted for in a Monte Carlo simulation by repeated calculations of H_{calc} , $CT_{\bullet\text{OH,calc}}$ and predicted abatements with each experimental data set 10⁴ times. According to Morgan *et al.*, (1990) [173], this is sufficient to have 95% confidence that the actual 50th percentile is within the estimated 49th and 51st percentiles for any distribution. In each repeated calculation,

the input parameters were assigned a random value around the measured value within the respective uncertainty, as described in Table B4 (Appendix B). The confidence intervals were evaluated after the repeated calculations by evaluating the 2.5 and 97.5 percentile values of H_{calc} , $CT_{\text{OH,calc}}$ and the predicted abatements, respectively.

H_{calc} and $CT_{\text{OH,calc}}$ could also be obtained by linear regression analysis using Eq. 4.1 and the abatement data of more than two probe compounds. This approach can potentially make the determination of these key parameters more robust against inaccuracies of kinetic parameters and analytical errors of single substances but was not tested in the original study.

Sensitivity Analysis. The sensitivities of the model outputs H_{calc} and $CT_{\text{OH,calc}}$ were assessed by the Gaussian error propagation. For a model output y as a function g of $i = 1, 2, 3, \dots, N$ non-correlated input variables $x_1, x_2, x_3, \dots, x_N$

$$y = g(x_1, x_2, x_3, \dots, x_N) \quad (4.9)$$

the combined variance $u_c^2(y)$ can be approximated by Eq. 4.10, neglecting higher-order terms in a Taylor series expansion [174]:

$$u_c^2(y) \approx \sum_{i=1}^N \left(\frac{\partial g}{\partial x_i} \right)^2 \times u^2(x_i) \quad (4.10)$$

$u^2(x_i)$ is the estimated standard uncertainty of an input variable x_i .

The partial derivatives $\frac{\partial g}{\partial x_i}$ for H_{calc} and $CT_{\text{OH,calc}}$ were computed by an online software (Wolfram Alpha LLC, 2020) and are described elsewhere [41]. Standard uncertainties of second-order rate constants are assumed to be uniformly distributed, wherefore $u^2(x_i)$ becomes [174]:

$$u^2(x_i) = \frac{(a_+ - a_-)^2}{12} \quad (4.11)$$

where, a_+ and a_- denote the upper and lower limits of the interval of uncertainty. For the sensitivity analysis, $u^2(x_i)$ of all kinetic constants was calculated with Eq. 4.11 with the assumption that kinetic constants are certain within a factor 2, i.e., a_+ as 2 times the kinetic constant and a_- as 0.5 times the kinetic constant, respectively.

A comparison of the estimated combined standard uncertainty $u_c(y) = \sqrt{u_c^2(y)}$ from the Gaussian error propagation with the results obtained from the Monte Carlo simulation validated that higher-order terms of the Taylor series expansion were of minor importance.

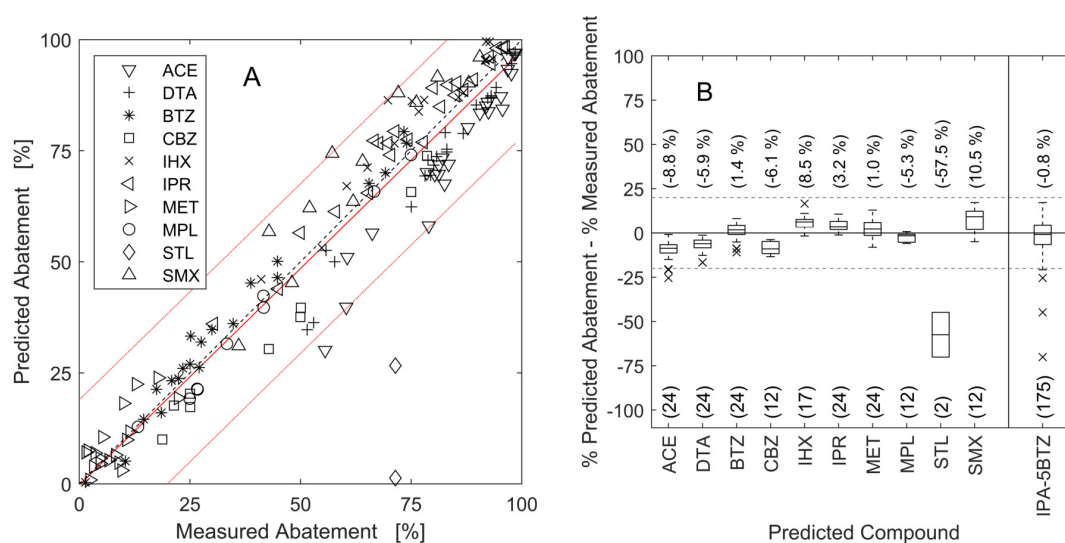


Figure 4.1: Predicted abatement of selected micropollutants by the probe compound combination iopamidol (IPA) and 5-methyl-1H-benzotriazole (5BTZ) in CBD laboratory experiments with river Rhine sand filtrate. A: Predicted relative abatement in comparison to the measured relative abatement. B: Box plots for the micropollutant-specific evaluation of the differences between the predicted and measured abatement ($\Delta\%$). The separate IPA-5BTZ box plot on the far right summarizes all box plots of the single micropollutants of the IPA-5BTZ model. Lower numbers in brackets: number of experiments with predictions for the respective micropollutant. Upper numbers in brackets: median values for $\Delta\%$. Grey dashed lines show $\pm 20\%$. [41]

Results and Discussion

Prediction of Abatement of Micropollutants.

Laboratory Experiments: Proof of Concept. Figure 4.1 shows the predicted and measured relative abatements of the selected MPs based on the model described with IPA and 5BTZ as internal probe compounds for river Rhine sand filtrate. The presented data are based on 24 CBD experiments, including six experiments without H₂O₂ addition ($H_{\text{set}} = 1'900$ to $8'000$ J m⁻², H₂O₂ dose = 0 to 8 mg L⁻¹. H_{set} is the UV fluence intended to be transferred to the sample). The combination of IPA and 5BTZ was selected because it was found to reproduce well the set UV fluence H_{set} in laboratory experiments (Figure 4.2), could be applied in many cases due to high detection frequencies in the river Rhine sand filtrate (Table 4.1) and has the lowest median value of the difference between % predicted and % measured abatement ($\Delta\% = -0.8\%$, Figure 4.3) of all investigated combinations of probe compounds.

Overall, the IPA-5BTZ model predicts abatements with a $\Delta\%$ within $\pm 20\%$ in 170 out of 175 data points (97 %, Figure 4.3). Five data points are outside this range: the two predictions for sotalol and three for acesulfame. These compounds are discussed later in the manuscript. The prediction accuracy was constant over the investigated range of H_{set} and H₂O₂.

Especially the $\Delta\%$ values of BTZ, IPR, and MET are mostly very small ($\leq 5\%$), with median values of -1.4 %, 3.2 % and 1.0 %, respectively. For BTZ and IPR, this might be explained by their similar $k_{\bullet\text{OH},\text{MP}}$ and $k_{\text{UV},\text{MP}}$ compared to the applied probe compounds. MET mainly reacted with $\bullet\text{OH}$ and was hardly abated under the investigated treatment conditions ($\leq 25\%$); hence, small values of $\Delta\%$ are expected.

Predictions of STL were unsatisfactory, not only with the IPA-5BTZ model, but also with all other combinations of probe compounds (Figure 4.3). STL was present only at very low concentrations in the filtrates, i.e., 7 ng L⁻¹ and 4 ng L⁻¹ in Rhine and Wiese, respectively. This is above the theoretical limit of quantification (1.6 ng L⁻¹) but outside the lower measurement range (10 ng L⁻¹). For this reason, analytical difficulties likely contribute to the unsatisfactory predictions. However, the observed under-predictions of STL abatement by the model could also result from disregarded reactions with $\text{CO}_3^{\bullet-}$, which were reported to react with STL with a second-order rate constant of $(2.2 \pm 1.7) \times 10^8 \text{ M}^{-1} \text{ s}^{-1}$, [92]. Assuming the $\text{CO}_3^{\bullet-}$ exposure is about two or three orders of magnitude higher than the $\bullet\text{OH}$ exposure, [172], the expected ln abatement by reactions with $\text{CO}_3^{\bullet-}$ is about 3- to 30-fold higher than the abatement via $\bullet\text{OH}$.

The CBD experiments with sand filtrates of rivers Rhine and Wiese were used to assess the significance of H_{calc} . H_{calc} and H_{set} correlated well in the laboratory experiments, as expected (Figure 4.2, combination of IPA and 5BTZ). From 24 assessed data sets, 95 % confidence intervals of H_{calc} of only four data sets did not include H_{set} , [41]. Three of these data sets were conducted with the same water sample, which might indicate a systematic experimental error for this series of experiments. This showcases the potential application of the model to check the consistency of experimental data.

Depending on the choice of the photo-sensitive probe compound, H_{calc} was found either higher or lower than H_{set} (Table B5, Appendix B). Small differences between H_{calc} and H_{set} were found for all combinations of probe compounds that used DTA, IHX, IPA or IPR as UV probe compound, except when STL was selected as the $\text{CT}\cdot\text{OH}$ probe compound. It can be concluded that H_{calc} can reproduce H_{set} , if a suitable combination of probe compounds is selected.

Figure 4.3 provides an overview of the prediction quality of all investigated combinations of internal probe compounds in laboratory experiments with sand filtrate of the river Rhine. For example, $\Delta\%$ of all models with ACE as a probe compound are grouped in the first block (far left) of Figure 4.3. The second probe compound is indicated in vertical text above the ACE label. The first boxplot shows results based on ACE and 5BTZ as probe compounds. Like the boxplot on the far right of Figure 4.1, one boxplot summarizes the prediction accuracy for the abatement of all other MPs (i.e., ACE and 5BTZ excluded) discussed in this paper. The number of distinct experiments and prediction results in each boxplot is indicated in vertical at the lower x-axis. The boxplot for ACE and 5BTZ as probe compounds represents 175 prediction results of DTA, IHX, IPA, IPR, SMX, BTZ, CBZ, MET, MPL and STL from 24 distinct laboratory

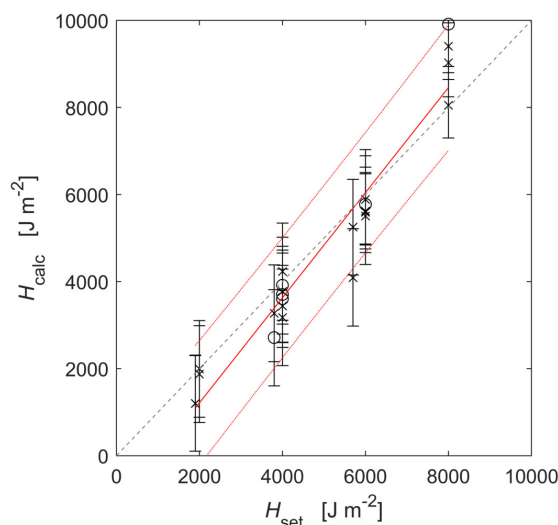


Figure 4.2: Calculated UV fluence (H_{calc}) in comparison to the set UV fluence (H_{set}). Probe compounds: iopamidol and 5-methyl-1H-benzotriazole of 24 CBD laboratory experiments with river Rhine sand filtrate. Circles show experiments without H₂O₂ addition, crosses with H₂O₂ addition. Error bars represent 95 % confidence intervals. [41]

experiments. At the upper x-axis, median values of $\Delta\%$ are indicated and the percentage of $\Delta\%$ inside the $\pm 20\%$ boundaries.

For most combinations of probe compounds, the prediction quality of the model was satisfactory, i.e., the predicted abatement of MPs was mostly within $\pm 20\%$ of the measured abatement. Similar results were obtained for river Wiese sand filtrate (Figure B3, Appendix B). Therefore, it can be concluded that the model generally works well in surface water sand filtrates to predict the abatement of other substances, based on the measured abatement of two probe compounds and the available kinetic information ($k_{\text{OH,MP}}$ and $k_{\text{UV,MP}}$).

A statistical assessment of the percentage of $\Delta\%$ inside the $\pm 20\%$ boundaries of all probe compounds in both filtrates showed that the average of all predictions is in the range of 68 % to 80 % with 95 % confidence, regardless of the choice of probe compounds (Table B6, Appendix B). However, STL performed significantly ($p < 0.05$) worse than the others, likely for the reasons discussed above. Also MET and SMX both showed a poorer average prediction performance when used as probe compounds, respectively, although statistically not significant ($p > 0.05$). Excluding MET, SMX and STL as probe compounds from the statistical evaluation, the average percentage of $\Delta\%$ inside the $\pm 20\%$ boundaries was in the range of 87 % to 92 % with 95 % confidence. Only predictions with ACE as probe compound were poorer on average, but not statistically significant ($p > 0.05$). In the later evaluation, IPA and IPR performed significantly better ($p < 0.05$) than the average. The UV resistant $CT_{\text{OH,calc}}$ probe compounds 5BTZ, BTZ, CBZ and MPL performed equally well.

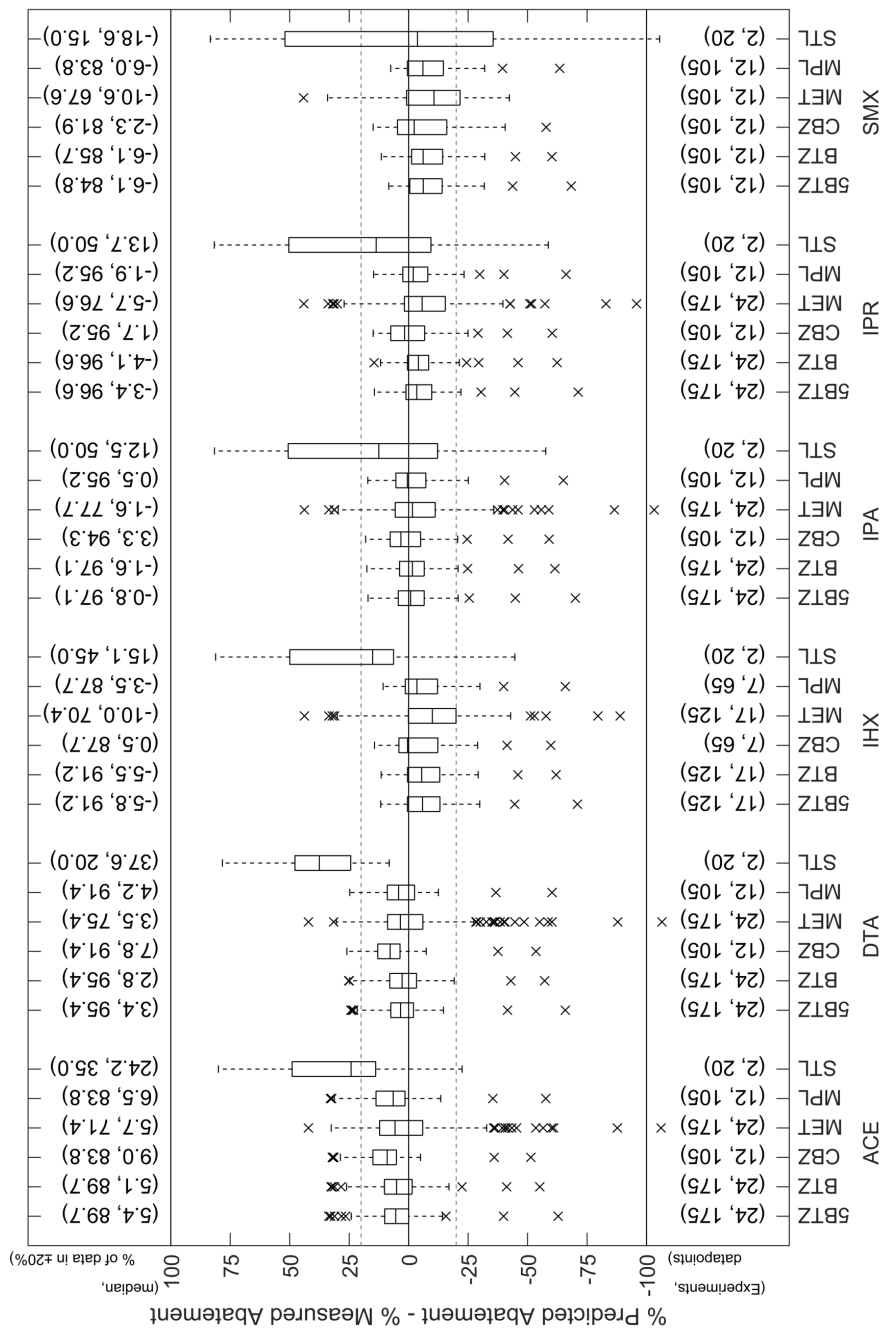


Figure 4.3: CBD laboratory experiments with river Rhine sand filtrate: Overview on differences between predicted and measured % abatement of possible combinations of probe compounds. Values in lower brackets: number of evaluated experiments, total number of predictions. Values in upper brackets: median of data points, share of data inside the $\pm 20\%$ range, shown by gray dashed lines. Horizontal names: UV susceptible probe compound. Vertical names: UV resistant CT_{OH} probe compound. [41]

MET was not well suited as probe compound under the treatment conditions investigated due to low % abatement measured in the range of -8 % to 22 % only. At low values of abatement, the model is very sensitive for analytical errors, as further discussed below. Negative values for % measured abatement are explained by analytical measurement uncertainties, which are relatively high for MET, i.e., standard uncertainty is 19 % (Table B3, Appendix B). In these cases, it can happen that % predicted abatements are negative, which causes an increase of the predicted MP concentration. In some cases, at the same time the % measured abatement was (strongly) positive, which explains results even below -100 % difference in Figure 4.3.

When SMX was used as UV probe compound, % abatement predictions tended to be lower than the % abatement measured. Comparing H_{set} and H_{calc} in CBD experiments, the calculated UV fluence was constantly below the set value, i.e., in the range of -48 % to -34 % (combination with STL excluded, Table B5, Appendix B). It is hypothesized that the literature value for $k_{\text{UV,SMX}}$ used in this study was too high (see also Table 4.2). This concurs with the previously observed reduction in $k_{\text{UV,SMX}}$ in real river water matrices compared to ultrapure water solutions, [90], and might indicate that dissolved organic matter partly inhibits the photochemical transformation of SMX by reduction of transformation intermediates back to the parent compound, [175]. Of note, SMX was reported to react with $\text{CO}_3^{\bullet-}$ with a second-order reaction rate of $(1.2 \pm 0.7) \times 10^8 \text{ M}^{-1} \text{ s}^{-1}$, [92], which implies that the expected ln abatement by reactions with $\text{CO}_3^{\bullet-}$ is about 2- to 20-fold higher than the abatement via $^{\bullet}\text{OH}$. In contrast to STL, predictions of SMX abatement are typically found within $\pm 20\%$ of the measured abatement. This is explained by the rapid abatement of SMX by photolysis, which is of higher importance than the abatement via radical species.

Similarly, when using ACE as a probe compound, H_{calc} in CBD experiments was systematically higher than H_{set} (Table B5, Appendix B), suggesting that $k_{\text{UV,ACE}}$ from the literature is too low (see also Table 4.2). This explains why the abatement of ACE was often under-estimated (Figure 4.1) and consequently, when using ACE as UV probe compound, abatements of UV-susceptible compounds tended to be over-predicted (Figure 4.3).

Pilot Plant Experiments: Application of the Model. The model was applied to predict the abatement of MPs in pilot plant experiments. A comparison of the $\Delta\%$ values for the investigated combinations of probe compounds is provided in Figures B4 (Appendix B) for river Rhine sand filtrate and in Figure B5 (Appendix B) for river Wiese sand filtrate.

An assessment of the percentage of $\Delta\%$ within the $\pm 20\%$ boundaries of all probe compounds in both filtrates showed no statistical differences between the mean values of the experiments performed in laboratory and pilot-scale, i.e., the average value is in the range of 74 % to 81 % with 95 % confidence (Table B7, Appendix B). Therefore, it can be concluded that the model is also applicable to sand filtrates at pilot-scale with a similar prediction performance.

However, some differences exist for single MPs, e.g., STL (better prediction performance) or MET (lower prediction performance). This might be due to effects of varying concentrations during the pilot trials. Another reason for the observed shifts in the prediction performance could be the influence of the water temperature on $k_{UV,SMX}$ and $k_{\bullet OH,MP}$. Water temperature (6.2 to 24.5 °C) is not included as an input parameter in the proposed model. Possible temperature effects, i.e., activation energies, likely differ between the investigated MPs, [154], which could explain the described discrepancies between laboratory and pilot-scale experiments. However, overall, it is concluded that the differences are not very large, because the average values of $\Delta\%$ inside the $\pm 20\%$ boundaries at both scales are statistically indifferent. In principle, temperature effects on the rate constants k could be accounted for by the Arrhenius equation:

$$k(T) = A \times \exp\left(-\frac{E_a}{R T}\right) \quad (4.12)$$

T (K) is the absolute temperature, R ($8.314 \text{ J K}^{-1} \text{ mol}^{-1}$) is the ideal gas constant, A is the pre-exponential factor, E_a (J mol^{-1}) is the activation energy. However, activation energies of for the relevant reaction rate constants of the selected MPs are not available in the published literature. Note that second-order rate constants for reactions of all water matrix constituents with $\bullet OH$ (including $\bullet OH$ scavengers) may also be impacted by the water temperature, which might lead to a net effect on MP abatement lower than expected.

In addition, the implementation of temperature-dependent values for $k_{UV,SMX}$ and $k_{\bullet OH,MP}$ is expected to improve the prediction quality of the model only moderately. This assumption is based on estimated activation energies for $k_{UV,SMX}$ and $k_{\bullet OH,MP}$ in the range of 5 to 22 kJ mol^{-1} , [154], [176], [177], which leads to a variation within a factor of 1.2 to 2.0 for the rate constants in the observed temperature range. This is in the range of uncertainty of experimentally determined kinetic parameters. Therefore, it is concluded that a temperature-independent model can be used for predictions within an accuracy of $\pm 20\%$ for the water temperature ranges in this study.

Published Data: Assessment of Wastewater Treatment with UV/H₂O₂. Published data from UV/H₂O₂ treatment of a wastewater effluent in laboratory experiments, [178], and in a pilot plant, [179], were assessed with the model to test its applicability in advanced wastewater treatment (Figure 4.4). Laboratory experiments were conducted on a CBD with tertiary wastewater effluent (0 to 12.8 $\text{mg H}_2\text{O}_2 \text{ L}^{-1}$; UV fluences: 400 to 20'000 J m^{-2} , [178], [179]). A pilot plant was continuously operated with tertiary wastewater effluent at a target dose of 10 $\text{mg H}_2\text{O}_2 \text{ L}^{-1}$ and a UV fluence of 8'000 J m^{-2} . Results include data from continuous monitoring over one week at dry weather conditions and another week during a rain event, [179]. Although the publication included the abatement of a more extensive set of MPs, only the MPs selected in the current study were evaluated (Table 4.1).

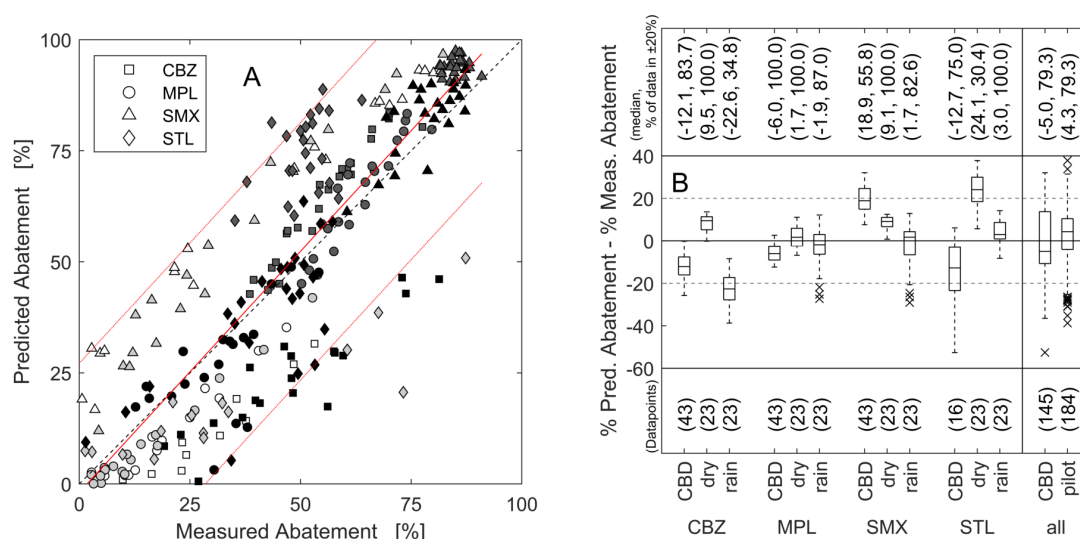


Figure 4.4: Assessment of published data for UV/H₂O₂ wastewater treatment iopromide (IPR) and 1H-benzotriazole (BTZ) as probe compounds. A: Predicted relative abatement in comparison to the measured relative abatement. White and light gray fillings: CBD experiments from [178] and [179], respectively. Dark gray and black fillings: pilot-scale experiments at dry weather ('dry') and during a rain event ('rain'), respectively, on a continuously operated pilot plant at 10 mg H₂O₂ L⁻¹, 8'000 J m⁻², [179]. B: Differences between predicted and measured % abatements from the respective micropollutants. Horizontal names: predicted micropollutant. Separate boxplots on the far right summarize all CBD experiments and all pilot plant experiments ('pilot') of all assessed micropollutants, respectively. [41]

Figure 4.4 shows the results for the probe compound combination IPR-BTZ for the prediction of CBZ, MPL, SMX and STL. The other MPs discussed here were not included in the measurements of [178] and [179]. IPR and BTZ were selected as probe compounds because this combination had the highest share of $\Delta\%$ inside the $\pm 20\%$ boundaries in the experiments with river Rhine sand filtrate.

Overall, the 95 % confidence intervals for the share of $\Delta\%$ within the $\pm 20\%$ boundaries of all possible combinations of probe compounds are in the range of 66 % to 82 % for CBD experiments and 68 % to 84 % for pilot plant experiments, respectively (Figure 4.4 B). This means that there is no statistical evidence that the measured % MPs abatement within $\pm 20\%$ in wastewater is predicted with a worse performance than in experiments with surface water, both on laboratory- and pilot-scale. In addition, there is no statistical difference between the share of $\Delta\%$ inside the $\pm 20\%$ boundaries at dry weather or during a rain event, evaluating the eight possible combinations of probe compounds. Therefore, it can be concluded that the model can be applied in a wide range of water matrices and, at least, at laboratory- and pilot-scale to predict the abatement of MPs based on the measured abatement of two MPs as internal probe compounds.

The prediction performance of the IPR-BTZ model for STL is much better in the wastewater than in the river sand filtrates. STL was present in the wastewater in the range of 32 ng L⁻¹ to 83 ng L⁻¹, which was well above the limit of quantification. This contributes to the overall better results for STL, compared to the experiments with the river sand filtrates where the influent concentrations of STL were often near the limit of quantification. Note that on the pilot plant, STL abatement tended to be overpredicted, even though carbonate radicals not considered in the model should add to the predicted abatement by photolysis and •OH. The reason for this result is currently unclear and further research is necessary to fully explain this observation.

Estimation of Kinetic Data for Micropollutants. The model was also tested for its applicability to obtain kinetic data. This can be an interesting application as a rough estimate of kinetic data that is not yet reported in literature. In a first step, the model is applied to back-calculate H_{calc} and $CT_{\text{OH,calc}}$ with Eqs. 4.7 and 4.8. In a second step, $k_{\text{UV,MP}}$ and $k_{\text{OH,MP}}$ are determined by linear regression analysis with Eq. 4.1, which is in principle possible if at least two experimental data points are available.

As a proof of concept, this approach was applied for well-described MPs from laboratory experiments with river Rhine sand filtrate with IPA and 5BTZ as internal probe compounds. Only positive, i.e., physically reasonable results for mean values of H_{calc} and $CT_{\text{OH,calc}}$ were used for the linear regression (data used: UV fluences: 1'900 to 8'000 J m⁻², 0 to 8 mg H₂O₂ L⁻¹). In Table 4.2, the fitting results of the model are compared with literature values (derived from Table 4.1).

The proposed approach leads to an agreement of predicted values for $k_{\text{UV,MP}}$ and $k_{\text{OH,CBZ}}$ and those from literature within a factor 2, except for one outlier ($k_{\text{UV,MP}}$). This is well within the range of accuracy that can be expected for kinetic parameters which are determined experimentally by different groups, [142].

For some MPs, rate constants were determined with high uncertainties ($k_{\text{UV,MP}}$ of CBZ, MET and MPL, or $k_{\text{OH,MP}}$ of DTA and IHX). Accurate estimates of rate constants are difficult to be obtained for substances that are either hardly abated by direct photolysis (CBZ, MET, MPL), or have very low values for $k_{\text{OH,MP}}$ (DTA) (Table 4.1). Nevertheless, the corresponding rate constants for the main pathway, i.e., the reaction with •OH (CBZ, MET, MPL) or direct photolysis (DTA), can still be determined with good agreement with the literature. For IHX the experiments with $H_{\text{set}} = 8'000 \text{ J m}^{-2}$ were excluded for fitting, because their inclusion led to physically impossible negative values for $k_{\text{OH,IHX}}$, likely due to analytical measurement errors at very low concentrations. The remaining data had a very narrow range of $CT_{\text{OH,calc}}$ (5.3×10^{-12} to $4.7 \times 10^{-11} \text{ M s}$). This explains the large confidence interval of the estimated $k_{\text{OH,IHX}}$ value. Furthermore, low abatement such as for MET (2 to 22 %) also leads to wide confidence intervals. Therefore, the suggested approach is only feasible if the target MP is abated to a sufficiently high extent to minimize uncertainties, e.g., from analytical measurements. Note

Chapter 4. Micropollutants as Internal Probe Compounds to Assess UV/H₂O₂ Treatment

Table 4.2: Laboratory experiments with river Rhine sand filtrate: Comparison of fitted rate constants for direct photolysis ($k_{UV,MP}$) and for reactions with $\bullet OH$ ($k_{\bullet OH,MP}$), along with the number of fitted data points (n), based on calculated UV fluences and $\bullet OH$ exposures from iopamidol and 5-methyl-1H-benzotriazole as internal probe compounds. Results show average values \pm half 95 % confidence intervals for fitted kinetic parameters. Ratios compare modelled values with literature values at pH 8.1.

Substance	n	$k_{UV,MP}/10^4$ (m ² J ⁻¹)			$k_{\bullet OH,MP}/10^9$ (M ⁻¹ s ⁻¹)		
		Fitted	Literature, ^a	k_{fitted}/k_{lit}	Fitted	Literature, ^b	k_{fitted}/k_{lit}
ACE	18	4.0 \pm 0.4	3.3	1.2	7.7 \pm 3.0	3.8	2.0
BTZ	18	0.28 \pm 0.07	0.29	1.0	7.4 \pm 0.5	8.3	0.9
CBZ	9	0.2 \pm 0.3	0.02	9.8	9.1 \pm 1.3	8.0	1.1
DTA	18	4.6 \pm 0.2	3.6	1.3	0.7 \pm 1.3	0.56	1.2
IHX	9	4.3 \pm 0.5	5.4	0.8	5.5 \pm 7.2	3.5	1.6
IPR	18	3.2 \pm 0.2	4.0	0.8	4.5 \pm 1.6	3.3	1.4
MET	17	0.03 \pm 0.07	0.06	0.5	1.2 \pm 0.5	1.4	0.8
MPL	9	0.2 \pm 0.2	0.1	1.8	7.6 \pm 0.8	7.7	1.0
SMX	9	2.2 \pm 0.6	3.8	0.6	7.5 \pm 3.1	5.9	1.3

^a Values were calculated using the ϵ and Φ values given in Table 4.1 and applying Eq. 4.2 and, if needed, the procedure to calculate speciation-dependent ϵ and Φ for pH 8.1 (Eqs. 4.3 and 4.4).

^b Values taken from Table 4.1, assumed to be pH-independent.

that in principle it is also possible to estimate the $\bullet OH$ scavenging rate of the water matrix, S , from H_{calc} , $CT_{\bullet OH,calc}$, and Eq. 4.5, but the discussed limitations are also valid for this approach.

Overall, these results show some benefits to estimate rate constants, but also serious limitations. Kinetic data are typically obtained by measurements of the abatement of a selected MP under controlled laboratory conditions, at concentration levels that are high enough to reduce analytical errors, and for optimized reaction times. Whenever possible, such an approach should be adopted to determine rate constants for individual micropollutants.

Sensitivity Analysis of the Model. This section provides an assessment of the role of experimental parameters on the quality of the modelling results. First, the impact of the measured abatement of the probe compounds on the combined standard uncertainties (u_c) of H_{calc} and $CT_{\bullet OH,calc}$ is assessed. In a second step, strategies to reduce the uncertainties of H_{calc} and $CT_{\bullet OH,calc}$ are discussed, which would lead to model outputs with increased confidence. Both assessments are based on the Gaussian error propagation.

H_{calc} and $CT_{\bullet OH,calc}$ depend on all parameters described in Eqs. 4.7 and 4.8, i.e., concentrations of both probe compounds before and after UV/H₂O₂ treatment and their respective kinetic parameters. To reduce the complexity, only the probe compound combination IPA-5BTZ is discussed here, because it was the main combination applied in this study. Analytical

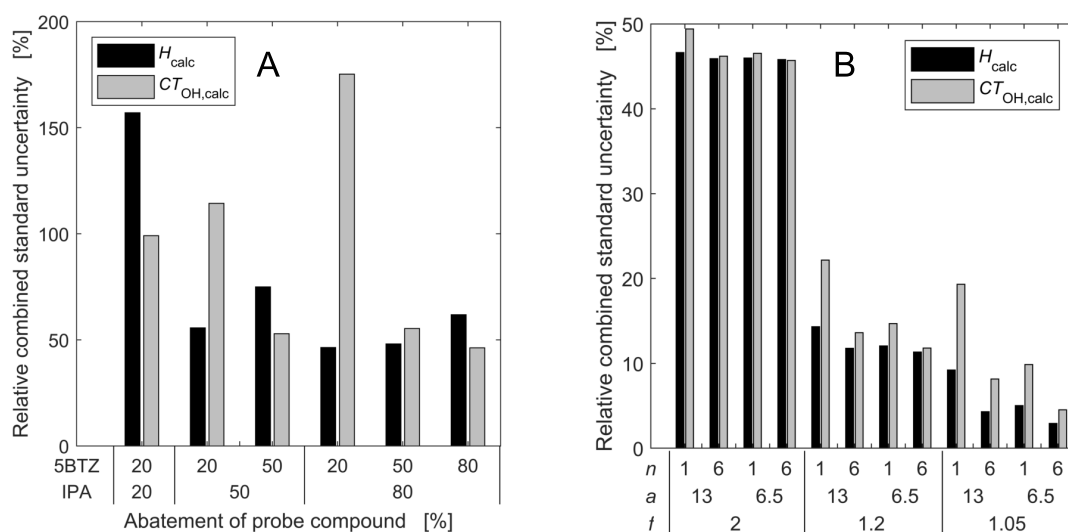


Figure 4.5: Sensitivity analysis of the model with iopamidol (IPA) and 5-methyl-1H-benzotriazole (5BTZ) as probe compounds. A: Impact of different levels of abatement of the probe compounds on the combined standard uncertainties (u_c) of the calculated UV fluence (H_{calc}) and the calculated \bullet OH exposure ($CT_{OH,calc}$) relative to H_{calc} or $CT_{OH,calc}$, respectively. B: Impact of strategies to minimize u_c for H_{calc} and $CT_{OH,calc}$, based on 93 % and 68 % abatement of IPA and 5BTZ, respectively. n : number of replicate measurements, a : analytical standard uncertainty in %, f : factor within which the experimentally determined rate constants are distributed around the precise value of the constants. [41]

measurement uncertainties for both probe compounds were 13 % in this study (Chapter 2). The uncertainty of the rate constants was assumed within a factor 2.

Figure 4.5 A shows u_c of H_{calc} and $CT_{OH,calc}$ at different levels of abatement of the probe compounds. Scenarios with a higher removal of 5BTZ compared to IPA are not of relevance for typical water treatment applications and therefore not discussed. For low relative abatements of the probe compounds (< 50%), the application of the model is not very useful, because u_c of H_{calc} and $CT_{OH,calc}$ can exceed 100 %. In such a case, if possible, a different pair of probe compounds has to be selected, with a higher extent of abatement. When both probe compounds are abated by at least 50 %, uncertainties of the rate constants dominate the calculations of H_{calc} and $CT_{OH,calc}$. Independent of the operational conditions, u_c of H_{calc} and $CT_{OH,calc}$ cannot be reduced below 43 %, even disregarding analytical uncertainties, due to the defined uncertainty for the rate constants within a factor 2.

Impacts of several strategies to improve the model outputs, i.e., replicate measurements, improvement of analytical measurements or precision of the rate constants, are shown in Figure 4.5 B for IPA and 5BTZ as probe compounds. Calculations were conducted for a relatively high abatement of the probe compounds, i.e., 93 % and 68 % for IPA and 5BTZ, respectively. These abatements result in $H_{calc} \approx 6200 \text{ J m}^{-2}$ and $CT_{OH,calc} \approx 1.1 \times 10^{-10} \text{ M s}$, which

corresponds to $\approx 4.1 \text{ mg H}_2\text{O}_2 \text{ L}^{-1}$, rearranging the $\bullet\text{OH}$ steady-state assumption (Eq. 4.5) and using the assumed S of an average river Rhine sand filtrate, i.e., $5.7 \times 10^4 \text{ s}^{-1}$. These treatment conditions are similar to those for the long-term pilot plant study.

Under these conditions, single measurements of IPA and 5BTZ with analytical uncertainties of 13 % and rate constants uniformly distributed within a factor 2 result in u_c of 47 % and 49 % for H_{calc} and $CT_{\bullet\text{OH,calc}}$, respectively. While for H_{calc} , the uncertainty of $k_{\text{UV,IPA}}$ has the highest importance (91 % of u_c^2 of H_{calc}), $k_{\bullet\text{OH,5BTZ}}$ contributes the most to the combined variance of $CT_{\bullet\text{OH,calc}}$ (68 %). Consequently, the improvement of analytical accuracy or replicate measurements do not significantly enhance the model outputs. Therefore, an optimization can only be achieved by more precise values for the rate constants.

Kinetic parameters can be estimated within a factor 1.2 by reviewing published rate constants of several independent research groups (as done, e.g., by Buxton et al., [151]), or by using relative rate constants from one lab determined under the same treatment conditions. By this, uncertainties of rate constants limit u_c of H_{calc} and $CT_{\bullet\text{OH,calc}}$ to $\geq 11\%$. Under these conditions, six replicate measurements can lower u_c of H_{calc} from 14 % to 12 % and u_c of $CT_{\bullet\text{OH,calc}}$ from 22 % to 14 %, respectively. Hence, replicate measurements (or improved analytical methods) can improve the predictions to some extent (especially hydroxyl radical exposure), but a considerable effort is required. At this level of precision, kinetic parameters should include temperature-dependencies (activation energies, Eq. 4.12), if the model is applied at other temperatures than 20 °C. Otherwise, the temperature impact on kinetic parameters can again increase the uncertainty of kinetic parameters, as discussed before. For u_c of H_{calc} , analytical uncertainties only play a significant role when the uncertainty of $k_{\text{UV,IPA}}$ is extremely low, i.e., accurate within a factor 1.05. With less accuracy for this rate constant, efforts to minimize analytical errors by repeated measurements or improved analytical methods are of minor relevance for H_{calc} .

Conclusions

A novel modeling tool based on the abatement of micropollutants acting as internal probe compounds was developed to determine the applied UV fluence and the hydroxyl radical exposure during laboratory- and pilot-scale UV/H₂O₂ treatment. This modeling approach has the advantage that water matrix parameters affecting the abatement of micropollutants (e.g., scavenging rate by background matrix, transmissivity of the water, etc.), as well as hydrodynamics and non-ideal characteristics of the UV-reactor are implicitly considered by the model. The following conclusions can be drawn:

- The model was proven to satisfactorily predict the abatement of compounds at laboratory- and pilot-scale, both for surface water sand filtrates and tertiary treated wastewater. The difference between measured and predicted abatements was typically within $\pm 20\%$ for

most combinations of probe compounds, even though water temperatures varied in the range of 5.0 to 24.5 °C during the pilot plant experiments.

- High reactivity of substances with other radical species than $\bullet\text{OH}$ might limit the application of the model for certain micropollutants, especially if they are at least moderately resistant against photolysis (e.g., sotalol). For such substances, the results should be interpreted with care, specifically in a water matrix with low contents of dissolved organic carbon or high carbonate concentrations, i.e., high ratio of $\text{CO}_3^{\bullet-}$ to $\bullet\text{OH}$. Vice versa, if the model largely underpredicts the abatement of a substance based on photolysis and reactions with $\bullet\text{OH}$, and the rate constants of the predicted substance were obtained from careful measurements in the laboratory, results might indicate significant contributions of other radical species to its abatement.
- This approach is suitable to monitor the absolute values of the UV fluence and hydroxyl radical exposure with reasonable confidence when the relative abatement of both probe compounds is at least 50 % and all rate constants are known with good precision (factor 1.2). Furthermore, concentrations of both probe compounds must be measured before and after the treatment by state-of-the-art analytical methods. When the used probe compounds are abated to a sufficiently high degree, e.g., when iopamidol and 5-methyl-1H-benzotriazole are abated by 93 % and 68 %, respectively, replicate measurements or improved analytical methods do not significantly improve the model results.
- Calculated UV fluences and hydroxyl radical exposures can be used to estimate unknown rate constants (second-order rate constant for the reaction with hydroxyl radicals, fluence-based rate constant for direct photolysis). The estimated rate constants were in most cases within the common range of accuracy of published kinetic data (factor 2). However, the accuracy of this approach strongly decreases when specific reactions are very slow. Thus, this approach provides a good first estimate of rate constants but cannot substitute careful measurement of rate constants under controlled laboratory conditions.

Dense Membrane Filtration before Soil Infiltration

Part III

5 Ozone Treatment of Concentrates

This chapter is a copy of a manuscript prepared for the submission to Water Research [42]:
Wünsch, R., Hettich, T., Prahtel, M., Thomann, M., Wintgens, T., and von Gunten, U.: Tradeoff Between Micropollutant Abatement and Bromate Formation during Ozonation of Concentrates from Nanofiltration and Reverse Osmosis Processes.

R.W.'s contributions: Design, preparation and execution of experiments; measurement of bulk water quality parameters, bromide and bromate; data analysis and interpretation; writing and critically reviewing the draft manuscript.

Abstract

To date, little is known on how the selection of a semi-permeable dense membrane impacts the dissolved organic matter in the concentrate and what the consequences are for micropollutant (MP) abatement and bromate formation during concentrate treatment with ozone. Laboratory ozonation experiments were performed with standardized concentrates produced by 3 membranes (2 NFs and 1 low-pressure reverse osmosis (LPRO) membrane) from 3 water sources (2 river waters and 1 lake water). The concentrates were standardized by adjustment of pH and concentrations of dissolved organic carbon, total inorganic carbon, selected micropollutants (MP) and bromide to exclude factors which are known to impact ozonation. NF membranes had a lower retention of bromide and MPs than the LPRO membrane, and if the permeate quality of the NF membrane meets the requirements, the selection of this membrane type is beneficial due to the lower bromate formation risks upon concentrate ozonation. The bromate formation was typically higher in standardized concentrates of LPRO membranes than of NF membranes, but the tradeoff between MP abatement and bromate formation upon ozonation of the standardized concentrates was not affected by the membrane type. Furthermore, there was no difference for the different source waters. Overall, ozonation of concentrates is only feasible for abatement of MPs with a high to moderate ozone reactivity with limited bromate formation. Differences in the DOM composition between NF and LPRO membrane concentrates are less relevant than retention of MPs and bromide by the membrane and the required ozone dose to meet a treatment target.

Introduction

Dense semi-permeable membranes, such as nanofiltration (NF) or reverse osmosis (RO), can be applied to simultaneously reject total dissolved solids, bacteria and viruses, salts and micropollutants (MPs) in drinking water production [180] or wastewater treatment [181]–[183]. In RO and NF applications, solutes are physically separated at the membrane from the product stream, i.e., the permeate. Separation is based on size exclusion, electrostatic interactions between the surface of the membrane and solutes such as MPs, as well as sorption and diffusion characteristics of a compound [184], [185]. During operation, additional effects can impact the rejection performance of the membranes, such as the applied pressure, water temperature, pH, hydrodynamic conditions in the membrane module, fouling status, membrane ageing, as well as changing feed water compositions [185], [186]. Typically, the rejection of solutes is specific for an application and transferability is only limited. For example, bromide (Br^-) rejection on NF membranes was found in the range of -4% to 10% in surface water treatment applications [187], [188], but can reach significantly higher relative rejection in highly saline feed water streams, e.g., from natural gas production [189], [190]. Further studies on bromide rejection by RO and NF are provided elsewhere [191].

One principal drawback of membrane applications is the production of a concentrated reject stream, often termed “brine”, “slurry” or “concentrate”. Here, rejected solutes such as MPs, natural and/or effluent organic matter, salts, bacteria and viruses, or process auxiliary substances such as chelating agents (antiscalants) are concentrated, depending on their specific rejection by the membrane and the water recovery. Depending on the local circumstances, the concentrates should be treated before their further use or discharge.

Possible treatment options for the abatement of MPs in the concentrates have been frequently discussed in literature, and they include the application of ozone or advanced oxidation processes, additional biological treatment or adsorption on activated carbon in granular or powdered form [192]–[199].

Ozone (O_3) has been applied for disinfection and MP abatement for more than a century [121], [135]. It reacts selectively and rapidly with electron-rich moieties, such as activated aromatic compounds, olefins, neutral amines and reduced sulfur species, [121]. In natural waters and wastewater effluents, dissolved organic matter (DOM) is usually the main consumer of O_3 , [40]. Hydroxyl radicals ($\cdot\text{OH}$) are always formed *in situ* as secondary oxidants during ozonation by various O_3 decomposition processes [121]. $\cdot\text{OH}$ react less selectively than ozone with second-order rate constants typically in the range of 10^9 to $10^{10} \text{ M}^{-1} \text{ s}^{-1}$, mostly by OH addition or by H abstraction reactions [200]. In environmental applications, the steady-state or transient concentration of $\cdot\text{OH}$ is determined by its main scavengers, i.e., DOM, carbonate (CO_3^{2-}), bicarbonate (HCO_3^-).

At given exposures of O_3 and $\cdot\text{OH}$, the abatement of a MP depends on its second-order

rate constants for reactions with O_3 ($k_{O_3,MP}$) and $\bullet OH$ ($k_{\bullet OH,MP}$). To facilitate a comparison between MPs with similar rate constants, they are often categorized into groups [160], i.e., (I), MPs with a high ozone reactivity ($k_{O_3,MP} \geq 10^5 \text{ M}^{-1} \text{ s}^{-1}$); (II), MPs with a moderate ozone reactivity ($10^1 \text{ M}^{-1} \text{ s}^{-1} \leq k_{O_3,MP} < 10^5 \text{ M}^{-1} \text{ s}^{-1}$); (III), ozone resistant MPs with a high $\bullet OH$ reactivity ($k_{O_3,MP} < 10^1 \text{ M}^{-1} \text{ s}^{-1}$ and $k_{\bullet OH,MP} \geq 5 \times 10^9 \text{ M}^{-1} \text{ s}^{-1}$); (IV), ozone resistant MPs with a moderate $\bullet OH$ reactivity ($k_{O_3,MP} < 10^1 \text{ M}^{-1} \text{ s}^{-1}$ and $1 \times 10^9 \text{ M}^{-1} \text{ s}^{-1} \leq k_{\bullet OH,MP} < 5 \times 10^9 \text{ M}^{-1} \text{ s}^{-1}$); (V), MPs resistant against ozone and $\bullet OH$ ($k_{O_3,MP} < 10^1 \text{ M}^{-1} \text{ s}^{-1}$ and $k_{\bullet OH,MP} < 1 \times 10^9 \text{ M}^{-1} \text{ s}^{-1}$).

During ozonation of bromide (Br^-)-containing waters, bromate (BrO_3^-) can be formed by a complex mechanism, including both reactions with ozone and $\bullet OH$ [51], [121], [201]. BrO_3^- is a possible human carcinogen and the WHO recommends a drinking water standard of $10 \mu\text{g L}^{-1}$, [202]. For wastewater, there is no BrO_3^- standard, but for example Switzerland proposed an environmental quality standard of $50 \mu\text{g L}^{-1}$ [203], [204]. Therefore, the application of ozone to abate MPs in bromide-containing concentrates is always a tradeoff between the desired MP abatement and the undesired formation of bromate.

Some studies investigated bromate formation upon ozonation of RO concentrates for MP abatement [205]–[208] and details are provided in Table C1 (Appendix C). All studies investigated MP abatement (and other aspects) in RO concentrates from real municipal wastewater treatment plants. Overall, the investigated concentrates had dissolved organic carbon (DOC) concentrations in the range of 22.5 to 86.7 mg L^{-1} (average: $45.6 \text{ mg DOC L}^{-1}$), while Br^- was present in concentrations between 1.2 to 9.64 mg L^{-1} (average: $3.0 \text{ mg Br}^- \text{ L}^{-1}$). The molar bromate yield (η) was calculated as bromide converted into bromate upon ozone treatment in relation to the bromide concentration before ozone treatment (5.1):

$$\eta = \frac{([BrO_3^-] - [BrO_3^-]_0) \times \frac{MW_{Br^-}}{MW_{BrO_3^-}}}{[Br^-]_0} \quad (5.1)$$

$[BrO_3^-]_0$ and $[BrO_3^-]$ (g L^{-1}) are bromate concentrations before and after ozonation, respectively. $MW_{Br^-} = 79.9 \text{ g mol}^{-1}$ and $MW_{BrO_3^-} = 127.9 \text{ g mol}^{-1}$ are the molecular weights of bromide and bromate, respectively. $[Br^-]_0$ (g L^{-1}) is the bromide concentration before ozone treatment. Overall, η was reported in the range of 0.4 to 10.2 % for specific ozone doses in the range of 0.17 to $1.0 \text{ mg O}_3 (\text{mg DOC})^{-1}$ (Table C1, Appendix C). However, only minimal data is available that allow for a systematic assessment of the tradeoff between MP abatement and bromate formation [207], [208].

Studies on ozonation of NF and RO concentrates from river or surface waters are lacking, despite the increasing demand for such treatment solutions. In addition, the effect of the membrane type on the subsequent concentrate ozonation is not yet well understood. Due to different rejection performances of NF and RO with respect to DOC, HCO_3^- , CO_3^{2-} , MPs and Br^- , both the MP abatement efficiency, as well as the risk of bromate formation upon ozonation are expected to differ between different membranes. In addition, hypothetically,

differences in the DOM compositions of NF and LPRO concentrates might exist if small DOM moieties are rejected by RO but not by NF and these could possibly influence, e.g., the ozone chemistry and the ensuing O_3 and $\cdot OH$ exposures.

This study aims to investigate, (i), how hypothetically differing DOM compositions in NF and RO concentrates impact the abatement of MPs and formation of bromate upon ozone treatment and, (ii), if the membrane type has an impact on the tradeoff between MP abatement and bromate formation. Two river water rapid sand filtrates (waters from River Rhine and River Wiese) and one lake water (Lake Biel) were treated with three membrane types, i.e., two NF membranes and one low-pressure RO (LPRO) membrane. Concentrates were standardized (same pH = 8.3 ± 0.1 and concentrations of DOC, total inorganic carbon (TIC) and Br^-) and spiked with seven MPs (atenolol, atrazine, 1H-benzotriazole, bezafibrate, carbamazepine, diclofenac, ibuprofen). The MPs were selected to cover a broad range of second-order rate constants for the reactions with O_3 and $\cdot OH$. The concentrates were characterized by electron donating capacity. Furthermore, the standardized concentrates were treated with various specific ozone doses in laboratory experiments. Finally, linking the membrane performance (MP rejection) with the benefits and limitations of the concentrate ozonation (abatement of MPs, formation of BrO_3^-), this study provides an overall evaluation of NF and RO membrane processes.

Materials and Methods

Concentrates were produced from different surface waters and membranes, as further detailed below. To rule out other known parameters affecting ozonation, the concentrates were standardized before ozone treatment, i.e., the only differences between the samples were, (i) the water source, (ii) the membrane type and, (iii) the concentrations of ions other than HCO_3^-/CO_3^{2-} , Br^- and borate, which was used as a buffer.

Raw Waters

IWB produces drinking water for the city of Basel (Switzerland) and surroundings, as described in Chapter 2. The treatment chain consists of a raw water abstraction from the River Rhine, rapid sand filtration and subsequent soil aquifer treatment in the “Lange Erlen” area (Chapter 2). A grab sample of the River Rhine water (RR, coordinates: 47° 33' 47" N, 7° 37' 49" E) was taken after rapid sand filtration on February 8, 2021.

The River Wiese flows through the Wiese valley in the southern Black Forrest in Germany and enters the River Rhine in Basel (Switzerland). In the “Lange Erlen” area in Basel, River Wiese water (RW) was abstracted from a side channel (coordinates: 47° 34' 27" N, 7° 37' 10" E). RW is used by IWB as a backup water resource and was therefore selected for investigations. After a

Table 5.1: Specifications of the investigated membranes according to the manufacturer.

Membrane abbreviation	NF1	NF2	LPRO
Manufacturer	Toray	Toray	Toray
Name	NE4040	HRM	TMH20A
Membrane type and material	Thin film composite, polyamide	Thin film composite, polyamide	Cross linked fully aromatic polyamide composite
Relative NaCl retention [%]	20 to 40	20 to 40	99.3
Permeability [$\text{L m}^{-2} \text{ h}^{-1} \text{ bar}^{-1}$]	8.5 ^a	9.8 ^b	6.8 ^c

^a Test conditions: 5.0 bar, 25 °C, pH 6.5 to 7, 15 % water yield.

^b Test conditions: 5.2 bar, 25 °C, pH 6.5 to 7, 15 % water yield.

^c Test conditions: 6.9 bar, 25 °C, pH 7, 15 % water yield.

pilot-scale rapid sand filtration, a RW grab sample was collected on November 30, 2020.

Energie Service Biel (ESB) produces drinking water for the city of Biel and surroundings from Lake Biel (Switzerland). A grab sample from ESB's intake of Lake Biel water (LB) without pretreatment was collected on March 10, 2021 (coordinates: 47° 7' 12" N, 7° 13' 34" E).

All samples were collected in intermediate bulk containers (IBC, material: HDPE, water volume: 0.6 m³) and transferred without cooling to the membrane pilot plant within less than 2 hours.

Experimental Setups and Procedures

Details on the investigated membranes are provided in Table 5.1. The retentions by the membranes of Br[−] and MPs present in RR without spiking were determined in bench-scale experiments with flat-sheet membranes (Figure C1, Appendix C). The test unit (Triple System, MMS Membrane Systems, Switzerland) was operated batch-wise for each membrane with a 2 L RR grab sample at a trans-membrane pressure of 5 bar and a controlled water temperature of 25°C. After filling the feed tank with the water sample, the operational set point was adjusted and the unit was left to stabilize for at least 1 hour, recycling the permeate back to the feed tank. Then, an initial sample of the water in the feed tank was taken for the analysis of the initial concentrations of Br[−] and MPs. Concentration of the sample was started by directing the permeate into a glass beaker, which was placed on a scale to measure the water recovery. Experiments were stopped at a water recovery of 75 % due to experimental constraints. Samples were of the final permeate and concentrate were taken. Analytical methods to determine the MP and Br[−] concentrations for these experiments are described in Chapter 2. The retention of a solute i was calculated by Equation 5.2 from the respective permeate ($[i]^{\text{Permeate}}$) and initial feed concentrations ($[i]_0^{\text{Feed}}$).

$$R_i = 1 - \frac{[i]^{\text{Permeate}}}{[i]_0^{\text{Feed}}} \quad (5.2)$$

Table 5.2: Averages and standard deviations of selected dissociation constants (pK_a) and observed second-order rate constants for reactions with ozone ($k_{O_3,MP}$) or hydroxyl radicals ($k_{\bullet OH,MP}$) for the investigated micropollutants (MP). Underlying data and references are provided in Table C2 (Appendix C). Group number according to Lee *et al.* (2013), [160].

Compound	pK_a [-]	$k_{O_3,MP}$ [M ⁻¹ s ⁻¹]	$k_{\bullet OH,MP}$ [M ⁻¹ s ⁻¹]	Group
Atenolol (ATO)	9.6 ± 0.1	$(4.0 \pm 0.6) \times 10^4$	$(8.0 \pm 0.5) \times 10^9$	II
Atrazine (ATZ)	4.2	$(7.0 \pm 1.3) \times 10^0$	$(2.3 \pm 0.4) \times 10^9$	IV
Benzotriazole (BTA)	8.4 ± 0.2	$(1.8 \pm 0.4) \times 10^3$	$(9.2 \pm 1.6) \times 10^9$	II
Bezafibrate (BZF)	3.6	$(3.3 \pm 3.9) \times 10^3$	$(7.8 \pm 0.3) \times 10^9$	II
Carbamazepine (CBZ)	16	3.0×10^5	$(7.0 \pm 2.7) \times 10^9$	I
Diclofenac (DCF)	4.2	1.0×10^6	$(9.7 \pm 2.5) \times 10^9$	I
Ibuprofen (IBU)	4.9	9.6×10^0	$(6.9 \pm 0.5) \times 10^9$	III

Concentrates for the ozonation experiments were produced on a pilot-scale membrane filtration plant (Figure C2, Appendix C) equipped with one 4" membrane module. 0.6 m³ water samples were delivered in IBCs. All membrane types described above (Table 5.1) were used in individual, successive runs to produce the respective concentrates. A polyphosphonic acid-based chelating agent (antiscalant) was added to all water samples in the same concentration to avoid potential scaling on the membranes (initial concentration: 2 mg L⁻¹, RPI-4000 A, Toray, Japan). Initially, the pilot plant (Figure C2, Appendix C) was set to the desired operational set point, i.e., permeate flow of 200 L h⁻¹, water yield of 85 % (achieved by adjusting a concentrate volume flow of 35.3 L h⁻¹), and a loop volume flow before the membrane of 1 m³ h⁻¹. The plant was left to run at least 1 hour to stabilize, recycling permeate and retentate back to the IBC feed tank. Finally, grab samples of the retentate were collected in annealed glass bottles, diverting the full concentrate stream into the bottle. During this time, the permeate was discarded into a separate permeate tank so that the feed water was not altered by dilution with permeate.

The concentrates were standardized before ozone treatment to guarantee good comparability. The standardization protocol is described in Appendix C. In brief, the concentrates were adjusted to the same pH = 8.3 ± 0.1 and concentrations of DOC, TIC, selected MPs (Table 5.2), bromide and borate as buffer. MPs were selected to represent a broad range of second-order rate constants.

Table C4 (Appendix C) provides water quality parameters before ozonation of the different standardized concentrates. Bromate was absent in all samples before ozonation. The MP concentrations in the range of 0.18 µM to 0.88 µM (C4, Appendix C) were selected to avoid sample preparation by solid phase extraction. The *pseudo* first-order scavenging rate constant of the background water matrix (S) was estimated by Equation 5.3.

$$S = \sum_i k_{\bullet OH,i} \times c_{i,0} \quad (5.3)$$

$k_{\text{OH},i}$ and $c_{i,0}$ are the second-order rate constant of the reaction of the $\bullet\text{OH}$ scavenger i with $\bullet\text{OH}$ and the concentrations of $\bullet\text{OH}$ scavenger i before ozonation, respectively. Typically, in surface waters, the main $\bullet\text{OH}$ scavengers are carbonate ($k_{\text{OH},\text{CO}_3^{2-}} = 3.9 \times 10^8 \text{ M}^{-1} \text{ s}^{-1}$, [151]), bicarbonate ($k_{\text{OH},\text{HCO}_3^-} = 8.5 \times 10^6 \text{ M}^{-1} \text{ s}^{-1}$, [151]) and dissolved organic matter ($k_{\text{OH},\text{DOC}} = (0.8 \text{ to } 3.3) \times 10^4 \text{ L (mg C)}^{-1} \text{ s}^{-1}$ with an average of $k_{\text{OH},\text{DOC}} = 2.4 \times 10^4 \text{ L (mg C)}^{-1} \text{ s}^{-1}$, [121], [164], [209]). Hence, S of the standardized concentrates was in the range of $1.7 \times 10^5 \text{ s}^{-1}$ ($(0.8 \text{ to } 2.3) \times 10^5 \text{ s}^{-1}$). The $\bullet\text{OH}$ scavenging rate by the spiked MPs never exceeded $0.2 \times 10^5 \text{ s}^{-1}$ and was typically $< 10\%$ of S . Therefore, the spiked MPs didn't interfere with the ozonation conditions, and the results can be transferred to real, i.e., non-spiked samples.

The standardized concentrates were ozonated at different specific ozone doses to investigate the abatement of MPs and formation of BrO_3^- . Details on the experimental standard protocol are provided in Appendix C. In brief, aliquots of the standardized concentrates were filled in glass vials, subsequently ozone was added from an ozone stock solution with a known ozone concentration.

Analytical Methods

The analytical methods are described in detail in Appendix C together with the limits of quantification, methods accuracies and the measurement ranges (Table C5, Appendix C). In brief, the electron donating capacity (EDC) was measured according to a modified standard protocol [210] by adding the radical cation of 2,2'-azino-bis(3-ethylbenzothiazoline-6-sulfonate) ($\text{ABTS}^{\bullet+}$) to dilution series of each concentrate buffered at pH 8.3 with 10 mM borate and subsequent measurement of the absorbance at 728 nm after 15 minutes reaction time. DOC was analyzed by size exclusion chromatography (SEC) coupled with an organic carbon detector (OCD) and an ultraviolet detector (UVD) at 254 nm (model 8b, DOC-Labor Dr. Huber, Germany). Micropollutants were measured by ultra-high pressure liquid chromatography (UHPLC) coupled with a tandem mass spectrometry (MS/MS). Bromide and bromate were separated by ion chromatography (IC) and measured by an inductively coupled plasma (ICP) coupled with MS/MS.

Results and Discussion

Relative Retentions by Membranes

The relative retentions of DOC, Br^- and MPs in bench-scale experiments with flat sheet membranes are provided in Table 5.3. While the DOC retentions were similar for all membranes, the membrane types strongly differ in their retentions of bromide and MPs. This means that the DOC is more efficiently concentrated in NF concentrates than Br^- . In contrast, in LPRO concentrates DOC and Br^- are concentrated to the same extend. In turn, this should make the

Chapter 5. Ozone Treatment of Concentrates

Table 5.3: Relative retentions of dissolved organic carbon (DOC), bromide (Br^-) and micropollutants (MP) by the investigated membranes (averages and standard deviations). Test conditions (unless stated otherwise): River Rhine rapid sand filtrate water (no spiking of MPs), 25 °C, 5.0 bar, pH 8.1, 75 % water recovery.

Membrane abbreviation	Molecular Weight [g mol ⁻¹]	NF1		NF2		LPRO	
		Rel. Retention		Rel. Retention		Rel. Retention ^a	
		[%]		[%]		[%]	
Solute		meas. ^b	estim. ^c	meas. ^b	estim. ^c	meas. ^b	estim. ^c
Dissolved organic carbon	-	97±0 ^d	-	96±0 ^d	-	97±0 ^d	-
Bromide	79.9	22±9	-	23±9	-	96±0	-
Benzotriazole (BTA)	119.1	24±18	-	36±15	-	86±3 ^e	-
Metformin (MET)	129.1	34±18	-	70±8	-	95±1	-
Diclofenac (DCF)	296.2	> 63±7 ^f	95±24	> 66±6 ^f	90±24	> 79±4	88±23
Iopromide (IPR)	791.1	> 90±1	97±11	> 90±1 ^e	100±12	> 96±0	93±11

^a Different pressure: 5.9 bar.

^b Relative measured (meas.) retentions were calculated with Equation 5.2. If $[i]^{\text{Permeate}}$ was < 0.01 µg L⁻¹, the measured retentions were calculated with $[i]^{\text{Permeate}} = 0.01 \mu\text{g L}^{-1}$ and retentions were marked with “>”.

^c Estimated (estim.) relative retentions were calculated if $[i]^{\text{Permeate}}$ was lower than the lowest calibrated concentration, i.e., 0.01 µg L⁻¹, with estimated permeate concentrations ($[i]^{\text{Permeate,*}}$) by closing the mass balance: $[i]^{\text{Permeate,*}} = [i]_0^{\text{Feed}} - 0.25 \times [i]^{\text{Concentrate}} / 0.75$, where $[i]^{\text{Concentrate}}$ is the concentration of a solute i in the feed tank at a water yield of 75 %.

^d Values from pilot-scale test with Lake Biel water at 85 % water yield.

^e The mass balance was not closed within a 95 % confidence interval of analytical uncertainties.

^f $c_{\text{Feed},0,i}$ was < 30 µg L⁻¹, i.e., < 3 times the lowest calibrated concentration.

NF concentrates more feasible than the LPRO concentrate for ozonation at similar specific ozone doses, because the relatively lower Br^- concentrations mean a lower bromate formation potential. Nevertheless, the membrane selection is typically determined by the permeate quality requirements with respect to the target MP concentrations and the LPRO membrane delivers a higher permeate quality.

Characterization of Standardized Concentrates

The EDC was measured as a parameter determining the phenol content of DOM, which is responsible for the initial ozone demand [211], [212]. Therefore, a high EDC indicates a high concentration of O_3 -reactive moieties [210], which for a given ozone dose might result in a lower O_3 exposure. Results of EDC measurements of the non-standardized concentrates are shown in Table 5.4. The absolute EDCs of standardized concentrates, shown in the respective second row of each cell in Table 5.4, varied within a factor of 2.2 and appeared to depend on the water source, i.e., the same order was observed for all investigated membranes: RW > RR > LB.

Table 5.4: Electron donating capacities (EDC) of non-standardized concentrates. All concentrates were measured at pH 8.3, buffered with 10 mM boric acid. EDCs are presented in the first rows. The second rows indicate the calculated absolute EDC of the standardized concentrates, i.e., EDC multiplied with DOC concentrations reported in Table C4 (Appendix C).

Membrane Water Source	LPRO	NF1	NF2
River Wiese (RW)	$3.8 \pm 0.1 \text{ mM e}^- (\text{g C})^{-1}$ $23 \pm 2 \text{ } \mu\text{M e}^-$	$3.7 \pm 0.1 \text{ mM e}^- (\text{g C})^{-1}$ $23 \pm 2 \text{ } \mu\text{M e}^-$	n.a. ^a
River Rhine (RR)	$2.3 \pm 0.2 \text{ mM e}^- (\text{g C})^{-1}$ $15 \pm 2 \text{ } \mu\text{M e}^-$	$3.5 \pm 0.1 \text{ mM e}^- (\text{g C})^{-1}$ $21 \pm 2 \text{ } \mu\text{M e}^-$	$4.2 \pm 0.1 \text{ mM e}^- (\text{g C})^{-1}$ $26 \pm 2 \text{ } \mu\text{M e}^-$
Lake Biel (LB)	$1.8 \pm 0.1 \text{ mM e}^- (\text{g C})^{-1}$ $12 \pm 1 \text{ } \mu\text{M e}^-$	$2.6 \pm 0.2 \text{ mM e}^- (\text{g C})^{-1}$ $16 \pm 2 \text{ } \mu\text{M e}^-$	$2.6 \pm 0.1 \text{ mM e}^- (\text{g C})^{-1}$ $16 \pm 1 \text{ } \mu\text{M e}^-$

^a not measured.

SEC-OCD or SEC-UVD chromatograms were not useful to detect differences between the standardized concentrates (data not shown). Minor differences were observed with respect to the water sources, which is explained by their different catchment areas. The membrane selection did not impact the SEC chromatograms.

The specific UV absorbances at 254 nm (SUVA_{254}) of the standardized concentrates were similar inside the standard uncertainty ($0.7 \text{ L mgC}^{-1} \text{ m}^{-1}$, estimated by the Gaussian error propagation rule, Table C4, Appendix C).

Treatment of Concentrates

Abatement of Micropollutants. The results for the abatement of MPs are shown in Figure C3 (Appendix C). The underlying data of all MP abatements and bromate yields discussed in this study are provided elsewhere in a “Dataset.csv” file, [42]. The abatements of MPs follow the order $\text{ATZ} < \text{IBU} < \text{BZF} \approx \text{BTA} < \text{ATO} < \text{CBZ} \approx \text{DCF}$. This agrees with the order expected from the second-order rate constants for reactions of the MPs with O_3 and $\bullet\text{OH}$ (Table 5.2). In the following, MPs with a high ozone reactivity are discussed, which are almost exclusively abated by reactions with O_3 (group I, i.e., CBZ and DCF). Then O_3 -resistant MPs are discussed, because their abatement can be mostly explained by reactions with $\bullet\text{OH}$ (groups III and IV, i.e., IBU and ATZ, respectively). Finally, MPs with a moderate ozone reactivity are discussed, where both reactions with O_3 and $\bullet\text{OH}$ are important for their abatement (group II, i.e., ATO, BTA and BZF).

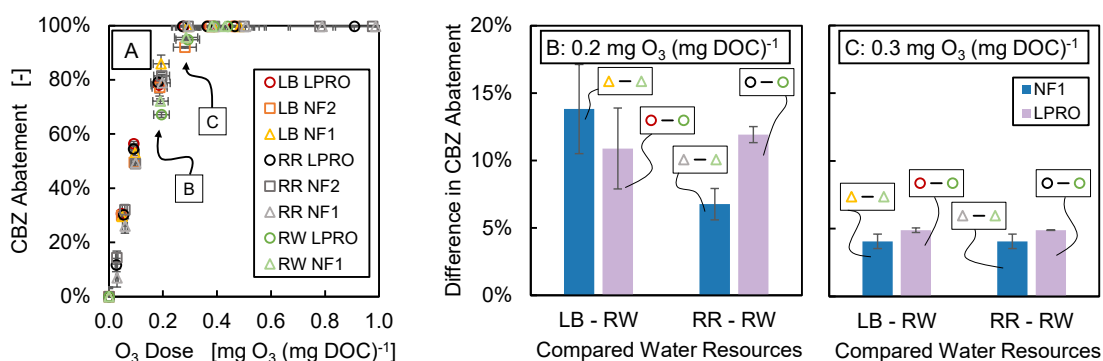


Figure 5.1: A: Abatement of carbamazepine (CBZ) as a function of the specific ozone dose. Error bars represent standard deviations of replicate experiments or, if no replicate experiment was conducted, calculated with the Gaussian error propagation rule. B and C: Differences in the relative abatements of CBZ in pair-wise comparisons between LB or RR and RW as reference, respectively, at specific O₃ doses of (B) 0.2 mg O₃ (mg DOC)⁻¹ and (C) 0.3 mg O₃ (mg DOC)⁻¹. Error bars represent standard deviations calculated with the Gaussian error propagation rule.

Micropollutants with High Ozone Reactivity. MPs with high ozone reactivity are abated to high extents even at relatively low specific O₃ doses. Typically, these compounds are abated predominantly by direct reactions with O₃, [213]. At about 0.2 mg O₃ (mg DOC)⁻¹, CBZ (Figure 5.1A) and DCF (Figure C4, Appendix C) were abated by 67 % to 86 % and 74 % to > 90 %, respectively, in different standardized concentrates with different raw waters. Figure 5.1B and C show the differences of the relative CBZ abatements of LB and RR compared to RW, respectively, for specific ozone doses of 0.2 and 0.3 mg O₃ (mg DOC)⁻¹. All differences between LB or RR and RW were significantly > 0 % ($p < 0.05$), which means a lower CBZ abatement in RW than in the other waters. The lower differences of about 5 % between RW and the other water sources at a specific ozone dose of 0.3 mg O₃ (mg DOC)⁻¹ can be explained by the already very high relative abatements close to 100 %. No statistically significant differences were observed between the other water sources or the membrane types. Similar results were obtained for DCF at 0.2 mg O₃ (mg DOC)⁻¹; at 0.3 mg O₃ (mg DOC)⁻¹, DCF was already abated to residual concentrations below the limit of quantification (Figure C4, Appendix C).

Based on the EDC values (Table 5.4), for a given specific O₃ dose, the ozone exposures were expected to follow the order: RW < RR < LB. Therefore, a lower abatement efficiency indicate for CBZ and DCF abatements in RW than in RR or LB can be expected, which is consistent with the results obtained in Figures 5.1 and C4 (Appendix C). This highlights that the ozone exposure was rather impacted by the water source and not by the membrane type.

Ozone Resistant Micropollutants. ATZ and IBU are almost exclusively abated by reactions with $\bullet\text{OH}$ (Table 5.2). It is known [157]–[159] that the $\bullet\text{OH}$ exposure can be calculated from the abatement of an ozone resistant probe compound from Equation 5.4:

$$\ln\left(\frac{[\text{MP}]}{[\text{MP}]_0}\right) = -k_{\bullet\text{OH},\text{MP}} \times \int [\bullet\text{OH}] \, dt - \underbrace{k_{\text{O}_3,\text{MP}} \times \int [\text{O}_3] \, dt}_{\approx 0} \quad (5.4)$$

$[\text{MP}]_0$ and $[\text{MP}]$ are the concentration of a MP before and after ozonation, respectively. $[\bullet\text{OH}]$ and $[\text{O}_3]$ are the time-dependent concentrations of $\bullet\text{OH}$ and O_3 , respectively.

IBU was used as a reference compound to assess the $\bullet\text{OH}$ exposure of the standardized concentrates. No statistically significant differences were found that indicated an impact of the membrane type or water source on the $\bullet\text{OH}$ exposure.

With small and similar contributions of reactions with ozone (Table 5.3), the ratio of $k_{\bullet\text{OH},\text{IBU}} / k_{\bullet\text{OH},\text{ATZ}} = 3.0 \pm 0.6$ (standard uncertainty calculated by Gaussian error propagation rule) determines the expected ratio of \ln abatements of these two MPs (black dashed line in Figure C5, Appendix C). However, the average ratio of the observed second-order rate constants was 1.4, i.e., about half the expected ratio, regardless of the water source or the membrane used. No analytical issues were observed for any of the MPs discussed here, i.e., linearity of the calibrations was acceptable throughout all measurement days ($R^2 > 0.995$ for all MPs) and matrix effects could be excluded from measurements of the MP recovery after spiking, both in ozonated and non-ozonated concentrates. The abatement of IBU was consistent with those of other MPs discussed below. Hence, ATZ was likely abated faster than expected, for unknown reasons. Further kinetic studies involving competition between ATZ and IBU are required to elucidate the reasons of this observation. Therefore, in the following, the discussions are based on IBU.

Micropollutants with Moderate Ozone Reactivity. Three MPs with moderate ozone reactivities were investigated in this study, i.e., ATO, BTA and BZF. Their abatement is expected to occur both by reactions with O_3 and $\bullet\text{OH}$. Plots of the negative natural logarithm of relative residual concentrations of BZF and BTA are shown in Figure 5.2 as functions of the negative natural logarithm of relative residual concentrations of IBU as $\bullet\text{OH}$ reference compound. The plots indicate that significant contributions of O_3 reactions only occurred at specific ozone doses $> 0.5 \text{ mg O}_3 (\text{mg DOC})^{-1}$ (highlighted data from experiments with RR standardized concentrates in Figure 5.2), because their abatements did not significantly exceed the abatement expected from reactions with $\bullet\text{OH}$ below this specific ozone dose. Based on the significant second-order rate constants for the reactions of BZF and BTA with ozone (Table 5.2), a more pronounced difference would be expected if the ozone exposures were significant for these specific ozone doses.

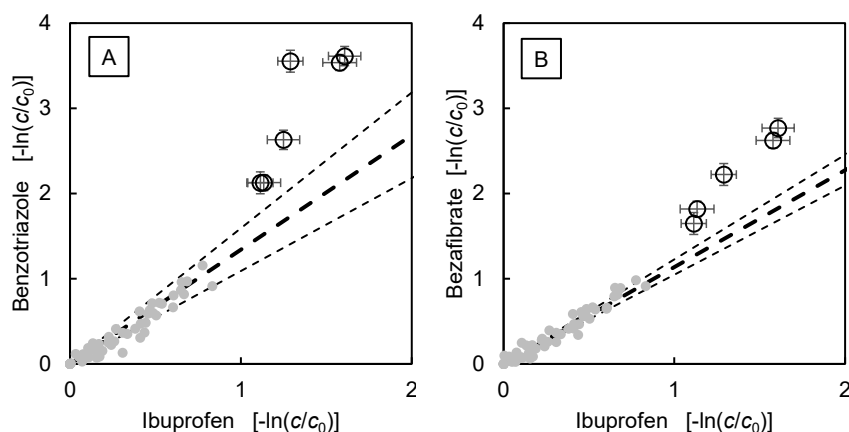


Figure 5.2: Negative natural logarithm of the relative residual concentrations of (A) benzotriazole and (B) bezafibrate as functions of the negative natural logarithm of the relative residual concentrations of ibuprofen. The bold black dashed lines represent expected ratios when the abatement is explained by reactions with $\bullet\text{OH}$ only, utilizing the corresponding second-order rate constants for reactions of the target compounds with $\bullet\text{OH}$ (Table 5.2). Standard deviations from the ratios of second-order rate constants are also shown in black dashed lines. Results of the experiments with standardized concentrates are shown as grey dots (without error bars for better readability of the plot). Experiments with specific O_3 doses $> 0.5 \text{ mg O}_3 (\text{mg DOC})^{-1}$ are shown as black circles. Error bars of the symbols represent standard deviations.

Formation of Bromate. Upon ozone treatment, bromate can be formed from bromide in a complex reaction mechanism including both O_3 and $\bullet\text{OH}$, [136], [201]. Results for η upon ozonation of the standardized concentrates are presented in Figure 5.3. For example, at a specific O_3 dose of about $0.4 \text{ mg O}_3 (\text{mg DOC})^{-1}$, $15 \pm 2 \mu\text{g BrO}_3^- \text{ L}^{-1}$ were formed on average (range: 11 to $19 \mu\text{g BrO}_3^- \text{ L}^{-1}$), corresponding to $\eta = 2.9 \pm 0.9 \%$ (range: 1.4 to 3.8 %). The bromate concentration is above the drinking water standard ($10 \mu\text{g BrO}_3^- \text{ L}^{-1}$), but below the proposed Swiss environmental quality standard ($50 \mu\text{g BrO}_3^- \text{ L}^{-1}$ [203], [204]).

For the same water source membrane-specific differences in bromate yields were observed, i.e., LPRO membrane (colored symbols in Figure 5.3) typically had higher bromate yields than the NF membranes. On average, η of the standardized LPRO membranes was $43 \pm 51 \%$ higher than those of the corresponding NF membranes at specific ozone doses in the range of 0.19 to $0.51 \text{ mg O}_3 (\text{mg DOC})^{-1}$. No statistical significance was observed except in RW at the highest specific ozone dose ($> 0.9 \text{ mg O}_3 (\text{mg DOC})^{-1}$) between LPRO and NF2.

The observed bromate yields are well within the range of those reported previously for municipal wastewater RO reject streams at a specific O_3 dose of $0.45 \text{ mg O}_3 (\text{mg DOC})^{-1}$ (Table C1, Appendix C, [207]), i.e., $3.1 \pm 1.5 \%$ (range: 0.8 to 4.5 %). The good agreement of the results was likely fortuitous because of the differences between the standardized concentrates investigated here and the non-standardized municipal wastewater concentrates investigated

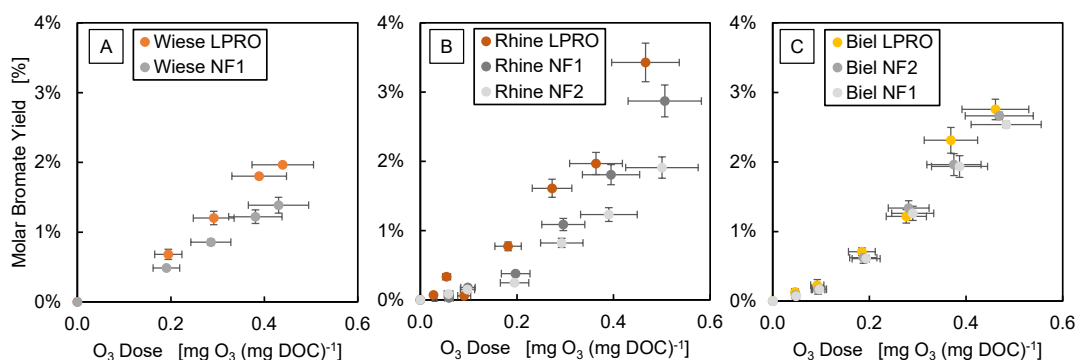


Figure 5.3: Molar bromate yields as a function of the specific ozone dose for various membrane concentrates in (A) RW, (B) RR and (C) LB. The yields were calculated according to Equation 5.1. The grey symbols represent the nanofiltration and the colored symbols the standardized low-pressure reverse osmosis concentrates, respectively. Initial bromide concentrations: 495 to 531 $\mu\text{g L}^{-1}$ (RW), 442 to 505 $\mu\text{g L}^{-1}$ (RR), 474 to 517 $\mu\text{g L}^{-1}$ (LB). Error bars represent standard deviations of replicate experiments or, if no replicate experiment was conducted, calculated with the Gaussian error propagation rule.

by King *et al.* (2020), [207]. In contrast, at a specific O_3 dose of about $0.2 \text{ mg O}_3 (\text{mg DOC})^{-1}$, η was $1.0 \pm 0.4 \%$ (range: 0.5 to 1.4 %), which was somewhat lower than η observed by Benner *et al.* (2008), [205]: 1.2 % at $0.17 \text{ mg O}_3 (\text{mg DOC})^{-1}$ and 1.8 % at $0.24 \text{ mg O}_3 (\text{mg DOC})^{-1}$ (Table C1, Appendix C, [205]). This highlights the dependence of the results on the water matrix composition and therefore underpins the necessity to standardize the concentrates in this study.

Tradeoff Between Micropollutant Abatement and Bromate Formation. Figure 5.4 shows the molar bromate yield in the standardized concentrates as functions of the abatement of representative MPs with high (DCF, group I) and moderate (BTA and ATO, group II) ozone reactivity and MPs of an ozone-resistant compound (IBU, group III). DCF and ATO were selected because they were studied before in ozonation of municipal wastewater RO concentrates and data was available for the corresponding bromate formation [207], [208]. IBU was compared with published results from diethyltoluamide (DEET) even though it has somewhat lower second-order rate constants for reactions with O_3 ($k_{\text{O}_3, \text{DEET}} = 0.1 \text{ M}^{-1} \text{ s}^{-1}$, [214]) and $\bullet\text{OH}$ ($k_{\bullet\text{OH}, \text{DEET}} = 5 \times 10^9 \text{ M}^{-1} \text{ s}^{-1}$, [215], i.e., group III).

Ozonation of standardized concentrates resulted in very similar abatements of MPs and formation of bromate. Hence, even if the water source or membrane selection impacted the O_3 and $\bullet\text{OH}$ exposures, this did not result in a change of the tradeoff between MP abatement and bromate formation. This finding is based on the connection of bromate formation and MP abatement by combinations of ozone and $\bullet\text{OH}$ reactions and the corresponding exposures. The results also highlight that the small differences in the dissolved organic matter composition between NF and LPRO membrane concentrates are of minor relevance for the treatment efficiency and the tradeoff between MP abatement and bromate formation.

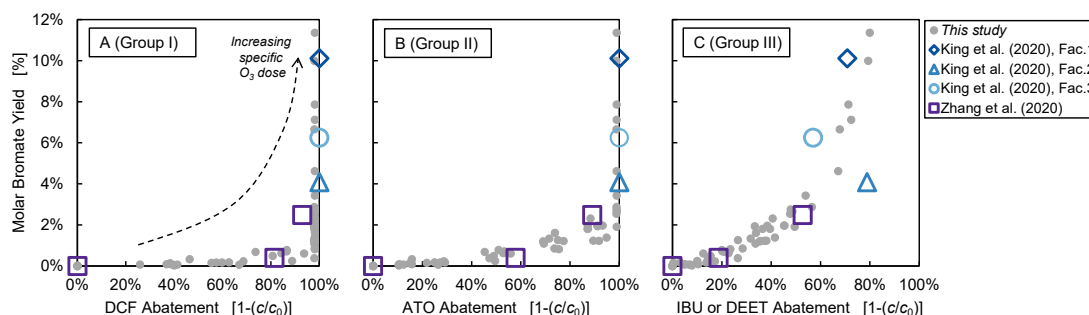


Figure 5.4: Bromate yields as functions of the abatement of selected micropollutants, A: diclofenac (DCF); B: atenolol (ATO); C: ibuprofen (IBU) or diethyltoluamide (DEET). The dashed black arrow in subplot A indicates the course of increasing specific O_3 doses, which is valid for all subplots. Classification into groups I to III according to the respective kinetic data (Table 5.2, [160]). Data from this study is presented in grey filled circles (without error bars for better readability of the plot). Results of this study are compared with previously published data from ozonation of municipal wastewater reverse osmosis concentrates with colored open symbols [207], [208]. Published abatements of DEET, [208], were used for comparison due to missing data for IBU and somewhat similar second-order rate constants, see text.

The data for the treatment of standardized concentrates from surface waters agree well with previously published data from non-standardized municipal wastewater RO concentrates, [207], [208], (colored open symbols in Figure 5.4), despite the highly different water qualities of the ozonated samples (colored open symbols in Figure 5.4) for specific ozone doses $> 1.0 \text{ mg } O_3 (\text{mg DOC})^{-1}$ despite the significantly different water qualities of the ozonated samples. Figure 5.4 highlights that the abatement of MPs in the standardized concentrates can be divided into three sections:

1. Low specific ozone doses $> 0.1 \text{ mg } O_3 (\text{mg DOC})^{-1}$ are sufficient for MPs with a high ozone reactivity such as DCF (group I, Figure 5.4A) to be abated by 50 % to 60 %. For the same doses, bromate yields are low, with $\eta < 0.2 \%$.
2. Moderate specific ozone doses in the range of 0.1 to $0.5 \text{ mg } O_3 (\text{mg DOC})^{-1}$ lead to an almost complete abatement of MPs with a high ozone reactivity (group I, Figure 5.4A) and are sufficient to abate MPs with a moderate ozone reactivity such as BTA (group II, Figure 5.4B) by up to 50 % to 60 %. In this range of specific ozone doses, the bromate yield linearly increases with the abatement of MPs and was typically $< 3 \%$. Therefore, bromide concentrations in the concentrate should be $< 200 \mu\text{g L}^{-1}$ to limit bromate formation to the drinking water standard of $10 \mu\text{g BrO}_3^- \text{ L}^{-1}$ at specific ozone doses around $0.5 \text{ mg } O_3 (\text{mg DOC})^{-1}$, i.e., the typical limit concentration for direct wastewater discharge, e.g., in Switzerland. This might limit the application of the investigated treatment chain in many cases. Considering the fact that municipal wastewater RO concentrates can contain bromide in concentrations in the range of 1 to 10 mg L^{-1} , this

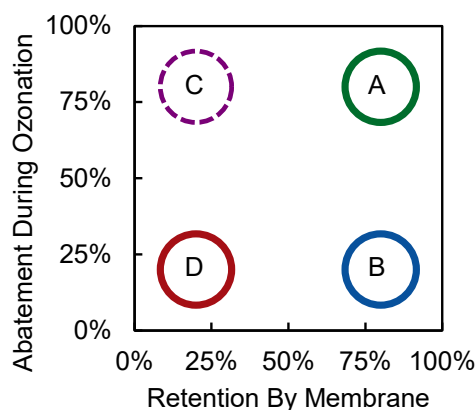


Figure 5.5: Representation of different types of micropollutants (MP) in the process chain of membrane filtration represented by the MP's retention (x axis) and subsequent abatement in concentrate ozonation (y axis). The different types of MPs, i.e., A to D, are discussed in Table 5.5. Type C is shown with a dashed edge because examples of this type are only known for nanofiltration membranes, e.g., benzotriazole (Table 5.5), but not for reverse osmosis membranes.

might result in bromate concentrations around 50 to 500 $\mu\text{g L}^{-1}$ (Table C1, Appendix C), i.e., in many cases even above the proposed Swiss environmental quality standard (50 $\mu\text{g BrO}_3^- \text{ L}^{-1}$ [203], [204]).

- Specific ozone doses $> 0.5 \text{ mg O}_3 (\text{mg DOC})^{-1}$ are required for an almost complete abatement of MPs with a moderate ozone reactivity (group II, Figure 5.4B) or to abate ozone resistant MPs such as IBU (group III, Figure 5.4C) by $> 50 \%$. For these specific ozone doses, bromate formation strongly increases with the ozone dose. An ozonation of concentrates with such specific ozone doses will be challenging considering the high bromate yields.

Overall, concentrate ozonation with significant abatement of MPs and limited bromate formation is only feasible for MPs from groups I and II (Figures 5.4A and B).

Evaluation of NF and RO Membrane Processes in Combination with Concentrate Ozonation

Ozonation of NF and LPRO concentrates were compared to assess the overall performance for MP abatement and bromate formation. Overall, four types of MP can conceptually be distinguished in process chains consisting of a membrane treatment with a subsequent concentrate ozonation, as illustrated in Figure 5.5, i.e., A, B, C and D and discussed in Table 5.5 in which the types of MPs are described.

First, the membrane treatment is evaluated (column “Treatment Step 1” in Table 5.5, i.e., x-axis in Figure 5.5). Compounds of types A or B are well retained by the membrane treatment, resulting in relatively low concentrations of these compounds in the permeate. In contrast, compounds of type C or D are retained to relatively low extents. A low retention results in relatively high concentrations of these compounds in the permeate. For this evaluation, the available experimental data with RR raw water samples was used (Table 5.3).

Then, the concentrate has to be treated for MP abatement before discharge with the corresponding necessary specific O_3 doses to achieve the local discharge limit concentrations of MPs and bromate. The abatement of the selected compounds upon ozonation of the concentrate is evaluated in Table 5.5 (column “Treatment Step 2”). This evaluation is based on experimental data for the abatement of BTA, DCF and IBU at specific ozone doses in the range of 0.24 to 0.61 mg O_3 (mg DOC)⁻¹ and the corresponding bromate yields for a non-standardized RW LPRO concentrate. This water source is different from membrane retention evaluation (RR); however, it was assumed that the MP abatement by ozonation does not significantly change with the water source, based on the findings presented above. Note that exposures of O_3 and $\bullet OH$ can significantly vary between real water sources due to differences, e.g., in the specific NOM’s ozone reactivity, $\bullet OH$ yield and $\bullet OH$ scavenging by the water background matrix, [121], [216], [217]. Nevertheless, in the context of the discussion here, these impacts are neglected.

The abatements of MPs in the non-standardized LPRO concentrate were comparable with those in the standardized LPRO concentrate (Appendix C). However, the molar bromate yields in the non-standardized LPRO concentrate were only about half the yields of the standardized LPRO concentrate at comparable specific O_3 doses (Figure C7, Appendix C). This is likely explained by the different ratios of Br^- : DOM and Br^- : S between the standardized and non-standardized concentrates and the different pH values.

The abatements of the ozone resistant MPs iopromide (IPR, group IV) and metformin (MET, group V) upon ozonation of the non-standardized LPRO concentrate were estimated based on the calculated $\bullet OH$ exposure from the abatement of IBU as $\bullet OH$ probe compound, [157]–[159], [161]. The calculations were performed with Eq. 5.4 with the corresponding second-order rate constants for the reactions with $\bullet OH$, $k_{\bullet OH, IPR} = 0.8 \times 10^9 \text{ M}^{-1} \text{ s}^{-1}$, [158], and $k_{\bullet OH, MET} = 0.5 \pm 0.8 \times 10^9$ (average and standard deviation of three reported values, [218]–[220]).

For compounds type A or C (MPs of groups I and II, [160]) in Figure 5.5 a good abatement during ozonation of the concentrate can be expected at specific ozone doses $\leq 0.6 \text{ mg } O_3 \text{ (mg DOC)}^{-1}$. In contrast, compounds type B or D are hardly abated during ozonation with specific O_3 doses $\leq 0.6 \text{ mg } O_3 \text{ (mg DOC)}^{-1}$.

Table 5.5: Retentions in dense membranes, observed second-order rate constants for ozone and hydroxyl radical, experimental or predicted relative abatements of selected micropollutants during ozonation, hydroxyl radical exposure and bromate yield in the non-standardized LPRO concentrate. For the retentions, the higher of the measured and estimated values reported in Table 5.3 was used here.

Compound	Treatment Step 1: Membrane Filtration		Treatment Step 2: Ozonation of Concentrate					Type of MP	Discussion
	Retentions in RR raw water (Table 5.3)		Kinetic data from literature	Experimentally determined abatements in RW non-standardized LPRO concentrate (pH 8.6)					
	Retention [%]		Second-order rate constants [M ⁻¹ s ⁻¹]	Specific O ₃ Dose [mg O ₃ (mg DOC) ⁻¹]					
	NF1	LPRO	k _{O₃,MP}	k [•] OH _{1MP} /10 ⁹	0.24	0.37	0.49		
Benzotriazole (BTA)	24	86	2.5 × 10 ³ⁱ	9.2 ⁱ	17 %	36 %	53 %	68 %	NF1: C LPRO: A If the low retention is sufficient for the required quality of the permeate, the concentrate treatment might be successful. Otherwise, a denser membrane has to be applied, which typically increases the subsequent bromate formation risk.
Diclofenac (DCF)	95	88	1.0 × 10 ³ⁱ	9.7 ⁱ	91 %	98 %	>99 %	> 99 %	A Treatment chain is well suited.
Ibuprofen (IBU)	-	-	9.6 × 10 ⁰ⁱ	6.9 ⁱ	20 %	28 %	38 %	46 %	- -
•OH exposure / 10 ⁻¹¹ [M s] ⁱⁱ	-	-	-	-	3.2	4.7	6.9	9.1	- -
	-	-	-	-	3.2	4.7	6.9	9.1	- -
Bromide (Br ⁻)	22	96	-	-	-	-	-	-	- -
Molar bromate yield (η)	-	-	-	-	0.2 %	0.4 %	1.0 %	1.5 %	- -
Metformin (MET) ^v	34	95	1.2 × 10 ⁰ⁱⁱⁱ	0.5 ± 0.8 ^{iv}	2 %	2 %	3 %	4 %	NF1: D LPRO: B The investigated treatment chain is not suited and other treatments have to be applied. Considering only the permeate quality, a denser membrane might be successful, but ozonation is not suited to abate MPs in the retentate.
Iopromide (IPR) ^v	97	>96	8.0 × 10 ^{-1vi}	3.3 ^{vi}	10 %	14 %	20 %	26 %	B High permeate quality can be reached, but a different concentrate treatment should be considered.

ⁱ From Table C2 (Appendix C); the observed second-order rate constant for reactions of BTA with O₃ was calculated for pH 8.6. ⁱⁱ Based on the abatement of IBU as reference compound and kinetic data reported in Table 5.2, neglecting small contributions of O₃ reactions to the abatement of IBU. ⁱⁱⁱ [147] ^{iv} Average and standard deviation of three reported values, [218]–[220]. ^v Abatement upon ozonation of the concentrate was predicted for MET and IPR. Predictions are based on oxidant exposures assessed with IBU as internal probe compound and referenced kinetic data reported from the literature, using Eq. 5.4. ^{vi} [158]

For an overall solution for MPs, the investigated treatment chain is well suited for type A compounds (Figure 5.5) such as DCF (Table 5.5), because they are well retained at the membrane and abated to high extends upon ozonation. Compounds of type B (Figure 5.5) such as IPR (Table 5.5) are well retained at the membrane, but their abatement in ozone treatment of the concentrate is limited. An additional activated carbon treatment after ozonation could improve the treated concentrate's quality to the accomplish the treatment goal, [221]. Hypothetical type C compounds (Figure 5.5, BTA for NF1 in Table 5.5, no compounds for LPRO) are retained to low extends by the NF1 membrane only. If retained, these compounds are well abated in the ozone treatment of the concentrate. For LPRO, there are no known compounds which fulfill these criteria. The worst case for the treatment chain are compounds of type D (Figure 5.5, MET for NF1 in Table 5.5, no compounds for LPRO), as they are hardly retained and hardly abated by ozone treatment in the concentrate. For LPRO, there are only very few examples such as chloroform and *N*-nitrosodimethylamide (NDMA), [25].

For compounds of type C and D using a NF membrane, the selection of a denser membrane might be suitable to improve the retention of such compounds, as in the case of BTA and MET (Table 5.5, compare "NF1" and "LPRO"). This can turn a compound type C to type A (Figure 5.5, e.g., BTA in Table 5.5) and a compound type D to type B (Figure 5.5, e.g., MET in Table 5.5). Nevertheless, for MET, a different concentrate treatment will be necessary, e.g., by a biological treatment [108].

Along with the retention of MPs and their abatement during ozonation of the concentrate, the retention of Br⁻ and the formation of BrO₃⁻ during concentrate ozonation is important for the assessment of the whole process train. An excessive formation of bromate might limit the application of the proposed treatment train. To compare the bromate formation risk for ozonation of NF1 and LPRO concentrates, the experimentally determined Br⁻ retention values (Table 5.3) were used to calculate Br⁻ concentrations in the concentrates. Given the retention R of a solute i at the membrane, the concentration in the concentrate can be calculated according to Eq. 5.5.

$$[i]^{\text{Concentrate}} = [i]^{\text{Feed}} \times \frac{1 - (W \times (1 - R_i))}{1 - W} \quad (5.5)$$

$[i]^{\text{Feed}}$ and $[i]^{\text{Concentrate}}$ are the concentrations in the membrane feed and concentrate, respectively. W is the water recovery, which was assumed to be $W = 85\%$ (Table 5.3) as for the production of the non-standardized concentrates. R_{Br^-} was known for bromide at $W = 75\%$ for a RR sample and assumed to be the same at $W = 85\%$ for a RW sample (Table 5.3). As a result, the Br⁻ concentrations in NF1 and LPRO concentrates are $2.2 \times [\text{Br}^-]^{\text{Feed}}$ and $6.4 \times [\text{Br}^-]^{\text{Feed}}$, respectively. Since the bromate formation is roughly proportional to the bromide concentration, the extent of bromate formation is about three times lower in the NF1 concentrate than in the LPRO concentrate.

To estimate the bromate yield upon concentrate ozonation, the resulting bromide concentration was multiplied with the experimentally determined. As discussed before, η of standardized NF1 concentrates were about 40 % lower than the standardized LPRO concentrates,

but no statistically relevant differences were found for specific O_3 doses $< 0.9 \text{ mg } O_3 \text{ (mg DOC)}^{-1}$. For this reason, non-standardized NF1 concentrates were assumed to have the same η as the non-standardized LPRO concentrate, which is a worst-case assumption for the NF1 concentrate treatment. Combining this information, bromate concentrations in the NF concentrate are estimated in the range of 0.4 % to 3.4 % $[Br^-]^{\text{Feed}} \times MW_{BrO_3^-} / MW_{Br^-}$, and for the LPRO concentrate in the range of 1.3 % to 9.7 % $[Br^-]^{\text{Feed}} \times MW_{BrO_3^-} / MW_{Br^-}$, respectively, depending on the investigated specific O_3 dose. To limit bromate concentrations in the treated concentrates to $\leq 10 \mu\text{g L}^{-1}$, $[Br^-]^{\text{Feed}}$ must therefore be $< 185 \mu\text{g L}^{-1}$ or $< 65 \mu\text{g L}^{-1}$ for the NF1 or LPRO membrane, respectively, for concentrate treatment with $0.61 \text{ mg } O_3 \text{ (mg DOC)}^{-1}$ and without additional bromate mitigation strategies (Figure C8, Appendix C).

Overall, the permeate quality with respect to MP concentrations is determined by the selection of the membrane. Denser LPRO membranes must be selected if only very low MP concentrations are acceptable in the permeate. However, this also considerably increases the risk of bromate formation, because the bromide concentration in the feed water should be $\lesssim 65 \mu\text{g L}^{-1}$. Therefore, during ozonation of concentrates, only MPs with a high or moderate ozone-reactivity are significantly abated with low to moderate specific O_3 doses, with acceptable bromate formation.

Conclusions

Concentrates of the rivers Rhine (RR) and Wiese (RW) and of Lake Biel (LB) waters were obtained from a low-pressure reverse osmosis (LPRO) membrane and two nanofiltration (NF) membranes. After standardization of the concentrates at $\text{pH} = 8.3 \pm 0.1$ and the same concentrations of dissolved organic carbon (DOC), total inorganic carbon (TIC), bromide (Br^-) and spiked micropollutants (MPs), the impact of the membrane selection and raw water type upon ozonation was investigated. The following conclusions can be drawn:

- It was demonstrated that the water source was the main factor impacting the electron donating capacity (EDC). The expected lower ozone exposures for higher EDCs are consistent with the lower abatement of diclofenac and carbamazepine in waters with higher EDCs ($RW < RR < LB$).
- Upon ozonation of the standardized concentrates, the investigated MPs (atenolol, atrazine, benzotriazole, bezafibrate, carbamazepine, diclofenac, ibuprofen) were abated to different degrees, in agreement with their second-order rate constants for the reactions with O_3 and $\cdot OH$. The tradeoff between the desired MP abatement and undesired bromate formation was neither impacted by the water source, nor by the membrane type. Ozonation of concentrates at limited bromate formation was only feasible for MPs with a high or moderate ozone reactivity.

- An assessment of the MP abatement and bromate formed upon ozonation for non-standardized concentrates highlighted the interplay of the membrane and the subsequent concentrate treatment. The LPRO membrane had a higher retention of MPs and bromide than the investigated NF membranes. Nevertheless, for lower MP retention requirements, NF membranes might be a better choice because their concentrates will lead to lower bromate concentrations upon ozonation.

Acknowledgements

Elisabeth Muck is acknowledged for her support to prepare and perform the ozonation experiments. Joanna Houska is acknowledged for measuring the electron donating capacities of the concentrates. Uwe Hübner is acknowledged for supervising Marlies Prahtel's master's thesis. Richard Wülser and his team are acknowledged for the measurement of the micropollutant concentrations of the membrane retention tests. Axel Jakob is acknowledged for providing the membrane modules. Energie Service Biel is acknowledged for providing the Lake Biel water sample. The analytical methods for the measurement of micropollutants was developed within the HLS research project "ANNETTe", funded by the FHNW School of Life Sciences. This study was conducted within the "OXIBIEAU" project, with co-funding from the Swiss Gas and Water Association (Schweizerischer Verein des Gas- und Wasserfaches, SVGW).

Which Way to Go? Part IV

6 Multi-Criteria Assessment of the Investigated Treatment Options

A multi-criteria assessment (MCA) of the investigated treatment options is conducted, i.e., (i) a full-stream UV/H₂O₂ treatment or, (ii), a side-stream LPRO treatment with concentrate ozonation. A similar assessment was conducted within the OXIBIEAU project. The final report is available for members of the Swiss Gas and Water Association (SVGW) [222].

Multi-criteria assessments (MCA) were published before to evaluate technologies for MP abatement in the fields of wastewater treatment [223]–[226], (in)direct potable reuse [227]–[229] and drinking water production [230], [231]. Table 6.1 provides an overview of the criteria assessed in these publications. MCAs are most relevant in (pre-)feasibility studies or the evaluation of process options and typically consist of the following steps:

First, different criteria are collected that are considered important for the decision-making. Typically, these criteria are based on technological considerations (e.g., feasibility of a technology, degree of (over-)fulfillment of a treatment target) and holistic sustainability categories, i.e., economic, environmental and social factors, see Table 6.1. It is advisable to analyze the selected criteria for inter-dependencies to avoid (unintended) weighting of single influencing parameters. Ideally, the selected criteria are independent from each other, although this can be hard to achieve. For example, operational expenditure (OPEX) is typically directly linked to specific electrical energy demand and the latter can also be connected to, e.g., environmental impacts such as the carbon dioxide footprint. Hence, if OPEX and CO₂ footprint are selected as criteria, both are typically affected by the specific electrical energy demand. Therefore, specific electrical energy demand might be a more useful parameter to assess as an independent parameter; otherwise, the evaluator should be aware of the inter-connection of the two other criteria and consider this in the interpretation of the results. To solve such issues connected to the inter-dependencies of criteria, in life cycle assessments, some methods allow for eval-

uations at mid-point (e.g., specific energy demand) or end-point level (e.g., consequences described above) [232]. However, this analysis was not yet conducted at any of the reviewed MCAs presented in Table 6.1 and should be subject of further research.

In a second step, a method to evaluate the assessed options with respect to all criteria is selected. Different methods were deployed for the evaluation of technologies for MP abatement and some can incorporate uncertainty of the underlying data [226, and references therein]. In principle, it is also possible to use multiple evaluation methods and, by this, test the sensitivity of the MCA result on the selected method.

Finally, by assigning weighting factors to certain criteria, it is possible to (willingly) prioritize certain criteria over others. Weighting is typically a matter of subjective and temporary decision. Some authors therefore calculated weighting factors based on the opinion of several experts to minimize potential biases by personal preferences [226], [230].

It is advisable to check the robustness of MCA results by including, e.g., a sensitivity analysis [226], [228], [230]. By this, factors can be identified that strongly impact the final results. In addition, a sensitivity analysis allows to check if one alternative is better suited to solve a certain task than another, or if they perform equally well within the range of (data) uncertainty.

Here, a modified MCA of the assessment conducted within the OXIBIEAU project [222] is presented, i.e., the assessed process trains are simplified compared to the OXIBIEAU project. The MCA includes:

- Technological aspects, i.e., both systems are designed to achieve a certain degree of MP abatement as a minimum requirement.
- Economic aspects in terms of a cost assessment including estimates of the capital expenditures (CAPEX) and operational expenditures (OPEX). The cost estimates are based on experts' estimates (technology vendors) for the equipment costs, which is multiplied by a factor to estimate the total CAPEX.
Cost assessment was preferred over the assessment of more fundamental parameters such as, e.g., specific electrical energy demand, because costs are typically easier to communicate to decision-makers in today's economy. Nevertheless, the costs are typically site specific due to, e.g., local energy and chemical prices.
- Environmental aspects by means of a simplified life cycle assessment (LCA), i.e., the LCA carried out considers the operational phase only. This simplification was considered valid in most cases because a more detailed LCA of the processes assessed demonstrated that the major environmental impacts are typically caused in the utilization phase of the technologies [44].
- Other aspects, such as disinfection efficiency. Social criteria were not assessed here and should be subject of future research.

This chapter is structured along this sequence of aspects and ends with a summary of the results and further research needs to complete a holistic MCA.

Table 6.1: Criteria considered in published multi-criteria assessments in the field of water treatment with a link to micropollutant abatement.

Field	Wastewater treatment			Potable reuse		Drinking water production		
Reference	Garrido-Baserba <i>et al.</i> (2016) [223]	Fernández-López <i>et al.</i> (2021) [225]	Salamiрад <i>et al.</i> (2021) [226]	Sadr <i>et al.</i> (2015) [227]	Yuan <i>et al.</i> (2019) [228]	Echevarría <i>et al.</i> (2020) [229]	Sudhakaran <i>et al.</i> (2013) [230]	Ribera <i>et al.</i> (2014) [231]
technological criteria	treatment effectiveness operation simplicity robustness space constrains innovation degree reliability cost-benefit analysis environmental benefit analysis	hydraulic retention time average annual temperature treatment capacity technology applied removal efficiencies (TSS, COD, BOD)	system efficiency complexity durability investment O&M ^a waste disposal improvement costs energy consumption impact of noise visual impacts odor impacts contribution to global warming carbon dioxide emission use of natural resources sludge production dangerous by-products public acceptance educational level of workers workforce requirement human health risks ^c water quality risks ^d hydro-geological risks occupational health, safety, and satisfaction government laws and regulations	adaptability ease of construction and deployment land requirement water quality and reliability capital cost O&M ^d energy consumption energy consumption impact on environment	treatability qualitative cost ranking qualitative environmental ranking ^b	water quality constrains average abatement of MPs	removal of MPs and NOM formation of by-products reliability/maintenance potential for modification residence time costs land use waste discharge carbon footprint use of energy and chemicals	
economic criteria						CAPEX + O&M ^a		
environmental criteria	eutrophication potential global warming potential					carbon footprint		Life cycle assessment (Recipe mid-point)
social criteria				community acceptance level of technological complexity			public acceptance professional skill required	human health risk ^e

^a i.e., operation and maintenance.

^b i.e., energy requirements, residual generation.

^c i.e., removal of bacteria, virus, protozoa, pathogens, residual toxicity and heavy metals.

^d i.e., salinity, nutrients, contribution to acidification.

^e i.e., cancer from trihalomethane formation potential.

Technological Aspects: Required Abatement and System Design

The proper dimensioning of the technical systems is of high relevance to fulfill the defined treatment goal(s) cost-efficiently. Here, the following two pretreatment scenarios are discussed before a soil infiltration and aquifer recharge:

1. An advanced oxidation process of the full-stream including a 4 mg H₂O₂ L⁻¹ dosage and subsequent radiation with ultraviolet light (UV dose: 5'800 J m⁻²) at an almost mono-chromatic wavelength of 254 nm (as investigated in Chapter 3).
2. A treatment of a side-stream by a low-pressure reverse osmosis which covers 72% of the water volume flow sent to the subsequent SAT treatment, and ozonation of the produced retentate with a specific O₃ dose of 0.4 mg O₃ (mg DOC)⁻¹ before its discharge, e.g., to a river (as investigated in Chapter 5).

For a fair comparison, both treatment systems were designed according to the same general boundaries. The nominal treatment capacity of each unit process was adjusted so that the pretreatment process train delivers an average water volume flow of 2'520 m³ h⁻¹. Peak flow volumes were not considered. Both pretreatments aimed at a maximum concentration of measured MPs of 0.1 µg L⁻¹ after a subsequent soil aquifer treatment. Hence, the pretreatment systems were designed to abate MPs that are present in the raw water (i.e., the river Rhine rapid sand filtrate water) in concentrations above this limit. Details on the derivations of the designs are provided in Appendix D.

Economic Aspects: Costs

Costs were assessed based on equipment costs provided by technology vendors. To estimate the CAPEX, the total investment costs (i.e., sum of costs for equipment, installation, yard piping, sitework landscaping, site electrics and controls, contractor overhead and profit, contingency, engineering, legal and admission), a factor method was used, i.e., the equipment costs were multiplied with 3.44 [43]. The estimated total costs are accurate within -30% to +50%, i.e., suitable for conceptual-level engineering-cost estimates [43].

The utilized factor (2.54 for estimates without engineering costs) is lower than typical Lang factors, which can be used to estimate the costs of projects in the chemical industry without engineering costs based on the costs of all essential plant elements, i.e., the equipment costs. Lang factors are $f_L = 3.10$ for simple processing plants, e.g., for stones, and $f_L = 3.63$ for simple chemical plants, [233]. The cause for the differences cannot be elucidated within the scope of this study. Nevertheless, for consistency with costs assessed by cost equations modified from Plumlee *et al.* (2014) (Appendix D), the same factors were used [43].

Estimates for CAPEX and OPEX of the UV/H₂O₂ pretreatment are shown in Tables 6.2 and

Table 6.2: Capital expenditures (CAPEX) of the UV/H₂O₂ treatment. Design: nominal flow rate: 2'520 m³ h⁻¹, 92% UV transmissivity, maximal UV fluence: 6'700 J m⁻² (one K143 12-24 UV reactor, Xylem), but operated at a UV fluence of 5'800 J m⁻². Annuities were calculated with an interest rate of 5.1% (weighted average cost of capital for utilities in Switzerland, January 2021 (www.waccexpert.com)) and the respective lifetime.

Item	Costs [€]	Lifetime [a]	Annuity (rounded to next 1'000) [€ p.a.]
Reactors	505'000	20	41'000
Quartz sleeves	167'000	7	29'000
H ₂ O ₂ dosing station	130'000	20	11'000
H ₂ O ₂ dosing pumps	20'000	10	3'000
Sub total	822'000		84'000
CAPEX equipment	822'000		
Factor	×3.44		
Total CAPEX (estimated, rounded)	2'830'000		
CAPEX except equipment	2'008'000	30	132'000
Total annuities (CAPEX)			216'000

6.3. OPEX estimates included costs for the electrical energy, H₂O₂, lamp replacement and service. Re-investment costs for the equipment were considered in the specific costs by the CAPEX annuities. Overall, the initial CAPEX was estimated around 2.8 million €. The OPEX for electrical energy, H₂O₂, lamp replacements and annual service was about 0.24 million € per year. Adding the annualized CAPEX to the OPEX yields the total specific costs of 0.021 € m⁻³. For comparison, the same treatment was calculated with the cost equations of Plumlee *et al.* (2014). The CAPEX was estimated with Equation D8 (Appendix D). With prices adjusted from the September 2011 (9'116 points) to the 2020 average *Engineering News-Record* (ENR) Construction Cost Index (CCI, 11'466 points), [234], and an exchange rate of 1€ = 1.1422\$ (average of 2020), the CAPEX was estimated to be 2.8 million €. This is in agreement with the estimated costs from the OXIBIEAU project. The OPEX was estimated with Equation D10 (Appendix D) and includes costs for H₂O₂, electrical energy and lamp replacements. The OPEX was estimated to be 0.29 million € per year. For the OPEX prices were not adjusted with the ENR CCI, because this adjustment is only relevant for construction. While the estimated OPEX by Plumlee *et al.* (2014) agrees well with the OPEX without re-investments (CAPEX annuities) estimated within the OXIBIEAU project, the similar values are rather fortuitous because different prices for electrical energy and H₂O₂ were assumed: Plumlee *et al.* (2014) used an energy price of 0.0865 € kWh⁻¹ and a H₂O₂ price around 540 € (t H₂O₂, 50% wt.)⁻¹. The corresponding data used for the assessments from the OXIBIEAU project are shown in Table 6.3.

Chapter 6. Multi-Criteria Assessment of the Investigated Treatment Options

Table 6.3: Operating expenditures (OPEX) of the UV/H₂O₂ treatment system assessed in the OXIBIEAU project. Details of the design are given in Table 6.2. The OPEX was calculated for a treatment of the nominal flow rate of 2'520 m³ h⁻¹ with a H₂O₂ dose of 4 mg L⁻¹ (i.e., 8 mg H₂O₂ L⁻¹ of the 50% wt. stock solution) and a UV fluence of 5'800 J m⁻².

Item	Value	Unit	Specific costs	Unit	Annual costs (€, rounded to next 10'000)
Energy	0.066	kWh m ⁻³	0.1	€ kWh ⁻¹	150'000
H ₂ O ₂ (50%)	8	mg L ⁻¹	410	€ ton ⁻¹	40'000
Lamp replacement					40'000
Manufacturer's service	1	p.a.	10'000	€ per execution	10'000
Subtotal OPEX					240'000
CAPEX annuities	see Table 6.2				216'000
Total annual costs					458'000
Total specific costs					0.021 € m ⁻³

Estimates for CAPEX and OPEX for the scenario of the side-stream LPRO treatment are shown in Tables 6.4 and 6.5. The CAPEX for the membrane pretreatment with concentrate ozonation was estimated around 10.6 million €. This is about 3.8-fold higher than the CAPEX of the UV/H₂O₂ scenario. Also, the OPEX was estimated to be around 0.71 million €, i.e., about a factor 3 higher than in the UV/H₂O₂ scenario and mainly caused by the higher costs for the electrical energy for the membrane treatment. The concentrate ozonation only added little to the equipment costs ($\approx 20\%$) and OPEX ($< 10\%$). The estimated treatment costs were lower than estimates by Echevarría *et al.* (2019) for ultrafiltration + RO (0.20 € m⁻³) or powdered activated carbon + NF (0.25 € m⁻³) systems for indirect potable reuse of municipal wastewater reclamation [229]. However, little information was provided by Echevarría *et al.* (2019) how the costs were derived and, hence, the costs from this study cannot be compared well.

Estimating the CAPEX with the modified cost functions from Plumlee *et al.* (2014), i.e., Equations D12 and D17 to D21 (Appendix D), the costs for the total treatment train were significantly higher, i.e., 59.7 million €. The main costs, i.e., 52.7 million €, were estimated for the membrane system. The cause for the significantly higher CAPEX estimated by the modified cost functions from Plumlee *et al.* (2014) is not clear. One reason might be higher demands for the materials, because the cost functions were developed for water reuse applications from municipal wastewater, which is a brackish water (500 to 2000 mg L⁻¹ total dissolved solids). Systems were presumably designed for an operation at 30 bar (Appendix D). In addition, hypothetically the membranes considered by Plumlee *et al.* (2014) had a lower flux than the membranes considered in this study, and this in combination with presumably higher prices per membrane module might lead to higher investment costs. The OPEX estimated with the modified cost functions from Plumlee *et al.* (2014), i.e., Equations D13 and D22 (Appendix D), was 3.2 million € per year, i.e., about 4.5 times higher than estimated in this

Table 6.4: Capital expenditures (CAPEX) of the low-pressure reverse osmosis (LPRO) membrane treatment with ozone treatment of the concentrate assessed in the OXIBIEAU project. Design: nominal flow: 2'520 m³ h⁻¹. The LPRO membranes (TMH20A, Toray) covers 72% of the total volume flow, i.e., 1'815 m³_{Permeate} h⁻¹ (three stage design, pressure vessels: 624, membrane modules: 3'744, membrane area per module: 41 m², feed pressure first stage: 8.2 bar). The concentrate treatment was designed to treat 320 m³ h⁻¹ with 0.4 mg O₃ (mg DOC)⁻¹ (assumed average feed DOC: 1.4 mg L⁻¹, DOC retention: 97%, i.e., 9.1 mg DOC L⁻¹). The subsequent ozone contact chambers were designed for a 15 minutes hydraulic residence time and its costs were estimated using Eqs. D17 to D20 (Appendix D). Annuities were calculated with an interest rate of 5.1% (weighted average cost of capital for utilities in Switzerland, January 2021 (www.waccexpert.com)) and the respective lifetime.

Item	Costs [€]	Lifetime [a]	Annuity (rounded to next 1'000) [€ p.a.]
Membrane system			
Pre-filters	160'000	20	13'000
Membranes	1'750'000	5	405'000
Racks and pressure vessels	370'000	20	30'000
Pumps	200'000	20	16'000
Dosing pump	20'000	10	3'000
Sub total	2'500'000		467'000
Concentrate treatment			
Ozone generators	490'000	20	40'000
Contactor chambers	100'000	30	7'000
Sub total	590'000		46'000
CAPEX equipment	3'090'000		
Factor	×3.44		
Total CAPEX (estimated, rounded)	10'630'000		
CAPEX except equipment	7'540'000	30	496'000
Total annuities (CAPEX)			1'009'000

Chapter 6. Multi-Criteria Assessment of the Investigated Treatment Options

Table 6.5: Operating expenditures (OPEX) of the low-pressure reverse osmosis (LPRO) membrane treatment with ozone treatment of the concentrate assessed in the OXIBIEAU project. The OPEX was calculated for a treatment of the nominal membrane feed flow rate of 2'135 m³ h⁻¹ and a water recovery rate of 85% (i.e., nominal permeate flow rate: 1'815 m³ h⁻¹, concentrate flow rate: 320 m³ h⁻¹) at an average water temperature of 13 °C. The concentrate ozonation was calculated with a specific O₃ dose of 0.4 mg O₃ (mg DOC)⁻¹ and an average DOC concentration of 9.1 mg L⁻¹.

Item	Value	Unit	Specific costs	Unit	Annual costs (€, rounded to next 10'000)
Membrane system					
Energy	0.364	kWh m ⁻³ _{permeate}	0.1	€ kWh ⁻¹	580'000
Antiscalant	1.68	mg L ⁻¹ _{membrane feed}	2.36	€ kg ⁻¹	70'000
Cleaning chemicals	divers	-	-	-	20'000
Sub total					670'000
Concentrate treatment					
Energy	0.036	kWh m ⁻³ _{concentrate}	0.1	€ kWh ⁻¹	10'000
LOX	11.6	kg LOX h ⁻¹	0.2	€ (kg LOX) ⁻¹	20'000
Cooling water	1.6	m ³ _{cooling water} h ⁻¹	0.1	€ m ⁻³ _{cooling water}	≈0
Manufacturer's service	1	p.a.	10'000	€ per execution	10'000
Sub total					40'000
Subtotal OPEX					710'000
CAPEX annuities	see Table 6.4				1'009'000
Total annual costs					1'719'000
Total specific costs					0.078 € m ⁻³

Table 6.6: Process inputs to the UV/H₂O₂ and membrane + concentrate ozonation processes during the operation.

Input	Unit	Value
Full-stream UV/H ₂ O ₂ treatment		
Electrical Energy	kWh m ⁻³	0.066
H ₂ O ₂ (50% wt/wt)	kg m ⁻³	8
Side-stream LPRO treatment with concentrate ozonation		
Electrical Energy	kWh m ⁻³ _{Permeate}	0.364
Ozone Processes		
Electrical Energy	kWh (kg O ₃) ⁻¹	8.7
Liquid Oxygen (LOX)	kg LOX (kg O ₃) ⁻¹	10

study. Considering the fact that the operating pressures in the estimates Plumlee *et al.* (2014) by were likely 3.6-fold higher than assumed by the LPRO membrane vendor, the higher OPEX is largely explained from higher electrical energy demands by the membrane treatment.

In conclusion, the costs of the UV/H₂O₂ pretreatment were about 3 to 4 times lower than by the LPRO pretreatment with concentrate ozonation. While the cost functions modified from Plumlee *et al.* (2014) yield the same cost estimates of the UV/H₂O₂, the equations are not suited for the estimate of surface water LPRO membrane systems.

Environmental Aspects: Life Cycle Assessment

LCA Method

In the light of the global environmental crisis, including climate change, it is reasonable to consider the environmental impacts of the pretreatment scenarios in a decision making process. Concerning the technologies under investigation here, a recent study by Roth *et al.* [44] showed that the majority of the environmental impacts are typically generated during the utilization phase of the technologies, i.e., by the electrical energy, H₂O₂ and liquid oxygen (LOX) [44], [222], [235]. Hence, the environmental impacts can be approximated considering only the impacts caused by these factors (Table 6.6). Combining the process specific inputs with their specific environmental impacts (Table 6.7), the environmental impact of the respective process train can be assessed.

The life cycle assessment (LCA) method is standardized in the ISO EN 14040. First, goal and scope are defined, e.g., the assessment of two treatment chains with the same treatment goal (abatement of MPs to a certain extend, see above). This includes the definition of system boundaries (UV/H₂O₂ process or membrane process with concentrate ozonation; construc-

Chapter 6. Multi-Criteria Assessment of the Investigated Treatment Options

Table 6.7: Environmental impact points of various process inputs. Data calculated with the European ILCD2011 method as single-score results [232]. 'Wind' and 'hydro' were newly created based on an existing country mix, replacing the energy sources by the respective form of electricity production. The new models therefore include production of electrical energy at high voltage, transformation to medium voltage and the transmission network.

Item	Type	Unit	Climate Change [kg CO ₂ -eq. per unit]	Single score [10 ⁻⁶ Pt per unit]
H ₂ O ₂ (50% wt/wt)	Market (Europe)	1 kg	1.02×10^0	2.60×10^2
Liquid Oxygen	Market (Europe)	1 kg	7.01×10^{-1}	7.05×10^1
Electricity (medium voltage)				
Europe	Market	1 kWh	4.98×10^{-1}	4.63×10^1
US	Market	1 kWh	6.56×10^{-1}	6.30×10^1
Global	Market	1 kWh	7.54×10^{-1}	6.73×10^1
Wind	Grid	1 kWh	2.32×10^{-2}	8.64×10^0
Hydro	Grid	1 kWh	9.99×10^{-3}	2.88×10^0

tion of the infrastructure, water as a resource, its treatments upstream and downstream the investigated processes, and formation of by-products in oxidative treatments were neglected). The functional unit is defined here as 1 m³ water treated for the subsequent treatment (soil infiltration in this case). As assessment method, the European method International Reference Life Cycle Data system (ILCD2011) was used, which describes environmental impacts in 16 impact categories [232]. 1 point (Pt) in the ILCD single score corresponds to the average annual environmental impact of one European citizen in 2010. The software SimaPro (V.9.0.0.48, PRé Consultants, The Netherlands) was used to build the LCA models, using the EcoInvent database (V.3.3, www.ecoinvent.org) for all background processes. Long-term emissions were generally excluded and all impacts were allocated to the point of substitution. Further details on the ILCD method are provided in Appendix D.

For the process inputs of the simplified life cycle inventory, Table 6.7 lists the impact on the climate change category and the single score result. Climate change was shown separately because this impact category is currently of great concern.

LCA Results and Discussion

Figure 6.1 shows ILCD2011 single score results of the investigated treatments, i.e., full-stream UV/H₂O₂ or side-stream treatment a LPRO membrane and subsequent concentrate ozonation. Different electrical energy sources were investigated to highlight country-specific differences along with two renewable energy sources.

For the investigated average electrical energy mixes of 2015 the UV/H₂O₂ treatment generates fewer environmental impacts than the side-stream LPRO treatment in every single impact

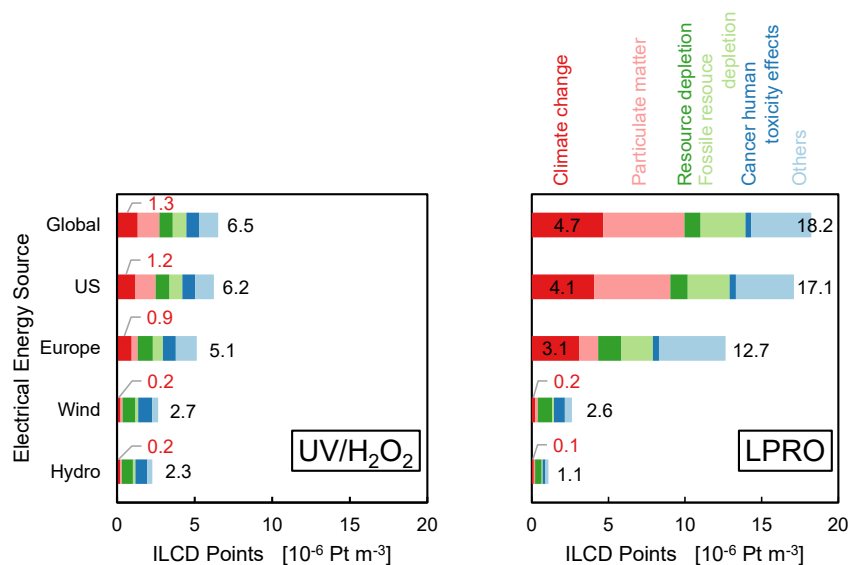


Figure 6.1: ILCD2011 single scores of the pretreatment scenarios. Three electricity energy country mixes (global average, US, Europe) or two renewable energy sources (onshore wind turbine, hydro power from run-of-river power plant) were assessed. Colors of the bars signify the ILCD2011 impact categories that contributed most to the total environmental impact. The black figures at the far right of each stacked bar show the total ILCD points. The dark red figures and those located in the dark red category indicate the points from the climate change category. All treatment trains were designed for a product volume flow of $2'520 \text{ m}^3 \text{ h}^{-1}$ from an average river Rhine rapid sand filtrate water ($1.4 \text{ mg DOC L}^{-1}$, UV absorbance at 254 nm : 3.6 m^{-1}). UV/H₂O₂ treatment with $4 \text{ mg H}_2\text{O}_2 \text{ L}^{-1}$ and a UV fluence of $5'800 \text{ J m}^{-2}$. Side-stream LPRO treatment with a nominal permeate flow rate of $1'815 \text{ m}^3 \text{ h}^{-1}$ (85% water recovery, 97% DOC rejection). Concentrate ozonation with a specific O₃ dose: $0.4 \text{ mg O}_3 (\text{mg DOC})^{-1}$.

category assessed (except cancer human toxic effects). In a European context, the additional treatments cause 5.1×10^{-6} and 12.7×10^{-6} ILCD points m^3 , respectively (Figure 6.1). Assuming an average daily drinking water consumption of about 200 L per person, the additional treatment would only account for about 0.3 to 0.9×10^{-3} ILCD points in one year, i.e., negligible environmental impacts are caused. For comparison, the conventional production of 1 m^3 drinking water from surface water (raw surface water intake, coagulation with aluminum sulfate, sedimentation, rapid sand filtration, UV disinfection, pressurizing for distribution) has an environmental impact of 0.2×10^{-3} ILCD points in a European context. This means that the additional treatment only adds little to the total environmental impact of drinking water production, regardless of the selected pretreatment. Note that the main impact (0.17×10^{-3} ILCD points, i.e., $> 85 \%$) of the conventional drinking water production is from the depletion of water resources, and, hence, the actual impact strongly depends on the region where the water is abstracted. Therefore, in a water-rich region, the additional pretreatment might also lead to a notable relative increase of environmental impacts of the drinking water production. With respect to the CO₂-equivalent (eq.) emissions, the production of 1 m^3 water for the

subsequent SAT causes 41.1 g CO₂-eq. and 136 g CO₂-eq. for the UV/H₂O₂ and LPRO treatment, respectively, with an average European electrical energy mix. This is explained by the overall lower specific energy demand of the UV/H₂O₂ treatment in comparison to the LPRO treatment, i.e., 0.066 kWh m⁻³_{Product} and 0.267 kWh m⁻³_{Product}, respectively. For comparison, the conventional production of 1 m³ drinking water causes the emission of about 260 g CO₂ equivalents in a European context. This means that, depending on the selected pretreatment, the specific CO₂-eq. emissions would rise by $\approx 20\%$ and $\approx 50\%$, respectively.

If the electrical energy is generated from wind or hydro power plants, an opposite result is obtained, i.e., the LPRO scenario causes less environmental burdens than the UV/H₂O₂ scenario in every single impact category assessed (except ionizing radiation). With respect to CO₂-eq. emissions, the UV/H₂O₂ and LPRO treatments would cause 8.5 g CO₂-eq. m⁻³_{Product} and 4.4 g CO₂-eq. m⁻³_{Product}, respectively. The higher environmental burdens from the UV/H₂O₂ treatment are explained by the environmental impact of the H₂O₂ production. Note that 37% of H₂O₂'s single score result is explained by cancer human toxicity effects. 92% of these effects could be traced back to anthraquinone used in the working solution of the H₂O₂ production, more specifically, to emissions of chromium to water. The EcoInvent database does not allow to further specify the reason for these emissions, but perhaps they come from the production of a catalyst used in the anthraquinone production process. Reducing the chromium emissions during anthraquinone production (or selecting a supplier that acts accordingly) can therefore significantly reduce the environmental impact of H₂O₂'s production. However, there is some uncertainty in the H₂O₂ single score result because the characterization factor for chromium emissions has to be interpreted with caution (level of quality: II/III [232]). On-site production of H₂O₂, e.g., in micro-reactors [236], [237] or by generation from an electrolysis process [238], [239] could be an alternative. Note that the UV/H₂O₂ process can accomplish a specific treatment goal, e.g., the abatement of a MP to a specific extend, with one degree of freedom (e.g., UV fluence as a function of H₂O₂, Figure D1, Appendix D). This gives the opportunity to optimize the UV/H₂O₂, e.g., towards a desired target, such as lowest treatment costs, lowest environmental impact or lowest CO₂-eq. emissions, as further discussed in Appendix D.

Other Aspects

Costs and environmental impacts are two important aspects which were assessed above. However, the decision which treatment to select might be further influenced by other aspects.

Disinfection Despite the systems assessed here were designed to treat micropollutants, another parameter of interest can be the disinfection efficiency and potential microbial inactivation credits (MIC) for the systems. MIC is the negative decadic logarithm of the ratio of a number, e.g., of cells, bacteria, viruses, etc. after a treatment (N_{out}) and the respective number

before the treatment (N_{in} , Equation 6.1).

$$MIC = -\log_{10} \left(\frac{N_{out}}{N_{in}} \right) \quad (6.1)$$

Both UV disinfection systems in AOP settings, as well the LPRO membrane system are generally capable to inactivate or remove pathogens and viruses during drinking water production to a high degree ($\geq 4 \log_{10}$, [126], [127], [228]) from, e.g., surface waters [126], [240]. For the validation of UV disinfection systems, detailed protocols exist, such as the German norm DVGW W 294, the Austrian norm ÖNORM M 5873, or the US EPA UV disinfection guideline manual [127]. Previous research confirmed that the UV/H₂O₂ treatment has an equal or even higher disinfection efficiency as UV systems alone [241], [242]. In addition, residual H₂O₂ can maintain a disinfection effect, e.g., by inhibiting bacterial regrowth at concentrations $\geq 0.3 \text{ mg L}^{-1}$ [38], [130]. To validate the disinfection effect of membrane systems, the US EPA published a membrane filtration guidance manual [243]. In addition to the validation of the systems, the constant monitoring of the integrity of the additional barrier can be challenging [127], [240], [243].

Inactivation of microorganisms by UV systems is related to, e.g., modifications of the deoxyribonucleic acid (DNA) upon photolysis, such as the formation of thymine-thymine dimers within the DNA [127]. In contrast, membrane systems physically remove microorganisms, protozoa and viruses from the permeate and these are concentrated in the retentate. To prevent the NF and LPRO membrane systems from, e.g., biofouling (e.g., bacterial growth on the membrane), they are periodically cleaned (and sanitized) in processes such as cleaning in place (CIP) utilizing chemicals [243].

Regarding the MICs of the treatment trains investigated here, the full-stream UV/H₂O₂ likely inactivates bacteria, protozoa and viruses by $\geq 4 \log_{10}$ [126], [228]. The \log_{10} removal for these potential human health risks in a side-stream LPRO treatment can be calculated by Equation 6.2 for the product water, i.e., the water sent to the subsequent treatment (e.g., soil aquifer treatment).

$$\frac{N_{SAT,in}}{N_0} = \frac{\dot{Q}_{Permeate}}{\dot{Q}_{SAT,in}} \times \underbrace{\frac{N_{Permeate}}{N_0}}_{=10^{-MIC_{Membrane}}} + \left(1 - \frac{\dot{Q}_{Permeate}}{\dot{Q}_{SAT,in}} \right) \quad (6.2)$$

For the LPRO side-stream treatment investigated here, with an assumed MIC of the LPRO system of ≥ 4 , the theoretical MICs are $0.55 \log_{10}$ due to the permeate fraction of 72% in the product water, i.e., the water sent to the subsequent SAT. Generally speaking, even if the membrane system itself has a MIC of $\geq 4 \log_{10}$, the MIC after mixing with the side stream is 0.5 if the permeate fraction is at least 68% or 1.0 for fractions above 90%. From a cost perspective, high fractions treated by the membrane are undesired because this requires higher treatment capacities of the membrane plant, which typically translates into increased investment costs for membranes and concentrate treatment (see Equations D12 and following, Appendix D).

Chapter 6. Multi-Criteria Assessment of the Investigated Treatment Options

Table 6.8: Behavior of selected features in non-target screening analysis. The selected features were produced upon UV/H₂O₂ treatment of river Rhine rapid sand filtrate water (4 mg H₂O₂ L⁻¹, 6'000 J m⁻²) and their behavior in a subsequent soil aquifer treatment (SAT) or biologically activated carbon (BAC) column was traced. Analytics and evaluation by IWB.

<i>m/z</i>	Ionization	Times detected	Behavior in SAT and GAC filters
224.9	negative	4/4	not detected after SAT or BAC
300.8	positive	3/4	not detected after SAT or BAC
165.0	negative	3/4	peak area decreased after SAT (factor 5), not detected after BAC
293.0	positive	4/4	no abatement in SAT or BAC
190.1	positive	3/4	no abatement in SAT or BAC
173.1	negative	3/4	no abatement in SAT or BAC

By-product formation during UV/H₂O₂ treatment Further considerations are related to the formation of potential by-products. It is known that, e.g., UV/H₂O₂ and ozone treatment can lead to the formation of potentially harmful oxidation by-products (BP), e.g., bromate upon ozonation of bromide-containing waters [51]) and disinfection by-products [40], [119], [244]. With respect to the UV/H₂O₂ treatment, the potential risks associated with the partial oxidative treatment occur directly in the product water, i.e., in the treatment chain to the drinking water. IWB conducted non-target screening analysis during the AquaNES project to investigate the formation of unknown reaction products upon the UV/H₂O₂ treatment and their fate in a subsequent SAT column. Grab samples were collected from the pilot plant described in Chapter 2 on four sampling days (20 March 2018; 10 April 2018; 11 June 2018; 14 August 2018). 250 µL of the samples were injected without further preparation on the HPLC system (Chapter 2). A mass spectrometer (Q Exactive, ThermoFisher Scientific, USA) was used to scan the range of 70 to 1'050 *m/z* in positive and negative ionization mode. Each sample was injected and measured three times. Data were processed by the software Compound Discoverer (ThermoFisher Scientific, USA). For a simple assessment of the fate of formed reaction products, only features were evaluated that fulfilled the following two criteria. First, the peak area of features increased upon UV/H₂O₂ treatment by at least a factor 2 with an adjusted *p* value < 0.001 (i.e., probability that the peak area actually increased: >99.9%). Second, only features were investigated for which the peak area increase was observed at least on three out of four sampling dates. These features were further traced for their behavior along the SAT column (described in Chapter 2) and a separate biological activated carbon filter operated in parallel (empty bed contact time ≈ 30 minutes; filter dimensions: 100 cm filter height, 28.8 cm inner diameter; filter material: F400; bed volumes filtered: ≈ 4'250 between March 2017 and August 2018).

Results are summarized in Table 6.8. Some reaction products were further abated by the biological filters investigated, others were not or only partially abated. It is unclear whether the abatement in the biological filters is based on adsorption, biological transformation or

even mineralization. These results agree with similar research on the formation of transformation products upon ozone treatment in wastewaters and their fate in subsequent biological treatments [245]–[247]. This highlights that the UV/H₂O₂ treatment potentially bears the risk associated with unknown compounds produced in the oxidation process to find their way to the drinking water. In addition, soils and aquifers are not necessarily protected from, e.g., pollution with unknown compounds.

To evaluate the risk from unknown compounds associated with the UV/H₂O₂ treatment, various ecotoxicological tests were conducted in the AquaNES project (4 mg H₂O₂ L⁻¹, 6'000 J m⁻²) [248]. Tests consisted of mutagenic tests (AMES II tests, strains TA98 and TA100, with and without addition of S9 enzyme; samples 10'000-fold concentrated by solid phase extraction (Oasis HLB, Waters)) and 18 other endpoints (CALUX tests for cytotoxicity; (anti-)androgenic activity; (anti-)estrogenic activity; (anti-)glucocorticoid activity; (anti-)progesterone activity; peroxisome proliferation (a2, d, g2); fast and slow dioxin receptor activation; xenobiotic metabolism; PXR receptor agonists; oxidative stress pathway; and DNA damage response with and without addition of S9 enzyme; all samples 6'666-fold concentrated by solid phase extraction (Oasis HLB, Waters, USA). Grab samples were taken on three dates (15 August 2017, 21 November 2017, 19 March 2018).

It was observed that none of the tested endpoints increased after the UV/H₂O₂ treatment. Instead, if there was a positive response for an endpoint before the UV/H₂O₂ treatment, typically this was either found at a similar or lower level after the UV/H₂O₂ treatment [248]. Other research showed that the formation potential for disinfection by-products upon chlorination increases after UV/H₂O₂ treatment, but is lower than the raw water when the UV/H₂O₂ effluent is subsequently treated by a biological activated carbon filtration [56], [117]–[119]. A biological treatment of UV/H₂O₂ treated water before finalization of the potable water is therefore recommended (Chapter 3). The biological treatment is also recommended because the UV/H₂O₂ treatment increases the biologically available organic carbon [38], and therefore, the bacterial regrowth potential [40], [60]. Note that this task probably can be fulfilled by a subsequent soil aquifer treatment (Chapter 3).

Summary

This chapter assessed two pretreatment options for MP abatement before an aquifer recharge in drinking water production, i.e., a full-stream UV/H₂O₂ and a side stream dense membrane treatment. The assessment was conducted for a case study which utilizes a river water after rapid sand filtration for soil infiltration, aquifer recharge and artificial groundwater augmentation. The systems were designed to abate known MPs to such an extent that each of their concentrations are below 0.1 µg L⁻¹ after a soil aquifer treatment simulated by columns. Nevertheless, as the assessment was conducted for the specific case study situation, the economic and environmental assessment are site specific. For a transfer of the cost assessment to other

sites, the modified equations derived from Plumlee *et al.* (2014) [43] proved feasible for cost estimates of the UV/H₂O₂ treatment, but not for the LPRO scenario. Table 6.9 summarizes the results of the assessed technical, economical, environmental and other aspects.

Both pretreatment options are considered feasible to fulfill the treatment task. The specific electrical energy demand of the UV/H₂O₂ treatment (0.066 kWh m⁻³_{Product}) was considerably lower than for the LPRO membrane treatment with concentrate ozonation (0.267 kWh m⁻³_{Product}, respectively). This figure impacts both the economical and environmental aspects assessed in this study. For the UV/H₂O₂ treatment, assuming the flexibility to select the UV fluence and H₂O₂ dose with one degree of freedom, the treatment design can be further optimized, e.g., towards lower operational costs or environmental impacts.

The concentrate treatment was assessed with a specific ozone dose of 0.4 mg O₃ (mg DOC)⁻¹ to abate on average 80% of moderately and quickly ozone-reactive compounds at limited bromate formation, i.e., below 10 µg L⁻¹. Although the research presented in Chapter 5 indicates the feasibility of this treatment, further research is needed to demonstrate this in a real application. The research should include the investigation of abatement of the chelating agent (if dosed before the membrane) and effect-based ecotoxicity tests to rule out possible adverse effects for the receiving aquatic system, e.g., from transformation products.

A full MCA required, as a next step, a weighting of the assessed criteria to derive at a single score or figure on which a decision is made. This is not done here because weighting can be very site-specific. In addition, this assessment focused on technical, economical and environmental aspects, but social aspects were not included. In their review on MCAs in the field of water resource management, Zolghadr-Asli *et al.* (2021) [249] highlighted the importance to account for legislative and political criteria next to economical and environmental aspects [249]. These criteria might be considered as part of the social pillar of an MCA, which might also include further aspects such as customer acceptance of the pretreatment scenarios. Therefore, further research focusing on various social aspects of the assessed pretreatment scenarios is therefore required to provide all data for a holistic MCA.

Table 6.9: Summary of the multi-criteria assessment of the investigated pre-treatment options before aquifer recharge for the "Lange Erlen" case study site, i.e., UV/H₂O₂ or dense membrane treatment with concentrate ozonation. Both systems are designed to deliver 2'520 m³ h⁻¹. Average bulk water quality parameters of the river Rhine rapid sand filtrate water, i.e., the feed water: 1.4 mg DOC L⁻¹, UV absorbance at 254 nm: 3.5 m⁻¹, pH 8.1, 28.5 mg total inorganic carbon L⁻¹, electrical conductivity: 320 µS cm⁻¹ [41].

Aspect	UV/H ₂ O ₂	LPRO
Technical		
Design:	Overall treatment goal: all MPs ≤ 0.1 µg L ⁻¹ after SAT column (Appendix D)	
	14% metformin abatement Full-stream treatment 4 mg H ₂ O ₂ L ⁻¹ , 5'800 J m ^{-2,a}	66% acesulfame retention Side-stream treatment 85% water recovery rate 72% permeate fraction
Electrical energy demand ^b	0.066 kWh m ⁻³	0.267 kWh m ⁻³
Protection of soil and aquifers	Compounds partially oxidized, transformation products are formed and might accumulate, others are not removed in SAT (or BAC) column treatment. No increased effects observed in various effect-based tests (AMES II, CALUX).	Compounds are rejected if their molecular weight is sufficiently high. No transformation products in process train to drinking water.
Economical		
CAPEX	2.8 Mio. €	10.6 Mio. €
OPEX	0.24 Mio. € a ⁻¹	0.71 Mio. € a ⁻¹
Total specific costs ^c	0.021 € m ⁻³	0.078€ m ⁻³
Environmental ^d		
ILCD2011	5.1 µPoints m ⁻³	12.7 µPoints m ⁻³
CO ₂ -equivalents	41.1 g m ^{-3,a}	136 g m ⁻³
Others		
Disinfection	≥ 4.0 log ₁₀	0.55 log ₁₀ ^e
Challenges	Transformation products, disinfection byproducts	Concentrate management (chelating agents, transformation products)

^a The design of the UV/H₂O₂ treatment can be further optimized as described in Appendix D.

^b Mind the impact of this parameter on the economical and environmental aspects.

^c Based on an interest rate of 5.1 %. See Tables 6.3 and 6.5.

^d For an average European electrical energy mix at market in 2015.

^e Value for the permeate mixed with the river rapid sand filtrate water.

7 Summary and Outlook

This study assessed two pretreatment options for the abatement of micropollutants (MPs) followed by a managed aquifer recharge (MAR) for drinking water production. One pretreatment was a full-stream UV/H₂O₂ process. The other was a side-stream nanofiltration (NF) or low-pressure reverse osmosis (LPRO) membrane treatment with a concentrate ozonation.

Results of this thesis and suggestions for further research

The effect of the UV/H₂O₂ treatment on MP abatement, dissolved organic matter (DOM) transformation and biological activity and on the subsequent MAR was investigated in soil column experiments (Chapter 3). The UV/H₂O₂ treatment abated the investigated MPs to the expected extent, depending on the photolysis efficiency and second-order rate constants for reactions with hydroxyl radicals ($\cdot\text{OH}$). The DOM was not mineralized by UV/H₂O₂ treatment, but its biodegradability increased slightly. The high applied UV fluence (6'000 J m⁻²) had a strong disinfection effect, which was maintained in the first few centimeters of the subsequent soil columns due to the residual H₂O₂ (concentration after UV treatment: 3.6 mg L⁻¹). The overall MP abatement was higher for the UV/H₂O₂ with subsequent soil column treatment compared to a soil column operated without UV/H₂O₂ pretreatment. The overall abatement could be explained by an additive effect of the relative abatements in each treatment step. DOM abatement was minimal in both soil columns, probably due to the short residence time of about day. No differences were observed in intact cell counts and microbial activity in the two soil column effluents. Overall, the UV/H₂O₂ process was a feasible pretreatment option for MP abatement followed by MAR, however, no synergistic effect of the two processes could be observed.

Further research is needed before the implementation of this process on a real site without H₂O₂ quenching. MP abatement by H₂O₂-based processes and the subsequent H₂O₂ quenching before infiltration by granular activated carbon (GAC) is practiced by e.g., Dunea in The Netherlands. Although the abatements of MPs and DOM in soil columns did not differ

significantly, the (long-term) effects of residual H_2O_2 on the microbial community were not investigated. In addition, not all transformation products formed upon the UV/ H_2O_2 treatment were abated in the soil column treatment, which is in agreement with a recent publication (Gulde et al., 2021). Hence, transformation products may ultimately enter the drinking water. No increase in various effect-based toxicity tests was observed, but the implementation of e.g., an additional activated carbon filter before MAR should be considered for risk minimization from residual H_2O_2 and from transformation products. Alternatively, an additional barrier for MPs could be assessed after the groundwater abstraction. This approach is likely more efficient than a treatment of the water before MAR because concentrations of micropollutants and dissolved organic matter are expected to be lower. Furthermore, for the UV/ H_2O_2 -MAR process likely more water needs to be treated, because often more water is infiltrated than abstracted. However, this approach would miss the additional protection of soil and aquifers.

MP abatement in the UV/ H_2O_2 process is mainly based on direct photolysis and reactions with *in situ* generated $\bullet\text{OH}$. Hence, the volume-averaged UV fluence (H) and $\bullet\text{OH}$ exposure ($CT_{\bullet\text{OH}}$) determine the average abatement of most MPs. A model was developed that facilitates the assessment of H and $CT_{\bullet\text{OH}}$ based on relative abatements of two MPs (*in situ* probe compounds) upon UV/ H_2O_2 treatment by considering their photolysis efficiency and second-order rate constants for the reaction with $\bullet\text{OH}$ (Chapter 4). With this information, the fate of other MPs with known fluence-based rate constants and second-order rate constants for reactions with $\bullet\text{OH}$ could be successfully predicted within $\pm 20\%$ of the measured abatements. These results were obtained both in bench-scale and pilot-scale experiments and for surface water and wastewater, respectively. A sensitivity analysis highlighted that the MPs selected as internal probe compounds should be abated by $> 50\%$, respectively, to avoid high uncertainties in estimated H and $CT_{\bullet\text{OH}}$ caused by measurements. At high extents of MP abatement, the uncertainties in H and $CT_{\bullet\text{OH}}$ are controlled by the uncertainties in second-order rate constants, molar absorption coefficients and quantum yields of the probe compounds.

The water temperature might impact, e.g., the second-order rate constants and quantum yields of the probe compounds to some extent. The water temperature was not included in the developed model. However, if a very accurate assessment of H and $CT_{\bullet\text{OH}}$ is required at water temperatures different from $20\text{ }^\circ\text{C}$, results from the sensitivity analysis of the model highlighted that these effects should be considered. In addition, for some compounds like sotalol, reactions with other reactive species such as carbonate radicals can be of significance to describe the fate of MPs. Therefore, further research is needed for the inclusion of temperature effects and other reactive species, such as the carbonate radical. This could facilitate a more complete and accurate assessment of the UV/ H_2O_2 process. In addition, the robustness of such calculations might be increased if more than two MP probe compounds are used for the calculation of H and $CT_{\bullet\text{OH}}$ by solving a linear equation system. It was shown previously that indirect *online* monitoring of the abatement of MPs is possible by correlations of relative MP abatements with surrogate parameters such as UV absorbance or fluorescence. These

correlations are purely empirical and, hence, water specific. Nevertheless, further research could investigate the options and limitations to monitor H and CT_{OH} by coupling these *online* measurements with the model. This could facilitate new control strategies of the UV/H₂O₂ process.

The interplay of the membrane selection for MP removal and subsequent concentrate ozonation was investigated in bench-scale experiments with standardized concentrates (Chapter 5). Neither the water source (River Rhine rapid sand filtrate water, River Wiese rapid sand filtrate water or Lake Biel raw water), nor the membrane type (two nanofiltration or one low-pressure reverse osmosis membrane) had a significant impact on the exposures of ozone or hydroxyl radicals for standardized conditions. Although the ozonation of standardized LPRO concentrates typically yielded a higher bromate formation than standardized NF membranes, this did not change the tradeoff between MP abatement and bromate formation, which was similar for all standardized concentrates of the assessed membranes and water sources. With respect to the permeate quality, NF membranes had lower relative retentions of MPs and bromide than the LPRO. This also results in lower bromide concentrations in NF concentrates compared to an LPRO concentrate. Therefore, the risk for bromate formation upon ozone treatment of NF concentrates is lower compared to LPRO concentrates. If for the whole treatment of membrane and concentrate ozonation, lower retentions of MPs are sufficient to reach a certain permeate quality, NF membranes are a better choice because their concentrates are more feasible for MP abatement by ozonation with limited bromate formation. Further research could focus on the development of membranes, e.g., on membranes with polyelectrolyte multilayer modified active layers, that have a high permeability, high retention of MPs (and DOM) and a low retention of bromide at the same time.

The electron donating capacity (EDC) proved to be the most sensitive parameter to describe differences in the concentrates, but the data base was too small to investigate correlations of the EDC with the abatement of MPs with high ozone reactivity. Therefore, the impact of membrane treatment on the EDC and its correlation with ozone exposure in the concentrate should be further investigated.

A multi-criteria assessment focused on technical, economic, and ecological aspects of the pretreatment options, as well as microbial removal credits (Chapter 6). It was found that typically, the full-stream UV/H₂O₂ treatment was advantageous over the side-stream membrane treatment with concentrate ozonation in all assessed categories (costs, environmental impacts, microbial removal credits). Only in cases where electricity was produced by wind or hydropower plants, the membrane-based pretreatment was in favor as it caused lower environmental burdens in these cases. In addition, tracking transformation products formed by the UV/H₂O₂ treatment showed that some of them might reach the drinking water, when they were not fully abated in the subsequent soil column treatment.

This thesis focused on the assessment of barriers against MPs at one treatment capacity (2'520 m³ h⁻¹). However, it is known that, e.g., specific treatment costs vary with changing

treatment capacities (Appendix D). Therefore, further research should clarify whether or not an additional treatment for MP abatement in drinking water production is useful at different treatment capacities. A holistic assessment should include social aspects in addition to the technical, economic, and ecological aspects assessed here. Social aspects include consumer acceptance and willingness to pay. In addition, a short literature review showed that many additional categories were considered by different assessments. Similarly, various methods are used to derive a ranking of the assessed options. Hence, the development of a framework or guideline for multi-criteria assessments in the context of (waste)water treatment would be beneficial if it provides guidance on assessment categories, minimal requirements of reported data and suggestions for weighting of categories, e.g., based on scientific evidence or political decisions. Such a framework could significantly improve the comparability of studies and support the design and evaluation of multi-criteria assessments. In many cases, the implementation of an additional barrier against MPs is only initiated as a response to driving forces such as political decisions, new scientific evidence or changes in risk patterns associated with the water resources. This thesis highlighted that both assessed pretreatment options caused substantial costs. Both pretreatment options added to the total environmental impact of the water treatment. It was shown before that the additional environmental burdens caused by the pretreatment do not weigh up the benefits of MP abatement, based on a Life Cycle Assessment with the ILCD2011 method that considered the toxicity effects of the MPs for humans and the environment [44]. Summarizing, the implementation of any of the pretreatments evaluated appears not to be justified, based on the selected assessment methodology.

Nevertheless, if an additional barrier against MPs is required, its implementation is likely more appropriate after the managed aquifer recharge [250]. This is because bulk water quality parameters lowering the efficiency of advanced treatments are typically partially abated during managed aquifer recharge. By this, the additional barrier is more efficient and can likely be designed smaller. This process arrangement could additionally protect the drinking water from potential contaminations of the groundwater from other sources than the MPs present in the infiltrated raw water, e.g., contamination after accidents in the water catchment area.

Outlook and future developments

Global challenges such as the environmental crisis, including climate change, the growing and ageing population and urbanization also affect the water sector. One result of these challenges is that water resources are increasingly stressed and polluted [251], [252]. Therefore, strategies for the adaption, e.g., of drinking water production to these challenges will likely gain importance in the future. As a result of the aging population, there is a risk of skilled worker shortage, and this might render complex treatment schemes less attractive in the future. Potentially, digitalization could be used to reduce the complexity to operate advanced water treatment processes, e.g., by reducing the need of workforce, facilitating new control strategies and/or remote service. Sustainable water management will probably become increasingly

important as the water sector plays a key role in the nexus between water, energy, food, and ecosystems. Additional drivers, such as new contaminants of emerging concern (CEC, such as per- and polyfluoroalkyl substances, PFAS) and increasing needs for citizen engagement will have to be considered. [251], [252]

According to the principles of circular economy (avoid, reduce, reuse, recover, replenish, [253]), the most efficient approaches to abate MPs, however, are source control by avoiding their use and/or a stringent emission control. Nevertheless, a complete ban or abatement of MPs before entering the (aquatic) environment is unrealistic. This highlights the need to raise public awareness for such issues. In this light, the need for simple and robust technologies providing an efficient barrier against MPs is clearly visible. Ideally, these technologies additionally support the above-mentioned requirements to respond to the global challenges at limited costs and resource consumption.

For the UV/H₂O₂ treatment, the results of the life cycle assessment highlight three topics with further research needs: (1) lowering the specific electrical energy demand, (2), lowering the environmental impact of H₂O₂ production, (3), increasing the H₂O₂ utilization efficiency. State-of-the-art low-pressure mercury arc UV lamps are already very mature, hence, drastic decreases in specific electrical energy demands are unlikely. Probably, additional energy savings could rather be accomplished by improved reactor design and control strategies. Regarding control strategies, the UV/H₂O₂ treatment might be optimized towards lowest costs and/or environmental impacts as described in this thesis (Appendix D). Furthermore, the use of UV light emitting diodes (UV-LEDs) might potentially lower the specific electrical energy demands, but current UV-LEDs have a limited applicability due to their relatively low output power per LED (30 mW, [100]) and low energy efficiency (1 to a few percent, [40]).

As discussed in Chapter 6, the environmental impacts of the H₂O₂ production could be reduced by onsite production of H₂O₂, e.g., with electrochemical methods. However, long-term studies that provide information on the feasibility of this technology in real environmental applications are currently missing. In addition, life cycle assessments are missing comparing conventional H₂O₂-based AOPs with, e.g., onsite electrochemical H₂O₂ production. Current UV/H₂O₂ processes typically only utilize < 10% of the dosed H₂O₂. Therefore, costs and environmental impacts of the H₂O₂ are at least ten times higher than actually needed, neglecting possible additional efforts for residual H₂O₂ quenching. Technologies that improve the H₂O₂ efficiency could improve the economic and ecologic footprint of the UV/H₂O₂ process, such as the use of heterogeneous catalysts [254], [255]. Further studies are required that demonstrate their beneficial application and long-term effectiveness in pilot- and full-scale in terms of cost and environmental aspects in comparison to UV/H₂O₂.

With respect to the membrane-based treatment, this thesis showed that the high specific electrical energy demand of dense membrane treatment and the high investment costs are the main limiting factors. The electrical energy demand directly influences the operational

costs and the environmental impacts. Hence, the development of novel membranes with high water permeability at low pressures without compromising the retention of target compounds such as MPs remains a rewarding task.

Membrane treatment separates the feed water into two water qualities, i.e., the (high-grade) permeate and the (low-grade) retentate. Further research should focus on potential uses of the concentrate such as the recovery of valuable salts and nutrients [256], [257] and irrigation purposes [258] after concentrate treatment for MP abatement (Chapter 5) and/or additional biological treatment, e.g., biological activated carbon, which would also act as an additional treatment to abate possible transformation products from the concentrate ozone treatment [78], [208], [259].

Current drinking water production schemes often already include a granular activated carbon (GAC) filtration. Typically, the exhausted GAC is reactivated and may be used in lower quality processes, such as wastewater treatment. However, options to reuse the GAC before its reactivation in the polishing of the concentrate could be investigated as this would extend the lifetime of the activated carbon (lower specific costs and environmental impacts), [260], [261].

Appendix A: Supporting Information for Chapter 3

This appendix is a copy of the post-print version of the supporting information (SI) of [38]:
Wünsch, R., Plattner, J., Cayon, D., Eugster, F., Gebhardt, J., Wülser, R., von Gunten, U., and
Wintgens, T.: Surface water treatment by UV/H₂O₂ with subsequent soil aquifer treatment:
impact on micropollutants, dissolved organic matter and biological activity. *Environ. Sci.:
Wat. Res. & Technol.*, **5** (2019), 10, 1709-1722. DOI: 10.1039/c9ew00547a.

Reproduced from [38] with permission from the Royal Society of Chemistry.

Appendix . Appendix A: Supporting Information for Chapter 3

Table A1: Device list of sensors and probes.

Parameter	Locations	Device	Manufacturer
UVA	Rhine river sand filtrate + after AOP	ColorPlus	SIGRIST-Photometer, Switzerland
pH, T	Rhine river sand filtrate + after AOP	CPS11D-7AS21*	Endress+Hauser, Switzer- land
Turbidity	Rhine river sand filtrate	Monitor AMI Tur- biwell 7027	SWAN Analytical Instru- ments, Switzerland
Electrical Conductivity	Rhine river sand filtrate + after AOP		Endress+Hauser, Switzer- land
H ₂ O ₂	After AOP	AquaDMS	SIGRIST-Photometer, Switzerland
Dissolved Oxygen	Rhine river sand filtrate + after AOP	COS22D- AA1A2B22	Endress+Hauser, Switzer- land
Redox	Rhine river sand filtrate + after AOP	CPS72D-7PT21**	Endress+Hauser, Switzer- land
Flow	Rhine river sand filtrate + after AOP	3021 25D 72014BT41 C1	GEMÜ Gebr. Müller Ap- paratebau, Germany
Flow	Soil column effluents	MIK- 5NA15AE34R	KOBOLD Messring, Ger- many

Table A2: Operational parameters of the UV/H₂O₂ process during the test phase (November 2017 until August 2018). Treatment target: 4 mg H₂O₂ before the UV reactor, 6'000 J m⁻² UV fluence.

Parameter	Unit	Median	Standard Deviation
Volume flow	L h ⁻¹	566	51
UV intensity	W m ⁻²	36.2	3.9
Residual H ₂ O ₂	mg L ⁻¹	3.6	0.7

Table A3: Operational parameters of the soil columns during the test phase (November 2017 until August 2018).

Parameter	Unit	Reference Column	Test Column
Feed water	-	Rhine river sand filtrate	UV/H ₂ O ₂ effluent
Volume flow	L h ⁻¹	7.3±2.6	6.4±3.2
Operating hours (flow >0.6 L h ⁻¹ , share of 7253 h)			
Operation	h	7121 (98%)	7019 (97%)
Stopped	h	132 (2%)	234 (3%)
Number of shutdowns	-	10	16
Mean duration of shutdown	h	13.2	14.6

Table A4: Selected properties of the investigated micropollutants. Values for the distribution constant (logD) were predicted for pH 7.4 by ACD/Labs, obtained at chemspider.com. For references, see publication [38].

Substance	CAS No.	Type	Molecular Weight [Da]	k_{OH} $10^9 [M^{-1} s^{-1}]$	ϵ_{254} $10^3 [M^{-1} cm^{-1}]$	Φ_{254} $10^{-2} [mol einstein^{-1}]$	logD [Da]	Meas. range [ng L ⁻¹]	Meas. uncertainty [%]	Theor. limit of quantification [ng L ⁻¹]
Ethylenediamine Tetraacetate (EDTA)	60-00-4	Chelating agent	292.2	2.0	7.89	56	-6.4	500 to 5'000	20	40
Acesulfame (ACE)	33665-90-6	Artificial sweetener	201.2	3.8 ± 0.3	≈ 31.6	26	-2.8	10 to 1'600	11	2.2
Iopamidol (IPA)	62883-00-5	X-ray contrast media	777.1	3.4 ± 0.3	22.7	3.3	-2.3	10 to 500	27	5.0
Iomeprol (IME)	78649-41-9	X-ray contrast media	777.1	2.0 ± 0.1	≈ 24.0	n.a.	-2.6	10 to 500	24	5.3
Metformin (MET)	657-24-9	Type 2 diabetes drug	129.2	1.4 ± 0.2	0.94 ± 0.09	1.4 ± 0.6	-3.4	10 to 800	39	3.4
1H-Benzotriazole (BTZ)	95-14-7	Anti-corrosive agent	119.1	8.3 ± 0.4	5.6	1.2	1.5	10 to 320	34	7.7
Iopromide (IPR)	73334-07-3	X-ray contrast media	791.1	3.3 ± 0.1	21.0 ± 0.2	3.9 ± 0.4	-2.1	10 to 500	12	5.0

Table A5: Overview on performance parameters of the applied analytical methods.

Analytical Method	Limit of quantification	Standard error [%]	Measuring range
Dissolved organic carbon by SEC-OCD	0.1 mg _C L ⁻¹	10	0.1 to 5.0 mg _C L ⁻¹
H ₂ O ₂ by titanium oxalate (photometric)	0.3 mg H ₂ O ₂ L ⁻¹	5	0.3 to 10 mg H ₂ O ₂ L ⁻¹
Intact cell counts by flow cytometry	200 cells mL ⁻¹	10	10 ³ to 10 ⁶ cells mL ⁻¹
ATP by luminescence	0.0004 nM	30	0.001 to 0.1 nM

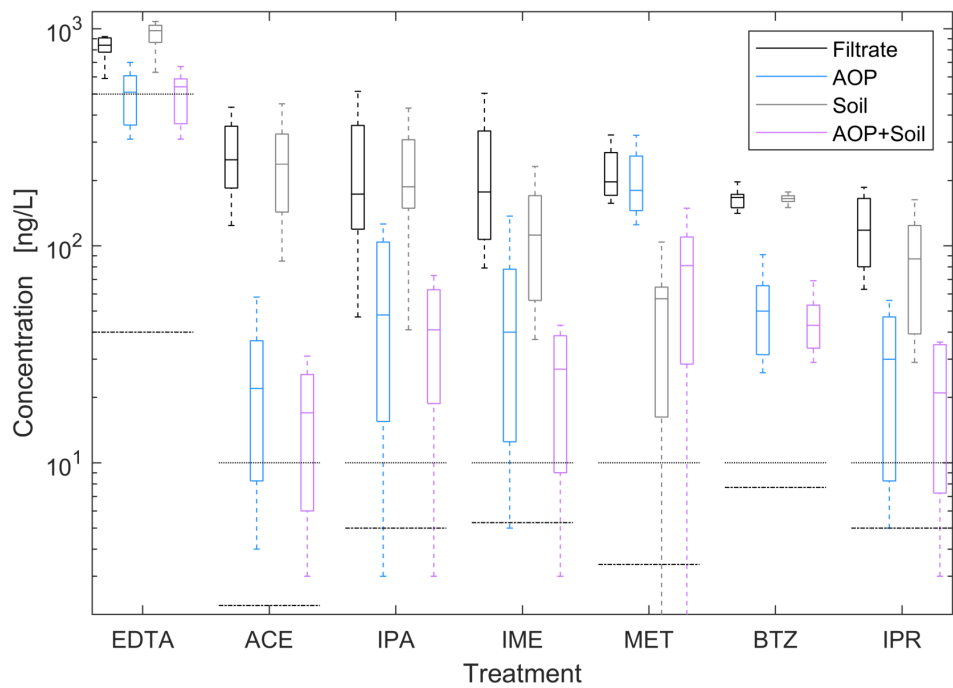


Figure A1: Concentrations of micropollutants along the treatment chains. $n = 7$ for all. Central mark of boxes: median; lower and upper edges of boxes: 25th and 75th percentiles, respectively; whiskers: minimum and maximum values. Dotted line: lowest concentration of calibration. Dot-stroked line: theoretical limit of quantification. Micropollutants: Ethylendiamine tetraacetate (EDTA), acesulfame (ACE), iopamidole (IPA), iomeprol (IME), metformin (MET), 1H-benzotriazole (BTZ), iopromide (IPR).

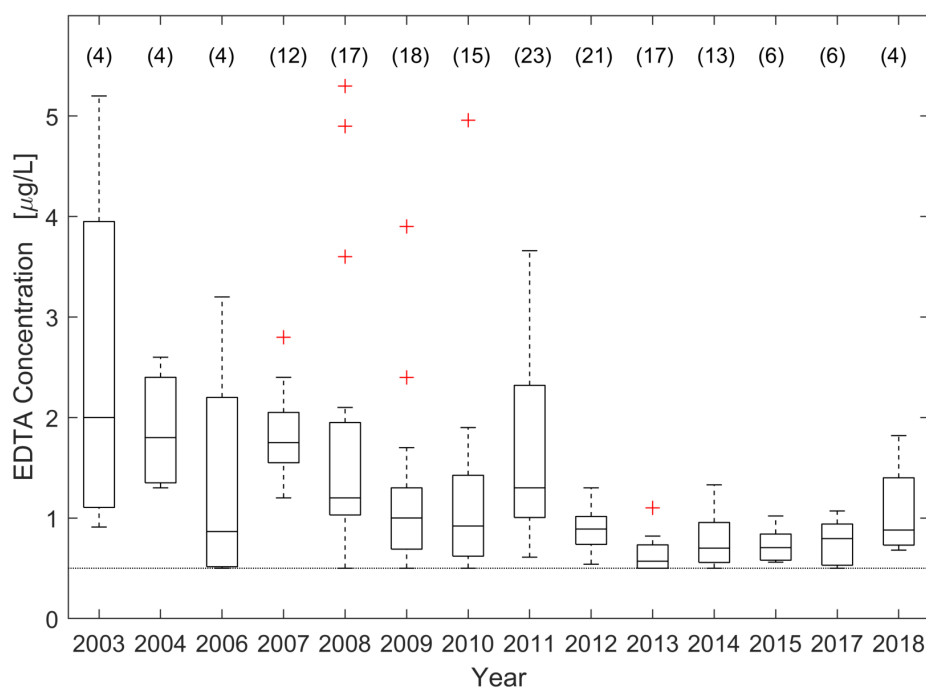


Figure A2: Concentrations of EDTA in the raw Rhine river water between 2003 and 2018. Values below the lowest point of calibration (i.e., $0.5 \mu\text{g L}^{-1}$) are reported as $0.5 \mu\text{g L}^{-1}$. n indicated in brackets for the respective year. Central mark of boxes: median; left and right edges of boxes: 25th and 75th percentiles, respectively; whiskers: minimum and maximum values. Outliers, i.e., values outside ± 2.7 standard deviations from median (99.3% coverage of normally distributed data), marked as a red cross. Dotted line: lowest calibrated concentration. Data from monitoring measurements by IWB.

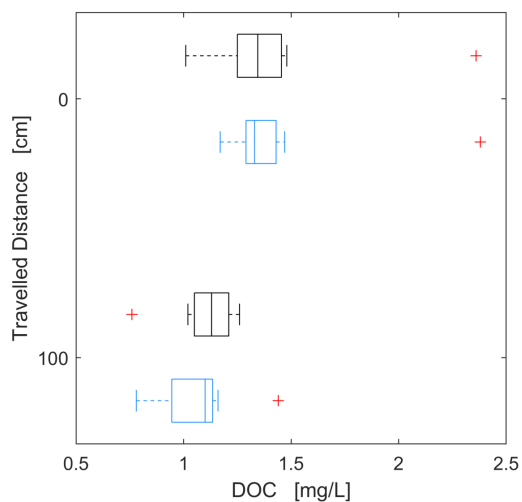


Figure A3: Dissolved organic carbon (DOC) concentrations along the soil columns, receiving Rhine river sand filtrate (black) and UV/H₂O₂ treated water (blue). $n = 8$ for all. Central mark of boxes: median; left and right edges of boxes: 25th and 75th percentiles, respectively; whiskers: minimum and maximum values. Outliers, i.e., values outside ± 2.7 standard deviations from median (99.3% coverage of normally distributed data), marked as a red cross. No statistically significant differences were detected between the groups at the influents (0 cm) and effluents (100 cm) of the columns.

Table A6: Evaluation by categories of the dissolved organic matter ($n = 8$, November 2017 to August 2018), median \pm standard deviation.

Treatment	DOC [mg L ⁻¹]	Chrom. [mg L ⁻¹]	DOC	Biopolymers [mg L ⁻¹]	Humic substances L ⁻¹]	Sub- [mg	HS Peak mum [min]	Building Blocks [mg L ⁻¹]	LMW A+N
Filtrate	1.3 \pm 0.4	1.2 \pm 0.4		0.1 \pm 0.0	0.8 \pm 0.1		43.9 \pm 0.5	0.2 \pm 0.0	0.1 \pm 0.1
AOP	1.3 \pm 0.4	1.2 \pm 0.4		0.1 \pm 0.0	0.9 \pm 0.1		44.5 \pm 0.5	0.2 \pm 0.1	0.2 \pm 0.1
Soil	1.1 \pm 0.2	1.1 \pm 0.2		0.0 \pm 0.0	0.7 \pm 0.1		43.8 \pm 0.5	0.2 \pm 0.0	0.1 \pm 0.0
AOP + Soil	1.1 \pm 0.2	1.1 \pm 0.2		0.0 \pm 0.0	0.8 \pm 0.1		44.2 \pm 0.5	0.2 \pm 0.0	0.1 \pm 0.0

Appendix . Appendix A: Supporting Information for Chapter 3

Table A7: p values of paired t-tests of the day-wise evaluation by categories of the dissolved organic matter ($n = 8$, November 2017 to August 2018).

	AOP	Soil	AOP+Soil
DOC			
Filtrate	0.6851	0.0195	0.0302
AOP	-	0.0236	0.0344
Soil	-	-	0.6636
Chromophoric DOC			
Filtrate	0.4036	0.0240	0.0597
AOP	-	0.0237	0.0508
Soil	-	-	0.8611
Biopolymers			
Filtrate	0.1991	0.0014	0.0024
AOP	-	0.0001	0.0002
Soil	-	-	0.1803
Humic Substances			
Filtrate	0.3847	0.0002	0.0068
AOP	-	0.0215	0.0129
Soil	-	-	0.3135
Humic Substances Peak Maximum			
Filtrate	0.3516	0.0013	0.0454
AOP	-	0.0015	0.0303
Soil	-	-	0.1575
Building Blocks			
Filtrate	0.4234	0.0108	0.0272
AOP	-	0.3653	0.3710
Soil	-	-	0.7110
Low Molecular Weight Acids and Neutrals			
Filtrate	0.2454	0.1910	0.2381
AOP	-	0.0654	0.0851
Soil	-	-	0.7799

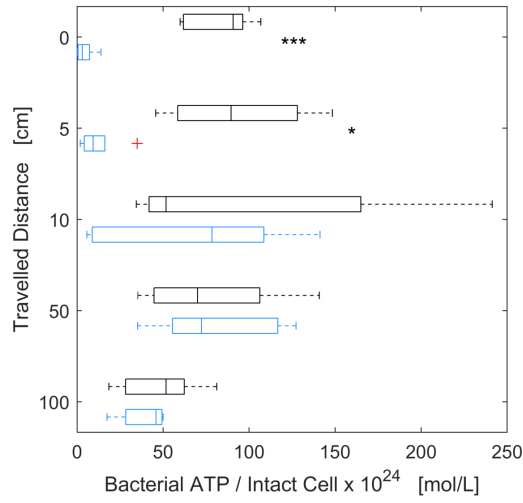


Figure A4: Bacterial ATP per intact cell in the water phase along the soil columns, receiving Rhine river sand filtrate (black) and UV/H₂O₂ treated water (blue). $n = 5$ for all, except $n = 4$ for Rhine river sand filtrate after 5 cm travelled distance. Central mark of boxes: median; left and right edges of boxes: 25th and 75th percentiles, respectively; whiskers: minimum and maximum values. Outliers, i.e., values outside ± 2.7 standard deviations from median (99.3% coverage of normally distributed data), marked as a red cross. Significant differences between groups in paired two-sided t-tests are marked with “*” and “***” for $p < 0.05$ and $p < 0.001$, respectively.

Appendix B: Supporting Information for Chapter 4

This appendix is a copy of the post-print version of the supporting information (SI) of [41]: Wünsch, R., Mayer, C., Plattner, J., Eugster, F., Wülser, R., Gebhardt, J., Hübner, U., Canonica, S., Wintgens, T., and von Gunten, U.: Micropollutants as internal probe compounds to assess UV fluence and hydroxyl radical exposure in UV/H₂O₂ treatment. *Wat. Res.* (2021), 116940. DOI: 10.1016/j.watres.2021.116940.

The article was published by Elsevier under a creative commons license (CC BY 4.0) [41].

Description of the collimated beam device

Figure B1 shows a scheme of the collimated beam device (CBD, provided by Xylem Services) used in this study, which was equipped with four low-pressure mercury lamps (NLR2036, Xylem Services) irradiating almost mono-chromatically at 254 nm. Relevant geometrical details are provided in Table B1. At the beginning of the collimated beam device experiments, the incident UV irradiance was measured at the height of the water level at 15 points each in x- and y- direction across the diameter by a calibrated radiometer (ILT1700, International Light Technology, MA, USA). This was done to determine the irradiance at the center of the sample dish and to calculate the Petri factor at the level of the water surface, i.e., the ratio of the average irradiance over the sample area and the irradiance in the center [262]. The fluence rate calculations were performed according to Bolton and Stefan (2002) [138] (see also Table B1). The target UV fluence was set by a timer, which controlled a shutter to open and close pneumatically. The irradiation time was calculated as described in Table B1. The calculation accounted for, e.g., sample volume (250 to 305 mL), diameter of the petri dish (18.5 cm, uncovered), transmissivity at 254 nm of the water sample, petri factor, distance to the UV lamps (36 cm), reflectance of UV light at the air-water interface at 254 nm (2.5 %), according to the calculation procedure described in Bolton and Stefan (2002) [138]. The temperatures

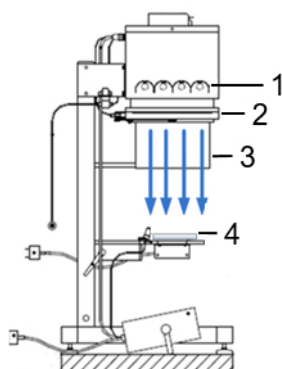


Figure B1: Scheme of a collimated beam device applied in this study. 1: Low-pressure mercury UV lamps. 2: Pneumatic shutter connected to a timer. 3: Tube to quasi-collimate the UV light and minimize scattered light. 4: Petri dish with sample. Copyright by Xylem Services, reprinted with permission.

before and after an experiment were measured and their average reported.

H₂O₂ was spiked before the laboratory experiments from a H₂O₂ stock solution (1 mg L⁻¹), prepared from a 35 % (w/w) sample by dilution with ultrapure water (>18 MΩ). The exact concentration of the 1 mg L⁻¹ stock solution was determined before use by permanganate titration [263].

Preparation of micropollutant stock solution for spiking

A mixed stock solution was prepared in ultrapure water at a concentration of 1 mg L⁻¹ of each of the following MPs: 5-methyl-1H-benzotriazole (5BTZ), metformin (MET), acesulfame (ACE), diatrizoic acid (DTA), iohexol (IHX), iopamidol (IPA) and iopromide (IPR).

MET and 5BTZ were dissolved as pure substances in ultrapure water at 10 mg L⁻¹ and 5 mg L⁻¹, respectively (solution 1). ACE was purchased as a stock solution at 10 mg L⁻¹ dissolved in ultrapure water (solution 2). DTA, IHX, IPA and IPR were purchased as stock solutions and diluted in a mix of acetonitrile, methanol and ultrapure water (1:1:1) to a concentration of each substance of 10 mg L⁻¹ (solution 3). Solutions 1 – 3 were mixed and diluted with ultrapure water to a final concentration of 1 mg L⁻¹ of each MP, except for 5BTZ (0.5 mg L⁻¹).

The MP stock solution contained both about 3.3% (v/v) methanol and acetonitrile and was diluted by a factor 1'000 by spiking. The second-order rate constants for methanol and acetonitrile are $9.7 \times 10^8 \text{ M}^{-1} \text{ s}^{-1}$ [151] and $2.2 \times 10^7 \text{ M}^{-1} \text{ s}^{-1}$ [264], respectively. Therefore, the pseudo first-order [•]OH scavenging rate of the added solvents, calculated by Eq. 4.6, are $S_{\text{Methanol}} = 7.9 \times 10^5 \text{ s}^{-1}$ and $S_{\text{Acetonitrile}} = 1.7 \times 10^4 \text{ s}^{-1}$, which is higher than the natural [•]OH scavenging rate of an average river Rhine sand filtrate ($5.7 \times 10^4 \text{ s}^{-1}$) by a factor 14. Thus, the spiking experiments do not allow to draw conclusions about MP abatement in natural, i.e., unspiked river sand filtrates. Nevertheless, for the purpose of this paper, these results can be

Table B1: Calculation scheme for the irradiation times at two different UV fluence rates in collimated beam device experiments with an average river Rhine sand filtrate sample, adapted from Bolton and Stefan (2002) [138].

Parameter	Unit	Low fluence	High fluence
UV fluence	J m^{-2}	2'000	6'000
H_2O_2	mg L^{-1}	2.0	4.0
Sample UV absorbance at 254 nm divided by path length (a)	m^{-1}	3.7	3.8
Petri dish diameter (d)	m		0.185
Water sample height (h)		$h = V_{\text{Sample}} / (\pi d^2 / 4)$	
	m		0.011
Reflection factor (RF), i.e., some irradiance is reflected on the water surface	-		0.975
Petri factor (PF), i.e., correction factor for not uniform fluence over the irradiated water surface (measured)	-		0.93
Water factor (WF), i.e., correction factor due to the absorption of the UV light along the irradiated pathway		$WF = (1 - 10^{-ah}) / (ah \ln(10))$	
	-	0.95	0.95
Divergence factor (DF), i.e., scattering of light inside the water sample		$DF = L / (L + h)$	
	-	0.97	0.97
Irradiance (E)	W m^{-2}		40.0
Volume averaged fluence rate		$\bar{E} = E \times RF \times PF \times WF \times DF$	
	W m^{-2}	33.5	33.5
Irradiation time (t)		$t = H / \bar{E}$	
	s	60	179

Table B2: List of suppliers and purity of utilized chemicals.

Chemical	Supplier	Chemical Purity
Micropollutant standards		
5-Methyl-1H-benzotriazole (5BTZ)	Neochema, Germany	≥98.94%
Acesulfame-K (ACE)	Neochema, Germany	≥99.9%
1H-Benzotriazole (BTZ)	Neochema, Germany	≥99.9%
Carbamazepine (CBZ)	Neochema, Germany	≥99.9%
Diatrizoic acid (DTA)	Neochema, Germany	≥94.1%
Iohexol (IHx)	Neochema, Germany	≥99%
Iopamidol (IPA)	Neochema, Germany	≥99.6%
Iopromide (IPR)	Neochema, Germany	≥98.6%
Metformin (MET)	Neochema, Germany	≥98.2%
Metoprolol (MPL)	Neochema, Germany	≥97%
Sulfamethoxazole (SMX)	Neochema, Germany	≥99.9%
Sotalol (STL)	Neochema, Germany	≥99.8%
Deuterated internal standards		
BTZ-d4	Neochema, Germany	≥99.9%
CBZ-d10	Neochema, Germany	≥97%
SMX-d4	Neochema, Germany	≥98.2%
MET-d6	Neochema, Germany	≥99%
STL-d4	Neochema, Germany	≥99%
IPA-d8	Toronto Research Chemicals	≥95%
DTA-d6	Toronto Research Chemicals	≥96%
ACE-d4	Toronto Research Chemicals	≥98.9%

used to investigate the applicability of the proposed model, because the model inherently accounts for these $\cdot\text{OH}$ scavenging effects.

Table B2 provides information on all utilized chemicals and their respective suppliers and purities.

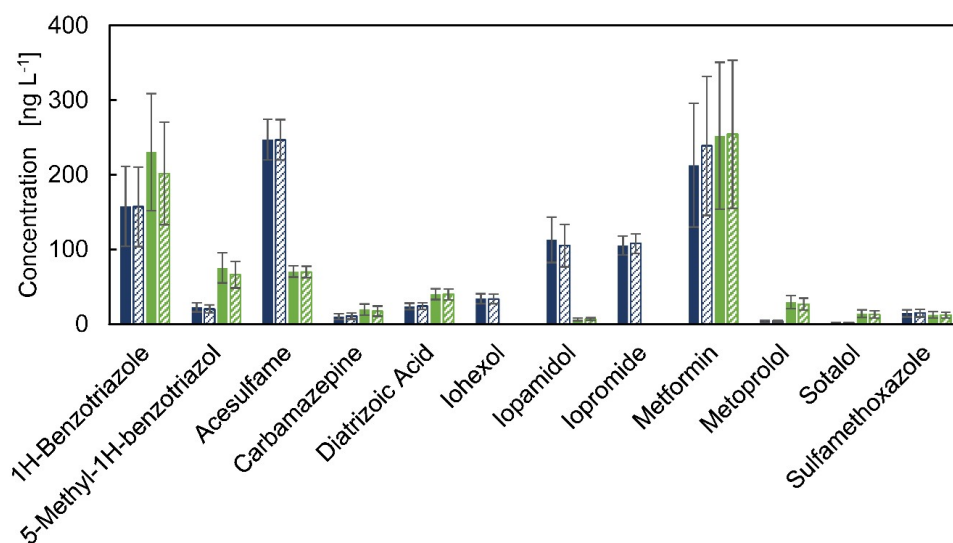


Figure B2: Measured concentrations before (full colored bar) and after (hatched bars) treatment with 4 mg L⁻¹ H₂O₂ and no UV fluence (“dark experiment”) in pilot plant experiments with sand filtrates of river Rhine (dark blue) and Wiese (green). Error bars: expanded analytical measurement uncertainty, i.e., 95% confidence intervals (see Table B3).

Table B3: Overview of analytical parameters for micropollutant analyses in this study. Standard analytical measurement uncertainties were determined along ISO 11352 and include, e.g., uncertainties of standards, pipettes, measurement devices, etc. The expanded standard analytical measurement uncertainty corresponds to a half 95% confidence interval of a single measurement for an absolute concentration.

Substance	Abbreviation	Theoretical LoQ [ng L ⁻¹]	Measurement range [ng L ⁻¹]	Standard analytical meas. uncert. (<i>u</i>) [%]	Expanded standard uncertainty, 2 × <i>u</i> [%]
5-Methyl-1H-benzotriazole	5BTZ	3.2	10 to 320	13	27
Acesulfame	ACE	2.2	10 to 1600	5	11
1H-Benzotriazole	BTZ	7.7	10 to 320	17	34
Carbamazepine	CBZ	0.2	10 to 320	19	38
Diatrizoic acid	DTA	0.8	10 to 500	9	18
Iohexol	IHX	8.3	10 to 500	9	19
Iopamidol	IPA	5.0	10 to 500	13	27
Iopromid	IPR	5.0	10 to 500	6	12
Metformin	MET	3.4	10 to 800	19	39
Metoprolol	MPL	0.7	10 to 320	15	30
Sulfamethoxazole	SMX	0.5	10 to 320	17	34
Sotalol	STL	1.6	10 to 320	19	37

Table B4: Uncertainties and types of distribution considered in the model to estimate confidence intervals.

Input parameter	Uncertainty	Type of distribution
pH	± 0.1	Uniform
k_{OH}	Substance specific, see Table 4.1	Normal
ε_{254} or ε_1 and ε_2	Substance specific, see Table 4.1	Normal
Φ_{254} or Φ_1 and Φ_2	Substance specific, see Table 4.1	Normal
Measured influent and effluent concentrations	Substance specific, see Table B3	Normal

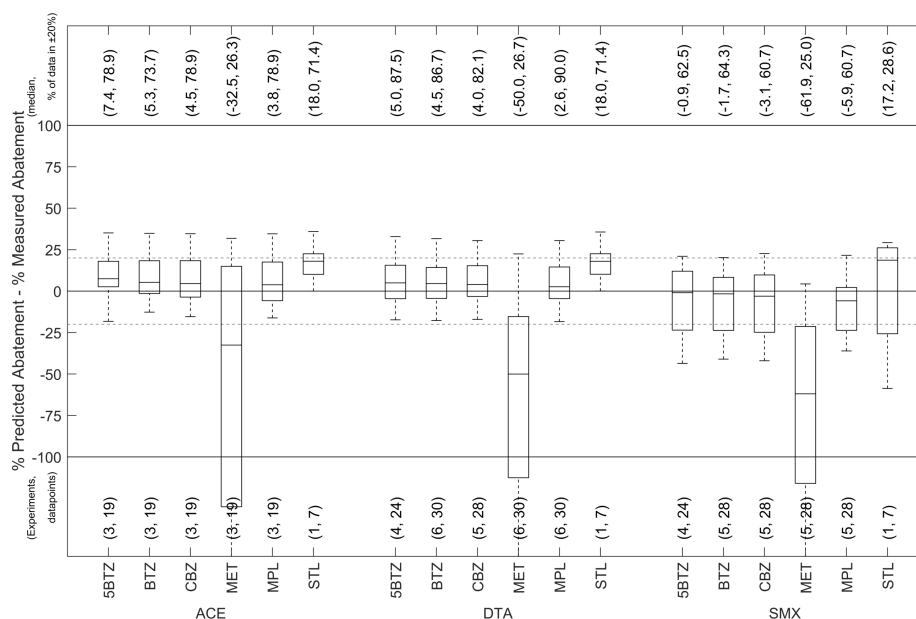


Figure B3: CBD laboratory experiments with river Wiese sand filtrate: Overview on differences between predicted and measured % abatement of possible combinations of probe compounds. Values in lower brackets: number of evaluated experiments, total number of predictions. Values in upper brackets: median of data points, share of data inside the $\pm 20\%$ range, shown by gray dashed lines. Horizontal names: UV susceptible probe compound, i.e., ACE, DTA, SMX: acesulfame, diatrizoic acid, sufamethoxazole, respectively. Vertical names: UV resistant CT_{OH} probe compound, i.e., 5BTZ, BTZ, CBZ, MET, MPL, STL: 5-methyl-1H-benzotriazole, 1H-benzotriazole, carbamazepine, metformin, metoprolol, sotalol, respectively.

Table B5: Relative differences in calculated UV fluences from models based on the indicated probe compounds and the set UV fluences, respectively. n : Number of evaluated experiments. Database: laboratory experiments with sand filtrates from rivers Rhine and Wiese (data set numbers: 13 – 30, [41]). H_{set} is the UV fluence set on the CBD device and H_{calc} is the calculated UV fluence from the model.

UV susceptible MP	UV resistant MP	n	$\frac{H_{\text{set}} - H_{\text{calc}}}{H_{\text{set}}}$	95% CI
ACE	5BTZ	15	39%	28% to 66%
	BTZ	15	41%	28% to 66%
	CBZ	15	32%	24% to 56%
	MET	15	42%	0% to 149%
	MPL	15	37%	22% to 58%
	STL	3	-43%	-63% to 35%
DTA	5BTZ	16	14%	-6% to 36%
	BTZ	18	13%	-6% to 37%
	CBZ	17	13%	-7% to 37%
	MET	18	15%	-6% to 48%
	MPL	18	13%	-6% to 37%
	STL	3	-3%	-8% to 34%
IHX	5BTZ	7	-1%	-21% to 20%
	BTZ	7	-1%	-29% to 20%
	CBZ	7	-6%	-30% to 11%
	MET	7	-22%	-63% to 17%
	MPL	7	-6%	-25% to 19%
	STL	2	-88%	-103% to -72%
IPA	5BTZ	12	-8%	-37% to 6%
	BTZ	12	-8%	-44% to 7%
	CBZ	12	-12%	-46% to -1%
	MET	12	-9%	-68% to 20%
	MPL	12	-10%	-42% to 5%
	STL	2	-113%	-123% to -102%
IPR	5BTZ	12	-24%	-49% to -7%
	BTZ	12	-23%	-54% to -6%
	CBZ	12	-26%	-56% to -12%
	MET	12	-20%	-77% to 6%
	MPL	12	-24%	-52% to -8%
	STL	2	-107%	-124% to -91%
SMX	5BTZ	16	-43%	-73% to -11%
	BTZ	17	-45%	-68% to -9%
	CBZ	17	-48%	-73% to -28%
	MET	17	-34%	-80% to 66%
	MPL	17	-43%	-61% to -13%
	STL	3	-144%	-178% to -100%

Appendix . Appendix B: Supporting Information for Chapter 4

Table B6: Percentage of predictions within $\pm 20\%$: statistical evaluation of single probe compounds. Data base: CBD laboratory experiments of sand filtrates of rivers Rhine and Wiese, as shown in Figures 4.3 and B3. Results present average values \pm half 95 % confidence intervals, n indicates the number of observations, respectively.

Substance	% predictions within $\pm 20\%$, all probe compounds	n	% predictions within $\pm 20\%$, MET, STL and SMX excluded	n
5BTZ	87 \pm 8	9	91 \pm 6	7
ACE	72 \pm 13	12	82 \pm 5	8
BTZ	87 \pm 9	9	90 \pm 8	7
CBZ	84 \pm 8	9	88 \pm 6	7
DTA	76 \pm 16	12	90 \pm 4	8
IHX	79 \pm 19	6	89 \pm 3	4
IPA	85 \pm 20	6	96 \pm 2	4
IPR	85 \pm 20	6	96 \pm 1	4
MET	57 \pm 18	9	-	0
MPL	85 \pm 8	9	89 \pm 6	7
SMX	60 \pm 16	12	-	0
STL	43 \pm 16	9	-	0
Average	74 \pm 6	54	89 \pm 3	28

Table B7: Percentage of predictions within $\pm 20\%$: statistical evaluation of single probe compounds. Data base: pilot-scale experiments of sand filtrates of rivers Rhine and Wiese, as shown in Figures B4 and B5. Results present average values \pm half 95 % confidence intervals, n indicates the number of observations, respectively.

Substance	% predictions within $\pm 20\%$, all probe compounds	n	% predictions within $\pm 20\%$, MET, STL and SMX excluded	n
5BTZ	78 \pm 7	12	83 \pm 5	8
ACE	84 \pm 7	12	91 \pm 2	8
BTZ	79 \pm 18	6	82 \pm 4	4
CBZ	76 \pm 13	6	83 \pm 5	4
DTA	80 \pm 13	6	87 \pm 4	4
IHX	70 \pm 7	12	-	0
IPA	84 \pm 6	9	87 \pm 5	7
IPR	85 \pm 6	9	87 \pm 4	7
MET	82 \pm 5	9	84 \pm 5	7
MPL	59 \pm 7	9	-	0
SMX	82 \pm 5	9	84 \pm 5	7
STL	73 \pm 9	9	-	0
Average	77 \pm 3	54	86 \pm 2	28

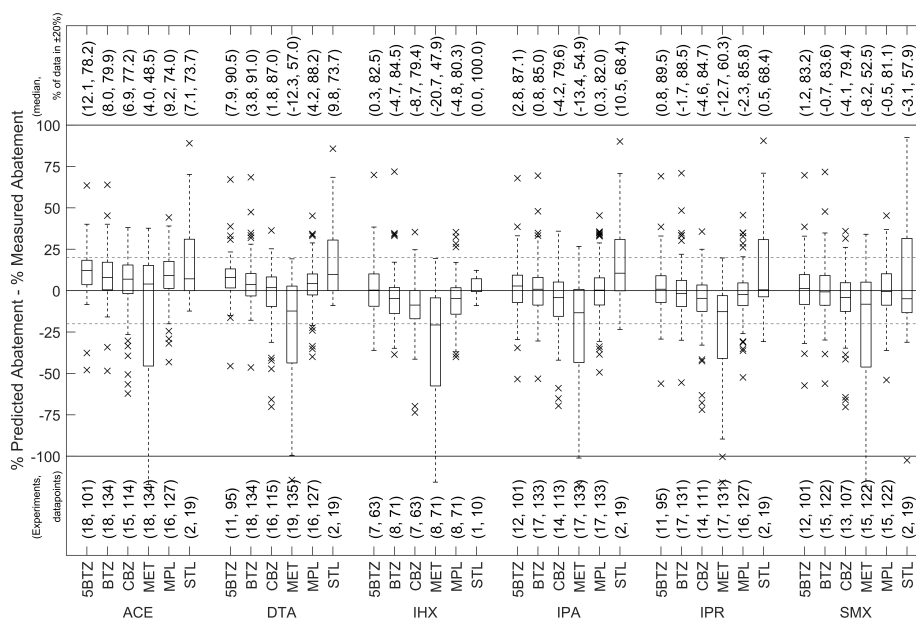


Figure B4: Pilot-scale experiments with river Rhine sand filtrate: Overview on differences between predicted and measured % abatement of possible combinations of probe compounds. Values in lower brackets: number of evaluated experiments, total number of predictions. Values in upper brackets: median of data points, share of data inside the $\pm 20\%$ range, shown by gray dashed lines. Horizontal names: UV susceptible probe compound, i.e., ACE, DTA, IHX, IPA, IPR, SMX: acesulfame, diatrizoic acid, iohexol, iopamidol, iopromide, sufamethoxazole, respectively. Vertical names: UV resistant CT_{OH} probe compound, i.e., 5BTZ, BTZ, CBZ, MET, MPL, STL: 5-methyl-1H-benzotriazole, 1H-benzotriazole, carbamazepine, metformin, metoprolol, sotalol, respectively.

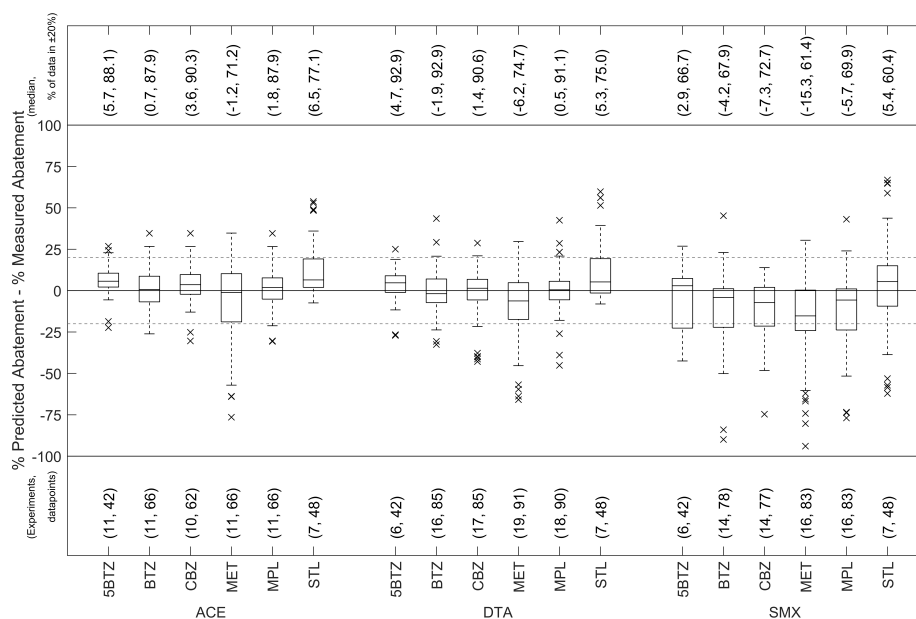


Figure B5: Pilot-scale experiments with river Wiese sand filtrate: Overview on differences between predicted and measured % abatement of possible combinations of probe compounds. Values in lower brackets: number of evaluated experiments, total number of predictions. Values in upper brackets: median of data points, share of data inside the $\pm 20\%$ range, shown by gray dashed lines. Horizontal names: UV susceptible probe compound, i.e., ACE, DTA, SMX: acesulfame, diatrizoic acid, sufamethoxazole, respectively. Vertical names: UV resistant CT_{OH} probe compound, i.e., 5BTZ, BTZ, CBZ, MET, MPL, STL: 5-methyl-1H-benzotriazole, 1H-benzotriazole, carbamazepine, metformin, metoprolol, sotalol, respectively.

Appendix C: Supporting Information for Chapter 5

This is a copy of the supporting information prepared for the submission to the Water Research journal [42]:

Wünsch, R., Hettich, T., Prahtel, M., Thomann, M., Wintgens, T., and von Gunten, U.: Tradeoff Between Micropollutant Abatement and Bromate Formation during Ozonation of Concentrates from Nanofiltration and Reverse Osmosis Processes.

Table C1: Studies reporting on bromate formation upon ozonation of reverse osmosis concentrates. The bromate yield calculated with Equation 5.1 (Chapter 5).

Study	RO ⁱ Feed	Concentrate Treatment	Treatment Goals	DOC ⁱⁱ [mg L ⁻¹]	pH [-]	Bulk Water Quality Parameters				BrO ₃ ⁻ [μg L ⁻¹]	Bromate After Ozonation		
						NH ₄ ⁺ [mg L ⁻¹]	NO ₂ ⁻ [mg L ⁻¹]	Alkalinity [mg CaCO ₃ L ⁻¹]	Br ⁻ [mg L ⁻¹]		Spec. O ₃ dose [mg (mg DOC) ⁻¹]	BrO ₃ ⁻ [μg L ⁻¹]	η [%]
Benner <i>et al.</i> (2008) ⁱⁱⁱ	Municipal wastewater after secondary treatment + ultrafiltration	O ₃	Abatement of MP ₅ ^{iv}	46.0	8.0	n.a. ^v	n.a. ^v	n.a. ^v	1.2	n.a. ^v	0.17	24	1.2
											0.24	35	1.8
Justo <i>et al.</i> (2013) ^{vi}	Municipal Wastewater after secondary treatment + ultrafiltration	UV/H ₂ O ₂ or O ₃	Abatement of MP ₅ ; removal of TOC ^{vii} and COD ^{viii} ; increase BOD ₅ -ix/COD	27.6 (TOC)	8.3	3.23	n.a. ^v	914	9.64	n.a. ^v	6.93	1100	7.1
King <i>et al.</i> (2020) ^x	Municipal wastewaters from five sites	O ₃	Abatement of micropollutants; precipitation of metals; pathogen indicator inactivation	22.5	7.3	n.d. ^{xi}	n.d. ^{xi}	385	2.1	110	0.45	250	4.2
				36.0	7.7	4.6	0.4	640	2.6	0	0.90	450	10.1
				42.9	7.4	3.1	1.1	808	2.4	0	0.45	70	1.7
				63.2	6.7	291	n.d. ^{xi}	664	1.8	15	0.90	170	4.1
				86.7	6.9	317	5.9	848	1.6	15	0.45	70	1.8
											0.90	240	6.4
Zhang <i>et al.</i> (2020) ^{xii}	Municipal wastewater after nitrification + microfiltration	O ₃ + biological activated carbon	Abatement of MP ₅ ; biological reduction of nitrate and bromate	40.0	7.7	n.a. ^v	< 0.64	660	2.7	< 2	0.45	120	3.6
											0.90	260	8.5
											0.45	35	0.8
											0.90	140	4.9

ⁱ RO: reverse osmosis. ⁱⁱ DOC: dissolved organic carbon. ⁱⁱⁱ [205] ^{iv} MP: micropollutant. ^v n.a.: not analyzed / not stated ^{vi} [206] ^{vii} TOC: total organic carbon. ^{viii} BOD₅: biological oxygen demand in a five-day aerobic biodegradation test. ^x [207] ^{xi} n.d.: not detected. ^{xii} [208]

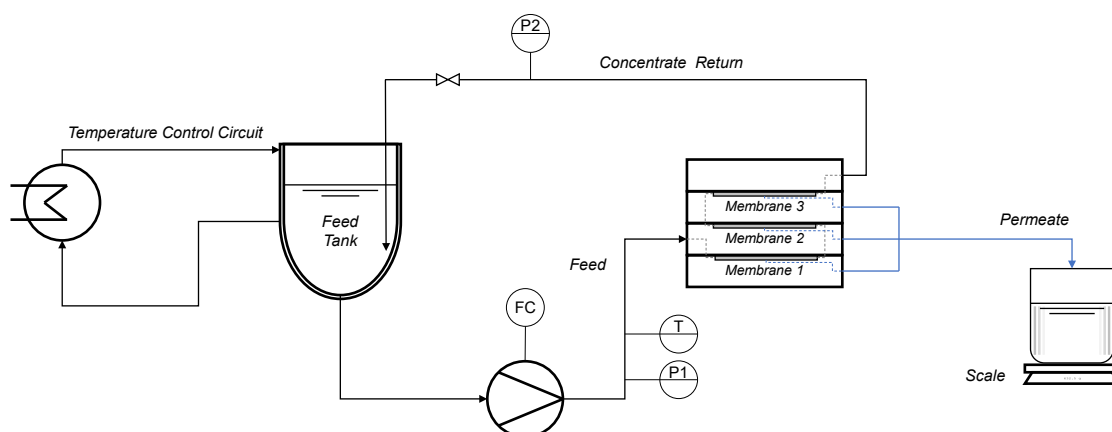


Figure C1: Membrane bench-scale test unit for the measurement of retentions of dissolved organic carbon, bromide and non-spiked micropollutants.

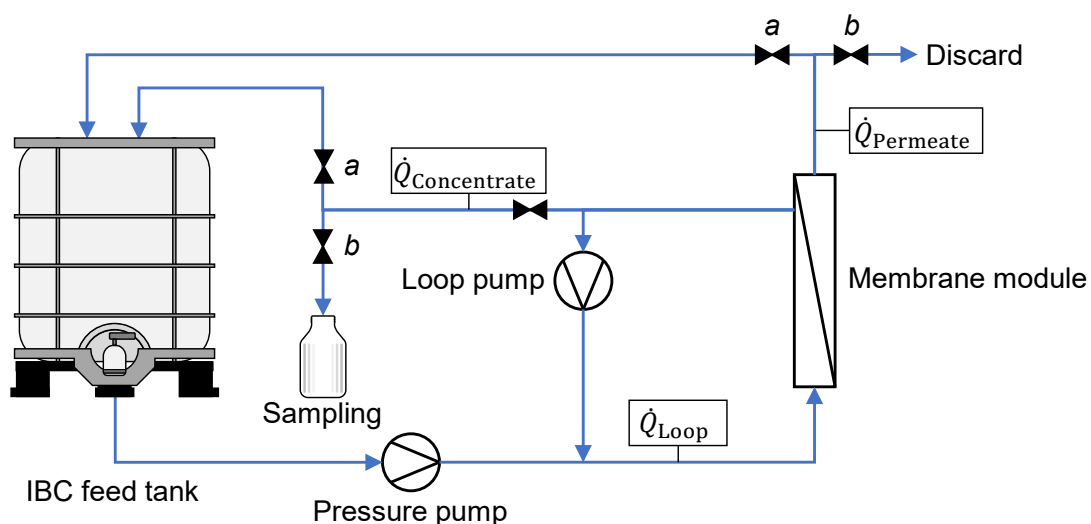


Figure C2: Scheme of the pilot plant used to produce the concentrates. Permeate flow ($\dot{Q}_{\text{Permeate}}$) was set to 200 L h^{-1} , water yield of 85 % was achieved by adjusting the concentrate volume flow ($\dot{Q}_{\text{Concentrate}}$) to 35.3 L h^{-1} . The loop volume flow before membrane (\dot{Q}_{Loop}) was set to $1 \text{ m}^3 \text{ h}^{-1}$ to assure turbulent flow conditions across the membrane. During the stabilization phase, permeate and retentate were recycled to the IBC feed tank by opening valves 'a' and closing valves 'b'. To take grab samples of the concentrate, valves 'b' were opened and 'a' were closed.

Appendix . Appendix C: Supporting Information for Chapter 5

Table C2: Selected micropollutants (MPs): Acid dissociation constants (pK_a) and observed second-order rate constants for reactions with ozone ($k_{O_3,MP}$) or hydroxyl radicals ($k_{OH,MP}$). pH was assumed to have a negligible effect on $k_{O_3,MP}$ if the respective compounds pK_a was at least two pH units above or below the pH of the investigated concentrates, i.e., 8.3 ± 0.1 . Otherwise, the pH-dependent value was calculated (see table footnotes ^{xvii} and ^{xxv}). pH was generally assumed to have limited impact on $k_{OH,MP}$, therefore all reported values were averaged.

Compound	pK_a	$k_{O_3,MP} / M^{-1} s^{-1}$ Value	pH	$k_{OH,MP} / 10^9 M^{-1} s^{-1}$ Value	pH
Group I: high ozone reactivity ($k_{O_3,MP} \geq 10^5 M^{-1} s^{-1}$)					
Carbamazepine (CBZ)	16 ⁱ	$\approx 3.0 \times 10^{5ii}$	7.0	8.8 ⁱⁱ	7.0
				5.85 ⁱⁱⁱ	7.0 (?) ^{iv}
				9.4 ^v	n.a. ^{vi}
				2.05 ^{vii}	5.0
				4.63 ^{viii}	3.0
				8.83 ^{ix}	3.0 (?) ^{iv}
				6.8 ^x	n.a. ^{vi}
				9.5 ^{xi}	n.a. ^{vi}
Average CBZ	16	3.0×10^5	7.0	7.0 ± 2.7	3.0 to 7.0
Diclofenac (DCF)	4.2 ⁱⁱ	$\approx 1.0 \times 10^{6ii}$	7.0	7.5 ⁱⁱ	7.0
				12.4 ^{xi}	n.a. ^{vi}
				9.3 ^{xii}	7.0
Average DCF	4.2	1.0×10^6	7.0	9.7 ± 2.5	7.0
Group II: moderate ozone reactivity ($10^1 M^{-1} s^{-1} \leq k_{O_3,MP} < 10^5 M^{-1} s^{-1}$)					
Atenolol (ATO)	9.64 ^{xiii}	1.7×10^{3xiv}	7.0	8.0 ± 0.5^{xiv}	7.0
		2.5×10^{3xvi}	7.0		
		6.2×10^{4xvi}	8.5		
Average ATO	9.6 ± 0.1	$(4.0 \pm 0.6) \times 10^{4xvii}$	8.3	8.0 ± 0.5	7.0
Benzotriazole (BTA)	8.6 ^{xviii}	1.8×10^{1xix}	2.0	7.6 and 9.0 ^{xx}	5.8 and 10.5
	8.2 ^{xxi}	2.2×10^{1xix}	5.0	8.34 ^{xxii}	7.0
	8.3 ^{xxii}	2.2×10^{2xxiii}	7.0	6.17 to 17.0	2.0 to 10.25
	8.62 ^{xxiii}	2.3×10^{3xvi}	8.5	(avg: 11.1) ^{xix}	
	8.37 ^{xxiv}				
Average BTA	8.4 ± 0.2	$(1.8 \pm 0.4) \times 10^{3xxv}$	8.3	9.2 ± 1.6	2.0 to 10.5

Table continues next page.

ⁱ Predicted by MarvinSketch (V.20.16, ChemAxon). ⁱⁱ [158] ⁱⁱⁱ [169] ^{iv} (?): Some data was stated, but it is unclear whether it refers to the reported rate constant. ^v [265] ^{vi} Data not available / not stated in respective publication. ^{vii} [266] ^{viii} [267] ^{ix} [268] ^x [269] ^{xi} [92] ^{xii} [270] ^{xiii} [271] ^{xiv} [205] ^{xv} [272] ^{xvi} [162] ^{xvii} Observed second-order rate constant for reactions of atenolol with O_3 at pH 8.3 were obtained by linear regression analysis of the reported $k_{O_3,ATO}$ as function of the protonated fraction ($\alpha = 1/(1 + 10^{pH-pK_a})$) utilizing the average pK_a , leading to the equation: $k_{O_3,ATO} \approx (8.4 \pm 0.6) \times 10^5 M^{-1} s^{-1} \times (1 - \alpha)$; the standard deviation was calculated with the Gaussian error propagation rule. ^{xviii} [273] ^{xix} [274] ^{xx} [275] ^{xxi} [276] ^{xxii} [141] ^{xxiii} [277] ^{xxiv} [278] ^{xxv} Observed second-order rate constant for reactions of 1H-benzotriazole with O_3 at pH 8.3 were obtained in the same way as atenolol, see ^{xvii}, leading to the equation: $k_{O_3,BTA} \approx (4.1 \pm 0.1) \times 10^3 M^{-1} s^{-1} \times (1 - \alpha)$; the standard deviation was calculated with the Gaussian error propagation rule.

<i>Table continued from previous page.</i>					
Compound	pK _a	$k_{\text{O}_3,\text{MP}} / \text{M}^{-1} \text{s}^{-1}$ Value	pH	$k_{\cdot\text{OH},\text{MP}} / 10^9 \text{M}^{-1} \text{s}^{-1}$ Value	pH
Bezafibrate (BZF)	3.6 ⁱⁱ	$5.9 \times 10^{2\text{ii}}$ 1.5×10^3 to 7.1×10^4 (avg: 6.1×10^3) ^{xxvi}	7.0 6.0 to 8.0	7.4 ⁱⁱ 8.0 ^{xxvii}	7.0 5.0 to 8.0
Average BZF	8.4 ± 0.2	$(3.3 \pm 3.9) \times 10^3$	6.0 to 8.0	8.0 ^{xxviii} 7.7 ± 0.3	7.0 5.0 to 8.0
Group III: ozone resistant ($k_{\text{O}_3,\text{MP}} < 10^1 \text{M}^{-1} \text{s}^{-1}$), high $\cdot\text{OH}$ reactivity ($k_{\cdot\text{OH},\text{MP}} \geq 5 \times 10^9 \text{M}^{-1} \text{s}^{-1}$)					
Ibuprofen (IBU)	4.9 ⁱⁱ	$9.6 \times 10^{0\text{ii}}$	7.0	7.4 ⁱⁱ 6.5 ^{xxix} 6.67 ^{xxx}	7.0 3.5 7.0
Average IBU	4.9	9.6×10^0	7.0	6.9 ± 0.5	3.5 to 7.0
Group IV: ozone resistant ($k_{\text{O}_3,\text{MP}} < 10^1 \text{M}^{-1} \text{s}^{-1}$), moderate $\cdot\text{OH}$ reactivity ($1 \times 10^9 \text{M}^{-1} \text{s}^{-1} \leq k_{\cdot\text{OH},\text{MP}} < 5 \times 10^9 \text{M}^{-1} \text{s}^{-1}$)					
Atrazine (ATZ)	4.2 ⁱ	$6.0 \times 10^{0\text{xxxi}}$ $7.9 \times 10^{0\text{xxxii}}$	2.0 n.a. ^{vi}	2.4 ⁱⁱ 2.4 ^{xxxiii} 1.7 ^{xxxiv} 2.6 ^{xxxv}	7.0 8.1 7.5 3.6
Average ATZ	4.2	$(7.0 \pm 1.3) \times 10^0$	2.0	2.3 ± 0.4	3.6 to 8.1
xxvi [279] xxvii [280] xxviii [281] xxix [282] xxx [283] xxxi [157] xxxii [284] xxxiii [285] xxxiv [286] xxxv [287]					

Standardization of concentrates

Preparation of micropollutant stock solutions: For each MP, an individual stock solution was prepared by weighting in the MPs in volumetric flasks (amber glass, previously cleaned with HPLC grade methanol). The MPs were dissolved in in methanol (HPLC grade). The single stock solutions were in the concentration range between 176.8 to 367.3 mg L⁻¹, according to the weight and solvent volume.

A mixed spiking solution was prepared by mixing defined volumes of the individual MP stock solutions with methanol. The mixed spiking solution had a concentration of 20 mg L⁻¹ of each MP, respectively.

Preparation of other stock solutions: A Br⁻ stock solution was prepared by weighting 564 mg NaBr in a 250 mL volumetric flask and dissolving it in ultra-purified water (≥ 18.2 M Ω , arium pro UV, Sartorius, Germany). The concentration of the Br⁻ stock solution was 21.9 mM.

A TIC stock solution was prepared by weighting 8.825 g Na₂CO₃ in a 1 L volumetric flask and dissolving it in ultra-purified water (≥ 18.2 M Ω). The concentration of the TIC stock solution was 83.3 mM TIC (1'000 (mg TIC) L⁻¹).

A boric acid stock solution was prepared by weighting 61.83 g H₃BO₃ in a 1 L volumetric flask and dissolving it with ultra-purified water (≥ 18.2 M Ω). The concentration of the boric acid stock solution was 1 M.

Preparation of concentrates: First, the concentrates were vacuum filtered to remove possible particles with glass fiber filters (GF5, Macherey-Nagel, Germany, nominal cut-off: 0.4 μ m). Aliquots of the filtered samples were analyzed for DOC and Br⁻. The filtered concentrate was acidified with HCl to pH 3 to 3.5, subsequently all inorganic carbon was purged overnight by bubbling nitrogen through the concentrates.

In parallel, the desired MPs were spiked by dosing a defined volume of the mixed spiking solution into an empty volumetric flask (1 L) previously cleaned with methanol (HPLC grade). After spiking, the methanol was evaporated under a constant nitrogen stream overnight [247]. A defined volume of the TIC-free concentrate was transferred to the MP-spiked flask. The transferred volume was calculated from the known DOC concentration of the concentrate, the volume of the volumetric flask (1 L) and the desired DOC of 6 mg L⁻¹ in the standardized concentrates. Similarly, with the known Br⁻ concentration of the concentrate, bromide was adjusted to the desired concentration of 450 μ g Br⁻ L⁻¹ by adding a defined volume of the Br⁻ stock solution. Then the TIC stock solution was added to adjust a TIC concentration of 30 mg L⁻¹ in the standardized concentrates. This Br⁻ concentration was selected based on the maximum 80-percentile Br⁻ concentration of the different feed waters from historic data (RR, about 180 μ g Br⁻ L⁻¹, 2003 to 2020) and a relative Br⁻ retention of 25 %, as observed in this range for the NF filtration membranes (Table 5.3, Chapter 5). The standardized concentrates were buffered by 10 mM boric acid, added from the boric acid stock solution. Then, the volumetric flasks were filled up to the 1 L mark with ultra-purified water (≥ 18.2 M Ω). Finally,

Table C3: Details on purities and suppliers of the used chemicals.

Compound	Molecular Weight	Minimal Purity	Supplier
Atenolol	266.2	98.0 %	Sigma-Aldrich
Atrazine	215.7	97.0 %	abcr
Benzotriazole	119.1	99.0 %	Sigma-Aldrich
Bezafibrate	361.1	98.0 %	Sigma-Aldrich
Carbamazepine	236.3	98.0 %	Sigma-Aldrich
Diclofenac (from Diclofenac-Na)	296.1	99.0 %	Molekula
Ibuprofen	206.1	98.0 %	Carbosynth
Methanol	32.0	99.9 %	Sigma-Aldrich
NaBr	102.9	99.0 %	Roth
Na ₂ CO ₃	106.0	99.5 %	Roth
H ₃ BO ₃	61.8	99.5 %	Sigma-Aldrich

the desired pH of 8.3 was adjusted with HCl and NaOH.

The prepared standardized concentrates were tightly closed and left overnight at room temperature to assure complete dissolution of the MPs.

Details on the chemical purities and manufacturers are listed in Table C3.

Table C4: Water quality parameters of the water samples before ozonation, except for pH values reported after ozonation as well. All samples before ozonation were analyzed in duplicates or triplicates.

Water Source		Membrane	Bulk Water Quality Parameters					Spiked Micropollutants								
			DOC ⁱ [mg L ⁻¹]	UVA ⁱⁱ [m ⁻¹]	SUVA ⁱⁱⁱ [L mg ⁻¹ m ⁻¹]	TIC ^{iv} [mg L ⁻¹]	pH	EC ^v [µg L ⁻¹]	Br ⁻ [µg L ⁻¹]	ATO ^{vi} [µg L ⁻¹]	ATZ ^{vii} [µg L ⁻¹]	BTA ^{viii} [µg L ⁻¹]	BZF ^{ix} [µg L ⁻¹]	CBZ ^x [µg L ⁻¹]	DCF ^{xi} [µg L ⁻¹]	IBU ^{xii} [µg L ⁻¹]
River Wiese water (RW)		LPRO ^{xiii}	6.2	16.9	2.7	32.4	8.35 - 8.39	n.d. ^{xiv}	531	75	66	61	81	66	68	69
		NF1 ^{xv}	6.3	16.8	2.7	33.1	8.38 - 8.41	n.d. ^{xiv}	495	77	68	67	78	67	70	67
River Rhine water (RR)		LPRO	6.6	15.6	2.4	30.7	8.29 - 8.33	2020	450	60	68	63	85	67	68	86
		NF1	6.1	16.6	2.7	30.2	8.25 - 8.28	1757	442	69	76	72	92	71	70	91
		NF2	6.2	17.2	2.8	30.1	8.29 - 8.33	1399	505	61	68	66	84	66	68	85
Lake Biel water (LB)		LPRO	6.5	16.6	2.5	27.9	8.30 - 8.32	1794	517	66	67	105	70	73	74	95
		NF1	6.2	16.5	2.7	27.9	8.27 - 8.33	1377	474	60	60	91	64	65	63	83
		NF2	6.4	17.0	2.7	27.7	8.33 - 8.34	1377	505	64	64	102	69	70	75	99

ⁱ Dissolved organic carbon. ⁱⁱ UV absorbance at 254 nm divided by the optical path length. ⁱⁱⁱ Specific UVA, i.e., UVA / DOC. ^{iv} Total inorganic carbon. ^v Electrical conductivity. ^{vi} Atenolol. ^{vii} Atrazine. ^{viii} 1H-benzotriazole. ^{ix} Bezafrilate. ^x Carbamazepine ^{xi} Diclofenac. ^{xii} Ibuprofen. ^{xiii} Low-pressure reverse osmosis. ^{xiv} not determined. ^{xv} NF: Nanofiltration.

Protocol of ozonation experiments

The standardized concentrates were ozonated at different specific ozone doses to investigate the abatement of MPs and formation of BrO_3^- .

Aliquots of the standardized concentrates were filled in glass vials (40 mL EPA screw neck vials) previously muffled at 500 °C for 5 h.

An ozone stock solution was prepared by saturating ice-cooled ultra-purified water ($\geq 18.2 \text{ M}\Omega$) with ozone produced from an ozone generator (803BT, BMT, Germany) supplied with pure oxygen. The ozone concentration of the saturated stock solution was measured directly by a spectrophotometer (Cary 100, Varian, USA) at 260 nm by adding 0.5 mL of the O_3 stock solution to 2 mL of 50 mM phosphoric acid in a closed quartz cuvette (1 cm optical pathlength) and using a molar absorption coefficient of ozone of $\epsilon_{\text{O}_3,260} = 3'200 \text{ M}^{-1} \text{ cm}^{-1}$, [121]. A constant ozone concentration of the ozone stock solution during the experiments was assured by continued ozone bubbling and monitoring the saturated solution with an online UV sensor (AVASPEC-ULS2048CL-EVO-RS with FDP-7UVIR200-2-1 2mm path dip probe, Avantes, The Netherlands).

To obtain similar dilution of all samples in an experimental series, ultra-purified water ($\geq 18.2 \text{ M}\Omega$) was added to samples that were prepared for lower ozone doses. Subsequently, the ozone stock solution was added using gas-tight glass syringes. Samples were vigorously stirred using a PTFE magnetic stir bar for about 10 seconds and then quickly capped with screw caps (silicone/PTFE septa). Sample volumes (35 mL sample) were selected to minimize headspace to < 4 mL after addition of ultra-purified water and the ozone stock solution. The relative standard deviation for the specific O_3 dose ($\text{mg O}_3 (\text{mg DOC})^{-1}$) was estimated $\pm 15 \%$ by the Gaussian error propagation rule.

Analytical methods

Dissolved organic carbon (DOC) was measured by size exclusion chromatography (SEC) coupled with an organic carbon detector (OCD) and a UV absorption detector at 254 nm (UVD) (model 8, DOC-Labor Dr. Huber, Germany), [54]. The DOC presented in Table C4 is the DOC in the bypass peak, accounting for both chromophoric and non-chromophoric DOC fractions [54]. The standard error of the DOC measured in the bypass was estimated 7 % from replicate injections of the same sample.

The total inorganic carbon (TIC) was measured with a TOC-L analyzer (Shimadzu, Japan) as purgeable carbon after acidification with phosphoric acid. pH was measured with a probe (TIX 940, WTW/Xylem Analytics Germany) freshly calibrated at pH 7 and 9. UV absorbance at 254 nm (UVA) was measured with a UV spectrophotometer (DR6000, Hach/Danaher, USA) with 1 cm optical pathlength disposable cuvettes (PMMA, Brand, Germany) without prior sample filtration.

Bromide and bromate were analyzed by ion chromatography (IC) coupled with an inductively coupled plasma (ICP), using a tandem mass spectrometer (MS/MS) as detector. No sample preparation was necessary. Samples were injected (100 μL) to the IC (ICS-2100, Thermo Fisher Analytics, USA) equipped with a guard column (Dionex IonPac AG-18, 2×50 mm, Thermo Fisher Analytics, USA) and a separation column (Dionex IonPac AS-18, 2×250 mm, Thermo Fisher Analytics, USA). KOH was applied as eluent with a gradient method. Bromide and bromate were detected as bromine at the ICP-MS/MS (8800 QqQ, Agilent Technologies, USA) in no-gas mode at mass 81, as this showed the highest sensitivity. The limit of detection (LoD) and limit of quantification (LoQ) were $0.7 \mu\text{g L}^{-1}$ and $2 \mu\text{g L}^{-1}$, respectively. The calibrated range was 2 to $20 \mu\text{g L}^{-1}$ for bromate and 100 to $600 \mu\text{g L}^{-1}$ for bromide, respectively, and the linearity in the calibrated range was given ($R^2 > 0.99$, five-point calibrations, respectively). Standard measurement errors were determined to be 8 % for both species from replicate standard injections. The relative standard deviation of η (Equation 5.1, Chapter 5) was estimated ± 11 % by the Gaussian error propagation rule.

MPs were measured with an Agilent 1260 Infinity II Prime HPLC system (Agilent Technologies, Switzerland). Samples were prepared by centrifugation at $13'700$ g for 5 minutes with a Spectrafuge 24D (Witec, Switzerland). The supernatant was transferred to a 300 μL fixed insert vial and an aliquot of 1 μL was injected (HALO AQ-C18 column, 2.1×50 mm; $2.7 \mu\text{m}$ particle size, Infocroma, Switzerland). A gradient method was used with eluents A (2 mM ammonium fluoride in ultra-purified water) and B (2 mM ammonium fluoride in HPLC-grade methanol). Mass spectrometry detection was performed with an Agilent Ultivo 6465B triple quadrupole equipped with an electrospray ionization (ESI) source operated in positive and negative mode. The mass spectrometer was run in multi reaction monitoring mode (MRM). The LC-MS/MS system was controlled under MassHunter Acquisition for Ultivo Version 1.2 (Agilent Technologies). Quantification of the samples was performed using an eight-point external calibration curve. A standard stock solution of 10 mg L^{-1} of each single MP was prepared freshly at the day of measurement in methanol and further diluted to concentrations in the range of 8 to $250 \mu\text{g L}^{-1}$. The linearity of the calibration curves was calculated by a least squares fitting without using the origin. $R^2 \geq 0.995$ was obtained each time and the accuracy was in the range of 80 to 120 % of the calibration point. The limits of detection for all MPs were in the range of $0.2 \mu\text{g L}^{-1}$ (carbamazepine) to $2.7 \mu\text{g L}^{-1}$ (ibuprofen, Table C5). Maximum standard deviations (σ) for all MPs are reported in Table C5, determined from the initial samples, i.e., the samples with an ozone dose of $0 \text{ mg O}_3 (\text{mg DOC})^{-1}$ measured in duplicates or triplicates. Blank samples and spiked samples were measured within each sequence run, serving as quality control for sample preparation. Every ten samples a reference standard with $20 \mu\text{g L}^{-1}$ of the respective compounds was measured. The standard uncertainty (u_c) of $\ln([i] / [i]_0)$ for a MP i , estimated by the Gaussian error propagation rule, is $\sqrt{2}\sigma$. The standard uncertainty of relative abatement, i.e., $1 - [i] / [i]_0$ (Equation 5.2, Chapter 5), depends on the degree of abatement and can be estimated by Equation C1 (Gaussian error propagation

rule).

$$u_c = \sqrt{2}\sigma \frac{[i]}{[i]_0} \quad (C1)$$

The electron donating capacity (EDC) was determined along a modified standard protocol, [210]. In brief, a stock solution containing the radical cation of 2,2'-azino-bis(3-ethylbenzothiazoline-6-sulfonate) (ABTS^{•+}) was prepared by dissolving ABTS (1 mM) in 7.5 mM sulfuric acid (pH 2) and adding 350 µL hypochlorite (1 mM) per milliliter ABTS stock. In contrast to the standard protocol, samples were measured at pH 8.3 using boric acid as buffer (10 mM) (according to the standard protocol, samples are typically measured at pH 7 using a phosphate buffer; phosphate buffer was avoided here due to formation of precipitates in some concentrates upon buffer addition). Previous research showed that the EDC of aquatic humic substances (HS) and natural organic matter (NOM) is typically higher at pH 7 than at pH 9 inside a range of about 0.1 to 1.0 mmol e⁻ (gHS)⁻¹ [288]. EDCs were measured from non-standardized concentrates. Samples were prepared by filtration over 0.45 µm PVDF syringe filters using 3 mL NORM-JECT PP/PE syringes without latex. After the addition of 1250 µL sample and 80 µL of buffer (1 M boric acid; final concentration: 50 mM) to a disposable semi micro-cuvette (1 cm optical pathlength, PMMA, Brand, Germany), 270 µL ABTS^{•+} stock solution was added and the solution was thoroughly mixed with polystyrene mixing spatulas. The reaction was timed (15 minutes) and subsequently the absorbance at 728 nm (*A*) was measured on a spectrophotometer (Cary 100, Varian, USA). The EDC was calculated according to Equation S2, [210].

$$EDC = \frac{A_{\text{Blank}} - A_{\text{Sample}}}{l \times \epsilon_{\text{ABTS}^{\bullet+}}} \times \frac{1}{[\text{DOC}]} \quad (C2)$$

*A*_{Sample} is the absorbance at 728 nm after 15 minutes reaction time. *A*_{Blank} is the absorbance at 728 nm with ultra-purified water (≥ 18.2 MΩ) used instead of sample. *l* is the optical pathlength (1 cm), $\epsilon_{\text{ABTS}^{\bullet+}}$ is the absorption coefficient (14'000 M⁻¹ cm⁻¹ at pH 7 and 728 nm,

Table C5: Limits of detection (LoD) and maximum standard measurement errors (σ) of the micropollutants. σ were determined from duplicate or triplicate analysis of the samples with 0 mg O₃ (mg DOC)⁻¹.

Compound	Limit of Detection [µg L ⁻¹]	Maximum Standard Measurement Error (σ) [%]
Atenolol (ATO)	0.7	3.1
Atrazine (ATZ)	0.3	3.3
1H-benzotriazole (BTA)	1.8	9.1
Bezafibrate (BZF)	0.7	3.1
Carbamazepine (CBZ)	0.2	2.6
Diclofenac (DCF)	1.4	3.3
Ibuprofen (IBU)	2.7	7.3

Appendix . Appendix C: Supporting Information for Chapter 5

Table C6: Slopes, their standard error and R^2 calculated from linear regression analysis for the EDC measurements of non-standardized concentrates.

Water Source	Membrane	Slope [mM e ⁻ (g C) ⁻¹]	Standard Error (slope)	R^2 [-]
RW	NF1	3.70	0.09	0.998
	LPRO	3.80	0.09	0.998
RR	NF1	3.51	0.11	0.997
	NF2	4.16	0.11	0.998
	LPRO	2.29	0.23	0.971
LB6	NF1	2.64	0.15	0.990
	NF2	2.57	0.08	0.997
	LPRO	1.85	0.07	0.995

[289], assumed to be the same at pH 8.3). [DOC] is the DOC concentration of the sample. All concentrates (range of [DOC]: 7.5 to 12.6 mg L⁻¹) were measured in dilution series with four dilution steps (dilution factors: 1.00, 1.14, 1.32, 1.56; diluted with ultra-purified water, ≥ 18.2 M Ω) and the EDC (unit: mM e⁻ (g C)⁻¹) of a concentrate was calculated from the resulting slope of the linear regression curve ($R^2 \geq 0.99$ for all, except $R^2 = 0.97$ for RR LPRO concentrate, Table C6).

The absolute EDC of standardized concentrates (Table C6) was calculated by multiplying the EDC of the non-standardized concentrates with the DOC concentration of the respective standardized concentrate (Table C4).

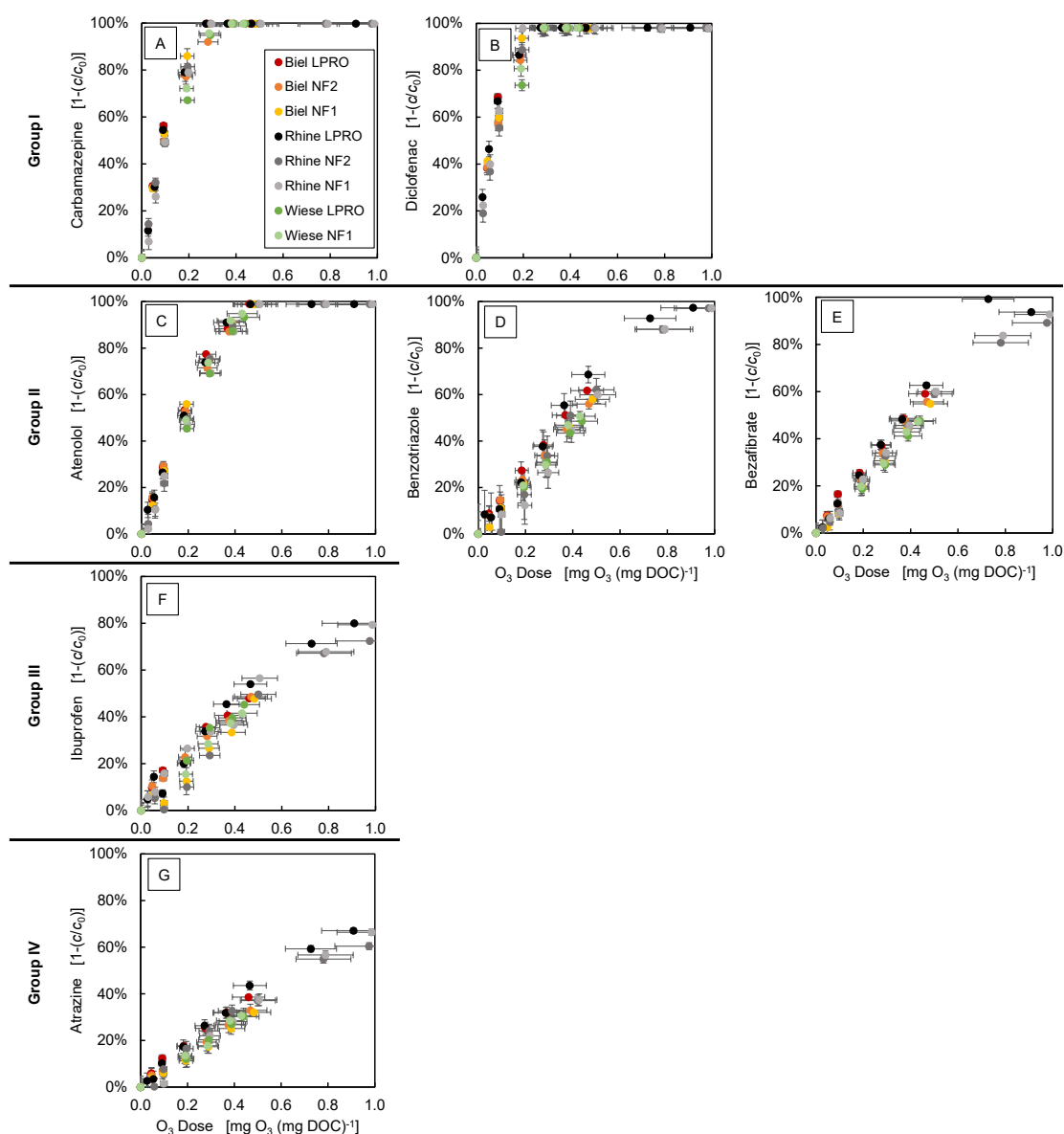


Figure C3: Relative abatement of micropollutants as a function of the specific O_3 dose in standardized concentrates. Classification in groups I to IV according to the kinetic data shown in Table 5.2 (Chapter 5), [160]. The color code is explained in the legend in subplot A. Error bars represent standard deviations of replicate experiments. If no replicate experiment was conducted, they were calculated with the Gaussian error propagation rule.

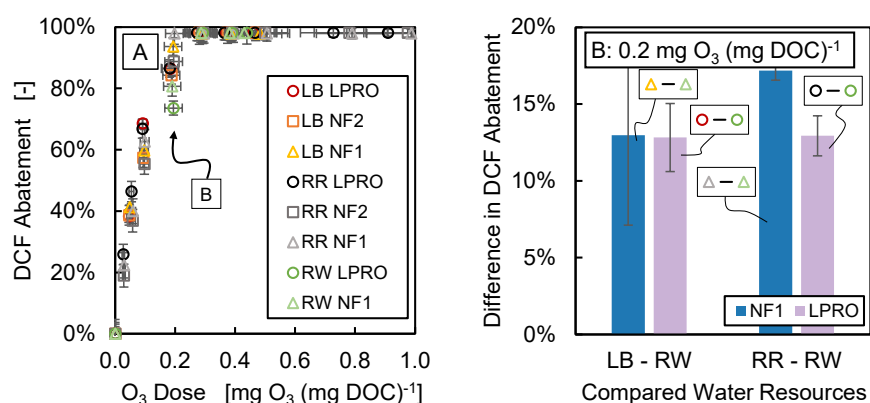


Figure C4: A: Abatement of diclofenac (DCF) as a function of the specific ozone dose. Error bars represent standard deviations of replicate experiments or, if no replicate experiment was conducted, calculated with the Gaussian error propagation rule. B: Differences in the relative abatements of DCF in pair-wise comparisons between LB or RR with RW as reference, respectively, at a specific O₃ dose of 0.2 mg O₃ (mg DOC)⁻¹. Error bars represent standard deviations calculated with the Gaussian error propagation rule.

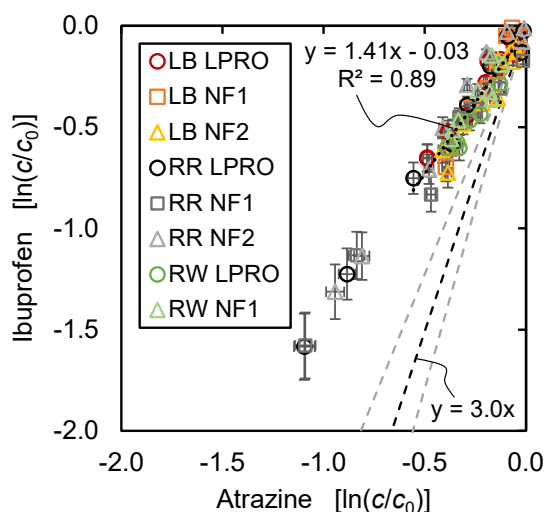


Figure C5: Natural logarithm of the relative residual concentration of ibuprofen as a function of the natural logarithm of the relative residual concentration of atrazine. The black dashed line represents the expected ratio for abatements by reactions with •OH only, utilizing the corresponding second-order rate constants for reactions with •OH (Table 5.2, Chapter 5). The grey dashed lines are standard deviations caused by the errors in the second-order rate constants. Error bars of the symbols represent standard deviations of the abatements. The black dotted line is the linear regression curve from all experimental abatements with specific ozone doses ≤ 0.5 mg O₃ (mg DOC)⁻¹.

Details on the evaluation of the membrane treatment with subsequent concentrate ozonation

A RW non-standardized LPRO concentrate was ozonated with different specific O_3 doses (0.24, 0.37, 0.49 and 0.61 mg O_3 (mg DOC) $^{-1}$). In contrast to the standardized RW LPRO concentrate, the RW non-standardized LPRO concentrate was neither pH adjusted nor were DOC and TIC concentrations corrected, but only MPs, bromide and borate were spiked (10 mM for buffering). Water quality parameters before ozonation were as follows: DOC: 15.1 mg L $^{-1}$, UVA: 39.7 m $^{-1}$, SUVA: 2.6 L mg $^{-1}$ m $^{-1}$, TIC: 160 mg L $^{-1}$, Br $^{-}$: 570 μ g L $^{-1}$. Spiked MP concentrations were: ATO: 197 μ g L $^{-1}$, ATZ: 173 μ g L $^{-1}$, BTA: 207 μ g L $^{-1}$, BZF: 170 μ g L $^{-1}$, CBZ: 177 μ g L $^{-1}$, IBU: 172 μ g L $^{-1}$. The pH remained constant during ozonation and was in the range of 8.52 to 8.60 after ozonation.

S of the RW non-standardized LPRO concentrate from DOC, HCO_3^- and CO_3^{2-} was estimated 5.6×10^5 s $^{-1}$ (range: (3.2 to 7.0×10^5 s $^{-1}$, Equation 5.3, Chapter 5). The *pseudo* first-order rate constant for reactions of the spiked MPs with $\bullet OH$ was 0.4×10^5 s $^{-1}$, i.e., typically < 10 % of S , and therefore the experiments with spiked MPs should still be comparable to non-spiked samples. However, it cannot be excluded that the spiking of MPs might have resulted in an alteration of the $\bullet OH$ scavenging compared to a water sample without spiking, which might limit the transferability of the results to real samples.

The abatements of the spiked MPs as functions of the specific O_3 dose are shown in Figure C6. Based on the comparison of IBU abatements, no statistically significant differences were detected between the $\bullet OH$ exposures of the RW standardized and non-standardized LPRO concentrates. In conclusion, the oxidant exposures of the non-standardized and standardized LPRO concentrates were similar.

For the evaluation of the concentrate treatments, the oxidant exposures in non-standardized NF concentrates were assumed to be similar to the RW non-standardized LPRO concentrate, based on the results presented in the main manuscript.

Molar bromate yields of the (non)-standardized concentrates are shown in Figure C7. Bromate formation was detected in the non-standardized LPRO concentrate for specific O_3 doses ≥ 0.24 mg O_3 (mg DOC) $^{-1}$ (Table 5.5, Chapter 5).

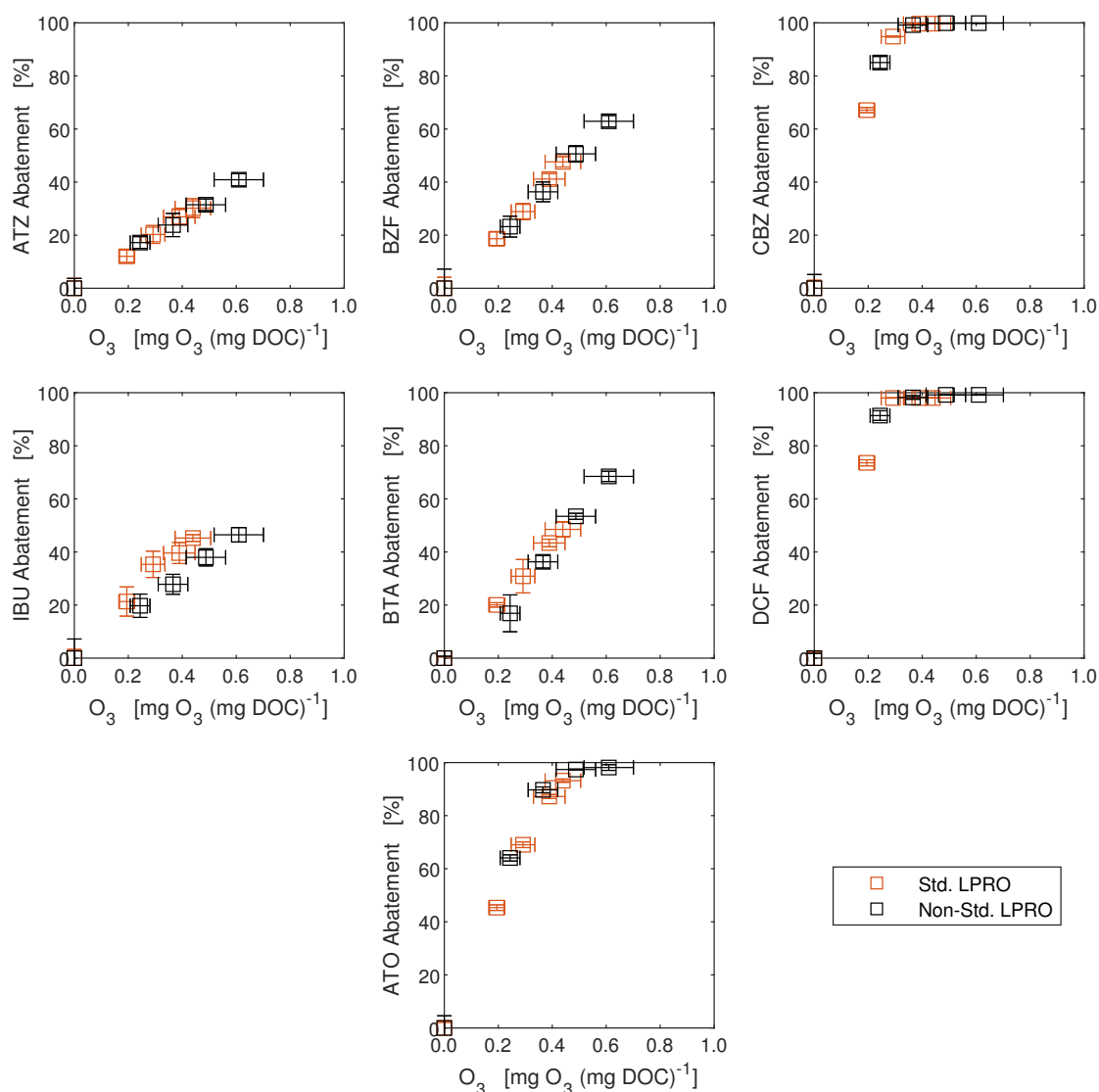


Figure C6: Relative abatements of micropollutants as a function of the specific ozone dose in standardized (orange) and non-standardized (black) River Wiese water LPRO concentrates. Error bars represent standard deviations of duplicate experiments or standard uncertainties estimated from the Gaussian error propagation rule. ATZ: atrazine, BZF: bezafibrate, CBZ: carbamazepine, IBU: ibuprofen, BTA: benzotriazole, DCF: diclofenac, ATO: atenolol.

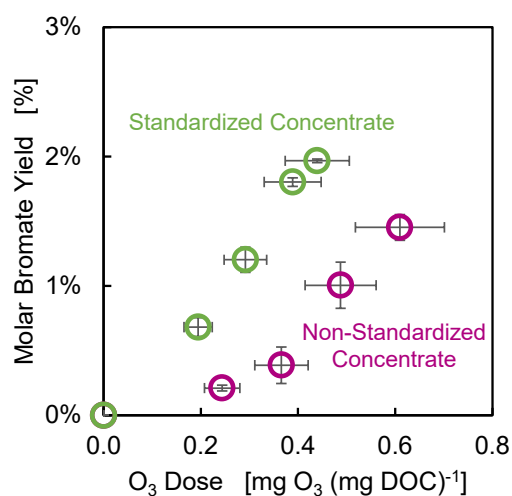


Figure C7: Molar bromate yields as a function of the specific ozone dose for RW standardized LPRO concentrate (green) and non-standardized LPRO concentrate (purple). The bromate yields were calculated according to Eq. 5.1 (Chapter 5). Experimental conditions: standardized concentrate: 6.2 mg DOC L⁻¹, 32.4 mg TIC L⁻¹, 495 to 531 µg Br⁻ L⁻¹ and pH 8.3 ± 0.1; non-standardized concentrate: 15.1 mg DOC LL⁻¹, 160 mg TIC L⁻¹, 573 to 613 µg Br⁻ L⁻¹ and pH 8.6 ± 0.1. Error bars represent standard deviations of replicate experiments or, if no replicate experiment was conducted, calculated with the Gaussian error propagation rule.

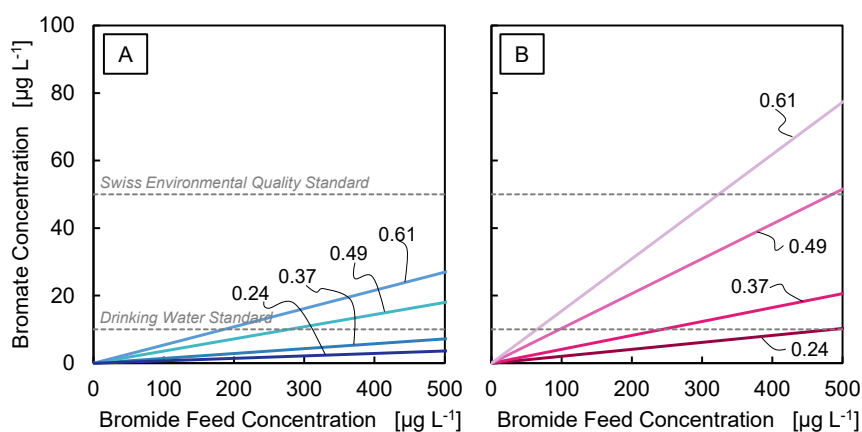


Figure C8: Estimated bromate concentrations after ozone treatment of the concentrates at different specific ozone doses (0.24, 0.37, 0.49 and 0.61 mg O₃ (mg DOC)⁻¹) as a function of the bromide concentration in the respective feed of (A) the NF1 membrane and (B) the LPRO membrane. The bromate concentrations of the drinking water standard, i.e., 10 µg BrO₃⁻ L⁻¹, and the proposed Swiss environmental quality standard, i.e., 50 µg BrO₃⁻ L⁻¹, are also shown (grey dashed lines). Estimates based on a water recovery of 85 %, as well as bromide retentions and molar bromate yields as shown in Table 5.5 (Chapter 5).

Appendix D: Supporting Information for Chapter 6

Determination of the designs of the pretreatment scenarios

Two pretreatment scenarios were investigated, i.e., one was based on a UV/H₂O₂ treatment of the full-stream, the other was based on a side-stream treatment with a low-pressure reverse osmosis (LPRO). Both pretreatments aimed at a maximum concentration of measured MPs of 0.1 µg L⁻¹ after a subsequent soil aquifer treatment. Hence, the pretreatment systems were designed to abate MPs that are present in the raw water (i.e., the river Rhine rapid sand filtrate water) in concentrations above this limit. Here, the respective 80 percentile MP influent concentration was used as calculation base for the required abatement efficiency by the technical system (Table D1).

The required abatement of MPs by the pretreatment process trains was calculated based on the observed abatement of the SAT columns in the AquaNES project (Chapter 3, [38]). It was assumed that the soil aquifer treatment (SAT) is operated sustainably (e.g., no loss of performance over time) and performs without any cost. With the knowledge of the MP abatement performance of the SAT, the maximum tolerable concentration before SAT $c_{\max,i}^{\text{in}}$ of the MP i can be calculated according to Equation D1. Here, the respective 20 percentile MP's abatement was used to account for seasonal lower abatement of MPs (Table D2).

$$c_{\max,i}^{\text{in}} = \frac{c_i^{\max}}{1 - A_i^{\text{SAT}}} \quad (\text{D1})$$

c_i^{\max} is the threshold concentration after SAT and can be MP specific. Here, it is 0.1 µg L⁻¹ for all investigated MPs. A_i^{SAT} is the compound-specific abatement in SAT. A_i^{SAT} was estimated from the SAT columns in the long-term pilot-scale experiment, utilizing the 20 percentile abatement of the SAT column with either the UV/H₂O₂ effluent or the river Rhine rapid sand filtrate water as feed (Table D2). Combining the resulting c_i^{\max} with the raw water concentration

Appendix . Appendix D: Supporting Information for Chapter 6

Table D1: Concentrations of micropollutants in the river Rhine rapid sand filtrate water, as reported previously [41]. Data obtained from grab samples obtained from the pilot plant are shown in Figure 2.3 (Chapter 2) between June 2017 and April 2019. All concentrations reported in ng L^{-1} . n : number of grab samples, avg: average, std: standard deviation.

Compound	n	Avg	\pm	Std	80-Percentile
Acesulfame	14	244	\pm	87	308
Metformin	14	204	\pm	68	259
Iopamidol	14	193	\pm	129	227
1H-benzotriazole	14	176	\pm	41	202
Iopromide	14	112	\pm	50	164

Table D2: Abatement of micropollutants in soil aquifer treatment (SAT) columns with different feed waters of the river Rhine rapid sand filtrate. Data were reported previously [38] and supplemented with data from the OXIBIEAU project. Data obtained from grab samples obtained from the pilot plant are shown in Figure 2.3 (Chapter 2) between November 2017 and February 2021. All abatements reported as percent relative to the respective column influent concentration. n : number of grab samples, avg: average, std: standard deviation.

SAT feed Compound	UV/H ₂ O ₂ Effluent					Rapid Sand Filtrate Water				
	n	Avg	\pm	Std	20-Percentile	n	Avg	\pm	Std	20-Percentile
Acesulfame	10	15	\pm	19	2	12	21	\pm	18	6
Metformin	12	70	\pm	16	55	12	80	\pm	17	67
Iopamidol	12	4	\pm	23	-11	12	4	\pm	14	-6
Benzotriazole	12	0	\pm	23	-19	12	2	\pm	13	-3
Iopromide	10	28	\pm	11	20	12	44	\pm	23	22

yields the required abatement by the UV/H₂O₂ process, $A_i^{\text{UV/H}_2\text{O}_2}$, or by the dense membrane process, A_i^{Mem} , as presented in Table D3. The different required abatements were used to account for the experimental findings described in Chapter 3, i.e., the abatement of metformin was significantly lower in the SAT column receiving the UV/H₂O₂ pretreated water than the river Rhine rapid sand filtrate water (Figure 3.2, Chapter 3). Differences between the SAT columns were statistically not significant for the other MPs considered here. Nevertheless, for consistency, the respective experimental result was used.

Operational Setpoint for UV/H₂O₂ Process

To determine an operational set point of the UV/H₂O₂ system, it is assumed that both the UV fluence H (J m^{-2}) and the H₂O₂ concentration $c_{\text{H}_2\text{O}_2}$ (M) can be selected with one degree of freedom. The operational set-point of the UV/H₂O₂ process is derived from a theoretical model for the river Rhine rapid sand filtrate water, describing the abatement of MPs as a function of the UV fluence and H₂O₂ dose.

Table D3: Required abatement of a UV/H₂O₂ or a membrane system before the soil aquifer treatment columns to comply with the treatment goal of 0.1 µg L⁻¹. A_i^{SAT} : compound-specific abatement in soil aquifer treatment (SAT), $c_{\text{max}}^{\text{in}}$: maximum tolerable concentration before SAT, $A_i^{\text{UV/H}_2\text{O}_2}$: required abatement by the UV/H₂O₂ process, A_i^{Mem} : required abatement by the dense membrane process. Values marked with '*' signify that A_i^{SAT} was <0% and no change of concentration in SAT was assumed here.

Compound	A_i^{SAT}	$c_{\text{max}}^{\text{in}}$	$A_i^{\text{UV/H}_2\text{O}_2}$	A_i^{Mem}
Acesulfame	2%	308	67%	66%
Metformin	55%	259	14%	0%
Iopamidol	0%*	227	56%	56%
Benzotriazole	0%*	202	50%	50%
Iopromide	20%	164	24%	22%

The parameters that determine the MP abatement performance of the UV/H₂O₂ process, i.e., H and the $\bullet\text{OH}$ exposure ($\int [\bullet\text{OH}] dt$), can be derived from the target abatement and known kinetic data, as described in Equations 4.1, 4.5 and 4.6 (Chapter 4). It is assumed that H is the (constant) fluence rate E multiplied with the treatment time t and that $\int [\bullet\text{OH}] dt$ can be calculated from the (constant) steady-state $\bullet\text{OH}$ concentration multiplied with t . Then H can be estimated as a function of the average H₂O₂ concentration from Eqn. D2.

$$H = \frac{\ln\left(\frac{c_{0,\text{MP}}}{c_{\text{MP}}}\right)}{k_{\text{UV,MP}} + k_{\bullet\text{OH,MP}} \times \left(\frac{\ln(10)}{10} \times \frac{\lambda}{h c N_A} \times \frac{\varepsilon_{\text{H}_2\text{O}_2} \times \Phi_{\text{H}_2\text{O}_2} \times c_{\text{H}_2\text{O}_2}}{S + k_{\bullet\text{OH,H}_2\text{O}_2} \times c_{\text{H}_2\text{O}_2}}\right)} \quad (\text{D2})$$

The *pseudo* first-order $\bullet\text{OH}$ scavenging rate of the background water matrix was previously estimated to be in the range of $(5.3 \text{ to } 5.7) \times 10^4 \text{ s}^{-1}$ [38], [41]. For the investigated MPs, possible operational set-points are shown in Figure D1. Obviously, metformin is the hardest MP to abate and therefore is decisive for the layout and design of the UV/H₂O₂ process. For example, at a dose of 4 mg H₂O₂ L⁻¹, the predicted required UV fluence is about 4'500 J m⁻² (450 mJ cm⁻²) to comply with the goal of 14% metformin abatement by the UV/H₂O₂ process. However, it was shown that the kinetic data reported for metformin might be inaccurate [41]. Using the fitted kinetic data (Table 4.2, Chapter 4, [41]), the required UV fluence is considerably higher: at 4 mg H₂O₂ L⁻¹, the predicted required UV fluence is about 5'800 J m⁻². This highlights the dependence of this *a priori* method from the accuracy of kinetic data. Hereafter, the higher UV fluence is used as a conservative design.

The accuracy of the abatement prediction was assessed with a small sub-set of the data presented previously [41] of five laboratory-scale experiments (2 to 6 mg H₂O₂ L⁻¹, 2'000 to 6'000 J m⁻²). This data set was selected because the experimental design was suitable to assess the UV/H₂O₂ at relevant process conditions covering the predicted operational set point;

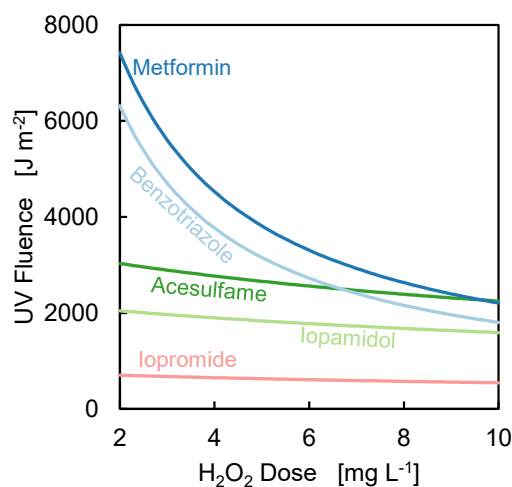


Figure D1: Possible designs of a UV/H₂O₂ process calculated with Equation D2, presented as UV fluence as a function of the average H₂O₂ concentration. The respective abatements comply with the required abatements described Table D3. Kinetic data used for the calculation are presented in Table 4.1 (Chapter 4). For the *pseudo* first-order [•]OH scavenging rate of the background water matrix, the average of the previously estimated values for the river Rhine rapid sand filtrate water was selected, i.e., $5.5 \times 10^4 \text{ s}^{-1}$ [38], [41].

and the data was inherently consistent when assessed with the model described in Chapter 4 (probe compounds: benzotriazole, iopamidole).

Overall, the predictions were in reasonable agreement with the experimental data, considering analytical uncertainties (Table D4). While the predictions based on kinetic data reported in the literature tended to over-predict the abatement, predictions were rather too low when the fitted kinetic constants were used. A water temperature effect can be excluded since all experiments were performed under controlled conditions at 20 °C. Comparing the experimental data of $c_{\text{H}_2\text{O}_2} = 2.0$ to $5.5 \text{ mg H}_2\text{O}_2 \text{ L}^{-1}$ and $H = 4'000$ to $6'000 \text{ J m}^{-2}$ with the prediction results, the operational set point predicted by the fitted kinetic data ($4 \text{ mg H}_2\text{O}_2 \text{ L}^{-1}$, $5'800 \text{ J m}^{-2}$) seems to be promising to fulfill the treatment goal (14% metformin abatement, Table D3). This set point is selected as the more conservative design. It is concluded that the presented approach to determine functions of possible combinations of H and $c_{\text{H}_2\text{O}_2}$ *a priori* is useful if reliable kinetic data is available and water-specific water quality parameters are known.

In a next step, the selected operational set point was assessed with data from a pilot-scale test. A similar operational set point as predicted by the *a priori* approach was investigated as described in Chapter 3 [38]. Concentrations of the relevant MPs before and after treatment with UV/H₂O₂ ($4 \text{ mg H}_2\text{O}_2 \text{ L}^{-1}$, $6'000 \text{ J m}^{-2}$) and the SAT column are shown in Figure D2. The defined treatment goal was achieved for all compounds on the twelve days when the experiments were performed. For two MPs, the treatment goal was not achieved each time. Benzotriazole was detected once at a concentration above $0.1 \mu\text{g L}^{-1}$ during the start-up phase

Table D4: Metformin abatements observed in laboratory experiments and two predictions based on Equation D2. Experimental data were obtained from a master's thesis [290] and published previously [41]. The respective kinetic data was either taken from the literature (k^{lit}) as reported in Table 4.1 or from the fitted kinetic constants described in Table 4.2 (Chapter 4, k^{fit}). H_2O_2 concentrations are average values of concentrations before and after the experiment measured by spectrophotometry after addition of titanium(IV) oxysulphate (Chapter 3).

H_2O_2 [mg L ⁻¹]	UV [J m ⁻²]	Experiment	Predicted k^{lit}	Predicted k^{fit}
2.0	2000	5%	4%	3%
6.2	2000	2%	9%	7%
3.8	4000	6%	12%	9%
2.0	6000	11%	11%	8%
5.5	6000	18%	22%	18%

of the SAT column. As the soil's microbiology was considered to be in an adaption phase at this time [38], this outlier is not considered relevant here. Metformin was observed twice at concentrations above $0.1 \mu\text{g L}^{-1}$. This is likely related to the water temperature and its effect on the SAT column's microbiological activity, because concentrations, e.g., $>0.05 \mu\text{g L}^{-1}$ (half of the set maximum concentration) in the SAT column's effluent were only detected when the respective water temperature was below 10°C (November 2017 to March 2018). It is concluded that the treatment with operational parameters derived from the *a priori* approach with k^{fit} is likely in compliance with the defined treatment goal in at least 80% of the cases.

Despite the good agreement between pilot-scale experiments with the treatment goal, the transferability of the results remains partially unclear. This is because the UV/ H_2O_2 treatment is designed for the abatement of metformin. Metformin is primarily abated in the SAT column, where the transferability to a real system might be limited for the several reasons. First, the water temperature strongly impacts the biological activity and therefore is decisive for the biological metformin abatement. The water temperatures were in the range of 6.2 to 24.5°C after the SAT column, i.e., after 1 m of traveling distance [38]. It is assumed that water temperatures of $>20^\circ\text{C}$ are uncommon at full-scale managed aquifer recharge sites in moderate climates. Since higher water temperatures correlate with a higher microbial activity, the observed abatement in the SAT columns might over-estimate real systems. Indeed, one study reported an average abatement of metformin of $87 \pm 4\%$ after infiltration of a lake water in a full-scale pond and an approximated traveling time of 0.5 d (traveling distance: 200 cm, observation period: April 2016 to October 2016) [291], which is in good agreement with the results of warm water temperatures presented here (complete abatement, Figure D2). The cited study did not cover colder seasons and water temperatures were not reported. Second, the investigated SAT columns had a relatively short residence time of 1 day only, while many full-scale applications have residence times in the range of 3 days to 96 months [17]. This might justify to assume a higher abatement of metformin than considered for the design of the

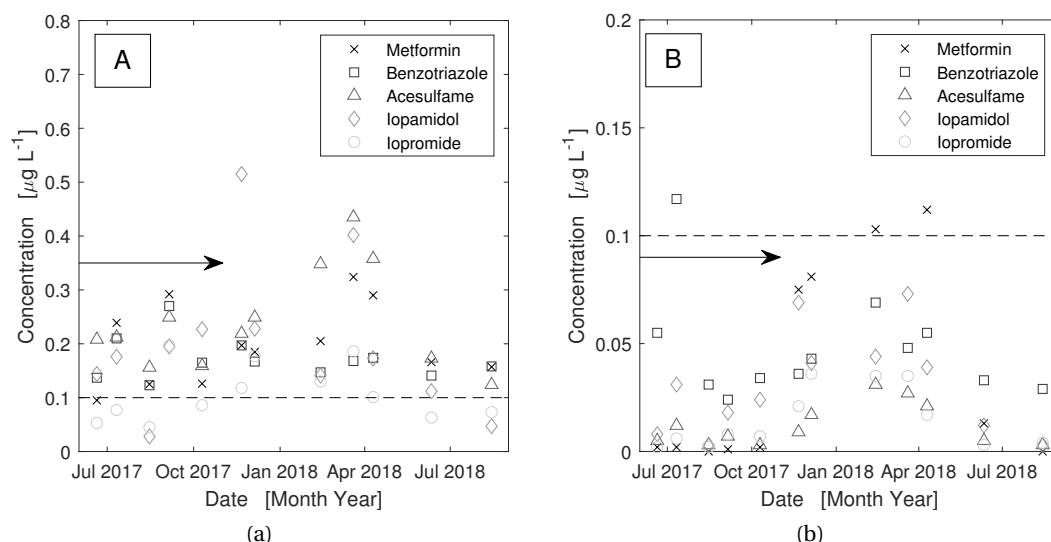


Figure D2: Assessment of the UV/H₂O₂ operational set point. A: Concentrations of relevant micropollutants in the river Rhine rapid sand filtrate water, i.e., before UV/H₂O₂ and soil aquifer treatment (SAT) column. B: Respective concentrations after UV/H₂O₂ and SAT column treatment. UV/H₂O₂ was operated with 4 mg H₂O₂ L⁻¹ and 6'000 J m⁻², as described in Chapter 3 [38]. Data from June 2017 to August 2018. The arrows mark the operation before November 2017 during which the microbiology in the SAT column was considered to be in an adaption phase [38]. Dashed black lines show the treatment goal after UV/H₂O₂ and SAT column treatment, i.e., 0.1 µg L⁻¹.

UV/H₂O₂ set point (Table D3) and, therefore, to select an operational setpoint of the UV/H₂O₂ process to assure sufficient abatement of the next hardest MP, i.e., benzotriazole. Finally, the SAT columns were operated in constant overflow mode, but many managed aquifer recharge sites are operated in a discontinued mode, e.g. to prevent clogging of the site [291].

Operational Setpoint for Dense Membrane Process

Membrane Selection. To select a membrane suitable for the rejection rates defined in Table D3, membrane screening tests were conducted on a bench-scale device (Triple System, MMS Membrane Systems, Switzerland) in a closed loop test. Grab samples of the river Rhine rapid sand filtrate water were spiked with 100 µg L⁻¹ bromide to assure quantification of the Br⁻ retention. All membranes were tested at the same transmembrane pressure (5 bar) and water temperature (25 °C). Results obtained in a master's thesis supervised by the author [292] are shown in Table D5 and were partly presented before in a conference paper [293].

As shown in Table D5, there is a tradeoff between the desired high retention of MPs and high permeabilities for bromide and water. A higher bromide retention potentially makes the concentrate ozone treatment more difficult due to the increasing risk to form bromate upon

Table D5: Permeability and retentions of different solutes in bench-scale membrane screening tests with river Rhine rapid sand filtrate waters at 5 bar and 25 °C after 75 % water recovery. The pressure of the LPRO was 5.9 bar. Samples were spiked with 100 µg Br⁻ L⁻¹. *Italic numbers* represent retention values calculated from closing mass balances, because their concentrations in the respective permeates were not quantifiable. NF1, NF2 and LPRO correspond to the membranes discussed before in Chapter 5. A_i^{Mem} is the required abatement by the membrane system repeated here from Table D3. Membrane data were obtained from a master's thesis [292] and partly presented previously [293].

Membrane	Unit	NF1	NF2	NF3	NF4	LPRO	A_i^{Mem}
Permeability	L m ⁻² h ⁻¹ bar ⁻¹	9.6	8.3	10.0	6.4	5.2	-
Retention							
Bromide	%	22	23	15	34	96	-
Acesulfame	%	63	85	85	71	92	66
Metformin	%	34	70	45	60	95	0
Iopamidol	%	96	93	98	86	93	56
Benzotriazole	%	24	36	8	67	86	50
Iopromide	%	97	100	83	86	93	22

ozone treatment of the concentrate, as discussed in Chapter 5. Comparing the observed MP retentions with the required MP abatement by the membrane system (Table D3), only two membranes show a sufficiently high retention of benzotriazole of >50%, i.e., NF4 and LPRO. The NF4 was a thin-film composite nanofiltration membrane (SR4, Koch Membrane Systems, USA) with a nominal molecular weight cut-off specified as 150 Da. The NF4's permeability determined here agreed well with other published results (6.5 L m⁻² h⁻¹ bar⁻¹, [294]). The LPRO was a cross-linked fully aromatic polyamide composite low-pressure reverse osmosis membrane (TMH20A, Toray Industries, Japan). For the LPRO, the permeability was lower than specified by the manufacturer (5.4 to 6.7 L m⁻² h⁻¹ bar⁻¹, [295]), probably due to the use of the rapid sand filtrate water instead of clean water and a higher water recovery rate (75% instead of 15%).

Assuming that the retention is similar in full-scale membrane systems and ignoring effects, e.g., from differing water rejection rates, up-scaling, membrane fouling and aging, water temperature, etc., the fraction of the permeate in the water stream sent to the SAT can be calculated from Equation D3 and the required abatement by the membrane treatment presented in Table D3.

$$\frac{\dot{Q}_{\text{Permeate}}}{\dot{Q}_{\text{SAT,in}}} = \frac{A_i^{\text{Mem}}}{R_i} \quad (\text{D3})$$

$\dot{Q}_{\text{Permeate}}$ and $\dot{Q}_{\text{SAT,in}}$ are the volume flows of the permeate and of the mixed water sent to the subsequent SAT, i.e., the permeate mixed with river Rhine rapid sand filter water. R_i is the rejection of solute i by the membrane. A_i^{Mem} is the required abatement of solute i

to accomplish the treatment task. For the investigated membranes, acesulfame was the compound that required the largest treated volume flow, i.e., 93% and 72% of the volume flow sent to the subsequent SAT. Note that the World Health Organization considers a daily uptake of up to 15 mg acesulfame-K (kg bodyweight)⁻¹ d⁻¹ as safe (acceptable daily intake [296]). For this reason, a design based on this compound is not necessarily required and the membrane systems could alternatively be designed to treat benzotriazole. However, to comply with the treatment target (all MPs ≤ 0.1 µg L⁻¹ after SAT), the design for acesulfame was selected.

A membrane system equipped with NF4 membranes had to produce about 1.29 times more permeate than a system equipped with the LPRO membrane to comply with the set treatment target. Considering that the measured permeabilities of the NF4 was about 1.25 times higher than the LPRO, the two membranes can be considered about equally well suited to comply with the treatment goal and should both be tested in a (long-term) pilot-scale trial. The NF4 concentrate is likely more favorable for the subsequent treatment by ozone due to the lower bromide retention.

Concentrate Treatment. The aim of the concentrate treatment is to abate fast and moderately ozone-reactive MPs by 80% on average at limited bromate formation. Experimental data from an ozonation of a concentrate from a similar river water as discussed here was presented in Chapter 5 and is summarized in Figure D3. Solving the linear regression line of the average abatement (Figure D3C) for an average abatement of 80%, the treatment goal should be accomplished at a specific O₃ dose of about 0.4 mg O₃ (mg DOC)⁻¹. At this dose, the interpolated molar bromate yield is about 0.6%_{Br⁻} (Figure D3B). Bromide concentrations vary in the raw water (Figure D3A). As discussed before, Br⁻ is retained by the membranes and, hence, can be found in the concentrates in concentrations at factors 2.9 (NF4) or 6.4 (LPRO) above the membrane feed concentration (Table D5). This means that bromate formation should be limited to < 5 µg L⁻¹ in NF4 concentrates and < 10 µg L⁻¹ in LPRO concentrates in 98% of the operation days at the specific O₃ dose of 0.4 mg O₃ (mg DOC)⁻¹. Therefore, the ozone treatment is considered feasible for both concentrates, but this should be validated in a long-term pilot trial. Nevertheless, for consistency with Chapter 5 and the data available from the OXIBIEAU project, only the LPRO membrane is further investigated here.

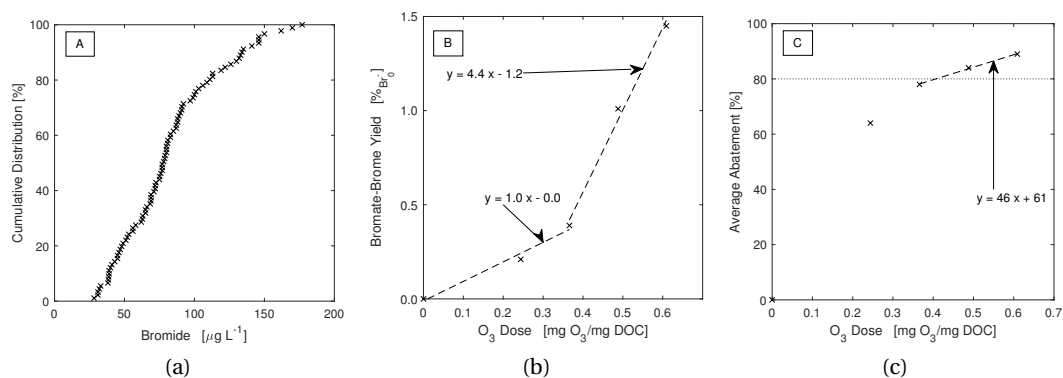


Figure D3: Assessment of the concentrate treatment by ozonation. A: Historical concentrations of bromide in the river Rhine raw water measured by IWB (May 2013 to October 2020). $n = 92$. B: Molar bromate yields as a function of the specific ozone dose. C: Average abatement of two fast ozone-reacting (carbamazepine, diclofenac) and one moderately ozone-reactive micropollutant (benzotriazole) as a function of the specific ozone dose. The dotted black line shows an average abatement of 80%. For B and C, data of a non-standardized concentrate produced from river Wiese rapid sand filtrate water with the LPRO membrane at 85% water recovery were presented in Chapter 5. Dashed lines are linear regression lines.

Modified Cost Functions from Plumlee *et al.* (2014)

Cost functions for the investigated treatment scenarios were derived from Plumlee *et al.* [43]. These cost estimates were developed as conceptual-level engineering-cost estimates for advanced wastewater reclamation technologies, i.e., with an accuracy of -30% to +50% [43]. All reported estimates were adjusted to the September 2011 *Engineering News-Record* (ENR) Construction Cost Index (CCI) [43]. These cost functions by Plumlee *et al.* (2014) were modified for the processes investigated in this study.

UV/H₂O₂ Treatment

The published cost equation for the total capital costs of the UV/H₂O₂ ($C_{UV/H_2O_2}^{tot,Cap}$) reads [43]:

$$C_{UV/H_2O_2}^{tot,Cap} = C_{UV/H_2O_2}^{Equipment} \times \underbrace{(1 + 0.3)}_{a_0=1.3} \times \underbrace{(1 + 0.1 + 0.05 + 0.2)}_{a_1=1.35} \times \underbrace{(1 + 0.15 + 0.3)}_{a_2=1.45} \times \underbrace{(1 + 0.35)}_{a_3=1.35} \quad (D4)$$

3.44

$C_{UV/H_2O_2}^{Equipment}$ are the costs of the UV/H₂O₂ system. a_0 are the installation costs (30%). a_1 accounts for costs for yard piping (10%), sitework landscaping (5%), and site electrics and controls (20%). a_2 are contractor overhead and profit (OH&P, 15%) and contingency (30%). a_3 are engineering, legal and administration costs (35%). In total, the equipment costs are therefore multiplied by a factor of 3.44 to estimate the costs of the total system.

Cost estimates for UV/H₂O₂ were reported for systems designed for a 1.2 log₁₀ (94%) abatement of NDMA and a 0.5 log₁₀ (68%) abatement of 1,4-dioxane in an RO permeate with a water transmission of 95% (UV absorbance: 2.2 m⁻¹). The H₂O₂ dose was specified to be in the range of 2.5 to 3.5 mg L⁻¹. Assessing the design with the model described before (Chapter 4), the UV fluence and hydroxyl radical exposure were calculated to be 12'300 J m⁻² and 4.1 × 10⁻¹⁰ M s, respectively. Kinetic data used for the assessment were $k_{\bullet OH,NDMA} = 0.4 \times 10^9 \text{ M}^{-1} \text{ s}^{-1}$ [150], $\epsilon_{NDMA} = 153 \text{ mol einstein}^{-1}$ [150], $\Phi_{NDMA} = 0.3$ [297]; and $k_{\bullet OH,1,4\text{-dioxane}} = 2.8 \times 10^9 \text{ M}^{-1} \text{ s}^{-1}$ [151], $\Phi_{1,4\text{-dioxane}} \approx 0$ [100]. For the abatement of 1.2 log₁₀ NDMA, UV fluences are typically selected in the range of about 8'000 to 13'000 J m⁻² (Xylem, personal communication), i.e., the calculated UV fluence is inside this expected range and, hence, considered realistic.

The cost functions of Plumlee *et al.* (2014) are only valid for a design as described above, i.e., at a specific UV fluence and UV transmission. To account for the impact of UV fluence and UV transmission on the design and to include the option to adopt the cost function for a different design, the capital cost function of Plumlee *et al.*, [43], was modified as described hereafter.

To ensure that the UV fluence is the same in two waters with differing UV absorbances, it is assumed that the same UV reactor type is used, but it is dimensioned differently by a factor of $A_{254,1} / A_{254,0}$ (Equation D5). $A_{254,0}$ is the UV absorbance at 254 nm of the original UV reactor design (95% UV transmission, i.e. $A_{254,0} = 2.2 \text{ m}^{-1}$, Eq. D6). $A_{254,1}$ is the UV absorbance at 254 nm of the different water sample. When the UV transmission of the different water sample is,

e.g., lower than 95% (higher UVA than in the original UV reactor design), the water factor WF increases and, therefore, the UV reactor must be sized larger.

$$WF = \frac{A_{254,1}}{A_{254,0}} \quad (D5)$$

The water transmission at 254 nm ($\%T_{254}$, %) is converted to the UV absorbance at 254 nm (A_{254} , cm^{-1}) by Equation D6.

$$A_{254} = -\log_{10} (\%T_{254}) \quad (D6)$$

Note that Equation D5 is only a very rough estimate to account for a different UV transmission than in the design considered by Plumlee *et al.* (2014). The design and layout of the UV reactor is commonly very specific for a certain UV transmission. Hence, details on the costs have to be clarified with a technology vendor. The approximation using Equation D5 was confirmed by a major UV reactor vendor to be accurate within $\pm 30\%$ for one reactor type, comparing transmissions of 95% and 88%.

To account for a UV fluence differing from the system layout presented in the original publication, it is assumed that the equipment can be linearly scaled to the required UV fluence. Hence, the UV reactor is selected by the ratio of the UV fluence required for the different water sample, H_1 , to the UV fluence of the original water, H_0 ($=12'300 \text{ J m}^{-2}$). In total, the adopted capital cost function is presented in Equation D7.

$$C_{\text{UV/H}_2\text{O}_2}^{\text{tot,Cap}} \approx C_{\text{UV/H}_2\text{O}_2}^{\text{Equipment}} \times 3.44 \times WF \times \frac{H_1}{12'300 \text{ J m}^{-2}} \quad (D7)$$

For systems with a capacity of 10 to 80 MGD ($1'577$ to $12'618 \text{ m}^3 \text{ h}^{-1}$), the total unit capital costs, i.e., $C_{\text{UV/H}_2\text{O}_2}^{\text{tot,Cap}} / \dot{Q}$, were reported to be constant at $0.21 \text{ \$M/MGD}$ [43]. Probably this is because for these system capacities no further scaling effect can be realized. The unit capital costs are therefore approximated by Equation D8 for systems with a capacity of 10 to 80 MGD and $\%T_{254,1}$ in the range of about 88 to 95%:

$$\frac{C_{\text{UV/H}_2\text{O}_2}^{\text{tot,Cap}}}{\dot{Q}} \approx 0.21 \text{ \$M/MGD} \times WF \times \frac{H_1}{12'300 \text{ J m}^{-2}} \quad (D8)$$

In addition to the capital costs, Plumlee *et al.* (2014) describe annual operating and maintenance (O&M) cost functions [43]. For the UV/ H_2O_2 systems, these costs accounted for H_2O_2 (2.5 to 3.5 mg L^{-1}), hypochlorite quenching, electrical energy (at $0.0988 \text{ \$ / kWh}$, [43]), and lamp replacements. For systems with a capacity of 5 MGD and above, the unit annual O&M costs were constant at $0.031 \text{ \$M/MGD}$ [43]. The published annual O&M cost function for systems with a capacity of ≥ 5 MGD can be approximated as follows [43]:

$$\frac{C_{\text{UV/H}_2\text{O}_2}^{\text{tot,O\&M}}}{\dot{Q}} = \left(\underbrace{0.005}_{\text{H}_2\text{O}_2} + \underbrace{0.008}_{\text{ClO}^- \text{ quenching}} + \underbrace{0.017}_{\text{El. Energy}} + \underbrace{0.002}_{\text{Lamp repl.}} \right) \text{ \$M/MGD} \quad (D9)$$

Costs for, e.g., electrical energy and H_2O_2 depend strongly on the local situation. The cost estimate can be adopted to a given situation as described in the following. The costs for a different H_2O_2 doses are assumed to linearly correlate with the doses. Hypochlorite was probably considered in the original equation to quench residual H_2O_2 . It is assumed that no hypochlorite is used for the surface water treatment by the UV/ H_2O_2 system, because the results presented in Chapter 3 [38] indicated that residual H_2O_2 should not be an issue for the subsequent SAT. Hence, the quenching costs are ignored here. The electrical energy is assumed to depend on the applied UV dose and the water's UV transmission (besides the UV system's energy consumption; back-calculated from the underlying data as 0.14 kWh/m^3 at the design point, [43]). Similarly, the lamp replacement costs depend on the number of lamps to replace. Hence, the costs of these two items are corrected by the system size as above. The estimated annual unit O&M costs therefore become:

$$\frac{C_{\text{UV/H}_2\text{O}_2}^{\text{tot,O\&M}}}{\dot{Q}} \approx \left(0.005 \times \frac{c_{\text{H}_2\text{O}_2}}{3 \text{ mg H}_2\text{O}_2 \text{ L}^{-1}} + 0.019 \times WF \times \frac{H_1}{12'300 \text{ J m}^{-2}} \right) \$\text{M/MGD} \quad (\text{D10})$$

For the calculation of the specific electrical energy demand to provide the UV fluence, Equation D11 can be used based on the data by Plumlee *et al.* [43] and the assumptions presented above.

$$\frac{\dot{E}_{\text{el}}}{\dot{Q}} \approx 0.14 \text{ kWh m}^{-3} \times WF \times \frac{H_1}{12'300 \text{ J m}^{-2}} \quad (\text{D11})$$

Note that the specific electrical energy demand calculated from Equation D11 for the UV reactor is about 0.11 kWh m^{-3} , which is almost a factor 2 higher than specified by the vendor (0.066 kWh m^{-3} , Chapter 6). This highlights the notable inaccuracies of the reported equations.

Membrane Treatment

The unit cost estimates for high-pressure membranes (NF and RO) by Plumlee *et al.* [43] read as follows:

$$\frac{C_{\text{NF\&RO}}^{\text{tot,Cap}}}{\dot{Q}} = \left(7.14 \times (\text{Plant Capacity, in MGD})^{-0.22} \right) \$\text{M/MGD} \quad (\text{D12})$$

$$\frac{C_{\text{NF\&RO}}^{\text{tot,O\&M}}}{\dot{Q}} = \left(0.44 \times (\text{Plant Capacity, in MGD})^{-0.13} \right) \$\text{M/MGD} \quad (\text{D13})$$

The systems were designed to treat brackish water (500 to 2000 mg L^{-1} total dissolved solids). Regardless of the membrane type (NF or RO), the systems were calculated to consume about 1.1 kWh m^{-3} permeate [43]. With an energy efficiency of the system without piping losses of 77.9% ($\eta_{\text{tot}} = \eta_{\text{motor}}(95\%) \times \eta_{\text{pump}}(82\%)$), the system pressure (p) is 30 bar (Equation D14).

$$p = \frac{\dot{E}_{\text{el}} \times \eta_{\text{tot}}}{\dot{Q}} \quad (\text{D14})$$

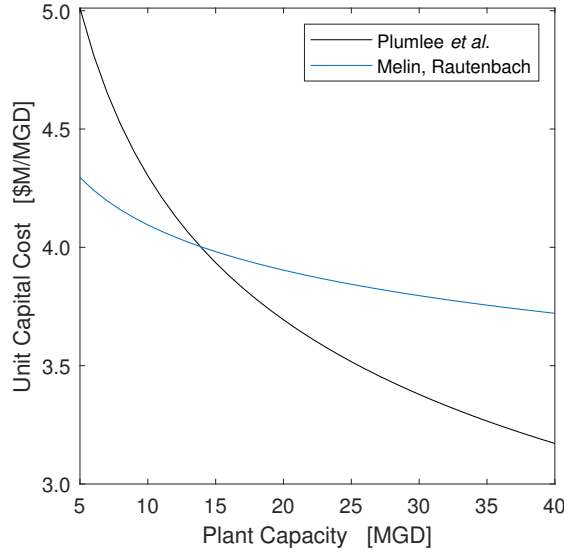


Figure D4: Unit capital cost of nanofiltration and reverse osmosis plants as a function of the plant capacity. Functions are based on Plumlee *et al.* (Equation D12, [43]) or Melin and Rautenbach (Equation D16, [233]) adjusted to the *Engineering News Record* Construction Cost Index in September 2011 (9'116 points).

It might therefore be reasonable to proportionally adjust the electrical energy costs to different values, as surface waters can often be treated at lower pressures, e.g., in the range of 5 to 10 bar. However, for an estimate with an accuracy of -30 to +50%, the suggested O&M cost functions were considered sufficient by Plumlee *et al.* (2014) [43].

Capital cost of 22 full-scale brackish water RO plants in nine countries that went into operation between 2000 and 2005 with capacities in the range of 4'361 to 153'000 m³ d⁻¹ (1.2 to 40 MGD) were reviewed [233]. The following capital investment cost equation was developed [233]:

$$C_{\text{NF\&RO}}^{\text{tot,O\&M}} = \left(3.72 \times (\text{Plant Capacity, in m}^3 \text{ d}^{-1})^{0.85} \right) \times 10^3 \$ \quad (\text{D15})$$

Adjusting the underlying data of Melin and Rautenbach [233] to the September 2011 ENR CCI and fitting the unit capital cost as a function of the plant capacity similar to the form of Plumlee *et al.*, the unit capital cost equation becomes:

$$\frac{C_{\text{NF\&RO}}^{\text{tot,Cap}}}{\dot{Q}} = \left(4.8 \times (\text{Plant Capacity, in MGD})^{-0.069} \right) \$\text{M/MGD} \quad (\text{D16})$$

The unit capital cost estimated by Equations D12 and D16 are shown in Figure D4. Higher costs are estimated by Plumlee *et al.* (2014) for plant capacities below 15 MGD. Above this capacity, the plants reviewed by Melin and Rautenbach had higher unit capital costs. Both equations are considered equally valid because they are uncertain in the range of -30% to +50% and, hence, have a common overlap. For consistency, Equation D12 is used hereafter.

Ozone Treatment

For water treatment at inland sites, it is assumed that the concentrate has to be treated before discharge into a river. Based on the results presented in Chapter 4, a specific ozone dose of about $0.4 \text{ mg O}_3 (\text{mg DOC})^{-1}$ is considered to be sufficient for an average abatement of 80% of fast to moderately O_3 -reactive MPs at limited bromate formation.

Cost estimates were developed for ozone treatment of wastewater before RO (6 mg TOC L^{-1}) by Plumlee *et al.* and base on project data of three vendors of facilities in the range of 10 to 535 MGD ($1'577$ to $84'383 \text{ m}^3 \text{ h}^{-1}$) [43]. These system dimensions are considerably larger than systems likely relevant for a concentrate treatment, since only 10% to 20% of the membrane feed volume stream have to be treated. As costs for facilities with treatment capacities <10 MGD steeply increase [43], the cost estimate equations by Plumlee *et al.* [43] must likely be regarded as too low. Instead, the underlying data of plants with capacities in the range of 10 to 52 MGD ($1'577$ to $8'202 \text{ m}^3 \text{ h}^{-1}$) were used to develop linear correlations presented below.

The ozone system selection is determined by the required ozone production capacity. The latter is determined by the ozone dose and the water quality, i.e., the DOC. To adopt the data from Plumlee *et al.* [43] to a different situation, Equations D17 to D19 were extracted:

$$C_{\text{O}_3}^{\text{Contactor, Cap}} = (1.3 \times (\text{Contactor Volume, in Mgal}) + 6.1 \times 10^{-2}) \text{ \$M} \quad (\text{D17})$$

$$C_{\text{O}_3}^{\text{Equipment, Cap}} = (1.6 \times 10^{-3} \times (\text{O}_3 \text{ Generator Capacity, in lb}_{\text{O}_3} \text{ day}^{-1}) + 1.7 \times 10^0) \text{ \$M} \quad (\text{D18})$$

$$C_{\text{O}_3}^{\text{System, Cap}} = \left(C_{\text{O}_3}^{\text{Contactor, Cap}} + \underbrace{1.3}_{a_0} \times C_{\text{O}_3}^{\text{Equipment, Cap}} \right) \times \underbrace{2.64}_{a_1 \times a_2 \times a_3} \text{ \$M} \quad (\text{D19})$$

The contactor volume can be calculated with Equation D20 from the hydraulic residence time t_{HR} (min) and the treated water flow \dot{Q} (MGD).

$$\text{Contactor Volume, in Mgal} = t_{\text{HR}} \times \dot{Q} \times \frac{1}{1440 \text{ min day}^{-1}} \quad (\text{D20})$$

The ozone generator capacity is calculated from \dot{Q} , the specific ozone dose c_{O_3} ($\text{mg O}_3 (\text{mg DOC})^{-1}$) and the DOC concentration c_{DOC} (mg DOC L^{-1}) (Equation D21).

$$\text{O}_3 \text{ Generator Capacity, in lb}_{\text{O}_3} \text{ day}^{-1} = \dot{Q} \times c_{\text{O}_3} \times c_{\text{DOC}} \times \underbrace{\frac{3785.4 \text{ m}^3 \text{ day}^{-1} \text{ MGD}^{-1} \times 10^3 \text{ L m}^{-3}}{10^6 \text{ mg}_{\text{O}_3} (\text{kg}_{\text{O}_3})^{-1} \times 0.454 \text{ lb}_{\text{O}_3} (\text{kg}_{\text{O}_3})^{-1}}}_{=8.34} \quad (\text{D21})$$

Equation D19 is plotted as a unit cost function, i.e., divided by the plant capacity, along with the corresponding function suggested by Plumlee *et al.* (2014) for systems with 6 mg TOC

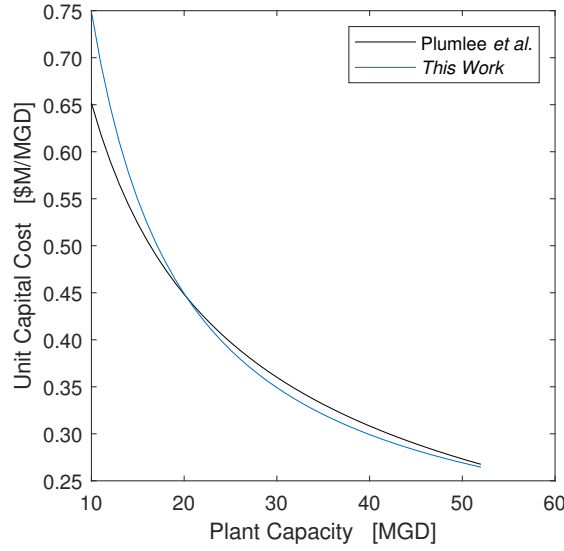


Figure D5: Unit capital cost of ozone systems, i.e., ozone generator and contactor, as a function of the plant capacity (10 to 52 MGD, i.e., 1'577 to 8'202 m³ h⁻¹). Functions are based on Plumlee *et al.* [43] or Equation D19 divided by the plant capacity.

L⁻¹, an ozone dose of 0.5 mg O₃ (mg DOC)⁻¹ and a hydraulic residence time of 5 min. Both functions give very similar results, hence, they are considered equally valid for the purpose of conceptual-level engineering-cost estimates. The advantage of the equation developed here is the flexibility to adopt the estimate to other treatment situations than the wastewater effluent and ozone dose assumed by Plumlee *et al.* (2014).

Cost estimates for O&M only account for energy costs of the ozone generator, i.e., other costs such as costs for oxygen supply were neglected [43]. For ozone generators with capacities in the range of 250 to 1'300 lb_{O₃} day⁻¹ (113 to 590 kg_{O₃} day⁻¹), the average specific energy consumption was 6.43 kWh/lb_{O₃} (14.2 kWh/kg_{O₃}) [43]. Therefore, the unit O&M cost function becomes a constant and reads:

$$\frac{C_{O_3}^{\text{tot,O\&M}}}{\dot{Q}} = (c_{O_3} \times c_{\text{DOC}} \times 8.34) \times 6.43 \text{ kWh (lb}_{O_3})^{-1} \times 0.0988 \text{ \$ kWh}^{-1} \times \frac{365 \text{ d a}^{-1}}{10^6 \text{ \$ (\$M)}^{-1}} \quad (\text{D22})$$

Note that more recent ozone generators can be more energy efficient and the energy demand might more accurately be described assuming values around 4.5 kWh/lb_{O₃} (10 kWh/kg_{O₃}) (Xylem Services, personal communication).

Further Details on the LCA Method

ILCD2011 provides suggestions for a characterization at midpoint or endpoint level. As the list for the endpoint levels is not complete, the method was applied at midpoint level. A midpoint method is "a characterization method that provides indicators for comparison of environmental interventions at a level of cause-effect chain between emissions/(resource consumption) towards endpoint level" [232]. For example, for climate change, the midpoint is a mass of CO₂-equivalents and the endpoints are, e.g., disability-adjusted life years (DALYs) and potentially disappeared number of species multiplied with time [232].

According to ISO EN 14040, the LCA inventories (here: Table 6.6 (Chapter 6) in combination with process specifications and mass flows) are first characterized by characterization factors (method specific). Note that the underlying models to calculate the characterization factors for the ILCD2011 methods were assigned to different levels of quality (I: recommended and satisfactory, II: recommended but in need of some improvements, III: recommended, but to be applied with caution) [232]. The following list gives insights to the levels of quality [232]:

- I: climate change; ozone depletion; particulate matter;
- II: ionizing radiation HH; photochemical ozone formation; acidification; eutrophication (terrestrial, freshwater and marine); mineral, fossil and renewable resource depletion.
- II/III: human toxicity (non-cancer and cancer effects); freshwater ecotoxicity;
- III: land use; water resource depletion;

In a next step, the importance of each impact category are normalized, e.g., to the average consumption of a European citizen. Finally, the different impact categories can be weighted against each other to yield at a single score. A weighting step is not included in the ISO EN 14040 because there is no scientific basis for the weighting factors. Nevertheless, weighting is useful and necessary for decision-making and can be based, e.g., on common (political) goals and is therefore commonly accepted. In ILCD2011, all normalized impact categories are weighted equally. Hence, 1 point (Pt) in the ILCD single score corresponds to the average annual environmental impact of one European citizen in 2010.

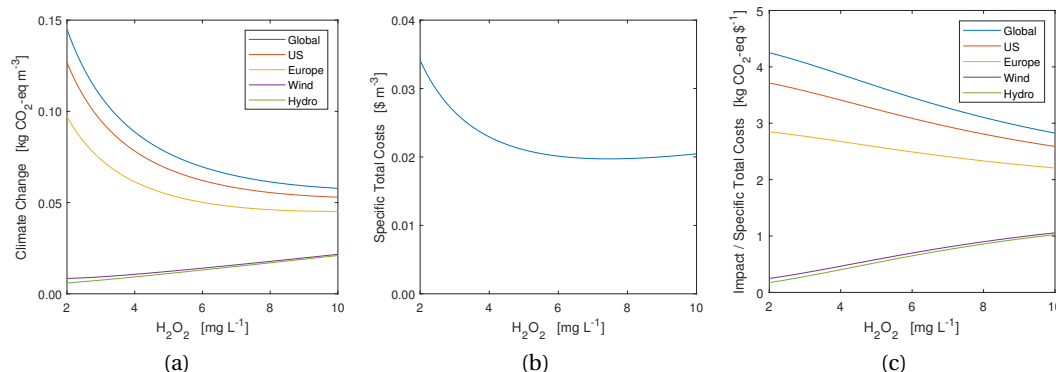


Figure D6: Optimization of the UV/H₂O₂ treatment with respect to the emission of CO₂ equivalents (CO₂-eq). Design of UV/H₂O₂ process with metformin as target compound (Figure D1) for the treatment of an average river Rhine rapid sand filtrate water (16.5 million m³ p.a., UV absorbance at 254 nm: 3.6 m⁻¹). A: Emissions of CO₂ equivalents as a function of the H₂O₂ dose. The UV fluences were calculated from Equation D2 with fitted rate constants from Table 4.2. Colors signify different electricity mixes (global average, US, Europe) or two renewable energy sources (onshore wind turbine, hydro power from run-of-river power plant). B: Total unit cost, i.e., sum of capital costs and operation and maintenance costs (Equations D8 and D10). Capital costs were converted to an annuity using an interest rate of 5.1% (weighted average cost of capital (WACC) for utilities in Switzerland, January 2021, www.waccexpert.com) and a project duration of 30 years. C: Ratio of functions from A and B.

Optimization of UV/H₂O₂ Treatment

Due to the principle flexibility in the UV/H₂O₂ to select UV fluence and H₂O₂ with one degree of freedom (Figure D1), one can optimize the treatment with respect to, e.g., lowest emission of CO₂-equivalents (Figure D6) or ILCD2011 single score (Figure D7). Combining the environmental impact with the treatment cost, it is also possible to search for the optimal treatment in terms of lowest impact per treatment cost.

For the climate change impact category, the optimum treatment conditions shift from high H₂O₂ concentrations and low UV fluences towards very low or absent H₂O₂ concentrations and high UV fluences the more the electrical energy is generated from renewable resources (Figure D6A). At the same time, a cost optimized treatment exists at 7.5 mg H₂O₂ L⁻¹ and 3'200 J m⁻² (minimum of the curve in Figure D6B), using Equations D8 and D10, an interest rate of 5.1% and a project duration of 30 years. Combining the climate change and costs to minimize the impact per cost yields (Figure D6C) a similar result as for the climate change, i.e., with a higher share of electrical energy from renewable sources, a treatment with low H₂O₂ concentrations is advantageous.

Assessing the treatment with the ILCD2011 method (Figure D7A), optimum treatment conditions exist for different country electrical mixes, i.e., at 7.1 mg H₂O₂ L⁻¹ and 3'600 J m⁻² (average global electrical energy mix), 6.9 mg H₂O₂ L⁻¹ and 3'700 J m⁻² (average US electrical

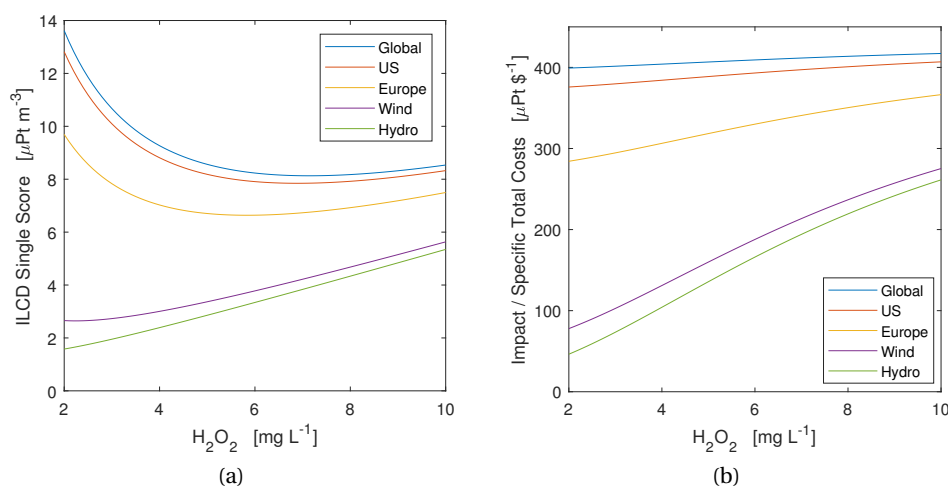


Figure D7: Optimization of the UV/H₂O₂ treatment with respect to the total environmental impact. Design of UV/H₂O₂ process with metformin as target compound (Figure D1) for the treatment of an average river Rhine rapid sand filtrate water (16.5 million m³ p.a., UV absorbance at 254 nm: 3.6 m⁻¹). A: ILCD single score as a function of the H₂O₂ dose. The UV fluence was calculated from Equation D2 with fitted rate constants from Table 4.2. Colors signify different electricity mixes (global average, US, Europe) or two renewable energy sources (onshore wind turbine, hydro power). B: Ratio of functions from A and specific total costs (Figure D6B).

energy mix) and 5.8 mg H₂O₂ L⁻¹ and 4'200 J m⁻² (average European electrical energy mix). With electrical energy solely from wind, the optimum is at 2.2 mg H₂O₂ L⁻¹ and 9'400 J m⁻², while for hydro energy, the optimum is outside the investigated range.

Regarding potential optimizations in the example presented above, specific total costs can be reduced, e.g., by 16% when changing the design from 4 to 7.5 mg H₂O₂ L⁻¹ and simultaneously reducing the UV fluence from 5'800 to 3'200 J m⁻² according to the possible treatment designs presented before (Figure D1). By this, the emission of CO₂-equivalents would drop by 31% in a European context. This optimization would lead to a reduction of ILCD2011 single score points by 3% only, which is about half of the optimization potential in this parameter (maximum 6%). A further increase of the H₂O₂ concentration, as suggested by the Impact per Specific Total Costs plot for CO₂-equivalents (Figure D6C) might not be useful from a technical point of view. This is because H₂O₂ also scavenges •OH and starts mediating the •OH reactions in this concentration range for an average river Rhine rapid sand filtrate water [222].

Optimization to the lowest ILCD2011 single score impact per specific total cost (Figure D7B) suggests to rather increase UV fluence than H₂O₂ doses. Changing the design from 4 to 2 mg H₂O₂ L⁻¹ and simultaneously increasing the UV fluence from 5'800 to 10'200 J m⁻², every € invested turns into 8% less total environmental impact from a global point of view in a European context. In the light of increasing shares of renewable electrical energy in the power grid,

this optimization direction seems to be more future-oriented. However, certain limitations to lower the H_2O_2 exist if one treatment requirement is the establishment of a barrier against MPs by means of $\cdot\text{OH}$. This barrier can be assessed, e.g., using Equation 4.5 (Chapter 4). Possibly, the adjustment of UV fluence and H_2O_2 is feasible during the operation to a certain degree. For example, if a facility does not (yet) obtain its electrical energy from renewable sources in large shares, more detailed analysis could explore the options of, e.g., investing in a larger UV reactor and beginning the operation with a lower UV fluence (e.g., at the optimum described above). With changes in the sources of the electrical energy received by the facility, the operational parameters could be adjusted accordingly. Ultimately, one could investigate options to connect the operational parameters with the electrical energy spot market and dynamically adjust UV fluence and H_2O_2 concentration, e.g., based on the current electrical energy source (or price) in the (local) power grid.

Summarizing, the UV/ H_2O_2 operation can be optimized to comply with a certain treatment goal and this optimization can be conducted *a priori*. This can yield great reductions of costs and/or environmental impacts. To achieve this, the following information are required:

- A mathematical description linking the treatment target to a UV fluence and H_2O_2 concentration, e.g., as shown in Equation D2 for compounds primarily abated by photolysis and/or reactions with $\cdot\text{OH}$. For this, kinetic information is necessary for the target compound as well as water-specific information, such as concentrations of $\cdot\text{OH}$ scavengers and their respective rate constants for reactions with $\cdot\text{OH}$. For many typical $\cdot\text{OH}$ scavengers, these rate constants are known. Commonly, the main unknown is the rate constant for reactions of $\cdot\text{OH}$ with the background organic matter. This parameter should be measured, e.g., in laboratory experiments [41], [148] or must be estimated (natural organic matter: $(0.8 \text{ to } 3.3) \times 10^4 \text{ L (mg DOC)}^{-1} \text{ s}^{-1}$ [164], [209]; effluent organic matter: $(1.0 \text{ to } 3.8) \times 10^4 \text{ L (mg DOC)}^{-1} \text{ s}^{-1}$ [160], [179], [209], [298]).
- The specific electrical energy demand of the UV reactor as a function of the UV fluence, e.g., as shown in Equations D11. If this mathematical description also includes changes in water quality parameters (UV transmission), the optimization could also be conducted for changing water qualities.
- Parameters that connect the electrical energy and H_2O_2 demand to a certain optimization goal, e.g., costs or environmental impacts (Table 6.7, Chapter 6). Note that specific total costs are more complex to estimate due to inter-dependencies, e.g., changing the UV fluences might require a different reactor size which is connected to the investment costs. Therefore, specific total cost optimizations require further mathematical descriptions like in Equations D8 and D10 along with additional information on project-specific accounting-related data (interest rate, project duration).

The suggested treatment parameters should be verified with experimental data. The accuracy

of the *a priori* optimization will depend on the accuracy of the kinetic data used to describe the target compound and the $\bullet\text{OH}$ scavenging of the background water matrix.

Bibliography

- [1] M. Stuart and D. Lapworth, “Emerging Organic Contaminants in Groundwater”, in *Smart Sensors for Real-Time Water Quality Monitoring*, S. C. Mukhopadhyay and A. Mason, Eds., Berlin Heidelberg: Springer Berlin Heidelberg New York Dordrecht London, 2013, ch. 12, pp. 259–284.
- [2] S. Jobling, M. Nolan, C. R. Tyler, G. Brighty, and J. P. Sumpter, “Widespread Sexual Disruption in Wild Fish”, *Environmental Science & Technology*, vol. 32, no. 17, pp. 2498–2506, Sep. 1998. DOI: 10.1021/es9710870.
- [3] E. Silva, N. Rajapakse, and A. Kortenkamp, “Something from “Nothing” - Eight Weak Estrogenic Chemicals Combined at Concentrations below NOECs Produce Significant Mixture Effects”, *Environmental Science & Technology*, vol. 36, no. 8, pp. 1751–1756, Apr. 2002. DOI: 10.1021/es0101227.
- [4] S. E. Hale, H. P. H. Arp, I. Schliebner, and M. Neumann, “Persistent, mobile and toxic (PMT) and very persistent and very mobile (vPvM) substances pose an equivalent level of concern to persistent, bioaccumulative and toxic (PBT) and very persistent and very bioaccumulative (vPvB) substances under REACH”, *Environmental Sciences Europe*, vol. 32, no. 1, p. 155, Dec. 2020. DOI: 10.1186/s12302-020-00440-4.
- [5] T. aus der Beek, F.-A. Weber, A. Bergmann, S. Hickmann, I. Ebert, A. Hein, and A. Küster, “Pharmaceuticals in the environment-Global occurrences and perspectives”, *Environmental Toxicology and Chemistry*, vol. 35, no. 4, pp. 823–835, Apr. 2016. DOI: 10.1002/etc.3339.
- [6] H. K. Khan, M. Y. A. Rehman, and R. N. Malik, “Fate and toxicity of pharmaceuticals in water environment: An insight on their occurrence in South Asia”, *Journal of Environmental Management*, vol. 271, p. 111 030, Oct. 2020. DOI: 10.1016/j.jenvman.2020.111030.
- [7] K. Vargas-Berrones, L. Bernal-Jácome, L. Díaz de León-Martínez, and R. Flores-Ramírez, “Emerging pollutants (EPs) in Latin América: A critical review of under-studied EPs, case of study Nonylphenol”, *Science of The Total Environment*, vol. 726, p. 138 493, Jul. 2020. DOI: 10.1016/j.scitotenv.2020.138493.

Bibliography

- [8] U. Szymańska, M. Wiergowski, I. Sołtyszewski, J. Kuzemko, G. Wiergowska, and M. K. Woźniak, “Presence of antibiotics in the aquatic environment in Europe and their analytical monitoring: Recent trends and perspectives”, *Microchemical Journal*, vol. 147, pp. 729–740, Jun. 2019. DOI: 10.1016/j.microc.2019.04.003.
- [9] J. C. Sousa, A. R. Ribeiro, M. O. Barbosa, M. F. R. Pereira, and A. M. Silva, “A review on environmental monitoring of water organic pollutants identified by EU guidelines”, *Journal of Hazardous Materials*, vol. 344, pp. 146–162, Feb. 2018. DOI: 10.1016/j.jhazmat.2017.09.058.
- [10] L. M. Bexfield, P. L. Toccalino, K. Belitz, W. T. Foreman, and E. T. Furlong, “Hormones and Pharmaceuticals in Groundwater Used As a Source of Drinking Water Across the United States”, *Environmental Science & Technology*, vol. 53, no. 6, pp. 2950–2960, Mar. 2019. DOI: 10.1021/acs.est.8b05592.
- [11] L. Charuau, E. Jarde, A. Jaffrezic, M.-F. Thomas, and B. Le Bot, “Veterinary pharmaceutical residues from natural water to tap water: Sales, occurrence and fate”, *Journal of Hazardous Materials*, vol. 361, pp. 169–186, Jan. 2019. DOI: 10.1016/j.jhazmat.2018.08.075.
- [12] A. Jurado, E. Vázquez-Suñé, J. Carrera, M. López de Alda, E. Pujades, and D. Barceló, “Emerging organic contaminants in groundwater in Spain: A review of sources, recent occurrence and fate in a European context”, *Science of The Total Environment*, vol. 440, pp. 82–94, Dec. 2012. DOI: 10.1016/j.scitotenv.2012.08.029.
- [13] European Commission, “Synthesis Report on the Quality of Drinking Water in the Union examining Member States’ reports for the 2011-2013 period, foreseen under Article 13(5) of Directive 98/83/EC”, Tech. Rep., 2016.
- [14] US National Service Center for Environmental Publications (NSCEP), “Factoids: Drinking Water and Ground Water Statistics for 2009”, Tech. Rep., 2009.
- [15] C. F. Couto, L. C. Lange, and M. C. Amaral, “Occurrence, fate and removal of pharmaceutically active compounds (PhACs) in water and wastewater treatment plants—A review”, *Journal of Water Process Engineering*, vol. 32, p. 100927, Dec. 2019. DOI: 10.1016/j.jwpe.2019.100927.
- [16] 7. Regnery, C. P. Gerba, E. R. Dickenson, and J. E. Drewes, “The Importance of Key Attenuation Factors for Microbial and Chemical Contaminants during Managed Aquifer Recharge: A Review”, *Critical Reviews in Environmental Science and Technology*, vol. 47, no. 15, pp. 1409–1452, 2017. DOI: 10.1080/10643389.2017.1369234.
- [17] S. K. Maeng, S. K. Sharma, K. Lekkerkerker-Teunissen, and G. L. Amy, “Occurrence and fate of bulk organic matter and pharmaceutically active compounds in managed aquifer recharge: A review”, *Water Research*, vol. 45, no. 10, pp. 3015–3033, 2011. DOI: 10.1016/j.watres.2011.02.017.

- [18] S. Mompelat, B. Le Bot, and O. Thomas, "Occurrence and fate of pharmaceutical products and by-products, from resource to drinking water", *Environment International*, vol. 35, no. 5, pp. 803–814, Jul. 2009. DOI: 10.1016/j.envint.2008.10.008.
- [19] P. Westerhoff, Y. Yoon, S. Snyder, and E. Wert, "Fate of Endocrine-Disruptor, Pharmaceutical, and Personal Care Product Chemicals during Simulated Drinking Water Treatment Processes", *Environmental Science & Technology*, vol. 39, no. 17, pp. 6649–6663, Sep. 2005. DOI: 10.1021/es0484799.
- [20] S. Bieber, S. A. Snyder, S. Dagnino, T. Rauch-Williams, and J. E. Drewes, "Management strategies for trace organic chemicals in water – A review of international approaches", *Chemosphere*, vol. 195, pp. 410–426, Mar. 2018. DOI: 10.1016/j.chemosphere.2017.12.100.
- [21] B. Petrie, R. Barden, and B. Kasprzyk-Hordern, "A review on emerging contaminants in wastewaters and the environment: Current knowledge, understudied areas and recommendations for future monitoring", *Water Research*, vol. 72, pp. 3–27, Apr. 2015. DOI: 10.1016/j.watres.2014.08.053.
- [22] E. R. Dickenson, S. A. Snyder, D. L. Sedlak, and J. E. Drewes, "Indicator compounds for assessment of wastewater effluent contributions to flow and water quality", *Water Research*, vol. 45, no. 3, pp. 1199–1212, Jan. 2011. DOI: 10.1016/j.watres.2010.11.012.
- [23] S. T. Glassmeyer, E. T. Furlong, D. W. Kolpin, J. D. Cahill, S. D. Z8g, S. L. Werner, M. T. Meyer, and D. D. Kryak, "Transport of Chemical and Microbial Compounds from Known Wastewater Discharges: Potential for Use as Indicators of Human Fecal Contamination", *Environmental Science & Technology*, vol. 39, no. 14, pp. 5157–5169, Jul. 2005. DOI: 10.1021/es048120k.
- [24] A. Kolkman, D. Vughs, R. Sjerps, P. J. F. Kooij, M. van der Kooi, K. Baken, J. Louisse, and P. de Voogt, "Assessment of Highly Polar Chemicals in Dutch and Flemish Drinking Water and Its Sources: Presence and Potential Risks", *ACS ES&T Water*, vol. 1, no. 4, pp. 928–937, Apr. 2021. DOI: 10.1021/acsestwater.0c00237.
- [25] E. L. Marron, W. A. Mitch, U. von Gunten, and D. L. Sedlak, "A Tale of Two Treatments: The Multiple Barrier Approach to Removing Chemical Contaminants during Potable Water Reuse", *Accounts of Chemical Research*, vol. 52, no. 3, pp. 615–622, 2019. DOI: 10.1021/acs.accounts.8b00612.
- [26] P. Dillon, "Future management of aquifer recharge", *Hydrogeology Journal*, vol. 13, no. 1, pp. 313–316, Mar. 2005. DOI: 10.1007/s10040-004-0413-6.
- [27] P. Dillon, P. Stuyfzand, T. Grischek, M. Lluria, R. D. G. Pyne, R. C. Jain, J. Bear, J. Schwarz, W. Wang, E. Fernandez, C. Stefan, M. Pettenati, J. van der Gun, C. Sprenger, G. Massmann, B. R. Scanlon, J. Xanke, P. Jokela, Y. Zheng, R. Rossetto, M. Shamrukh, P. Pavelic, E. Murray, A. Ross, J. P. Bonilla Valverde, A. Palma Nava, N. Ansems, K. Posavec, K. Ha, R. Martin, and M. Sapiano, "Sixty years of global progress in managed aquifer recharge",

- Hydrogeology Journal*, vol. 27, no. 1, pp. 1–30, Feb. 2019. DOI: 10.1007/s10040-018-1841-z.
- [28] C. Stefan and N. Ansems, “Web-based global inventory of managed aquifer recharge applications”, *Sustainable Water Resources Management*, vol. 4, no. 2, pp. 153–162, Jun. 2018. DOI: 10.1007/s40899-017-0212-6.
 - [29] S. Grünheid, G. Amy, and M. Jekel, “Removal of bulk dissolved organic carbon (DOC) and trace organic compounds by bank filtration and artificial recharge”, *Water Research*, vol. 39, no. 14, pp. 3219–3228, 2005. DOI: 10.1016/j.watres.2005.05.030.
 - [30] S. Alam, A. Borthakur, S. Ravi, M. Gebremichael, and S. K. Mohanty, “Managed aquifer recharge implementation criteria to achieve water sustainability”, *Science of The Total Environment*, vol. 768, p. 144 992, May 2021. DOI: 10.1016/j.scitotenv.2021.144992.
 - [31] J. Filter, V. Zhiteneva, C. Vick, A. S. Ruhl, M. Jekel, U. Hübner, and J. E. Drewes, “Varying attenuation of trace organic chemicals in natural treatment systems – A review of key influential factors”, *Chemosphere*, vol. 274, p. 129 774, Jul. 2021. DOI: 10.1016/j.chemosphere.2021.129774.
 - [32] T. Wintgens, R. Hochstrat, C. Kazner, P. Jeffrey, B. Jefferson, and T. Melin, “Managed Aquifer Recharge as a component of sustainable water strategies - a brief guidance for EU policies”, in *Water Reclamation Technologies for Safe Managed Aquifer Recharge*, C. Kazner, T. Wintgens, and P. Dillon, Eds., London: IWA Publishing, 2012, ch. 22.
 - [33] A. Nauta and A. Roelandse, *Het effect van de industriële lozing van Chemours op de aanwezigheid van PFOA in (oever)grondwater*, Gouda (Netherlands), 2016.
 - [34] UNEP (United Nations Environment Program), *Report of the Persistent Organic Pollutants Review Committee on the work of its thirteenth meeting. Addendum: Risk management evaluation on pentadecafluorooctanoic acid (CAS No: 335-67-1, PFOA, perfluorooctanoic acid), its salts and PFOA-related compounds*, Rome, Oct. 2017.
 - [35] S. Sudhakaran, S. K. Maeng, and G. Amy, “Hybridization of natural systems with advanced treatment processes for organic micropollutant removals: New concepts in multi-barrier treatment”, *Chemosphere*, vol. 92, no. 6, pp. 731–737, 2013. DOI: 10.1016/j.chemosphere.2013.04.021.
 - [36] K. Hellauer, D. Mergel, A. Ruhl, J. Filter, U. Hübner, M. Jekel, and J. E. Drewes, “Advancing Sequential Managed Aquifer Recharge Technology (SMART) Using Different Intermediate Oxidation Processes”, *Water*, vol. 9, no. 3, p. 221, Mar. 2017. DOI: 10.3390/w9030221.
 - [37] Y. Yu, Y. H. Choi, J. Choi, S. Choi, and S. K. Maeng, “Multi-barrier approach for removing organic micropollutants using mobile water treatment systems”, *Science of the Total Environment*, vol. 639, pp. 331–338, 2018. DOI: 10.1016/j.scitotenv.2018.05.079.

- [38] R. Wünsch, 7. Plattner, D. Cayon, F. Eugster, J. Gebhardt, R. Wülser, U. von Gunten, and T. Wintgens, “Surface water treatment by UV/H₂O₂ with subsequent soil aquifer treatment: impact on micropollutants, dissolved organic matter and biological activity”, *Environmental Science: Water Research & Technology*, vol. 5, no. 10, pp. 1709–1722, 2019. DOI: 10.1039/C9EW00547A.
- [39] K. Lekkerkerker-Teunissen, J. Scheideler, S. K. Maeng, A. Ried, J. Q. J. C. Verberk, A. H. Knol, G. L. Amy, and J. C. Van Dijk, “Advanced oxidation and artificial recharge: A synergistic hybrid system for removal of organic micropollutants”, *Water Science and Technology: Water Supply*, vol. 9, no. 6, pp. 643–651, 2009. DOI: 10.2166/ws.2009.696.
- [40] U. von Gunten, “Oxidation Processes in Water Treatment: Are We on Track?”, *Environmental Science & Technology*, vol. 52, no. 9, pp. 5062–5075, May 2018. DOI: 10.1021/acs.est.8b00586.
- [41] R. Wünsch, C. Mayer, 7. Plattner, F. Eugster, R. Wülser, J. Gebhardt, U. Hübner, S. Canonica, T. Wintgens, and U. von Gunten, “Micropollutants as internal probe compounds to assess UV fluence and hydroxyl radical exposure in UV/H₂O₂ treatment”, *Water Research*, p. 116 940, Feb. 2021. DOI: 10.1016/j.watres.2021.116940.
- [42] R. Wünsch, T. Hettich, M. Prahtel, M. Thomann, T. Wintgens, and U. von Gunten, “Tradeoff Between Micropollutant Abatement and Bromate Formation during Ozonation of Concentrates from Nanofiltration and Reverse Osmosis Processes (in preparation)”,
- [43] M. H. Plumlee, B. D. Stanford, J.-F. Debroux, D. C. Hopkins, and S. A. Snyder, “Costs of Advanced Treatment in Water Reclamation”, *Ozone: Science & Engineering*, vol. 36, no. 5, pp. 485–495, Sep. 2014. DOI: 10.1080/01919512.2014.921565.
- [44] C. Roth, R. Wünsch, F. Dinkel, C. Hugli, R. Wülser, R. Antes, and M. Thomann, “Micropollutant abatement with UV/H₂O₂ oxidation or low-pressure reverse osmosis? A comparative life cycle assessment for drinking water production”, *Journal of Cleaner Production*, p. 130 227, Dec. 2021. DOI: 10.1016/j.jclepro.2021.130227.
- [45] D. Rüetschi, “BASLER TRINKWASSERGEWINNUNG IN DEN LANGEN ERLLEN Biologische Reinigungsleistungen in den bewaldeten Wasserstellen”, PhD Thesis, University of Basel, Basel (Switzerland), 2004.
- [46] K. Schütz, “Artificial groundwater recharge in forests - soil fauna and microbiology”, PhD Thesis, University of Basel, 2008.
- [47] IWB. (2021). “Trinkwasserversorgung IWB”, [Online]. Available: <https://www.iwb.ch/Fuer-Zuhause/Wasser/Trinkwasser-Versorgung.html> (visited on 08/06/2021).
- [48] F. R. Storck, “Fate of dissolved organic carbon and organic trace pollutants in the artificial groundwater recharge site Lange Erlen (Basel)”, PhD Thesis, Technical University Berlin, 2014.

Bibliography

- [49] J. Zawadzka, E. Gallagher, H. Smith, and R. Corstanje, "Ecosystem services from combined natural and engineered water and wastewater treatment systems: Going beyond water quality enhancement", *Ecological Engineering*, vol. 142, p. 100 006, 2019. DOI: 10.1016/j.ecoena.2019.100006.
- [50] M. Ruff, M. S. Mueller, M. Loos, and H. P. Singer, "Quantitative target and systematic non-target analysis of polar organic micro-pollutants along the river Rhine using high-resolution mass-spectrometry – Identification of unknown sources and compounds", *Water Research*, vol. 87, pp. 145–154, Dec. 2015. DOI: 10.1016/j.watres.2015.09.017.
- [51] U. von Gunten, "Ozonation of drinking water: Part II Disinfection and by-product formation in the presence of bromide", *Water Research*, vol. 37, no. 37, pp. 1469–1487, 2003.
- [52] P. Dillon, S. Toze, D. Page, J. Vanderzalm, E. Bekele, J. Sidhu, and S. Rinck-Pfeiffer, "Managed aquifer recharge: rediscovering nature as a leading edge technology", *Water Science and Technology*, vol. 62, no. 10, pp. 2338–2345, Nov. 2010. DOI: 10.2166/wst.2010.444.
- [53] 7. Plattner, F. Eugster, J. Svojitka, R. Wünsch, J. Gebhardt, R. Wülser, and T. Wintgens, "Removal of Micropollutants and Formation of Harmful By-Products in Advanced Oxidation Process with UV and H₂O₂ in Surface Water", in *9th IWA Eastern European Young Water Professionals Conference, Budapest, 24.-27. May 2017*, 2017, pp. 1–2.
- [54] S. A. Huber, A. Balz, M. Abert, and W. Pronk, "Characterisation of aquatic humic and non-humic matter with size-exclusion chromatography - organic carbon detection - organic nitrogen detection (LC-OCD-OND)", *Water Research*, vol. 45, no. 2, pp. 879–885, 2011. DOI: 10.1016/j.watres.2010.09.023.
- [55] R. Geschke and M. Zehringer, "A new method for the determination of complexing agents in river water using HPLC", *Fresenius' Journal of Analytical Chemistry*, vol. 357, no. 6, pp. 773–776, Mar. 1997. DOI: 10.1007/s002160050247.
- [56] S. R. Sarathy, M. I. Stefan, A. Royce, and M. Mohseni, "Pilot-scale UV/H₂O₂ advanced oxidation process for surface water treatment and downstream biological treatment: effects on natural organic matter characteristics and DBP formation potential", *Environmental Technology*, vol. 32, no. 15, pp. 1709–1718, Nov. 2011. DOI: 10.1080/09593330.2011.553843.
- [57] K. Lekkerkerker-Teunissen, E. T. Chekol, S. K. Maeng, K. Ghebremichael, C. J. Houtman, A. Verliefde, J. Q. J. C. Verberk, G. L. Amy, and J. C. Van Dijk, "Pharmaceutical removal during managed aquifer recharge with pretreatment by advanced oxidation", *Water Science and Technology: Water Supply*, vol. 12, no. 6, pp. 755–767, 2012. DOI: 10.2166/ws.2012.050.

-
- [58] K. E. Black and P. R. Bérubé, “Rate and extent NOM removal during oxidation and biofiltration”, *Water Research*, vol. 52, pp. 40–50, Apr. 2014. DOI: 10.1016/j.watres.2013.12.017.
- [59] H. C. Kim, W. M. Lee, S. Lee, J. Choi, and S. K. Maeng, “Characterization of organic precursors in DBP formation and AOC in urban surface water and their fate during managed aquifer recharge”, *Water Research*, vol. 123, pp. 75–85, 2017. DOI: 10.1016/j.watres.2017.06.038.
- [60] S. A. Parsons, *Advanced Oxidation Processes for Water and Wastewater Treatment*, S. A. Parsons, Ed. London: IWA Publishing, 2004.
- [61] C. Kazner, T. Wintgens, and P. Dillon, Eds., *Water Reclamation Technologies for Safe Managed Aquifer Recharge*. London: IWA Publishing, 2012, p. 460.
- [62] M. K. Yoon, J. E. Drewes, and G. L. Amy, “Fate of bulk and trace organics during a simulated aquifer recharge and recovery (ARR)-ozone hybrid process”, *Chemosphere*, vol. 93, no. 9, pp. 2055–2062, 2013. DOI: 10.1016/j.chemosphere.2013.07.038.
- [63] M. Alidina, J. Shewchuk, and J. E. Drewes, “Effect of temperature on removal of trace organic chemicals in managed aquifer recharge systems”, *Chemosphere*, vol. 122, pp. 23–31, Mar. 2015. DOI: 10.1016/j.chemosphere.2014.10.064.
- [64] 7. Regnery, J. Barringer, A. D. Wing, C. Hoppe-Jones, J. Teerlink, and J. E. Drewes, “Start-up performance of a full-scale riverbank filtration site regarding removal of DOC, nutrients, and trace organic chemicals”, *Chemosphere*, vol. 127, pp. 136–142, 2015. DOI: 10.1016/j.chemosphere.2014.12.076.
- [65] WWAP (United Nations World Water Assessment Programme)/UN-Water, “The United Nations World Water Development Report 2018: Nature-Based Solutions for Water”, UNESCO, Paris, Tech. Rep., 2018.
- [66] J. E. Drewes and M. Jekel, “Behavior of DOC and AOX using advanced treated wastewater for groundwater recharge”, *Water Research*, vol. 32, no. 10, pp. 3125–3133, Oct. 1998. DOI: 10.1016/S0043-1354(98)00064-5.
- [67] J. Schumacher, Y. Pi, and M. Jekel, “Ozonation of persistent DOC in municipal WWTP effluent for groundwater recharge”, *Water Science and Technology*, vol. 49, no. 4, pp. 305–310, Feb. 2004. DOI: 10.2166/wst.2004.0291.
- [68] 7. Hollender, S. G. Zimmermann, S. Koepke, M. Krauss, C. S. Mc Ardell, C. Ort, H. Singer, U. von Gunten, and H. Siegrist, “Elimination of Organic Micropollutants in a Municipal Wastewater Treatment Plant Upgraded with a Full-Scale Post-Ozonation Followed by Sand Filtration”, *Environmental Science & Technology*, vol. 43, no. 20, pp. 7862–7869, Oct. 2009. DOI: 10.1021/es9014629.

Bibliography

- [69] U. Hübner, U. Miehe, and M. Jekel, "Optimized removal of dissolved organic carbon and trace organic contaminants during combined ozonation and artificial groundwater recharge", *Water Research*, vol. 46, no. 18, pp. 6059–6068, Nov. 2012. DOI: 10.1016/j.watres.2012.09.001.
- [70] M. K. Yoon and G. L. Amy, "Reclaimed water quality during simulated ozone-managed aquifer recharge hybrid", *Environmental Earth Sciences*, pp. 7795–7802, 2015. DOI: 10.1007/s12665-014-3412-5.
- [71] I. Zucker, H. Mamane, H. Cikurel, M. Jekel, U. Hübner, and D. Avisar, "A hybrid process of biofiltration of secondary effluent followed by ozonation and short soil aquifer treatment for water reuse", *Water Research*, vol. 84, no. 8ust, pp. 315–322, Nov. 2015. DOI: 10.1016/j.watres.2015.07.034.
- [72] S. Echigo, M. Nakatsuji, Y. Takabe, and S. Itoh, "Effect of preozonation on wastewater reclamation by the combination of ozonation and soil aquifer treatment", *Water Science and Technology: Water Supply*, vol. 15, no. 1, pp. 101–106, 2015. DOI: 10.2166/ws.2014.089.
- [73] Y. Lester, D. S. Aga, N. G. Love, R. R. Singh, I. Morrissey, and K. G. Linden, "Integrative Advanced Oxidation and Biofiltration for Treating Pharmaceuticals in Wastewater", *Water Environment Research*, vol. 88, no. 11, pp. 1985–1993, Nov. 2016. DOI: 10.2175/106143016X14504669767454.
- [74] 7. Regnery, A. D. Wing, J. Kautz, and J. E. Drewes, "Introducing sequential managed aquifer recharge technology (SMART) - From laboratory to full-scale application", *Chemosphere*, vol. 154, pp. 8–16, 2016. DOI: 10.1016/j.chemosphere.2016.03.097.
- [75] U. Hübner, S. Kuhnt, M. Jekel, and J. E. Drewes, "Fate of bulk organic carbon and bromate during indirect water reuse involving ozone and subsequent aquifer recharge", *Journal of Water Reuse and Desalination*, vol. 6, no. 3, pp. 413–420, Nov. 2016. DOI: 10.2166/wrd.2015.222.
- [76] H. C. Kim, S. H. Park, J. H. Noh, J. Choi, S. Lee, and S. K. Maeng, "Comparison of pre-oxidation between O₃ and O₃/H₂O₂ for subsequent managed aquifer recharge using laboratory-scale columns", *Journal of Hazardous Materials*, vol. 377, no. March, pp. 290–298, 2019. DOI: 10.1016/j.jhazmat.2019.05.099.
- [77] A. Lakretz, H. Mamane, H. Cikurel, D. Avisar, E. Gelman, and I. Zucker, "The Role of Soil Aquifer Treatment (SAT) for Effective Removal of Organic Matter, Trace Organic Compounds and Microorganisms from Secondary Effluents Pre-Treated by Ozone", *Ozone: Science and Engineering*, vol. 39, no. 5, pp. 385–394, 2017. DOI: 10.1080/01919512.2017.1346465.

- [78] M. Bourgin, B. Beck, M. Boehler, E. Borowska, 7. Fleiner, E. Salhi, R. Teichler, U. von Gunten, H. Siegrist, and C. S. McArdell, "Evaluation of a full-scale wastewater treatment plant upgraded with ozonation and biological post-treatments: Abatement of micropollutants, formation of transformation products and oxidation by-products", *Water Research*, vol. 129, pp. 486–498, 2018. DOI: 10.1016/j.watres.2017.10.036.
- [79] J. E. Drewes and N. Horstmeyer, "Strategien und Potenziale zur Energieoptimierung bei der Wasserwiederverwendung", *Österreichische Wasser- und Abfallwirtschaft*, vol. 68, no. 3-4, pp. 99–107, Apr. 2016. DOI: 10.1007/s00506-016-0298-3.
- [80] K. Lekkerkerker-Teunissen, A. H. Knol, J. G. Derks, M. B. Heringa, C. J. Houtman, R. C. H. M. Hofman-Caris, E. F. Beerendonk, A. Reus, J. Q. J. C. Verberk, and J. C. Van Dijk, "Pilot Plant Results with Three Different Types of UV Lamps for Advanced Oxidation", *Ozone: Science & Engineering*, vol. 35, no. 1, pp. 38–48, 2013. DOI: 10.1080/01919512.2013.721317.
- [81] J. Scheideler, K. Lekkerkerker-Teunissen, T. Knol, A. Ried, J. Q. J. C. Verberk, and H. C. Van Dijk, "Combination of O_3/H_2O_2 and UV for multiple barrier micropollutant treatment and bromate formation control – an economic attractive option", *Water Practice & Technology*, vol. 6, no. 4, pp. 1–2, Dec. 2011. DOI: 10.2166/wpt.2011.0063.
- [82] K. Lekkerkerker-Teunissen, A. H. Knol, L. P. Van Altena, C. J. Houtman, J. Q. J. C. Verberk, and J. C. Van Dijk, "Serial ozone/peroxide/low pressure UV treatment for synergistic and effective organic micropollutant conversion", *separation and Purification Technology*, vol. 100, pp. 22–29, 2012. DOI: 10.1016/j.j9pur.2012.08.030.
- [83] M. M. Bazri, B. Barbeau, and M. Mohseni, "Impact of UV/ H_2O_2 advanced oxidation treatment on molecular weight distribution of NOM and biostability of water", *Water Research*, vol. 46, no. 16, pp. 5297–5304, Oct. 2012. DOI: 10.1016/j.watres.2012.07.017.
- [84] U. technologies. (). "Titanium Oxalate (Spectrophotometric)", [Online]. Available: <http://www.h2o2.com/technical-library/analytical-methods/default.aspx?pid=71%7B%5C&%7Dname=Titanium-Oxalate-Spectrophotometric> (visited on 04/10/2019).
- [85] G. Eisenberg, "Colorimetric Determination of Hydrogen Peroxide", *Industrial & Engineering Chemistry Analytical Edition*, vol. 15, no. 5, pp. 327–328, May 1943. DOI: 10.1021/i560117a011.
- [86] W. Jäggi, "Die Bestimmung der CO_2 -Bildung als Mass der bodenbiologischen Aktivität", *Schweiz. landw. Forschung*, vol. 15, pp. 371–380, 1976.
- [87] Agroscope, "Band 2: Bodenuntersuchungen zur Standort-Charakterisierung", in *Schweizerische Referenzmethoden der Eidg. landwirtschaftlichen Forschungsanstalten*, 2015th ed., 1996, ch. B-BA-IS.

Bibliography

- [88] E. Prest, F. Hammes, S. Köttsch, M. van Loosdrecht, and J. Vrouwenvelder, “Monitoring microbiological changes in drinking water systems using a fast and reproducible flow cytometric method”, *Water Research*, vol. 47, no. 19, pp. 7131–7142, Dec. 2013. DOI: 10.1016/j.watres.2013.07.051.
- [89] F. Hammes, F. Goldschmidt, M. Vital, Y. Wang, and T. Egli, “Measurement and interpretation of microbial adenosine tri-phosphate (ATP) in aquatic environments”, *Water Research*, vol. 44, no. 13, pp. 3915–3923, Jul. 2010. DOI: 10.1016/j.watres.2010.04.015.
- [90] S. Canonica, L. Meunier, and U. von Gunten, “Phototransformation of selected pharmaceuticals during UV treatment of drinking water”, *Water Research*, vol. 42, no. 1-2, pp. 121–128, 2008. DOI: 10.1016/j.watres.2007.07.026.
- [91] F. X. Tian, B. Xu, Y. L. Lin, C. Y. Hu, T. Y. Zhang, and N. Y. Gao, “Photodegradation kinetics of iopamidol by UV irradiation and enhanced formation of iodinated disinfection by-products in sequential oxidation processes”, *Water Research*, vol. 58, pp. 198–208, 2014. DOI: 10.1016/j.watres.2014.03.069.
- [92] B. A. Wols, D. J. Harmsen, E. F. Beerendonk, and R. C. H. M. Hofman-Caris, “Predicting pharmaceutical degradation by UV (LP)/H₂O₂ processes: A kinetic model”, *Chemical Engineering Journal*, vol. 255, pp. 334–343, Nov. 2014. DOI: 10.1016/j.cej.2014.05.088.
- [93] J. Lati and D. Meyerstein, “Oxidation of first-row bivalent transition-metal complexes containing ethylenediaminetetra-acetate and nitrilotriacetate ligands by free radicals: a pulse-radiolysis study”, *Journal of the Chemical Society, Dalton Transactions*, vol. 0, no. 9, pp. 1105–1118, 1978. DOI: 10.1039/DT9780001105.
- [94] M. Sörensen, S. Zurell, and F. H. Frimmel, “Degradation Pathway of the Photochemical Oxidation of Ethylenediaminetetraacetate (EDTA) in the UV/H₂O₂-process”, *Acta hydrochimica et hydrobiologica*, vol. 26, no. 2, pp. 109–115, Mar. 1998. DOI: 10.1002/(SICI)1521-401X(199803)26:2<109::AID-AHEH109>3.0.CO;2-C.
- [95] B. Müller, *ChemEQL (V. 3.2.1)*, 2015.
- [96] B. A. Wols, R. C. H. M. Hofman-Caris, D. J. Harmsen, and E. F. Beerendonk, “Degradation of 40 selected pharmaceuticals by UV/H₂O₂”, *Water Research*, vol. 47, no. 15, pp. 5876–5888, 2013. DOI: 10.1016/j.watres.2013.07.008.
- [97] H. Khouri, F. Collin, D. Bonnefont-Rousselot, A. Legrand, D. Jore, and M. Gardes-Albert, “Radical-induced oxidation of metformin”, *European Journal of Biochemistry*, vol. 271, no. 23-24, pp. 4745–4752, Dec. 2004. DOI: 10.1111/j.1432-1033.2004.04438.x.
- [98] B. A. Wols, D. J. Harmsen, J. Wanders-Dijk, E. F. Beerendonk, and R. C. H. M. Hofman-Caris, “Degradation of pharmaceuticals in UV (LP)/H₂O₂ reactors simulated by means of kinetic modeling and computational fluid dynamics (CFD)”, *Water Research*, vol. 75, no. 0, pp. 11–24, 2015. DOI: 10.1016/j.watres.2015.02.014.

- [99] J. M. Gleason, G. McKay, K. P. Ishida, and S. P. Mezyk, "Temperature dependence of hydroxyl radical reactions with chloramine species in aqueous solution", *Chemosphere*, vol. 187, pp. 123–129, Nov. 2017. DOI: 10.1016/j.chemosphere.2017.08.053.
- [100] M. I. Stefan, *Advanced Oxidation Processes for Water Treatment*, 15. London: IWA Publishing, 2018, p. 686. DOI: 10.1021/jz300929x.
- [101] R. Zellner, M. Exner, and H. Herrmann, "Absolute OH quantum yields in the laser photolysis of nitrate, nitrite and dissolved H₂O₂ at 308 and 351 nm in the temperature range 278–353 K", *Journal of Atmospheric Chemistry*, vol. 10, no. 4, pp. 411–425, May 1990. DOI: 10.1007/BF00115783.
- [102] Z. He, "UV Lamp Temperature Characteristics", *IUVA News*, vol. 14, no. 4, pp. 13–17, 2012.
- [103] Eidgenössische Departement des Innern (EDI), *Verordnung des EDI über Trinkwasser sowie Wasser in öffentlich zugänglichen Bädern und Duschanlagen (TBDV)*, 817.022.11, 2018.
- [104] J. L. Kormos, M. Schulz, and T. A. Ternes, "Occurrence of Iodinated X-ray Contrast Media and Their Biotransformation Products in the Urban Water Cycle", *Environmental Science & Technology*, vol. 45, no. 20, pp. 8723–8732, Oct. 2011. DOI: 10.1021/es2018187.
- [105] A. G. Asimakopoulos, A. Ajibola, K. Kannan, and N. S. Thomaidis, "Occurrence and removal efficiencies of benzotriazoles and benzothiazoles in a wastewater treatment plant in Greece", *Science of The Total Environment*, vol. 452–453, pp. 163–171, May 2013. DOI: 10.1016/j.scitotenv.2013.02.041.
- [106] C. Götz, J. Otto, and H. Singer, "Überprüfung des Reinigungseffekts", *Aqua+Gas*, vol. 2, pp. 34–40, 2015.
- [107] C. Trautwein and K. Kümmerer, "Incomplete aerobic degradation of the antidiabetic drug Metformin and identification of the bacterial dead-end transformation product Guanylylurea", *Chemosphere*, vol. 85, no. 5, pp. 765–773, 2011. DOI: 10.1016/j.chemosphere.2011.06.057.
- [108] M. Scheurer, A. Michel, H. J. Brauch, W. Ruck, and F. Sacher, "Occurrence and fate of the antidiabetic drug metformin and its metabolite guanylylurea in the environment and during drinking water treatment", *Water Research*, vol. 46, no. 15, pp. 4790–4802, 2012. DOI: 10.1016/j.watres.2012.06.019.
- [109] B. Blair, A. Nikolaus, C. Hedman, R. Klaper, and T. Grundl, "Evaluating the degradation, sorption, and negative mass balances of pharmaceuticals and personal care products during wastewater treatment", *Chemosphere*, vol. 134, pp. 395–401, 2015. DOI: 10.1016/j.chemosphere.2015.04.078.

Bibliography

- [110] A. Kot-Wasik, A. Jakimska, and M. Śliwka-Kaszyńska, "Occurrence and seasonal variations of 25 pharmaceutical residues in wastewater and drinking water treatment plants", *Environmental Monitoring and Assessment*, vol. 188, no. 12, 2016. DOI: 10.1007/s10661-016-5637-0.
- [111] M. Markiewicz, C. Jungnickel, S. Stolte, A. Białk-Bielińska, J. Kumirska, and W. Mroziak, "Primary degradation of antidiabetic drugs", *Journal of Hazardous Materials*, vol. 324, pp. 428–435, 2017. DOI: 10.1016/j.jhazmat.2016.11.008.
- [112] S. Tisler and C. Zwiener, "Formation and occurrence of transformation products of metformin in wastewater and surface water", *Science of the Total Environment*, vol. 628–629, pp. 1121–1129, 2018. DOI: 10.1016/j.scitotenv.2018.02.105.
- [113] J. E. Drewes, D. Li, 7. Regnery, M. Alidina, A. Wing, and C. Hoppe-Jones, "Tuning the performance of a natural treatment process using metagenomics for improved trace organic chemical attenuation", *Water Science and Technology*, vol. 69, no. 3, pp. 628–633, 2014. DOI: 10.2166/wst.2013.750.
- [114] U. Hübner, U. von Gunten, and M. Jekel, "Evaluation of the persistence of transformation products from ozonation of trace organic compounds – A critical review", *Water Research*, vol. 68, pp. 150–170, Jan. 2015. DOI: 10.1016/j.watres.2014.09.051.
- [115] U. Hübner, B. Seiwert, T. Reemtsma, and M. Jekel, "Ozonation products of carbamazepine and their removal from secondary effluents by soil aquifer treatment – Indications from column experiments", *Water Research*, vol. 49, no. 1, pp. 34–43, Feb. 2014. DOI: 10.1016/j.watres.2013.11.016.
- [116] M. Prévost, P. Laurent, P. Servais, and J.-C. Joret, Eds., *Biodegradable Organic Matter in Drinking Water Treatment and Distribution*. Denver (CO): AWWA, 2005, pp. xiii, 300.
- [117] A. D. Dotson, O. S. Keen, D. Metz, and K. G. Linden, "UV/H₂O₂ treatment of drinking water increases post-chlorination DBP formation", *Water Research*, vol. 44, no. 12, pp. 3703–3713, Jun. 2010. DOI: 10.1016/j.watres.2010.04.006.
- [118] H.-C. Lin and G.-S. Wang, "Effects of UV/H₂O₂ on NOM fractionation and corresponding DBPs formation", *Desalination*, vol. 270, no. 1-3, pp. 221–226, Apr. 2011. DOI: 10.1016/j.desal.2010.11.049.
- [119] R. Toor and M. Mohseni, "UV-H₂O₂ based AOP and its integration with biological activated carbon treatment for DBP reduction in drinking water", *Chemosphere*, vol. 66, no. 11, pp. 2087–2095, 2007. DOI: 10.1016/j.chemosphere.2006.09.043.
- [120] S. R. Sarathy, M. M. Bazri, and M. Mohseni, "Modeling the Transformation of Chromophoric Natural Organic Matter during UV/H₂O₂ Advanced Oxidation", *Journal of Environmental Engineering*, vol. 137, no. 10, pp. 903–912, 2011. DOI: 10.1061/(ASCE)EE.1943-7870.0000390..

- [121] C. von Sonntag and U. von Gunten, *Chemistry of Ozone in Water and Wastewater Treatment: From Basic Principles to Applications*, C. von Sonntag and U. von Gunten, Eds. London: IWA Publishing, 2012, p. 302. DOI: 10.2166/9781780400839.
- [122] C. Prasse, B. Ford, D. K. Nomura, and D. L. Sedlak, “Unexpected transformation of dissolved phenols to toxic dicarbonyls by hydroxyl radicals and UV light”, *Proceedings of the National Academy of Sciences*, vol. 115, no. 10, pp. 2311–2316, Mar. 2018. DOI: 10.1073/pnas.1715821115.
- [123] A. Parkinson, M. J. Barry, F. A. Roddick, and M. D. Hobday, “Preliminary toxicity assessment of water after treatment with UV-irradiation and UVC/H₂O₂”, *Water Research*, vol. 35, no. 15, pp. 3656–3664, Oct. 2001. DOI: 10.1016/S0043-1354(01)00096-3.
- [124] E. H. Goslan, F. Gurses, J. Banks, and S. A. Parsons, “An investigation into reservoir NOM reduction by UV photolysis and advanced oxidation processes”, *Chemosphere*, vol. 65, no. 7, pp. 1113–1119, Nov. 2006. DOI: 10.1016/j.chemosphere.2006.04.041.
- [125] K. Hellauer, J. Uhl, M. Lucio, P. Schmitt-Kopplin, D. Wibberg, U. Hübner, and J. E. Drewes, “Microbiome-Triggered Transformations of Trace Organic Chemicals in the Presence of Effluent Organic Matter in Managed Aquifer Recharge (MAR) Systems”, *Environmental Science and Technology*, vol. 52, no. 24, pp. 14 342–14 351, 2018. DOI: 10.1021/acs.est.8b04559.
- [126] W. A. M. Hijnen, E. F. Beerendonk, and G. J. Medema, “Inactivation credit of UV radiation for viruses, bacteria and protozoan (oo)cysts in water: A review”, *Water Research*, vol. 40, no. 1, pp. 3–22, 2006. DOI: 10.1016/j.watres.2005.10.030.
- [127] US EPA, *Ultraviolet Disinfection Guidance Manual for the Final Long Term 2 Enhanced Surface Water Treatment Rule (EPA 815-R-06-007)*, 2006.
- [128] G. Chevretils, É. Caron, H. Wright, G. Sakamoto, P. Payment, B. Barbeau, and B. Cairns, “UV Dose Required to Achieve Incremental Log Inactivation of Bacteria, Protozoa and Viruses”, *IUVA News*, vol. 8, no. 1, pp. 38–45, 2006.
- [129] K. Lautenschlager, C. Hwang, F. Ling, W.-T. Liu, N. Boon, O. Köster, T. Egli, and E. Hammes, “Abundance and composition of indigenous bacterial communities in a multi-step biofiltration-based drinking water treatment plant”, *Water Research*, vol. 62, pp. 40–52, Oct. 2014. DOI: 10.1016/j.watres.2014.05.035.
- [130] F. Wang, D. van Halem, G. Liu, K. Lekkerkerker-Teunissen, and J. P. van der Hoek, “Effect of residual H₂O₂ from advanced oxidation processes on subsequent biological water treatment: A laboratory batch study”, *Chemosphere*, vol. 185, pp. 637–646, Oct. 2017. DOI: 10.1016/j.chemosphere.2017.07.073.
- [131] J. C. Kruithof, P. C. Kamp, and B. J. Martijn, “UV/H₂O₂ treatment: A practical solution for organic contaminant control and primary disinfection”, *Ozone-Science & Engineering*, vol. 29, no. 4, pp. 273–280, 2007. DOI: 10.1080/01919510701459311.

Bibliography

- [132] S. L. Roback, K. P. Ishida, and M. H. Plumlee, "Influence of reverse osmosis membrane age on rejection of NDMA precursors and formation of NDMA in finished water after full advanced treatment for potable reuse", *Chemosphere*, vol. 233, pp. 120–131, 2019. DOI: 10.1016/j.chemosphere.2019.05.259.
- [133] R. S. Trussell, G. Lai-Blum, M. Chaudhuri, and G. Johnson, "Developing a regional recycled water program in Southern California", *Water Practice and Technology*, vol. 14, no. 3, pp. 570–578, 2019. DOI: 10.2166/wpt.2019.042.
- [134] J. Lee, U. von Gunten, and J.-H. Kim, "Persulfate-Based Advanced Oxidation: Critical Assessment of Opportunities and Roadblocks", *Environmental Science & Technology*, vol. 54, no. 6, pp. 3064–3081, Mar. 2020. DOI: 10.1021/acs.est.9b07082.
- [135] D. B. Miklos, C. Remy, M. Jekel, K. G. Linden, J. E. Drewes, and U. Hübner, "Evaluation of advanced oxidation processes for water and wastewater treatment – A critical review", *Water Research*, vol. 139, pp. 118–131, 2018. DOI: 10.1016/j.watres.2018.03.042.
- [136] U. von Gunten and Y. Oliveras, "Advanced Oxidation of Bromide-Containing Waters: Bromate Formation Mechanisms", *Environmental Science & Technology*, vol. 32, no. 1, pp. 63–70, Jan. 1998. DOI: 10.1021/es970477j.
- [137] E. J. Rosenfeldt and K. G. Linden, "The $R_{\text{OH,UV}}$ Concept to Characterize and the Model UV/H₂O₂ Process in Natural Waters", *Environmental Science & Technology*, vol. 41, no. 7, pp. 2548–2553, Apr. 2007. DOI: 10.1021/es062353p.
- [138] J. R. Bolton and M. I. Stefan, "Fundamental photochemical approach to the concepts of fluence (UV dose) and electrical energy efficiency in photochemical degradation reactions", *Research on Chemical Intermediates*, vol. 28, no. 7, pp. 857–870, 2002. DOI: 10.1163/15685670260469474.
- [139] National Institute of Standards and Technology. (2002). "NIST Standard Reference Database 40", [Online]. Available: <https://kinetics.nist.gov/solution/> (visited on 08/06/2021).
- [140] D. Minakata, P. Westerhoff, and J. C. Crittenden, "Development of a Group Contribution Method To Predict Aqueous Phase Hydroxyl Radical (HO•) Reaction Rate Constants", *Environmental Science & Technology*, vol. 43, no. 16, pp. 6220–6227, 2009. DOI: 10.1021/es900956c.
- [141] S. Bahnmüller, C. H. Loi, K. L. Linge, U. von Gunten, and S. Canonica, "Degradation rates of benzotriazoles and benzothiazoles under UV-C irradiation and the advanced oxidation process UV/H₂O₂", *Water Research*, vol. 74, pp. 143–154, May 2015. DOI: 10.1016/j.watres.2014.12.039.
- [142] B. A. Wols and R. C. H. M. Hofman-Caris, "Review of photochemical reaction constants of organic micropollutants required for UV advanced oxidation processes in water", *Water Research*, vol. 46, no. 9, pp. 2815–2827, Jun. 2012. DOI: 10.1016/j.watres.2012.03.036.

- [143] R. O. Rahn, "Potassium Iodide as a Chemical Actinometer for 254 nm Radiation: Use of Iodate as an Electron Scavenger", *Photochemistry and Photobiology*, vol. 66, no. 4, pp. 450–455, 1997. DOI: 10.1111/j.1751-1097.1997.tb03172.x.
- [144] W. R. Haag and J. Hoigné, "Photo-sensitized oxidation in natural water via $\bullet\text{OH}$ radicals", *Chemosphere*, vol. 14, no. 11-12, pp. 1659–1671, Jan. 1985. DOI: 10.1016/0045-6535(85)90107-9.
- [145] J. Hoigné, "Inter-calibration of $\bullet\text{OH}$ radical sources and water quality parameters", *Water Science and Technology*, vol. 35, no. 4, pp. 1–8, 1997. DOI: 10.1016/S0273-1223(97)00002-4.
- [146] J. E. Donham, E. J. Rosenfeldt, and K. R. Wigginton, "Photometric hydroxyl radical scavenging analysis of standard natural organic matter isolates", *Environmental Science: Processes & Impacts*, vol. 16, no. 4, p. 764, 2014. DOI: 10.1039/c3em00663h.
- [147] O. S. Keen, G. McKay, S. P. Mezyk, K. G. Linden, and F. L. Rosario-Ortiz, "Identifying the factors that influence the reactivity of effluent organic matter with hydroxyl radicals", *Water Research*, vol. 50, pp. 408–419, Mar. 2014. DOI: 10.1016/j.watres.2013.10.049.
- [148] C. Wang, E. Rosenfeldt, Y. Li, and R. Hofmann, "External Standard Calibration Method To Measure the Hydroxyl Radical Scavenging Capacity of Water Samples", *Environmental Science & Technology*, vol. 54, no. 3, pp. 1929–1937, Feb. 2020. DOI: 10.1021/acs.est.9b06273.
- [149] M. Kwon, S. Kim, Y. Yoon, Y. Jung, T.-M. Hwang, and J.-W. Kang, "Prediction of the removal efficiency of pharmaceuticals by a rapid spectrophotometric method using Rhodamine B in the UV/ H_2O_2 process", *Chemical Engineering Journal*, vol. 236, pp. 438–447, Jan. 2014. DOI: 10.1016/j.cej.2013.10.064.
- [150] Y. Lee, D. Gerrity, M. Lee, S. Gamage, A. Pisarenko, R. A. Trenholm, S. Canonica, S. A. Snyder, and U. von Gunten, "Organic Contaminant Abatement in Reclaimed Water by UV/ H_2O_2 and a Combined Process Consisting of $\text{O}_3/\text{H}_2\text{O}_2$ Followed by UV/ H_2O_2 : Prediction of Abatement Efficiency, Energy Consumption, and Byproduct Formation", *Environmental Science & Technology*, vol. 50, no. 7, pp. 3809–3819, Apr. 2016. DOI: 10.1021/acs.est.5b04904.
- [151] G. V. Buxton, C. L. Greenstock, W. P. Helman, and A. B. Ross, "Critical Review of rate constants for reactions of hydrated electrons, hydrogen atoms and hydroxyl radicals ($\bullet\text{OH}/\bullet\text{O}^-$) in Aqueous Solution", *Journal of Physical and Chemical Reference Data*, vol. 17, no. 2, pp. 513–886, Apr. 1988. DOI: 10.1063/1.555805.
- [152] J. C. Crittenden, S. Hu, D. W. Hand, and S. A. Green, "A kinetic model for $\text{H}_2\text{O}_2/\text{UV}$ process in a completely mixed batch reactor", *Water Research*, vol. 33, no. 10, pp. 2315–2328, Jul. 1999. DOI: 10.1016/S0043-1354(98)00448-5.

- [153] D. Minakata, D. Kamath, and S. Maetzold, "Mechanistic Insight into the Reactivity of Chlorine-Derived Radicals in the Aqueous-Phase UV–Chlorine Advanced Oxidation Process: Quantum Mechanical Calculations", *Environmental Science & Technology*, vol. 51, no. 12, pp. 6918–6926, Jun. 2017. DOI: 10.1021/acs.est.7b00507.
- [154] B. A. Wols, D. J. Harmsen, T. van Remmen, E. F. Beerendonk, and C. H. Hofman-Caris, "Design aspects of UV/H₂O₂ reactors", *Chemical Engineering Science*, vol. 137, pp. 712–721, 2015. DOI: 10.1016/j.ces.2015.06.061.
- [155] D. Gerrity, Y. Lee, S. Gamage, M. Lee, A. N. Pisarenko, R. A. Trenholm, U. von Gunten, and S. A. Snyder, "Emerging investigators series: Prediction of trace organic contaminant abatement with UV/H₂O₂: Development and validation of semi-empirical models for municipal wastewater effluents", *Environmental Science: Water Research and Technology*, vol. 2, no. 3, pp. 460–473, 2016. DOI: 10.1039/c6ew00051g.
- [156] H. W. Yu, T. Anumol, M. Park, I. Pepper, J. Scheideler, and S. A. Snyder, "On-line sensor monitoring for chemical contaminant attenuation during UV/H₂O₂ advanced oxidation process", *Water Research*, vol. 81, pp. 250–260, 2015. DOI: 10.1016/j.watres.2015.05.064.
- [157] J. L. Acero, K. Stemmler, and U. von Gunten, "Degradation kinetics of atrazine and its degradation products with ozone and •OH radicals: A predictive tool for drinking water treatment", *Environmental Science and Technology*, vol. 34, no. 4, pp. 591–597, 2000. DOI: 10.1021/es990724e.
- [158] M. M. Huber, S. Canonica, G. Y. Park, and U. von Gunten, "Oxidation of pharmaceuticals during ozonation and advanced oxidation processes", *Environmental Science and Technology*, vol. 37, no. 5, pp. 1016–1024, 2003. DOI: 10.1021/es025896h.
- [159] U. Hübner, S. Keller, and M. Jekel, "Evaluation of the prediction of trace organic compound removal during ozonation of secondary effluents using tracer substances and second order rate kinetics", *Water Research*, vol. 47, no. 17, pp. 6467–6474, 2013. DOI: 10.1016/j.watres.2013.08.025.
- [160] Y. Lee, D. Gerrity, M. Lee, A. E. Bogeat, E. Salhi, S. Gamage, R. A. Trenholm, E. C. Wert, S. A. Snyder, and U. von Gunten, "Prediction of Micropollutant Elimination during Ozonation of Municipal Wastewater Effluents: Use of Kinetic and Water Specific Information", *Environmental Science & Technology*, vol. 47, no. 11, pp. 5872–5881, 2013. DOI: 10.1021/es400781r.
- [161] I. Zucker, D. Avisar, H. Mamane, M. Jekel, and U. Hübner, "Determination of oxidant exposure during ozonation of secondary effluent to predict contaminant removal", *Water Research*, vol. 100, pp. 508–516, Sep. 2016. DOI: 10.1016/j.watres.2016.05.049.
- [162] Y. Lee, L. Kovalova, C. S. Mc Ardell, and U. von Gunten, "Prediction of micropollutant elimination during ozonation of a hospital wastewater effluent", *Water Research*, vol. 64, pp. 134–148, 2014. DOI: 10.1016/j.watres.2014.06.027.

- [163] Y. Lester, I. Ferrer, E. M. Thurman, and K. G. Linden, "Demonstrating sucralose as a monitor of full-scale UV/AOP treatment of trace organic compounds", *Journal of Hazardous Materials*, vol. 280, pp. 104–110, Sep. 2014. DOI: 10.1016/j.jhazmat.2014.07.009.
- [164] P. L. Brezonik and J. Fulkerson-Brekken, "Nitrate-Induced Photolysis in Natural Waters: Controls on Concentrations of Hydroxyl Radical Photo-Intermediates by Natural Scavenging Agents", *Environmental Science & Technology*, vol. 32, no. 19, pp. 3004–3010, Oct. 1998. DOI: 10.1021/es9802908.
- [165] Landesanstalt für Umwelt Baden-Württemberg. (2021). "Daten- und Kartendienst der LUBW", [Online]. Available: <https://udo.lubw.baden-wuerttemberg.de/public/pages/home/welcome.xhtml> (visited on 01/15/2021).
- [166] N. Froloff, E. Lloret, J.-M. Martinez, and A. Faurion, "Cross-adaptation and Molecular Modeling Study of Receptor Mechanisms Common to Four Taste Stimuli in Humans", *Chemical Senses*, vol. 23, no. 2, pp. 197–206, Apr. 1998. DOI: 10.1093/chemse/23.2.197.
- [167] J. E. Toth, K. A. Rickman, A. R. Venter, J. J. Kiddle, and S. P. Mezyk, "Reaction Kinetics and Efficiencies for the Hydroxyl and Sulfate Radical Based Oxidation of Artificial Sweeteners in Water", *The Journal of Physical Chemistry A*, vol. 116, no. 40, pp. 9819–9824, Oct. 2012. DOI: 10.1021/jp3047246.
- [168] H. W. Yu, M. Park, S. Wu, I. J. Lopez, W. Ji, J. Scheideler, and S. A. Snyder, "Strategies for selecting indicator compounds to assess attenuation of emerging contaminants during UV advanced oxidation processes", *Water Research*, p. 115 030, Aug. 2019. DOI: 10.1016/j.watres.2019.115030.
- [169] V. J. Pereira, H. S. Weinberg, K. G. Linden, and P. C. Singer, "UV degradation kinetics and modeling of pharmaceutical compounds in laboratory grade and surface water via direct and indirect photolysis at 254 nm", *Environmental Science and Technology*, vol. 41, no. 5, pp. 1682–1688, 2007. DOI: 10.1021/es061491b.
- [170] F. J. Real, F. J. Benitez, J. L. Acero, J. J. P. Sagasti, and F. Casas, "Kinetics of the Chemical Oxidation of the Pharmaceuticals Primidone, Ketoprofen, and Diatrizoate in Ultra-pure and Natural Waters", *Industrial & Engineering Chemistry Research*, vol. 48, no. 7, pp. 3380–3388, Apr. 2009. DOI: 10.1021/ie801762p.
- [171] J. Jeong, J. Jung, W. J. Cooper, and W. Song, "Degradation mechanisms and kinetic studies for the treatment of X-ray contrast media compounds by advanced oxidation/reduction processes", *Water Research*, vol. 44, no. 15, pp. 4391–4398, Aug. 2010. DOI: 10.1016/j.watres.2010.05.054.
- [172] S. Canonica, T. Kohn, M. Mac, F. J. Real, J. Wirz, and U. von Gunten, "Photosensitizer Method to Determine Rate Constants for the Reaction of Carbonate Radical with Organic Compounds", *Environmental Science & Technology*, vol. 39, no. 23, pp. 9182–9188, Dec. 2005. DOI: 10.1021/es051236b.

Bibliography

- [173] M. G. Morgan, M. Henrion, and M. Small, *Uncertainty: A Guide to Dealing with Uncertainty in Quantitative Risk and Policy Analysis*. Cambridge: Cambridge University Press, 1990, p. 332.
- [174] ISO/IEC, *ISO/IEC Guide 98-3:2008. Uncertainty of measurement. Part 3: Guide to the expression of uncertainty in measurement (GUM:1995)*, 2008.
- [175] J. H. Wenk, U. von Gunten, and S. Canonica, "Effect of Dissolved Organic Matter on the Transformation of Contaminants Induced by Excited Triplet States and the Hydroxyl Radical", *Environmental Science & Technology*, vol. 45, no. 4, pp. 1334–1340, Feb. 2011. DOI: 10.1021/es102212t.
- [176] H. Christensen, K. Sehested, and H. Corfitzen, "Reactions of hydroxyl radicals with hydrogen peroxide at ambient and elevated temperatures", *The Journal of Physical Chemistry*, vol. 86, no. 9, pp. 1588–1590, Apr. 1982. DOI: 10.1021/j100206a023.
- [177] A. J. Elliot and A. S. Simsons, "Rate constants for reactions of hydroxyl radicals as a function of temperature", *Radiation Physics and Chemistry (1977)*, vol. 24, no. 2, pp. 229–231, Jan. 1984. DOI: 10.1016/0146-5724(84)90056-6.
- [178] D. B. Miklos, W. L. Wang, K. G. Linden, J. E. Drewes, and U. Hübner, "Comparison of UV-AOPs (UV/H₂O₂, UV/PDS and UV/Chlorine) for TOrC removal from municipal wastewater effluent and optical surrogate model evaluation", *Chemical Engineering Journal*, vol. 362, no. 11, pp. 537–547, 2019. DOI: 10.1016/j.cej.2019.01.041.
- [179] D. B. Miklos, R. Hartl, P. Michel, K. G. Linden, J. E. Drewes, and U. Hübner, "UV/H₂O₂ process stability and pilot-scale validation for trace organic chemical removal from wastewater treatment plant effluents", *Water Research*, vol. 136, pp. 169–179, Jun. 2018. DOI: 10.1016/j.watres.2018.02.044.
- [180] K. Kiefer, T. Bader, N. Minas, E. Salhi, E. M.-L. Janssen, U. von Gunten, and J. Hollender, "Chlorothalonil transformation products in drinking water resources: Widespread and challenging to abate", *Water Research*, vol. 183, p. 116066, Sep. 2020. DOI: 10.1016/j.watres.2020.116066.
- [181] I. Michael-Kordatou, C. Michael, X. Duan, X. He, D. Dionysiou, M. Mills, and D. Fatta-Kassinos, "Dissolved effluent organic matter: Characteristics and potential implications in wastewater treatment and reuse applications", *Water Research*, vol. 77, pp. 213–248, Jun. 2015. DOI: 10.1016/j.watres.2015.03.011.
- [182] C. Y. Tang, Z. Yang, H. Guo, J. J. Wen, L. D. Nghiem, and E. Cornelissen, "Potable Water Reuse through Advanced Membrane Technology", *Environmental Science & Technology*, vol. 52, no. 18, pp. 10215–10223, Sep. 2018. DOI: 10.1021/acs.est.8b00562.

- [183] D. M. Warsinger, S. Chakraborty, E. W. Tow, M. H. Plumlee, C. Bellona, S. Loutatidou, L. Karimi, A. M. Mikelonis, A. Achilli, A. Ghassemi, L. P. Padhye, S. A. Snyder, S. Curcio, C. D. Vecitis, H. A. Arafat, and J. H. Lienhard, "A review of polymeric membranes and processes for potable water reuse", *Progress in Polymer Science*, vol. 81, pp. 209–237, Jun. 2018. DOI: 10.1016/j.progpolymsci.2018.01.004.
- [184] M. Taheran, S. K. Brar, M. Verma, R. Surampalli, T. Zhang, and J. Valero, "Membrane processes for removal of pharmaceutically active compounds (PhACs) from water and wastewaters", *Science of The Total Environment*, vol. 547, pp. 60–77, Mar. 2016. DOI: 10.1016/j.scitotenv.2015.12.139.
- [185] J. Wang, D. S. Dlamini, A. K. Mishra, M. T. M. Pendergast, M. C. Wong, B. B. Mamba, V. Freger, A. R. Verliefde, and E. M. Hoek, "A critical review of transport through osmotic membranes", *Journal of Membrane Science*, vol. 454, pp. 516–537, Mar. 2014. DOI: 10.1016/j.memsci.2013.12.034.
- [186] Y. Luo, W. Guo, H. H. Ngo, L. D. Nghiem, F. I. Hai, J. Zhang, S. Liang, and X. C. Wang, "A review on the occurrence of micropollutants in the aquatic environment and their fate and removal during wastewater treatment", *Science of The Total Environment*, vol. 473–474, pp. 619–641, Mar. 2014. DOI: 10.1016/j.scitotenv.2013.12.065.
- [187] S. Chellam, "Effects of nanofiltration on trihalomethane and haloacetic acid precursors removal and speciation in waters containing low concentrations of bromide ion", *Environmental Science and Technology*, vol. 34, no. 9, pp. 1813–1820, 2000. DOI: 10.1021/es991153t.
- [188] K. Listiarini, J. T. Tor, D. D. Sun, and J. O. Leckie, "Hybrid coagulation-nanofiltration membrane for removal of bromate and humic acid in water", *Journal of Membrane Science*, vol. 365, no. 1–2, pp. 154–159, 2010. DOI: 10.1016/j.memsci.2010.08.048.
- [189] N. Pagès, M. Reig, O. Gibert, and J. L. Cortina, "Trace ions rejection tuning in NF by selecting solution composition: Ion permeances estimation", *Chemical Engineering Journal*, vol. 308, pp. 126–134, 2017. DOI: 10.1016/j.cej.2016.09.037.
- [190] P. Xu, J. E. Drewes, and D. Heil, "Beneficial use of co-produced water through membrane treatment: technical-economic assessment", *Desalination*, vol. 225, no. 1–3, pp. 139–155, 2008. DOI: 10.1016/j.desal.2007.04.093.
- [191] K. Watson, M. Farré, and N. Knight, "Strategies for the removal of halides from drinking water sources, and their applicability in disinfection by-product minimisation: A critical review", *Journal of Environmental Management*, vol. 110, pp. 276–298, Nov. 2012. DOI: 10.1016/j.jenvman.2012.05.023.
- [192] H. Deng, "A review on the application of ozonation to NF/RO concentrate for municipal wastewater reclamation", *Journal of Hazardous Materials*, vol. 391, p. 122 071, Jun. 2020. DOI: 10.1016/j.jhazmat.2020.122071.

Bibliography

- [193] O. González, B. Bayarri, J. Aceña, S. Pérez, and D. Barceló, "Treatment Technologies for Wastewater Reuse: Fate of Contaminants of Emerging Concern", in 7, vol. 45, 2016, pp. 5–37. DOI: 10.1007/698-2015-363.
- [194] S. J. Khan, D. Murchland, M. Rhodes, and T. D. Waite, "Management of Concentrated Waste Streams from High-Pressure Membrane Water Treatment Systems", *Critical Reviews in Environmental Science and Technology*, vol. 39, no. 5, pp. 367–415, Apr. 2009. DOI: 10.1080/10643380701635904.
- [195] C. Mansas, J. Mendret, S. Brosillon, and A. Ayrat, "Coupling catalytic ozonation and membrane separation: A review", *Separation and Purification Technology*, vol. 236, p. 116221, Apr. 2020. DOI: 10.1016/j.seppur.2019.116221.
- [196] A. Pérez-González, A. Urtiaga, R. Ibáñez, and I. Ortiz, "State of the art and review on the treatment technologies of water reverse osmosis concentrates", *Water Research*, vol. 46, no. 2, pp. 267–283, Feb. 2012. DOI: 10.1016/j.watres.2011.10.046.
- [197] M. Umar, F. Roddick, and L. Fan, "Recent advancements in the treatment of municipal wastewater reverse osmosis concentrate - An overview", *Critical Reviews in Environmental Science and Technology*, vol. 45, no. 3, pp. 193–248, 2015. DOI: 10.1080/10643389.2013.852378.
- [198] B. Van der Bruggen, L. Lejon, and C. Vandecasteele, "Reuse, Treatment, and Discharge of the Concentrate of Pressure-Driven Membrane Processes", *Environmental Science & Technology*, vol. 37, no. 17, pp. 3733–3738, Sep. 2003. DOI: 10.1021/es0201754.
- [199] Q. Xiang, Y. Nomura, S. Fukahori, T. Mizuno, H. Tanaka, and T. Fujiwara, "Innovative Treatment of Organic Contaminants in Reverse Osmosis Concentrate from Water Reuse: a Mini Review", *Current Pollution Reports*, vol. 5, no. 4, pp. 294–307, 2019. DOI: 10.1007/s40726-019-00119-2.
- [200] C. von Sonntag, P. Dowideit, X. Fang, R. Mertens, X. Pan, N. M. Schuchmann, and H.-P. Schuchmann, "The fate of peroxy radicals in aqueous solution", *Water Science and Technology*, vol. 35, no. 4, 1997. DOI: 10.1016/S0273-1223(97)00003-6.
- [201] U. von Gunten and J. Hoigné, "Bromate Formation during Ozonation of Bromide-Containing Waters: Interaction of Ozone and Hydroxyl Radical Reactions", *Environmental Science & Technology*, vol. 28, no. 7, pp. 1234–1242, 1994. DOI: 10.1021/es00056a009.
- [202] World Health Organization, *WHO guidelines for drinking-water quality*, 4th ed. Geneva (Switzerland): World Health Organization, 2011, pp. 1–564.
- [203] Oekotoxzentrum, *Environmental Quality Standard (EQS) - Vorschlag des Oekotoxentrums für: Bromat*, 2015.
- [204] F. Soltermann, C. Abegglen, C. Götz, S. G. Zimmermann-Steffens, and U. von Gunten, "Bromid im Abwasser", *Aqua+Gas*, vol. 96, no. 10, pp. 64–71, 2016.

- [205] J. Benner, E. Salhi, T. Ternes, and U. von Gunten, "Ozonation of reverse osmosis concentrate: Kinetics and efficiency of beta blocker oxidation", *Water Research*, vol. 42, no. 12, pp. 3003–3012, 2008. DOI: 10.1016/j.watres.2008.04.002.
- [206] A. Justo, O. González, J. Aceña, S. Pérez, D. Barceló, C. Sans, and S. Esplugas, "Pharmaceuticals and organic pollution mitigation in reclamation osmosis brines by UV/H₂O₂ and ozone", *Journal of Hazardous Materials*, vol. 263, pp. 268–274, 2013. DOI: 10.1016/j.jhazmat.2013.05.030.
- [207] J. F. King, A. Szczuka, Z. Zhang, and W. A. Mitch, "Efficacy of ozone for removal of pesticides, metals and indicator virus from reverse osmosis concentrates generated during potable reuse of municipal wastewaters", *Water Research*, vol. 176, p. 115 744, 2020. DOI: 10.1016/j.watres.2020.115744.
- [208] Z. Zhang, J. F. King, A. Szczuka, Y. H. Chuang, and W. A. Mitch, "Pilot-scale ozone/biological activated carbon treatment of reverse osmosis concentrate: Potential for synergism between nitrate and contaminant removal and potable reuse", *Environmental Science: Water Research and Technology*, vol. 6, no. 5, pp. 1421–1431, 2020. DOI: 10.1039/d0ew00013b.
- [209] P. Westerhoff, S. P. Mezyk, W. J. Cooper, and D. Minakata, "Electron Pulse Radiolysis Determination of Hydroxyl Radical Rate Constants with Suwannee River Fulvic Acid and Other Dissolved Organic Matter Isolates", *Environmental Science & Technology*, vol. 41, no. 13, pp. 4640–4646, Jul. 2007. DOI: 10.1021/es062529n.
- [210] N. Walpen, J. Houska, E. Salhi, M. Sander, and U. von Gunten, "Quantification of the electron donating capacity and UV absorbance of dissolved organic matter during ozonation of secondary wastewater effluent by an assay and an automated analyzer", *Water Research*, vol. 185, p. 116 235, Oct. 2020. DOI: 10.1016/j.watres.2020.116235.
- [211] M. Aeschbacher, M. Sander, and R. P. Schwarzenbach, "Novel Electrochemical Approach to Assess the Redox Properties of Humic Substances", *Environmental Science & Technology*, vol. 44, no. 1, pp. 87–93, Jan. 2010. DOI: 10.1021/es902627p.
- [212] J. Houska, E. Salhi, N. Walpen, and U. von Gunten, "Oxidant-reactive carbonous moieties in dissolved organic matter: Selective quantification by oxidative titration using chlorine dioxide and ozone", *Water Research*, vol. 207, p. 117 790, Dec. 2021. DOI: 10.1016/j.watres.2021.117790.
- [213] Y. Lee and U. von Gunten, "Advances in predicting organic contaminant abatement during ozonation of municipal wastewater effluent: reaction kinetics, transformation products, and changes of biological effects", *Environmental Science: Water Research & Technology*, vol. 2, no. 3, pp. 421–442, 2016. DOI: 10.1039/C6EW00025H.

Bibliography

- [214] F. J. Benitez, J. L. Acero, F. J. Real, G. Roldan, and E. Rodriguez, “Photolysis of model emerging contaminants in ultra-pure water: Kinetics, by-products formation and degradation pathways”, *Water Research*, vol. 47, no. 2, pp. 870–880, Feb. 2013. DOI: 10.1016/j.watres.2012.11.016.
- [215] W. Song, W. J. Cooper, B. M. Peake, S. P. Mezyk, M. G. Nickelsen, and K. E. O’Shea, “Free-radical-induced oxidative and reductive degradation of N,N-diethyl-m-toluamide (DEET): Kinetic studies and degradation pathway”, *Water Research*, vol. 43, no. 3, pp. 635–642, Feb. 2009. DOI: 10.1016/j.watres.2008.11.018.
- [216] M. S. Elovitz and U. von Gunten, “Hydroxyl Radical/Ozone Ratios During Ozonation Processes. I. The R_{ct} Concept”, *Ozone: Science & Engineering*, vol. 21, no. 3, pp. 239–260, Jan. 1999. DOI: 10.1080/01919519908547239.
- [217] J. Staehelin and J. Hoigné, “Decomposition of ozone in water in the presence of organic solutes acting as promoters and inhibitors of radical chain reactions”, *Environmental Science & Technology*, vol. 19, no. 12, pp. 1206–1213, Dec. 1985. DOI: 10.1021/es00142a012.
- [218] Y. Fu, G. Wu, J. Geng, J. Li, S. Li, and H. Ren, “Kinetics and modeling of artificial sweeteners degradation in wastewater by the UV/persulfate process”, *Water Research*, vol. 150, pp. 12–20, Mar. 2019. DOI: 10.1016/j.watres.2018.11.051.
- [219] H.-P. Kaiser, O. Köster, M. Gresch, P. M. Périsset, P. Jäggi, E. Salhi, and U. von Gunten, “Process Control For Ozonation Systems: A 11el Real-Time Approach”, *Ozone: Science & Engineering*, vol. 35, no. 3, pp. 168–185, May 2013. DOI: 10.1080/01919512.2013.772007.
- [220] M. Minella, S. Giannakis, A. Mazzavillani, V. Maurino, C. Minero, and D. Vione, “Phototransformation of Acesulfame K in surface waters: Comparison of two techniques for the measurement of the second-order rate constants of indirect photodegradation, and modelling of photoreaction kinetics”, *Chemosphere*, vol. 186, pp. 185–192, Nov. 2017. DOI: 10.1016/j.chemosphere.2017.07.128.
- [221] Y.-T. Ahn, D.-W. Cho, A. N. Kabra, M.-K. Ji, Y. Yoon, J. Choi, I.-H. Choi, J.-W. Kang, J. R. Kim, and B.-H. Jeon, “Removal of Iopromide and Its Intermediates from Ozone-Treated Water Using Granular Activated Carbon”, *Water, Air, & Soil Pollution*, vol. 226, no. 10, p. 346, Oct. 2015. DOI: 10.1007/s11270-015-2594-0.
- [222] S. Bressmer, A. Jacob, 7. Plattner, M. Thomann, U. von Gunten, T. Wintgens, R. Wülser, and R. Wünsch, “Abschlussbericht OXIBIEAU (in german)”, Schweizerischer Verein des Gas- und Wasserfaches (SVGW), Muttentz, Tech. Rep., 2021.
- [223] M. Garrido-Baserba, R. Reif, M. Molinos-Senante, L. Larrea, A. Castillo, M. Verdaguer, and M. Poch, “Application of a multi-criteria decision model to select of design choices for WWTPs”, *Clean Technologies and Environmental Policy*, vol. 18, no. 4, pp. 1097–1109, Apr. 2016. DOI: 10.1007/s10098-016-1099-x.

- [224] Z. Visanji, S. M. K. Sadr, M. B. Johns, D. Savic, and F. A. Memon, "Optimising wastewater treatment solutions for the removal of contaminants of emerging concern (CECs): a case study for application in India", *Journal of Hydroinformatics*, vol. 22, no. 1, pp. 93–110, Jan. 2020. DOI: 10.2166/hydro.2019.031.
- [225] C. Fernández-López, M. González García, and J. M. Sánchez-Lozano, "Analysis of WWTPs technologies based on the removal efficiency of Pharmaceutical Activated Compounds for water reuse purposes. A Fuzzy Multi-Criteria Decision Making approach", *Journal of Water Process Engineering*, vol. 42, p. 102098, Aug. 2021. DOI: 10.1016/j.jwpe.2021.102098.
- [226] A. Salamirad, S. Kheybari, A. Ishizaka, and H. Farazmand, "Wastewater treatment technology selection using a hybrid multicriteria decision-making method", *International Transactions in Operational Research*, p. 12979, Apr. 2021. DOI: 10.1111/itor.12979.
- [227] S. Sadr, D. Saroj, S. Kouchaki, A. Ilemobade, and S. Ouki, "A group decision-making tool for the application of membrane technologies in different water reuse scenarios", *Journal of Environmental Management*, vol. 156, pp. 97–108, Jun. 2015. DOI: 10.1016/j.jenvman.2015.02.047.
- [228] J. Yuan, M. I. Van Dyke, and P. M. Huck, "Selection and evaluation of water pretreatment technologies for managed aquifer recharge (MAR) with reclaimed water", *Chemosphere*, vol. 236, p. 124886, Dec. 2019. DOI: 10.1016/j.chemosphere.2019.124886.
- [229] C. Echevarría, I. Martin, M. Arnaldos, X. Bernat, C. Valderrama, and J. L. Cortina, "Multicriteria Evaluation of Novel Technologies for Organic Micropollutants Removal in Advanced Water Reclamation Schemes for Indirect Potable Reuse", in 2020, pp. 215–217. DOI: 10.1007/978-3-030-13068-8_53.
- [230] S. Sudhakaran, S. Lattemann, and G. L. Amy, "Appropriate drinking water treatment processes for organic micropollutants removal based on experimental and model studies - A multi-criteria analysis study", *Science of the Total Environment*, vol. 442, pp. 478–488, 2013. DOI: 10.1016/j.scitotenv.2012.09.076.
- [231] G. Ribera, F. Clarens, X. Martínez-Lladó, I. Jubany, V. Martí, and M. Rovira, "Life cycle and human health risk assessments as tools for decision making in the design and implementation of nanofiltration in drinking water treatment plants", *Science of the Total Environment*, vol. 466–467, pp. 377–386, 2014. DOI: 10.1016/j.scitotenv.2013.06.085.
- [232] European Commission, Joint Research Centre, Institute for Environment and Sustainability, *Characterisation factors of the ILCD Recommended Life Cycle Impact Assessment methods. Database and supporting information*. Luxembourg, 2012.
- [233] T. Melin and R. Rautenbach, *Membrantrennverfahren - Grundlagen der Modul- und Anlagenauslegung*, 3rd ed. Springer Berlin Heidelberg New York, 2007, pp. 1–589.
- [234] Engineering News-Record, *Construction Cost Index History*, 2021.

Bibliography

- [235] C. Roth, “Life Cycle Assessment of Two Alternative Treatment Approaches for the Elimination of Micropollutants in Drinking Water Production”, Master Thesis, University Koblenz-Landau, 2020.
- [236] J. M. Campos-Martin, G. Blanco-Brieva, and J. L. G. Fierro, “Hydrogen Peroxide Synthesis: An Outlook beyond the Anthraquinone Process”, *Angewandte Chemie International Edition*, vol. 45, no. 42, pp. 6962–6984, Oct. 2006. DOI: 10.1002/anie.200503779.
- [237] C. Samanta, “Direct synthesis of hydrogen peroxide from hydrogen and oxygen: An overview of recent developments in the process”, *Applied Catalysis A: General*, vol. 350, no. 2, pp. 133–149, Nov. 2008. DOI: 10.1016/j.apcata.2008.07.043.
- [238] W. Yao, Q. Qu, U. von Gunten, C. Chen, G. Yu, and Y. Wang, “Comparison of methylisoborneol and geosmin abatement in surface water by conventional ozonation and an electro-peroxone process”, *Water Research*, vol. 108, pp. 373–382, Jan. 2017. DOI: 10.1016/j.watres.2016.11.014.
- [239] J. J. Mekes and Hpnw, *Electrifying Advanced Oxidation Processes*, 2021.
- [240] US EPA, *Long Term 2 Enhanced Surface Water Treatment Rule Toolbox Guidance Manual (EPA 815-R-09-016)*, 2010.
- [241] U. Alkan, A. Teksoy, A. Atesli, and H. S. Baskaya, “Efficiency of the UV/H₂O₂ process for the disinfection of humic surface waters”, *Journal of Environmental Science and Health, Part A*, vol. 42, no. 4, pp. 497–506, Mar. 2007. DOI: 10.1080/10934520601188375.
- [242] N. Augsburger, N. Zaouri, H. Cheng, and P.-Y. Hong, “The use of UV/H₂O₂ to facilitate removal of emerging contaminants in anaerobic membrane bioreactor effluents”, *Environmental Research*, vol. 198, p. 110479, Jul. 2021. DOI: 10.1016/j.envres.2020.110479.
- [243] US EPA, *Membrane Filtration Guidance Manual (EPA 815-R-06-009)*, 2005.
- [244] R. Sadiq and M. Rodriguez, “Disinfection by-products (DBPs) in drinking water and predictive models for their occurrence: a review”, *Science of The Total Environment*, vol. 321, no. 1-3, pp. 21–46, Apr. 2004. DOI: 10.1016/j.scitotenv.2003.05.001.
- [245] J. E. Schollée, M. Bourgin, U. von Gunten, C. S. McArdell, and J. Hollender, “Non-target screening to trace ozonation transformation products in a wastewater treatment train including different post-treatments”, *Water Research*, vol. 142, pp. 267–278, Oct. 2018. DOI: 10.1016/j.watres.2018.05.045.
- [246] J. E. Schollée, J. Hollender, and C. S. McArdell, “Characterization of advanced wastewater treatment with ozone and activated carbon using LC-HRMS based non-target screening with automated trend assignment”, *Water Research*, vol. 200, p. 117209, Jul. 2021. DOI: 10.1016/j.watres.2021.117209.

- [247] R. Gulde, M. Rutsch, B. Clerc, J. E. Schollée, U. von Gunten, and C. S. McArdell, “Formation of transformation products during ozonation of secondary wastewater effluent and their fate in post-treatment: From laboratory- to full-scale”, *Water Research*, vol. 200, p. 117 200, Jul. 2021. DOI: 10.1016/j.watres.2021.117200.
- [248] R. Wünsch, R. Wülser, and T. Wintgens, “Organische Mikroverunreinigungen in der Wasseraufbereitung: Kombinierte technische und naturnahe Verfahren (in german)”, *Aqua+Gas*, vol. 100, no. 4, pp. 50–55, 2020.
- [249] B. Zolghadr-Asli, O. Bozorg-Haddad, M. Enayati, and X. Chu, “A review of 20-year applications of multi-attribute decision-making in environmental and water resources planning and management”, *Environment, Development and Sustainability*, vol. 23, no. 10, pp. 14 379–14 404, Oct. 2021. DOI: 10.1007/s10668-021-01278-3.
- [250] A. Auckenthaler and U. von Gunten, “Regionale Wasserversorgung Basel-Landschaft 21 Gesamtsynthese”, Amt für Umweltschutz und Energie Basel-Landschaft; Eawag, Liestal, Dübendorf (Switzerland), Tech. Rep., 2016, pp. 1–64.
- [251] Water Joint Programming Initiative (JPI), “Water JPI Strategic Research and Innovation Agenda 2025”, Tech. Rep., 2020.
- [252] American Water Works Association (AWWA), *Resource Topics*, 2022.
- [253] ARUP, Anteagroup, and Ellen MacArthur Fondation, “Water and Circular Economy - A Whitepaper”, Tech. Rep., 2019.
- [254] Z. Xie, J. Zhou, J. Wang, C. P. François-Xavier, and T. Wintgens, “Novel Fenton-like catalyst γ -Cu-Al₂O₃-Bi₁₂O₁₅Cl₆ with electron-poor Cu centre and electron-rich Bi centre for enhancement of phenolic compounds degradation and H₂O₂ utilization: The synergistic effects of σ -Cu-ligand, dual-reaction centres and oxygen vaca”, *Applied Catalysis B: Environmental*, vol. 253, pp. 28–40, Sep. 2019. DOI: 10.1016/j.apcatb.2019.04.032.
- [255] S. Xu, H. Zhu, W. Cao, Z. Wen, J. Wang, C. P. François-Xavier, and T. Wintgens, “Cu-Al₂O₃-g-C₃N₄ and Cu-Al₂O₃-C-dots with dual-reaction centres for simultaneous enhancement of Fenton-like catalytic activity and selective H₂O₂ conversion to hydroxyl radicals”, *Applied Catalysis B: Environmental*, vol. 234, pp. 223–233, Oct. 2018. DOI: 10.1016/j.apcatb.2018.04.029.
- [256] H. Valdés, A. Saavedra, M. Flores, I. Vera-Puerto, H. Aviña, and M. Belmonte, “Reverse Osmosis Concentrate: Physicochemical Characteristics, Environmental Impact, and Technologies”, *Membranes*, vol. 11, no. 10, p. 753, Sep. 2021. DOI: 10.3390/membranes11100753.
- [257] M. Kumar, M. Badruzzaman, S. Adham, and J. Oppenheimer, “Beneficial phosphate recovery from reverse osmosis (RO) concentrate of an integrated membrane system using polymeric ligand exchanger (PLE)”, *Water Research*, vol. 41, no. 10, pp. 2211–2219, May 2007. DOI: 10.1016/j.watres.2007.01.042.

Bibliography

- [258] A. R. Ben Ali, M. K. Shukla, B. J. Schutte, and C. C. Gard, "Irrigation with RO concentrate and brackish groundwater impacts pecan tree growth and physiology", *Agricultural Water Management*, vol. 240, p. 106 328, Oct. 2020. DOI: 10.1016/j.agwat.2020.106328.
- [259] R. C. Scholes, J. F. King, W. A. Mitch, and D. L. Sedlak, "Transformation of Trace Organic Contaminants from Reverse Osmosis Concentrate by Open-Water Unit-Process Wetlands with and without Ozone Pretreatment", *Environmental Science & Technology*, vol. 54, no. 24, pp. 16 176–16 185, Dec. 2020. DOI: 10.1021/acs.est.0c04406.
- [260] J. Hu, R. Shang, B. Heijman, and L. Rietveld, "Reuse of spent granular activated carbon for organic micro-pollutant removal from treated wastewater", *Journal of Environmental Management*, vol. 160, pp. 98–104, Sep. 2015. DOI: 10.1016/j.jenvman.2015.06.011.
- [261] M. Luján-Facundo, M. Iborra-Clar, J. Mendoza-Roca, and M. Alcaina-Miranda, "Pharmaceutical compounds removal by adsorption with commercial and reused carbon coming from a drinking water treatment plant", *Journal of Cleaner Production*, vol. 238, p. 117 866, Nov. 2019. DOI: 10.1016/j.jclepro.2019.117866.
- [262] J. R. Bolton, I. Mayor-Smith, and K. G. Linden, "Rethinking the Concepts of Fluence (UV Dose) and Fluence Rate: The Importance of Photon-based Units – A Systemic Review", *Photochemistry and Photobiology*, vol. 91, pp. 1252–1262, 2015. DOI: 10.1111/php.12512.
- [263] C. E. Huckaba and F. G. Keyes, "The Accuracy of Estimation of Hydrogen Peroxide by Potassium Permanganate Titration", *Journal of the American Chemical Society*, vol. 70, no. 4, pp. 1640–1644, Apr. 1948. DOI: 10.1021/ja01184a098.
- [264] P. Neta and R. H. Schuler, "Rate constants for the reaction of O[•] radicals with organic substrates in aqueous solution", *Journal of Physical Chemistry*, vol. 79, no. 1, pp. 1–6, 1975. DOI: 10.1021/j100568a001.
- [265] M. W. Lam and S. A. Mabury, "Photodegradation of the pharmaceuticals atorvastatin, carbamazepine, levofloxacin, and sulfamethoxazole in natural waters", *Aquatic Sciences*, vol. 67, no. 2, pp. 177–188, May 2005. DOI: 10.1007/s00027-004-0768-8.
- [266] D. Vogna, R. Marotta, R. Andreozzi, A. Napolitano, and M. D'Ischia, "Kinetic and chemical assessment of the UV/H₂O₂ treatment of antiepileptic drug carbamazepine", *Chemosphere*, vol. 54, no. 4, pp. 497–505, Jan. 2004. DOI: 10.1016/S0045-6535(03)00757-4.
- [267] R. Xiao, J. Ma, Z. Luo, W. Zeng, Z. Wei, R. Spinney, W.-P. Hu, and D. D. Dionysiou, "Experimental and theoretical insight into hydroxyl and sulfate radicals-mediated degradation of carbamazepine", *Environmental Pollution*, vol. 257, p. 113 498, Feb. 2020. DOI: 10.1016/j.envpol.2019.113498.

- [268] F. Ali, J. A. Khan, N. S. Shah, M. Sayed, and H. M. Khan, "Carbamazepine degradation by UV and UV-assisted AOPs: Kinetics, mechanism and toxicity investigations", *Process Safety and Environmental Protection*, vol. 117, pp. 307–314, Jul. 2018. DOI: 10.1016/j.psep.2018.05.004.
- [269] L. Furatian and M. Mohseni, "Temperature dependence of 185 nm photochemical water treatment – The photolysis of water", *Journal of Photochemistry and Photobiology A: Chemistry*, vol. 356, pp. 364–369, Apr. 2018. DOI: 10.1016/j.jphotochem.2017.12.030.
- [270] H. Yu, E. Nie, J. Xu, S. Yan, W. J. Cooper, and W. Song, "Degradation of Diclofenac by Advanced Oxidation and Reduction Processes: Kinetic Studies, Degradation Pathways and Toxicity Assessments", *Water Research*, vol. 47, no. 5, pp. 1909–1918, Apr. 2013. DOI: 10.1016/j.watres.2013.01.016.
- [271] H. Wan, A. G. Holmén, Y. Wang, W. Lindberg, M. Englund, M. B. Någård, and R. A. Thompson, "High-throughput screening of pKa values of pharmaceuticals by pressure-assisted capillary electrophoresis and mass spectrometry", *Rapid Communications in Mass Spectrometry*, vol. 17, no. 23, pp. 2639–2648, Dec. 2003. DOI: 10.1002/rcm.1229.
- [272] K. Box, C. Bevan, J. Comer, A. Hill, R. Allen, and D. Reynolds, "High-Throughput Measurement of pKa Values in a Mixed-Buffer Linear pH Gradient System", *Analytical Chemistry*, vol. 75, no. 4, pp. 883–892, Feb. 2003. DOI: 10.1021/ac020329y.
- [273] P. Li, M. A. Khan, M. Xia, W. Lei, S. Zhu, and F. Wang, "Efficient preparation and molecular dynamic (MD) simulations of Gemini surfactant modified layered montmorillonite to potentially remove emerging organic contaminants from wastewater", *Ceramics International*, vol. 45, no. 8, pp. 10 782–10 791, Jun. 2019. DOI: 10.1016/j.ceramint.2019.02.152.
- [274] N. K. Vel Leitner and B. Roshani, "Kinetic of benzotriazole oxidation by ozone and hydroxyl radical", *Water Research*, vol. 44, no. 6, pp. 2058–2066, Mar. 2010. DOI: 10.1016/j.watres.2009.12.018.
- [275] D. Naik and P. Moorthy, "Studies on the transient species formed in the pulse radiolysis of benzotriazole", *Radiation Physics and Chemistry*, vol. 46, no. 3, pp. 353–357, Sep. 1995. DOI: 10.1016/0969-806X(94)00129-8.
- [276] J. Ye, P. Zhou, Y. Chen, H. Ou, J. Liu, C. Li, and Q. Li, "Degradation of 1H-benzotriazole using ultraviolet activating persulfate: Mechanisms, products and toxicological analysis", *Chemical Engineering Journal*, vol. 334, pp. 1493–1501, 2018. DOI: 10.1016/j.cej.2017.11.101.
- [277] R. Andreozzi, V. Caprio, A. Insola, and G. Longo, "Photochemical degradation of benzotriazole in aqueous solution", *Journal of Chemical Technology & Biotechnology*, vol. 73, no. 2, pp. 93–98, Oct. 1998. DOI: 10.1002 / (SICI) 1097-4660(1998100)73:2<93::AID-JCTB910>3.0.CO;2-7.

Bibliography

- [278] B. Yang, G.-G. Ying, L.-J. Zhang, L.-J. Zhou, S. Liu, and Y.-X. Fang, "Kinetics modeling and reaction mechanism of ferrate(VI) oxidation of benzotriazoles", *Water Research*, vol. 45, no. 6, pp. 2261–2269, Mar. 2011. DOI: 10.1016/j.watres.2011.01.022.
- [279] R. F. Dantas, M. Canterino, R. Marotta, C. Sans, S. Esplugas, and R. Andreozzi, "Bezafibrate removal by means of ozonation: Primary intermediates, kinetics, and toxicity assessment", *Water Research*, vol. 41, no. 12, pp. 2525–2532, 2007. DOI: 10.1016/j.watres.2007.03.011.
- [280] X.-T. Shi, Y.-Z. Liu, Y.-Q. Tang, L. Feng, and L.-Q. Zhang, "Kinetics and pathways of Bezafibrate degradation in UV/chlorine process", *Environmental Science and Pollution Research*, vol. 25, no. 1, pp. 672–682, Jan. 2018. DOI: 10.1007/s11356-017-0461-9.
- [281] B. Razavi, W. Song, W. J. Cooper, J. Greaves, and J. Jeong, "Free-Radical-Induced Oxidative and Reductive Degradation of Fibrate Pharmaceuticals: Kinetic Studies and Degradation Mechanisms", *The Journal of Physical Chemistry A*, vol. 113, no. 7, pp. 1287–1294, Feb. 2009. DOI: 10.1021/jp808057c.
- [282] J. L. Packer, J. J. Werner, D. E. Latch, K. McNeill, and W. A. Arnold, "Photochemical fate of pharmaceuticals in the environment: Naproxen, diclofenac, clofibric acid, and ibuprofen", *Aquatic Sciences - Research Across Boundaries*, vol. 65, no. 4, pp. 342–351, Dec. 2003. DOI: 10.1007/s00027-003-0671-8.
- [283] F. Yuan, C. Hu, X. Hu, J. Qu, and M. Yang, "Degradation of selected pharmaceuticals in aqueous solution with UV and UV/H₂O₂", *Water Research*, vol. 43, no. 6, pp. 1766–1774, Apr. 2009. DOI: 10.1016/j.watres.2009.01.008.
- [284] V. Camel and A. Bermond, *The use of ozone and associated oxidation processes in drinking water treatment*, Nov. 1998. DOI: 10.1016/S0043-1354(98)00130-4.
- [285] J. De Laat, N. Chramosta, M. Doré, H. Suty, and M. Pouillot, "Constantes cinétiques de réaction des radicaux hydroxyles sur quelques sous-produits d'oxydation de l'atrazine par O₃ ou par O₃/H₂O₂", *Environmental Technology*, vol. 15, no. 5, pp. 419–428, May 1994. DOI: 10.1080/09593339409385446.
- [286] N. Chramosta, J. De Laat, M. Dore, H. Suty, and M. Pouillot, "Determination des constantes cinétiques de réaction des radicaux hydroxyles sur quelques s-triazines", *Environmental Technology*, vol. 14, no. 3, pp. 215–226, Mar. 1993. DOI: 10.1080/09593339309385283.
- [287] W. R. Haag and C. C. D. Yao, "Rate constants for reaction of hydroxyl radicals with several drinking water contaminants", *Environmental Science & Technology*, vol. 26, no. 5, pp. 1005–1013, May 1992. DOI: 10.1021/es00029a021.
- [288] M. Aeschbacher, C. Graf, R. P. Schwarzenbach, and M. Sander, "Antioxidant Properties of Humic Substances", *Environmental Science & Technology*, vol. 46, no. 9, pp. 4916–4925, May 2012. DOI: 10.1021/es300039h.

- [289] N. Walpen, M. H. Schroth, and M. Sander, "Quantification of Phenolic Antioxidant Moieties in Dissolved Organic Matter by Flow-Injection Analysis with Electrochemical Detection", *Environmental Science & Technology*, vol. 50, no. 12, pp. 6423–6432, Jun. 2016. DOI: 10.1021/acs.est.6b01120.
- [290] C. Mayer, "Comparing Advanced Oxidation Processes for Micropollutant Abatement in Drinking Water Treatment", Master Thesis, RWTH Aachen University, 2019.
- [291] K. Hellauer, S. Karakurt, A. Sperlich, V. Burke, G. Massmann, U. Hübner, and J. E. Drewes, "Establishing sequential managed aquifer recharge technology (SMART) for enhanced removal of trace organic chemicals: Experiences from field studies in Berlin, Germany", *Journal of Hydrology*, vol. 563, pp. 1161–1168, Aug. 2018. DOI: 10.1016/j.jhydrol.2017.09.044.
- [292] M. Prahtel, "Impact of membrane selection and transmembrane pressure on micropollutant removal, DOC removal and bromide passage in surface water treatment", Master Thesis, Technical University of Munich, 2019.
- [293] R. Wünsch, M. Prahtel, M. Thomann, T. Wintgens, and U. von Gunten, "Ozon-Behandlung von Konzentraten dichter Membranen in der Trinkwasseraufbereitung: Einfluss der Membran auf die Bromatbildung", in *Proceedings of 14. Aachener Tagung Wassertechnologie*, Aachen: ISA and AVT (RWTH Aachen University), 2021.
- [294] G. Rice, S. Kentish, A. O'Connor, A. Barber, A. Pihlajamäki, M. Nyström, and G. Stevens, "Analysis of separation and fouling behaviour during nanofiltration of dairy ultrafiltration permeates", *Desalination*, vol. 236, no. 1-3, pp. 23–29, Jan. 2009. DOI: 10.1016/j.desal.2007.10.046.
- [295] Toray Industries. (2021). "TMHA Series", [Online]. Available: [https://www.water.toray/products/ro/pdf/TMHA\(C\)_v0_202104.pdf](https://www.water.toray/products/ro/pdf/TMHA(C)_v0_202104.pdf) (visited on 08/16/2021).
- [296] Joint FAO/WHO Expert Committee on Food Additives (JECFA), *Evaluations of certain food additives and contaminants*, 1991.
- [297] C. M. Sharpless and K. G. Linden, "Experimental and Model Comparisons of Low- and Medium-Pressure Hg Lamps for the Direct and H₂O₂ Assisted UV Photodegradation of N-Nitrosodimethylamine in Simulated Drinking Water", *Environmental Science & Technology*, vol. 37, no. 9, pp. 1933–1940, May 2003. DOI: 10.1021/es025814p.
- [298] I. A. Katsoyiannis, S. Canonica, and U. von Gunten, "Efficiency and energy requirements for the transformation of organic micropollutants by ozone, O₃/H₂O₂ and UV/H₂O₂", *Water Research*, vol. 45, no. 13, pp. 3811–3822, 2011. DOI: 10.1016/j.watres.2011.04.038.

Curriculum Vitae

- 01/2018 – 12/2021 School of Architecture, Civil and Environmental Engineering
 (ENAC), Ecole Polytechnique Fédérale de Lausanne (EPFL),
 Switzerland
 PhD Student
- 09/2016 – 12/2021 FHNW University of Applied Sciences and Arts Northwestern
 Switzerland, School of Life Sciences, Institute for Ecopreneurship,
 Switzerland
 Scientific Assistant and Internship
- 04/2014 – 05/2016 RWTH Aachen University, Germany
 Master Degree in Chemical Engineering
- 09/2009 – 11/2013 RWTH Aachen University, Germany
 Bachelor Degree in Mechanical Engineering
 Specialization in Chemical Engineering
- 08/1999 – 06/2008 Evangelisches Gymnasium Meinerzhagen, Germany
 German Abitur

Lörrach, 12 November 2021

Robin Wünsch